GIS based assessment of climate-induced landslide susceptibility of sensitive marine clays in the Ottawa region, Canada

Submitted by

Mohammad Al-Umar

Under the supervision of
Dr. Mamadou Fall

and

Co-supervision of
Dr. Bahram Daneshfar

A thesis submitted to the
Faculty of Engineering Graduate Studies
In partial fulfillment of the requirements
for the degree of
Doctor of Philosophy
in Civil Engineering

Department of Civil Engineering
Faculty of Engineering
University of Ottawa

To the soul of my Mother

Abstract

Landslides are relatively frequent in Ottawa due to the presence of sensitive marine clays (Leda clay or Champlain Sea clay), and the presence of natural or climatic triggers such as rainfall or snowmelt. A geographic information system (GIS) based modeling tool has been developed to assess and predict climate (rainfall and snowmelt)-induced landslides in the sensitive marine clays of the Ottawa region. The Transient Rainfall Infiltration and Grid-based Regional Slope-Stability (TRIGRS) model is used in a GIS framework to investigate the influence of rainfall and snowmelt on shallow landslides through the Ottawa region, with respect to time and location.

First, the GIS and TRIGRS models are combined to assess landslide susceptibility with respect to rainfall. The GIS-TRIGRS approach requires topographic, geologic, hydrologic, and geotechnical information of the study area. In addition to this technical information (input data), rainfall intensity data for different durations (5 minutes, and 6, 12, 18, and 24 hours), and historical data of the regional landslides is required. This data is used to verify the locations of predicted landslide-susceptible areas with respect to historical landslide maps in the area. The generated results from the GIS-TRIGRS model were verified by comparing the predicted and historical locations of shallow landslides induced by rainfall throughout the Ottawa region. The comparison results showed a high correlation between the predicted areas of landslides and the previously reported landslides. In addition, the results also indicated that not all previous landslides in Leda clays were triggered by rainfall.

The second application of the developed GIS-TRIGRS approach was used to assess and predict snowmelt-induced landslides in areas of sensitive marine clay in the Ottawa region. Similar to the first analysis, the approach requires the following input data: topographic, geologic, hydrologic, geotechnical, snowmelt intensity data for various periods (6–48 hours, 3–15 days, 25 days, and 30 days), This approach also requires data indicating the location of historical landslides in the study area. Using this data, we examine both the timing and location of shallow landslides due to snowmelt in a GIS-based framework. The developed model was validated by comparing the predicted landslide-susceptible areas to historical landslide maps in the study area. A high correlation between predicted and historical landslide location trends was obtained, confirming that the developed GIS-TRIGRS model can predict the snowmelt-induced landslide susceptibility in the sensitive marine clays relatively well. The model results reinforced the conclusion that areas with high slopes and sensitive marine clays were more prone to snowmelt-induced landslides.

Finally, in a Geographic Information System (GIS) the landslide occurrence susceptibility in the Ottawa area was modeled. Results of such models are presented as maps showing landslide susceptibility in Champlain Sea clays (Leda clays) in the Ottawa area due to both rainfall and snowmelt. Various input data was collected and entered into a GIS and TRIGRS model. The main categories of such inputs are climate, topography, geology, hydrology, and geotechnical data. The rainfall and snowmelt intensity data was extracted for 24 to 48 hour periods from Environment and Climate Change Canada historical climate records. Thereafter, the factor of safety was calculated in order to determine the stability of slopes across the study area. The model assesses the effects of rainfall and snowmelt on landslide occurrence, and based on the calculated factor of safety at each pixel of the study area, the model calculates the landslide susceptibility.

The results presented in this thesis will provide a geotechnical basis for making appropriate engineering decisions during slope management and land use planning in the Ottawa region.

ACKNOWLEDGEMENTS

First and foremost, thank you to God, Allah, for granting me the strength and opportunity to learn and for your endless bounties in all aspects of life.

This thesis was completed in this form with the assistance of several people, that I am sincerely thankful and appreciative of:

My supervisor, **Dr. Mamadou Fall**, and co-supervisor, **Dr. Bahram Daneshfar**, for their kind support and encouragement offered to me during the progression of my graduate work. My supervisors were especially helpful in helping my research flourish and overcome its obstacles. Thank you very much.

I would like to express my great thanks to my family (My father "**Thegeel Nema Al-Umar"**, My wife "**Zahraa"** and kids "**Maryam**, **Narjis**, **Heba**, **Muntathar"**), for their patient and positive support which I would never reach this stage of my life without it. I also thank my brothers and sisters for their emotional support.

My colleagues – **Professor Andraos Skaff**, **Dr. Muslim Majeed**, and **Mr. Imad Alainachi** – thank you for your unending, unconditional, and unstoppable support and help through this journey.

Mr. Rene Duplain, Mr. Pierre Leblanc (from the University of Ottawa library) for providing me with technical assistance, thank you for your support.

Last, I hope that my work fills your heart with joy and makes you proud.

Table of Contents

List of Figures

List of Tables

CHAPTER 1

1 General Introduction

1.1 Problem Statement

Sensitive marine clays (also known as Leda clays) cover large areas throughout Eastern Canada (e.g., Ontario, Quebec). There are thick deposits of these sensitive clays in the provinces of Ontario, and especially throughout the Ottawa region (Haché et al. 2015; Taha, 2010). The populations of the Ottawa region have increased at a steady rate, reaching around 1 million at the beginning of 2016 (City of Ottawa 2016). A sudden surge in local infrastructure construction has occurred in the area, contributing to the development of new residential areas, transportation ways, and utilities. Due to a large amount of infrastructure development, it is difficult to avoid the spread of these facilities throughout the Ottawa region, including across areas with problematic pockets of sensitive clays (Nader et al., 2015; Taha, 2010; Quinn, 2009).

Sensitive marine clay in Canada and other parts of the world are a challenging soil to work with from a geotechnical engineer's point of view because the soil behaves very differently than other types of soils. Leda clay characteristics also vary in comparison to other clays. The sensitive marine clays of Canada are young glacial deposits - less than 12,000 years old. The micro-structure of the clay particles of Leda clay are arranged in an orientation that resembles a card house structure; when disturbed, the entire structure collapses. During remolding and excessive wetting, Leda clay can suddenly collapse and flow like a liquid (Haché et al., 2015; Nader et al., 2015). This kind of soil has caused many geotechnical problems, such as landslides. Landslides have taken place in areas containing Leda clay throughout Eastern Canada over the course of the past several decades (Taha and Fall, 2014; Taha, 2010; Quinn, 2009). In the history of the Ottawa region, slopes of Leda clay occur in many areas within the cities of Orleans, Gloucester, and Casselman, and have thus been prone to landslide events. Elsewhere, most landslides cover a large area, and could rapidly take place without any warning (Aylsworth et al., 1997).

Rainfall, snowmelt, and seismic activity can trigger landslides in locations with sensitive marine clay formations, particularly in the Ottawa region (Quinn, 2009). Regarding climate, Ottawa is warm and humid during the relatively short summer. Rainfall reaches its maximum during June and July. Throughout the winter season, the duration of rain and snowfall is unstable throughout typical Ottawa winters. Regardless, from November to March there are significant amounts of snowfall each year. The

snow cover begins from mid-December until early April. During this time, freezing rain and high wind chills are also very common in the region. Most recently in Ottawa, the overall amount and duration of rainfall and snowmelt have increased with time (EEPL, 2014; Auld et al., 2009).

1.2 Research Objectives

The primary objective of this thesis is to assess the influence of rainfall and snowmelt on landslide susceptibility in areas of sensitive marine clays in Ottawa. This objective was achieved by:

1- Developing a GIS-based geotechnical model to conduct an assessment of the effect that various rainfall intensities and durations may have on landslide occurrence. This data was used to create rainfall-induced landslide danger maps for affected areas.

2- Developing a GIS-based geotechnical model to conduct an assessment of the effect that various snowmelt intensities and durations may have on landslide occurrence. This data was used to create snowmelt-induced landslide danger maps for affected areas.

3- Developing a map of climate-induced (rainfall and snowmelt) landslides in Ottawa sensitive marine clays.

These results will provide a geotechnical basis for making appropriate engineering decisions during slope management and land use planning.

1.3 Research Methodology and Approach

The research approach illustrated in Figure (1-1) (presented at the end of this section) was adopted to achieve the objectives of this study. This approach includes five main stages.

In the first step, a comprehensive literature review is conducted to observe both similar work and related data. Furthermore, background information is acquired, then and given, in order to facilitate the understanding of the main concepts used in the present manuscript and of the results presented in this thesis.

The second step includes gathering the geographical, geomorphological, geological, geotechnical and climate background information and data about the study area (Ottawa, Canada). The information and data were collected from several publications and sources with a good work history in the region, including governmental agencies, consulting firms, academic researchers and technical firms. All the

data gained from this stage was then used as the input data for the GIS-based landslide susceptibility assessment with respect to rainfall (Part 3) and snowmelt (Part 4).

In the third part of this thesis, a GIS-based geotechnical model was developed to assess and predict rainfall-induced landslides in Ottawa areas containing sensitive marine clays (this GIS-TRIGRS model is presented in Technical Paper 1, Section 4). The geotechnical model was developed using the Transient Rainfall Infiltration and Grid-based Regional Slope-stability (TRIGRS) model. The landslide susceptibility assessment required the rainfall intensity data for different periods of time as well as the following input data: topographic, geologic, hydrologic, and geotechnical information of the study area. The rainfall-induced landslides areas predicted by the developed model were compared with the locations of the historical landslides in the study area for validation purpose. The validation shows a relatively good agreement between the predicted landslide areas and the mapped historical landslide areas. Spatial analyses were conducted by combining the use of rainfall intensity records of different durations (5 minutes and 6, 12, 18, and 24 hours), and the historical landslide data in the study area. The developed model was used to evaluate rainfall's effect on shallow landslide susceptibility in the Ottawa region with respect to time and location.

In the fourth part of this work, another GIS-TRIGRS model was developed to assess and predict snowmelt-induced landslides in Ottawa areas containing sensitive marine clays (see Technical Paper 2, Section 5). Topographic, geologic, hydrologic, and geotechnical information was required for the study area, in addition to snowmelt intensity data for several different periods (6 to 48 hours, 3 to 15 days, 25 days, and 30 days). Snowmelt intensity records and historical landslide information from the study area was used during the spatial analysis in order to examine both the timing and location of shallow landslides due to snowmelt across the Ottawa region in a GIS-based framework. These models were validated via similar means as those presented in Technical Paper 1.

In the fifth part of this work the influence of rainfall and snowmelt on landslide susceptibility was evaluated, which resulted in the development of climate-induced landslides map for the study area (see Technical Paper 3, Section 6).

The final portion of this research approach includes a compilation of the results, main conclusions, and recommendations.

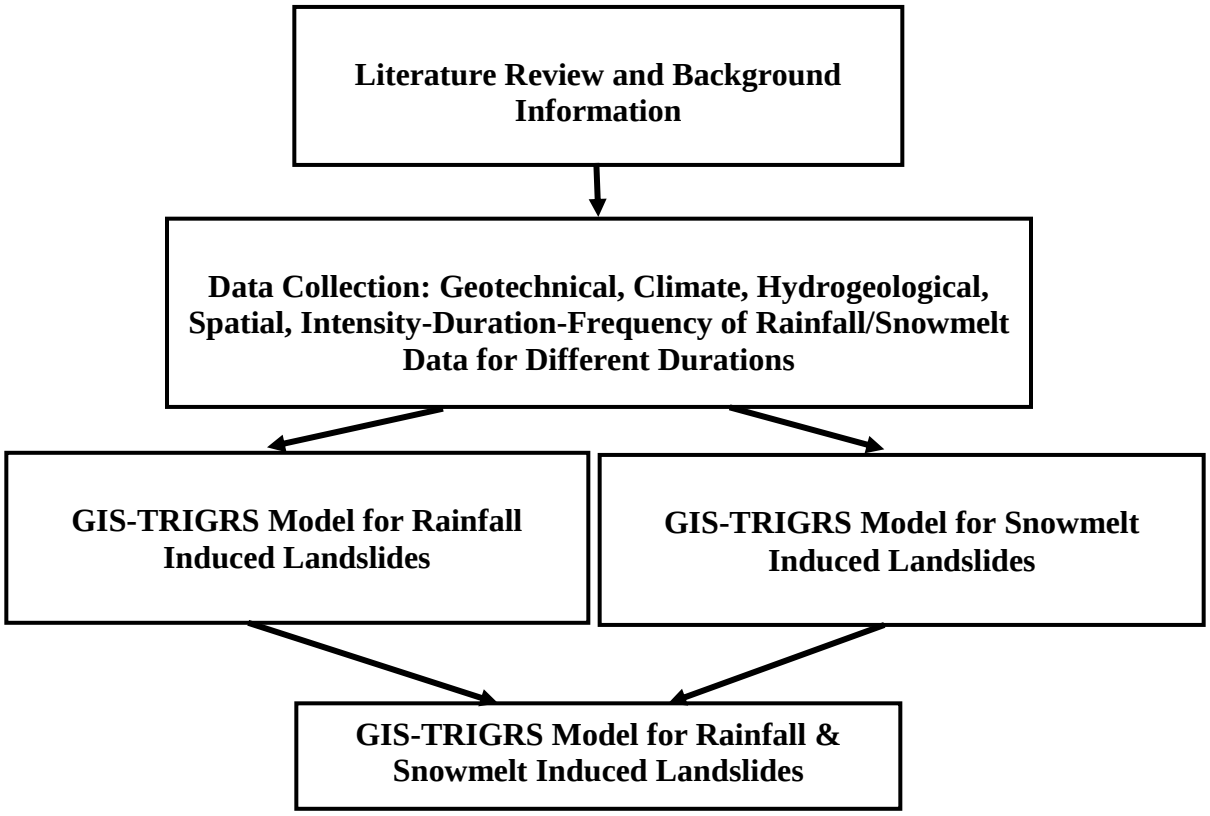

Figure 1-1 Research and Study Approach

1.4 Thesis Organization

This thesis is organized in the form of technical papers and contains eight chapters (see Figure (1-2)) below).

- ✓ Chapter 1: presents the general introduction, in which the problem statement, the thesis research objectives, the adopted research methodology and approach, and the organization of the thesis are presented and discussed.
- ✓ Chapter 2: provides relevant background information on the sensitive marine clay throughout Canada (including the Ottawa region). This chapter also contains relevant background information about Geographic Information System (GIS) and the Transient Rainfall Infiltration and Grid-based Regional Slope-stability (TRIGRS) model as a tool for landslide assessment. This chapter also provides a detailed literature review on previous studies using GIS based assessments of landslide susceptibility induced by rainfall and snowmelt.

- ✓ Chapter 3: provides information on the study area including the geographic setting, geomorphology, the geotechnical and geological characteristics of the sensitive marine clays of the Ottawa region, and the impact of climatic conditions like rainfall and snowmelt.
- ✓ Chapter 4: consists of the Technical Paper 1 - GIS based modeling of rainfall-induced landslide susceptibility for sensitive marine clays in the Ottawa region.
- ✓ Chapter 5: consists of the Technical Paper 2 - GIS based modeling of snowmelt-induced landslide susceptibility for sensitive marine clays in the Ottawa region.
- ✓ Chapter 6: consists of the Technical Paper 3 - Mapping Combined Effect of Rainfall and Snowmelt-Induced Landslide Susceptibility of Sensitive Marine Clays in Ottawa Area.
- ✓ Chapter 7: syntheses the overall thesis results.
- ✓ Chapter 8: presents the conclusions and recommendations of this thesis.

It should be emphasized that since a paper-based thesis format is adopted, some of the contents in the papers may be repeated because each paper is independently written, and crafted according to manuscript instructions for the specified publication.

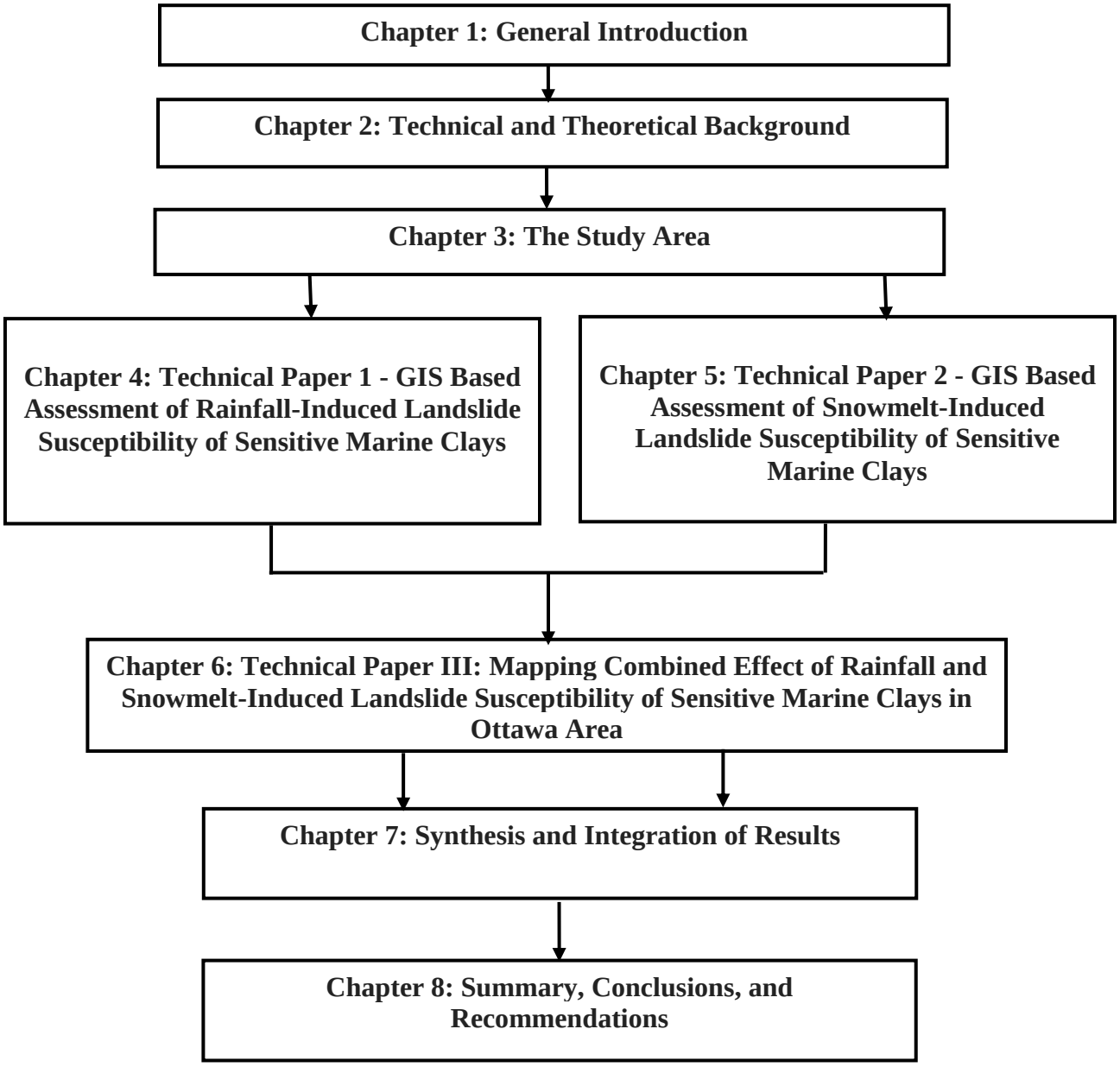

Figure 1-2 Schematic diagram that illustrates the organization of the thesis

1.5 References

Auld, H., Don, M., Joan, K., Shouquan, C., Neil. C., Sharon, F. 2009. Adaptation by design: climate, municipal infrastructure & buildings in the Ottawa area. Environment Canada.

Aylsworth, J.M., Lawrence, D.E. and Evans, S.G., 1997. Landslide and settlement problems in sensitive marine clay, Ottawa Valley. Geological Association of Canada/Mineralogical Association of Canada.

City of Ottawa, 2015 http://ottawa.ca/en/long-range-financial-plans/economy-and-demographics/population.

Energy East Pipeline Project (EEPL) 2014, Prepared for Energy East Pipeline Ltd. Calgary, Alberta.

Haché, R., Nader A., Gudina S., Fall, M., 2015. Evaluation of the undrained shear strength of Champlain Sea clays (Leda) in Ottawa. Geo Quebec 2015 – the 68th Canadian Geotechnical Conference (CGC) and 7th Canadian Permafrost Conference, Sep. 20-23 2015, Quebec, Canada CD rom.

Nader, A., Fall, M. and Hache, R., 2015. Characterization of sensitive marine clays by using cone and ball penetrometers: example of clays in Eastern Canada. Geotechnical and Geological Engineering, 33(4), pp.841-864.

Quinn, P., 2009. Large landslides in sensitive clay in eastern Canada and the associated hazard and risk to linear infrastructure.

Taha, A.M., 2010. Interface shear behavior of sensitive marine clays-Leda clay (Doctoral dissertation, University of Ottawa (Canada).

Taha, A. and Fall, M., 2014. Shear behavior of sensitive marine clay–steel interfaces. Act a Geotechnical, 9(6), pp. 969-980.

Trow Associates Inc., 2010. Updated geotechnical investigation proposed residential development 280-282 Crichton Street, Ottawa, Ontario, Trow Associates Inc., Accessed http://webcast.ottawa.ca/plan/All_Image%20Referencing_Site%20Plan%20Application_Image%20Reference_Geotechnical%20Study%20D07-12-10-0219.PDF

CHAPTER 2

2 Theoretical and Technical Backgrounds

2.1 Introduction

In order to develop a tool for the assessment of landslide susceptibility induced by rainfall and/or snowmelt in the sensitive marine clays in the Ottawa region, the combined use of Geographic Information System (GIS) technology, and the Transient Rainfall Infiltration and Grid-based Regional Slope-stability (TRIGRS) is necessary. Therefore, to facilitate the understanding of the main results presented in this thesis, theoretical and technical background on sensitive marine clays, GIS and TRIGRS are provided in this chapter. Furthermore, a literature review on previous studies that dealt with GIS-based assessment of landslides induced by rainfall or snowmelt is provided in this chapter to underline the uniqueness of the results presented in this thesis.

2.2 Background on Sensitive Marine Clays

In Canadian geotechnical engineering literature, the sensitive marine clay is often referred to as "Leda" or Champlain Sea clay (Nader et al., 2015; Taha and Fall, 2014). At a micro-level, the structure of the clay is similar to a card house - the clay collapses and flows when excessively wet and remolds accordingly (Nader et al., 2015). Due to their microstructure, these clays are susceptible to landslide, as seen in the past years and decades in the landslide events that occurred in the sensitive marine clays of Eastern Canada. For a thorough investigation and analysis of landslide occurrences in Leda clay slopes, a good understanding of the features and mechanics of sensitive clays is required.

Sensitive marine clays have many unique characteristics. For example, sensitive marine clays behave like a brittle material with a well-defined peak resistance. Initially, the particle structure is open, parallel, and flocculated. As high stresses are induced, and the critical resistance is reached, these bonds begin to fail. With little time to readjust and resist shear forces, particle failure occurs rapidly until the particles become stable and reach equilibrium once again. Here, the process of cementation becomes important, because it allows the soil's open, parallel, and flocculated structure to remain (Nader et al., 2015; Taha and Fall, 2014). Alternatively, as salt water in the marine clay leaches out from the previous glacier, a brittle mineral structure is left. Ultimately, the sensitive marine clay has a unique feature that causes it to collapse from a brittle material into a liquid mass flow upon disturbance (Taha and Fall, 2014). Mitchell, 1970 reported that the low stress fissured clay tests were executed on Leda clay in six

different locations in the Ottawa region up to 20 meters in depth. Most of the clay samples failure had a low stress envelope and a nodular structure (see Figure 2-1). In Ottawa area, The Leda clay deposit shows that the clay lightly pre-compressed with shear strength that slightly increases with depth as shown in Figure (2-2) (Eden and Crawford, 1957). The plasticity index relationship present in Norwegian marine clays is not supported or confirmed by these findings.

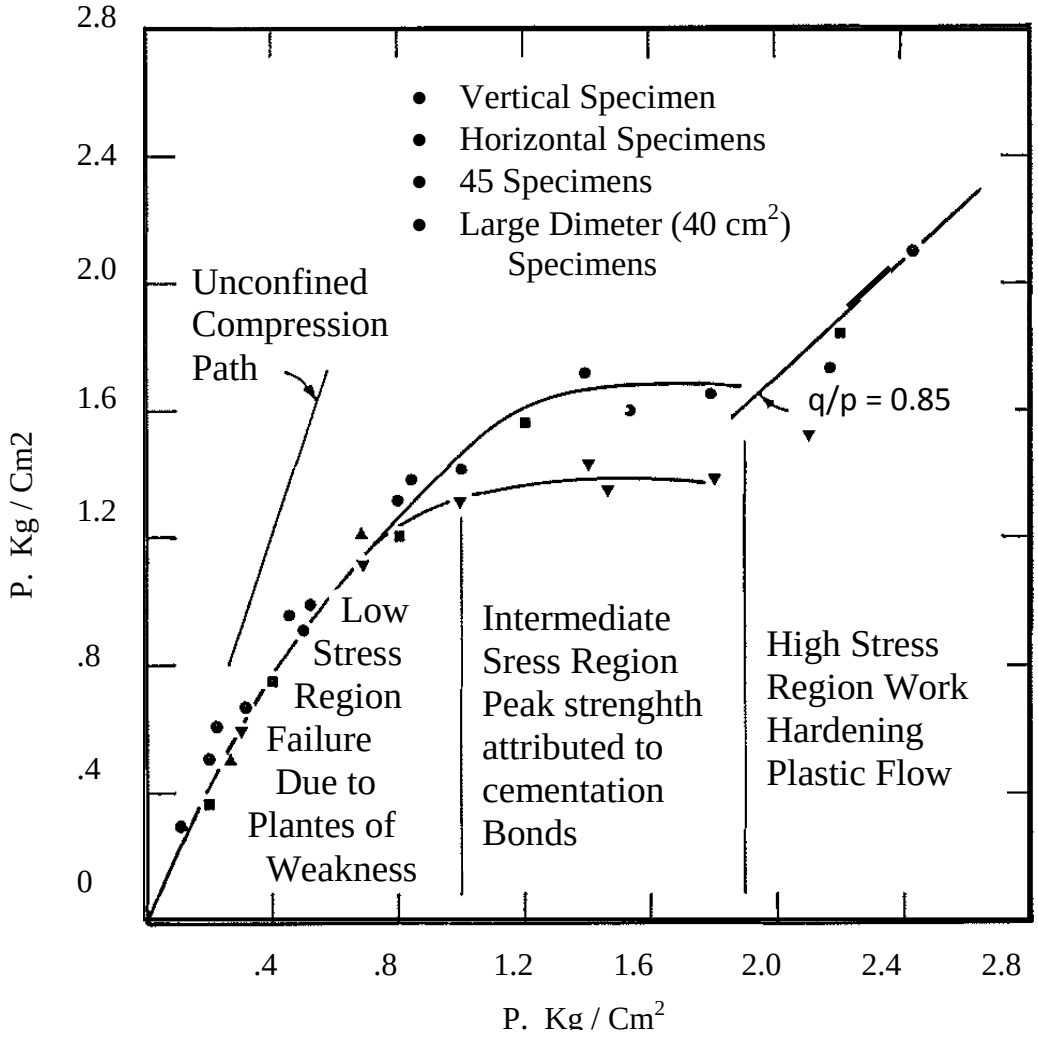

Figure 2-1 Mechanical strength of Leda Clay (Modified from Mitchell R.J. 1970)

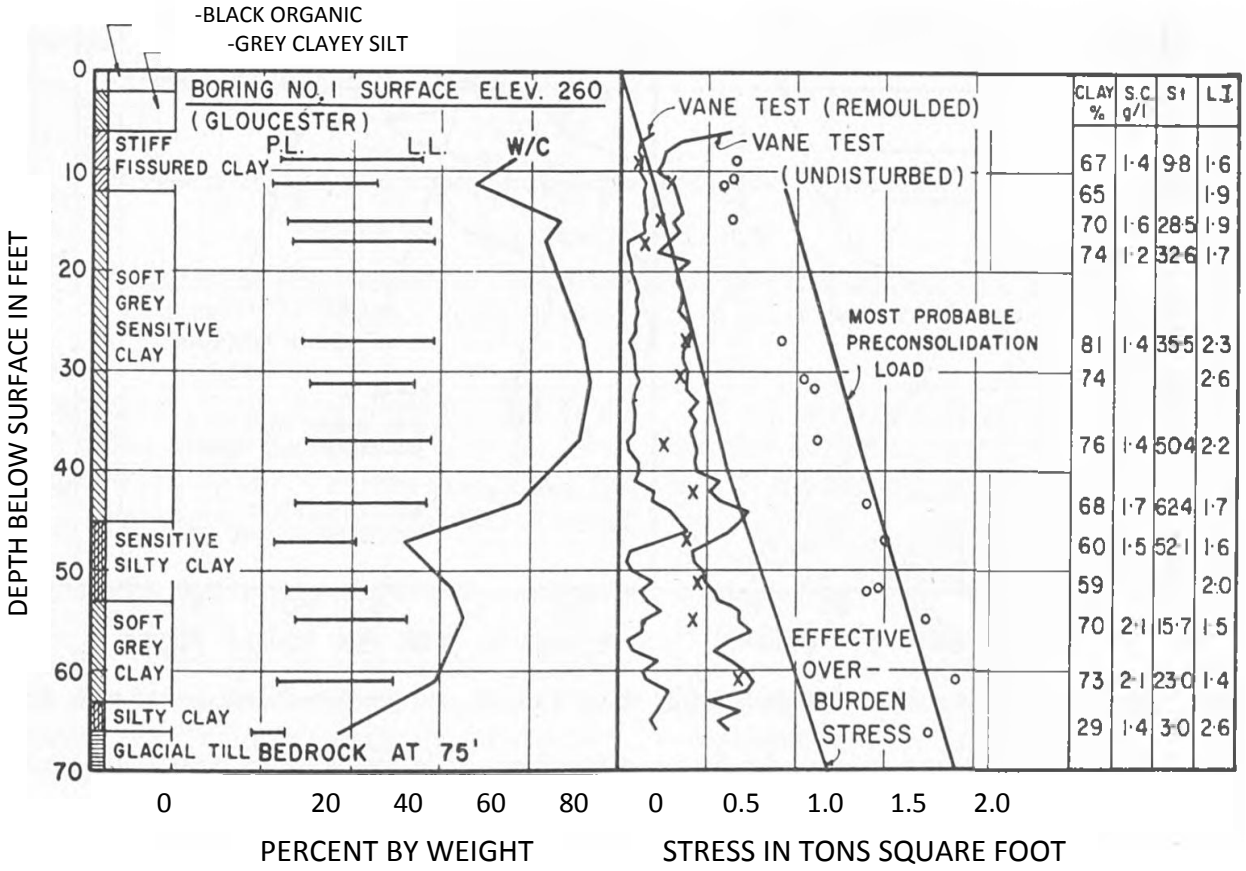

Figure 2-2 Variation of water content, Atterberg limits, shear strength, and pre-consolidated load with depth (Modified from Eden and Crawford, 1957)

Historically, numerous landslide occurrences have been recorded in regions around the world with these sensitive clays of clay, such as Scandinavia (e.g, Sweden, Norwegian), Japan, and Canada. Many recent events have occurred due to the disruption of these sediments (Won J.Y. 2013; Aylsworth et al., 2004; Benjumea et al., 2003).

The sensitive clays in Sweden are located in three main parts: Surte, Hogstorp, and Grästorp (Taha, 2010). In general, the particulate structure of Sweden's soil consists of two parts: 1) the coarse particles consist of quartz and feldspar and 2) the finer particles consist mostly of hydrous mica (illite Group). Hydrous mica is considered to be a type of clay most prone to failure. The illites present in the Swedish soil may have pre-glacial origins, or consist of other transformed minerals. The till and glaciofluvial deposits formed beneath the ice or near retreating ice, are considerably more permeable in comparison to the much finer clay sediments deposited near the ice front. The thickness of the coarse-grained sediments varies based upon location (approximately 0 to 50 meters), and their distribution is

dependent on the distance to glacial flow, bedrock morphology, subglacial melt water drainage patterns, and the distance to geographic stand still positions of the ice front (Persson, 2014).

Generally, Norwegian clays are coarser than Swedish clays. Research conducted on Norwegian clays, such as the Rosenqvist publication (1949, 1960 and other publications), reported that the illite is not prevalent in these soils, but may consist of chlorite.. At the peak of post-glaciation, about 10,000 years ago, the weight of ice pushed the land down. In the surrounding ocean, all the rock that was deposited lifted from the ground and emerged to the surface of the water, which had extended far inland. The particles of silt and clay were deposited as loose soil in the marine environment and formed into unusual flakes. The connections between the soil skeletons were very strong because the particles of soil were glued together as a result of the sea salt ions (Tilahun, 2013; Rankka and others, 2004).

In Canada, increased knowledge of the geotechnical characteristics of these marine clay soils was required due to extensive infrastructure developments. Research done in the regions with marine clays offered significant details about the sensitive soil (e.g., Nader, 2014; Taha and Fall, 2014; Quinn, 2009). For example, many types of sediment formed in the pro-glacial lake basins producing sensitive clay throughout Canada. Ice front freshwater lakes (like Lake Eriein South Ontario) are considered to be the first place in which these sensitive clay minerals were deposited in 13,000 BP. The Lake Erie basin includes Paleozoic shales and carbonates which create clay minerals. These materials were formed as a result of the erosion of the glacier. Moreover, illite, chlorite, calcite, and dolomite formed a large proportion of the deposits of clay components (Nader, 2014; Gadd, 1986).

In the Ottawa area, the Champlain Sea covered St. Lawrence Lowlands during the period between 12,500 to 10,000 BP. However, as a result of the high ground, the sea shrunk over time, and the retreated sheet of ice in the North lead to the isostatic rebound (Nader, 2014; Andrews, 1986). The combination of water gained from the melting ice, the rebound rate of the ice sheet, and the retreat and damming of drainage terraces lead to the formation of the sea, pro-glacial lakes, and postglacial lakes (Carrivick et al., 2013). The Champlain Sea deposits in the Ottawa region are concentrated at the base of the sea, which includes fine sand, silt, and clay. Most of the region's deposits include silt and clay, which cover the deepest areas of the sea bottom and lower land, sand covers the shallower parts close to the beach, and sand and gravel compose the deposits on the sea shore. These deposits are in the form of lines of different levels along the beach (Nader, 2014; Carrivick et al., 2013).

The Champlain marine clay (Leda clays) in Ottawa was first studied by Johnston (1917). He said that the water resulting from the melting of the ice was a major reason for the sedimentation of Leda

clay. Following Johnston's study, new researchers gave many details of the properties of the marine clay in the Ottawa Valley, such as Antevs (1925) and Gadd (1962). In 1977, Fransham et al. reported that clay and silt deposits represent the main component of Leda clay. These sediments arise in both salt and fresh water: in salt water, during the transgression of the Champlain Sea, and in fresh water, with fluviodeltaic clay and silt. The Champlain Sea sequence of transgression and regression, as well as the progress in the drainage system, led to the varied stratigraphic units within the sensitive clay deposits.

Freeman-Lynde et al. (1980) determined the stratigraphic sequences of the Champlain sea marine deposits, by collecting Piston cores from Lake Champlain. They demonstrated that the fresh water lakes are concentrated in the Ottawa-St. Lawrence-Champlain Lowlands region, due to the northward extension of one or more glacial lake phases of the Lake Ontario basin. Thereafter, the transgression of the Champlain Sea occurred.

In the last decade, Taha (2010) studied the geotechnical characteristics, interface problems, and engineering behavior of Leda clay. Taha (2010) found the lower of matrix suction of Leda clay increases the interface of friction angles and decreased interface contraction. In 2014, Nader et al. studied the characterization of sensitive marine clay in the Ottawa region. Nader found that the sensitive marine clays in Ottawa have different behavior than other marine clays in other parts of Canada and the world. Field and laboratory testing was used to determine clay characteristics including key engineering parameters for these specific clays (Nader, 2014).

2.3 Background on GIS

2.3.1 Definition

Spatial data can be mapped and visualized, queried, analyzed, modelled and integrated in a Geographic Information System (GIS). It enables us to do various types of analysis including simulating and modelling natural processes and to study the relationships, patterns, and trends in spatial data. GIS relates features of maps to attributes stored in a database (Dohare, 2014; Tsihrintzis et al., 1996). GIS provides solutions and tools to more efficiently manage map and non-graphic attribute data. There are several core components present in each GIS software, although many have varying capabilities (Dohare, 2014; Tsihrintzis et al., 1996). One core component includes, a data input system used to collect and process spatial data (Meaden et al., 2013; Tsihrintzis et al., 1996).

Another core GIS component is a storage and retrieval system that can organize spatial data in order to be easily retrieved for future analysis or, updates. Various types and formats of spatial data can be applied in GIS, for example, land cover, soil imagery, topography, and water information. The third core component of any GIS system includes a data manipulation and analysis subsystem that converts data, produces estimates, and constrains optimization and simulation models. The final component is a data reporting subsystem that displays the final output, including a portion of the original database as well as the manipulated data as an output from the spatial models as a table or map (Dohare, 2014; Meaden et al., 2013; Tsihrintzis et al., 1996).

2.3.2 GIS Data Structures

The majority of spatial data required in a GIS-based analysis is either vector or raster data. Vector data includes data represented as points, lines, and polygons that can be used to represent the spatial data in a vector model. Vector models are defined by coordinate pairs that precisely identify the spatial locations of features. Each coordinate point can be connected together to form lines, and each line can be linked to form polygons. Alternatively, raster data is represented by pixels in a raster model. Raster models are a spatial representation of an object composed of a grid of pixels and cells that are organized by a row and column of numbers (Meaden et al., 2013; Numetu, 2005). Raster data has a value for each parameter held in a cell or pixel, within a grid. Pixel values represent variable values at different locations of the grid. For example, a digital elevation model (DEM) as a raster, stores the elevation values for each pixel of the grid. The grid-based system that raster data is based upon facilitates an efficient and accurate overlay of analytical functions and integration of spatial data (Meaden et al., 2013; Numetu, 2005).

2.3.3 GIS Data Structures Conversion

Spatial data for projects may be available in a variety of formats and file structures. For example, for one project, the remote sensing imagery, DEM data, and geotechnical data may be based on various scales in both vector and raster model (Jha et al., 2007; Numetu, 2005). Therefore, it is often necessary to convert files between different data structures to work with multiple kinds of spatial data. When working with GIS, conversions between vector and raster models are often possible and straight forward. GIS can be applied to integrate spatial data. For instance, maps representing areas prone to landslide can be created in GIS based on outputs of the equations of models. GIS can be easily utilized to visualize the results in 2D or 3D (Jha et al., 2007; Numetu, 2005).

The GIS package used for this research is ArcGIS 10.1, developed by the Environmental Research Institute (ESRI) in Redlands, California. The package was originally developed for mapping and land planning, but it has the capabilities to expand into several fields: engineering, hydrology, geology, physics, statistics, remote sensing, business, and many others (Numetu, 2005; Malczewski, 2004).

2.4 Background on TRIGRS

The TRIGRS (Transient Rainfall Infiltration and Grid-based Regional Slope stability) model is a FORTRAN program used to display the timing of a shallow, rainfall induced landslide (Baum et al., 2002, 2008). Originally, TRIGRS was created by Baum et al. (2002) using the Richards equation set developed by Iverson (2000). The TRIGRS model is founded upon partial differential equations that produce analytical results including, transient pore pressure due to vertical infiltration and changes in slope stability. This approach is used due to the model's one-dimensional, vertical flow in isotropic and homogenous, and saturated or unsaturated soil materials (Baum et al., 2008).

The initial analysis methodology followed Iverson's outlined method (2000). The second version expanded to also address the scenario of soil infiltration into a partially, unsaturated surface layer lying above the water table. This objective was achieved by using the Richards equation for vertical infiltration that was originally sourced from Srivastava and Yeh (1991). Theoretical infiltration models, subsurface rainfall water flow, runoff direction, and slope stability were combined to evaluate the effects of rainfall flows on soil stability (Park et al., 2013).

TRIGRS analyses can be applied to areas that typically see shallow precipitation induced landslides. To apply this model, the following assumptions are made: the area has a stable and recorded water table elevation, a steady flux, and isotropic, homogeneous hydrologic properties (Baum et al., 2008).

The TRIGRS models evaluate changes in the transient pore-pressure and the factor of safety (slope stability), due to the infiltration of rainfall on a gridded, elevation model of the area. TRIGRS requires an initialization file. This file contains all of the input files, output files, and data needed to run the program successfully. Variations of hydraulic, soil infiltration, and slope stability input parameters across the mapped area is considered in order to accurately analyze complex storm sequences and to take into account variability of geological and terrain conditions. In order to achieve mass balance, an optional routing scheme may be used to find a balance between rainfall, soil infiltration, and water runoff across

the mapped grid. This balance is achieved by allowing excess water to flow downslope to cells that have yet to absorb any direct precipitation received. TRIGRS outputs are saved in series of text files representing output rasters. These text files can be imported into GIS to convert them into workable rasters (Baum et al., 2008 and 2002).

Baum et al. (2008) have extended this model to incorporate the scenarios of 1) an impervious basal boundary at a finite depth, 2) an unsaturated part over the water table, and 3) a simple runoff routing scheme that diverts excess water from cells seeing a higher rainfall application rate to those without exceeded soil infiltration capacities (Baum et al., 2008). The model results are determined by the initial conditions of the study area, the steadiness of the flow, and initial water table depth. However, the magnitudes of uncertainty and errors present in the model have not been evaluated, so the model may create inaccurate outcomes in the case that the initial water table depth is not estimated properly.

Slope stability is evaluated based on a variety of conditions and factors. For example, the saturated initial conditions for groundwater flow are modeled in the steady and transient state. Steady-state seepage and flow are dependent on the water table levels and infiltration rate. The flow is analyzed along the horizontal and vertical axes (x and z planes), and also accounts for hydraulic conductivity and slope angle (Iverson, 2000; Baum et al., 2008). Alternatively, transient groundwater flow is modeled as one dimensional (moving vertically downward). Transient groundwater flow is affected by time-varying flux of fixed duration and intensity, at the ground surface, with a zero flux condition for times greater than the starting time (Baum et al., 2002). Slope stability is ultimately determined by the calculated factor of safety values obtained from the TRIGRS model. These values are easily affected by initial steady seepage conditions; therefore, accurate estimation of initial conditions is important for modeling scenarios. Accurate initial conditions can be obtained through field observation and steady flow modeling. Inaccurate initial conditions make TRIGRS only applicable to the modeling of hypothetical situations (Godt et al., 2008; Baum et al., 2002).

A series of Heaviside step functions are used within the TRIGRS model. Heaviside step functions may be used along with the TRIGRS model in order to analyze constant rainfall intensities with time, or varied rainfall intensities in association with changes in the rainfall durations (Baum et al., 2002, 2008). The following formula (2-1) accomplishes this objective (Iverson, 2000; Park et al., 2013; Liao et al., 2011; Kim et al., 2010):

$$\Psi(Z,t) = (Z-d) + 2\sum_{n=1}^{N}\frac{I_{nz}}{K_s}\left\{H(\mathrm{t}-\mathrm{t_n})[\mathrm{D_1}(\mathrm{t}-\mathrm{t_n})]^{\frac{1}{2}}\mathrm{ierfc}\left[\frac{\mathrm{Z}}{2[\mathrm{D_1}(\mathrm{t}-\mathrm{t_n})]^{\frac{1}{2}}}\right]\right\} - 2\sum_{\mathrm{n=1}}^{\mathrm{N}}\frac{\mathrm{I_{nz}}}{\mathrm{K_s}}\left\{\mathrm{H(t}-\mathrm{t_{n+1}})[\mathrm{D1}(\mathrm{t}-\mathrm{t_{n+1}})]^{\frac{1}{2}}\mathrm{ierfc}\left[\frac{\mathrm{Z}}{2[\mathrm{D_1}(\mathrm{t}-\mathrm{t_{n+1}})]^{\frac{1}{2}}}\right]\right\} \qquad (2-1)$$

Where:

t = is time,

$\mathrm{Z} = \mathrm{z}/\cos\delta$, Z is the vertical coordinate direction, where z is the slope-normal coordinate direction,

$\beta = cos^2\delta - (I_{ZLT}/K_s)$, Ks is the hydraulic conductivity in the Z direction,

I_{ZLT} = is the steady surface flux,

$\mathrm{I_{nz}}$ = is the surface flux of a given intensity of the n**th** time interval,

$\mathrm{D_1} = \mathrm{D_0}/\cos^2\delta$, where $\mathrm{D_0}$ is the saturated hydraulic diffusivity,

N = is the total number of intervals,

$\mathrm{H}(\mathrm{t}-\mathrm{t_n})$ = is the Heavy side step function,

$\mathrm{t_n}$ = is the time at nth time interval in the rainfall infiltration sequence.

Formula (2-1) consists of two terms. The first term represents the steady component of the solution. The second term represents the transient component of flow (Godt et al., 2008). The first several expressions of this infinite series are considered acceptable; therefore, formula (2-1) is most effective when used across broad areas, on a cell-by-cell basis, and within a GIS framework that produces time varied pore pressure and safety factor for each cell within the grid (Baum et al., 2002).

The second formula (2-2) determines $\mathrm{Ierfc}(\eta)$, the complementary error function (Godt et al., 2008):

$$\mathrm{Ierfc}(\eta) = \frac{\mathrm{I}}{\sqrt{\pi}\exp(-\eta^2)} - \eta\mathrm{erfc}(\eta) \qquad (2\text{-}2)$$

Note that TRIGRS models allow limitations to be imposed. For example, at any given depth, a maximum pressure head may be set to not exceed a water table at the ground surface (Godt et al., 2008, Baum et al., 2002). This is depicted in formula (2-3):

$$\Psi(Z,t) \leq Z\beta \qquad (2\text{-}3)$$

To expand the TRIGRS model applicability to a wider range of initial conditions and situations, the model provides an additional solution. This additional analytical solution is an alternative method for estimating the infiltration of flow at the ground surface in an unsaturated state. This solution assumes the soil is a two-layer system: a saturated zone with a capillary fringe and an unsaturated zone (Baum et al., 2002). The unsaturated zone is assumed to soak up water and allow any remaining water to rise over the unsaturated zone beyond the initial water table. This soil strata is assumed to have a lower permeability that prevents and reduces surface infiltration to deeper ground. Using the four factors ,θs, θr, α, and Ks, SWCC was produced to model the wetting and infiltration process of the unsaturated soil (Srivastava and Yeh, 1991).

As depicted in the one-dimensional model, infiltrating water moves to the bottom of the unsaturated layer causing the water table to rise. The rise in the water table diffuses the pressure wave, thus increasing the pore pressure. For hillsides, with thin saturated zones, pressure waves quickly spread to the basal boundary. Richard's equation was applied for the infiltration at the ground surface and straight up flow (one dimensional form) through the unsaturated zone (Baum et al., 2008). A coordinate transformation is applied and explains the effects of a sloping ground surface (Iverson, 2000):

$$\frac{\partial\theta}{\partial t} = \frac{\partial}{\partial z}\left[K(\Psi)\left(\frac{1}{\cos^2\delta}\frac{\partial\Psi}{\partial z} - 1\right)\right] \qquad (2\text{-}4)$$

Hydraulic conductivity, K (Ψ), and volumetric content, θ, is determined from the Richard's equation as shown in formulas (2-5) and (2-6) respectively, below (Baum et al., 2008).

$$K(\Psi) = Ks\exp(\alpha\Psi^*) \qquad (2\text{-}5)$$

$$\theta = \theta r + (\theta s - \theta r)\exp(\alpha\Psi^*) \qquad (2\text{-}6)$$

Where:

Ψ = the pressure head,

Ψ* = Ψ - Ψo, where Ψo is a constant,

Ks = the saturated hydraulic conductivity,

K (Ψ) = the hydraulic conductivity function,

θ = the volumetric water content,

θr = the residual water content, and

θs = the water content at saturation.

The parameter, α, is determined using equation 2-6 to fit the parameter to a characteristic curve for the soil. Substituting equations (2-3) and (2-4) into equation (2-2) gives a linear partial differential equation. The solution of this formula is found in equations (2-7) and (2-8) below (Srivastava and Yeh, 1991). Note that the coordinate conversion for the sloping ground surface uses the following relationship: $\alpha 1 = \alpha \cos 2\delta$.

$$q(d_u, t) = \begin{Bmatrix} I_z - 4\,(I_z - I_{ZLT})\exp\left(\frac{\alpha_1\ d_u}{2}\right)\exp\left(-D_\Psi \frac{t}{4}\right) \\ \sum_{m=1}^{\infty} \frac{\Lambda_m \sin(\Lambda_m \alpha_1 d_u)}{1+\frac{\alpha_1 d_u}{2}+2\Lambda_m^2 \alpha_1 d_u}\exp[-\Lambda_m^2 D_\Psi t] \end{Bmatrix} \qquad (2\text{-}7)$$

$$D_\Psi = \frac{\alpha_1 K_s}{(\theta_s - \theta_r)} \qquad (2\text{-}8)$$

Where:

D_Ψ = the soil-water diffusivity,

$D_\Psi t$ = is equivalent to non-dimensional time, and

$\alpha_1 d_u$ = corresponds to the non-dimensional depth used by Srivastava and Yeh (1991).

d_u = is the vertical depth to the top of the capillary fringe, and the values of Λm are the roots of the equation given in Baum et al. (2008). All other parameters are identical to those used previously (Srivastava and Yeh, 1991).

The infinite slope stability model is also used in TRIGRS in order to determine the stability of a slope. This model assumes that landslides have a shallow depth with respect to their surface area (length and width). Figure (2-1) depicts a conceptual example of the infinite slope model's applicability to the computation of the factor of safety for TRIGRS models.

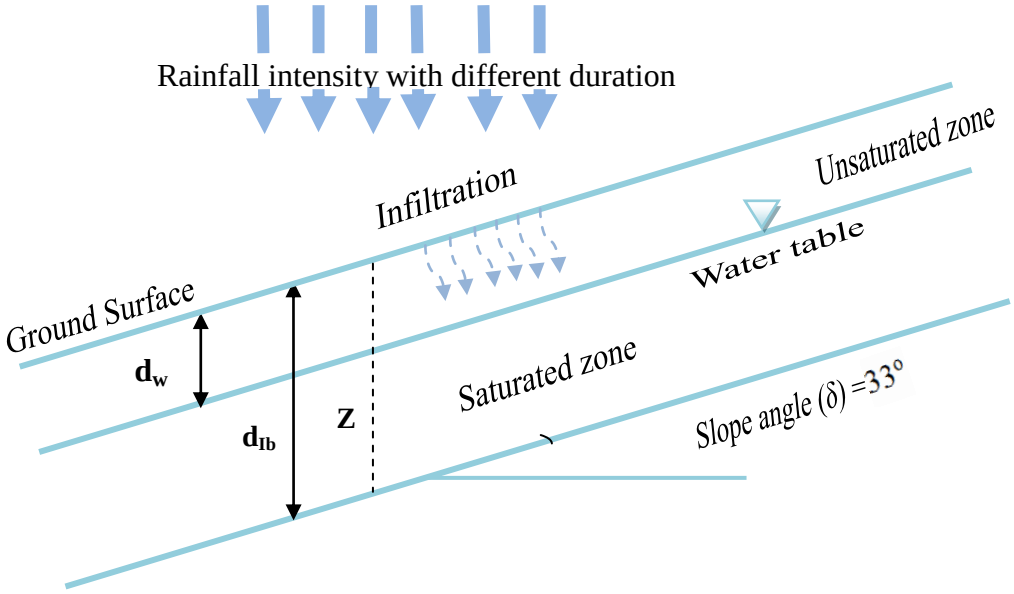

Figure 2-3 Proposed infinite slope stability analysis of studied area

This example depicts the upper portion of the slope in an unsaturated state, and the initial ground water table level was reconstructed based on observed and interpolated groundwater levels in PGMN wells. Lastly, the infinite slope model is used to calculate the factor of safety by rainfall water infiltration at a varied depth (Terzaghi, 1943; Salciarini et al., 2008). Shallow depths are most appropriate for this technique because infinite slope stability analysis is characterized by the amount of friction resisting the driving stress. The equation below is used within the TRIGRS model to calculate the safety factor for any given slope. A slope is considered stable in this approach if the Factor of Safety (FS) is greater than one (FS > 1), in equilibrium when FS equals 1 (FS = 1), and unstable when the FS is less than 1 (FS < 1). Therefore, landslides are initiated when the factor of safety transforms from a slope in equilibrium (FS = 1) to instability (FS < 1).

$$FS = \frac{\tan\phi'}{\tan\delta} + \frac{c' - \Psi(Z,t)\,\gamma_w \tan\phi'}{\gamma_s d_{Ib} \sin\delta \cos\delta} \qquad (2-9)$$

Where:

c' = is soil cohesion,

ϕ' = is soil friction angle,

Ψ = is ground-water pressure head as a function of depth Z and time t,

δ = is slope angle,

γ_w, γ_s = The unit weights of water and soil, respectively.

The TRIGRS model uses a simple method for modeling and routing surface runoff for saturated cells. Surface runoff routing is also known as the infiltrability of saturated and tension-saturated soils (Godt et al., 2008; Baum et al., 2008). Surface runoff must be routed in order to guide excess surface water flow to less infiltrated soil cells further downslope. By doing so, the loss of excess rainfall that does not infiltrate the soil is prevented. Runoff occurred when the precipitation and runoff supplied to a cell exceeds its infiltrability (Godt et al., 2008; Baum et al., 2008; Raia et al., 2013). This approach can support the improved performance of urbanized and impervious areas. When storm drains are used to guide excess runoff, runoff routing is no longer needed.

In the formulas below, infiltration, I is computed using the sum of the precipitation, P, (including additional runoff from upslope cells, R_u. The runoff cannot exceed the saturated hydraulic conductivity, K_s.

$$I = P + R_u \quad \text{if} \quad I = P + R_u \leq K_s \qquad (2-10)$$

$$I = K_s \quad \text{if} \quad P + R_u > K_s \qquad (2-11)$$

TRIGRS uses a simple approach to calculate runoff routing (for infiltration less than the saturated hydraulic conductivity) (Baum et al., 2002, 2008). At each cell where $P + R_u$ is greater than the saturated hydraulic conductivity, K_s the excess flow is considered runoff, R_u and is diverted to adjacent cells.

$$R_d = P + R_u - K_s, \quad \text{if} \quad P + R_u - K_s \geq 0 \qquad (2-12)$$

$$R_d = 0, \quad \text{if} \quad P + R_u - K_s < 0 \qquad (2-13)$$

This model does not incorporate overland flow, but it is typically assumed that overland flow between adjacent cells is instant. Because overland flow is not incorporated into this model, individual storm periods must be long enough to allow surface water to flow between cells. This model's runoff routing method ensures mass balance throughout a storm, indicating that all cell precipitation must equal the water infiltrating and flowing out of the region's boundary (Baum et al., 2008; Raia et al., 2013; Park et al., 2013). Therefore, excess precipitation must infiltrate cells further downslope. Using mass-balance calculations for a storm verifies that the rainfall applied (as an input), is reasonably accounted for as an output (Godt et al., 2008; Baum et al., 2008; Raia et al., 2013; Park et al., 2013). The TRIGRS model does not carry runoff between time steps, or track water was exiting a system (through storm drains).

This model design means that excess water from a soil cell will infiltrate a different cell in the model with time (Baum et al., 2008; Park et al., 2013). This model also assumes water leaves cells and runs to adjacent cells further downslope because the water table is assumed to be at the ground surface. This case indicates that the infiltration rate will initially be steady and become negative with time. The TRIGRS model uses mass balance calculations to ensure that all precipitation exits the model's border. Instead of iterating, this model analyzes the cell saturation at the surface and later at deeper soil depths. To ensure successful mass balance, the area's topographic data must be indexed correctly when using the TRIGRS model. Alternatively, in GIS, the topography can be modified based on a digital elevation model (DEM) by raising or lowering the elevation of each cell.

2.5 Literature Review on Previous Studies of GIS Based Assessment of Landslides Induced by Rainfall

In the past decades, numerous GIS modeling studies of landslides induced by rainfall have been conducted. Key recent past studies are described and discussed below.

Barredo et al. (2000) developed a GIS technique (weighted linear sum formula) to evaluate landslide hazard in the Barranco de Tirajana basin, Gran Canarias Island. The primary data used to produce the landslide hazard map was rainfall. The average annual rainfall in the study area ranges from370 millimeters, in the bottom of the basin, to 890 millimeters at the basins top. The experts' opinions believe that the main causes of the landslides in the study area are heavy rainfall, and additionally, slope angle, the activity of landslide, and proximity to reservoirs and drainage channels. The final results illustrated that the landslide hazards map could be classified by a 'high' hazards region. The previous recordings in the study area proved most regions had landslide occurrences in a period of heavy rainfall ('moderate' and 'very low' hazard areas were present too). The study results provided information to manage and mitigate natural disasters.

In Bhagirathi Valley, Himalaya, Saha et al. (2002) successfully created landslide hazard zonation maps using GIS-based methodology (the Landslide Hazard Index formula). This allowed for improvements and enhancements of various topographic, geological, structural, and land use/land cover data sets. In some cases, landslides caused road closures and posed real threats due to local heavy monsoonal rains. The study results have generated the five zones on the Landslide Hazard Zonation (LHZ) scale as follows: 'very low', 'low', 'moderate', 'high', and 'very high'.

Chau et al. (2003) studied 1,448 landslides causing extensive damage to infrastructure in the region of Hong Kong. The study represented the number of landslides which occurred in these areas

between1984 to 1998. The reason for these landslides is geological, geomorphologic, and rainfall. Chau's work is focused on the possibility of data use alongside GIS to generate landslide hazard and risk maps. GIS (multi-dimensional regression analysis) was used to develop the maps drawn from the study area, to give a clear picture to users, who can predict the risks of landslides.

Lee (2005) used GIS and remote sensing technology to assess the hazard of landslides in Penang, Malaysia. Through the interpretations obtained from aerial photographs and field surveys, the location of previous landslides that occurred within the study area was identified and used to verify the accuracy of the model. The input data used included rainfall, geological and topographical information, and images obtained from satellites. The final results of the landslide hazard analysis were verified based on the locations of previous landslides. The verification process confirmed that the model could be used to calculate the probability of a landslide hazard.

Flentje et al. (2005) developed a GIS model to inventory detailed information on landslides, including the size and the real-time to the occurrence in the Illawarra escarpment. The inventory presented information for landslide occurrence and frequency for about 569 of all 956 landslides. Heavy rainfall was the main cause of the landslide occurrences. Meteorological data for the study area recorded the average annual rainfall to be about 1,200 to 1,600 millimeters. This information has been recognized around the world, and planners have benefited from it in risk management and mitigation. Through GIS, researchers could expand their inventory, yet narrow their focus to landslides caused by rainfall, in order to better understand and take precautionary measures to deal with such natural disasters.

Sarkar et al. (2006) used the GIS model (weighted and integrate data) to predict landslide susceptibility while mapping the Indian Himalayas. Rainfall and earthquakes were determined to be the two most important factors regarding landslide occurrence. The parameters used in GIS were lithology, fault, drainage, slope, slope aspect, and land use. A few of the different thematic data layers were prepared using satellite images, topographic maps, field data, and additional available maps. Landslide susceptible zones were classified into five classes: 'very low', 'low', 'moderate', 'high' and 'very high'. Validation of the final result (landslide susceptibility map) was done in the study area, and it was found that there was a connection instability circumstances between events.

Salciarini et al. (2006) used the TRIGRS and GIS models to predict shallow landslides induced by rainfall in Central Italy. The input parameters used in the model include rainfall intensity for different durations, topography slope, colluvial thickness, initial ground water table depth, the strength of material, and hydraulic characteristics. In their study, the TRIGRS model used analytical solutions, one-dimensional analysis, and the analysis of infinite-slope stability to calculate the factor of safety and the

variance in pore-pressure response due to rainfall infiltration. Additional information on the TRIGRS approach can be found in Park et al. (2013), Liao et al. (2011), Kim et al. (2010), and Baum et al. (2008). Results obtained from this analysis (with respect to time and location) showed regions that incurred landslides due to rainfall. These landslides were compared with the landslides previously affecting the area, and a match of 80 percent was confirmed. Verification of the model confirmed that both TRIGRS and GIS applications are good tools to predict landslides.

Lin et al. (2006) used the GIS spatial analysis feature to predict debris-flow (landslide) hazards in the watershed of the Chen-Yu-Lan River in Central Taiwan. The input dataset utilized rock formation, fault length, slope angle, slope aspect, and stream slope data to evaluate landslide hazards. Meteorological data of the study area recorded an average annual rainfall of 2,500 millimeters. This rainfall represents the main reason for landslide occurrence- because rainfall raises the ground water level, which leads to weakening of the geotechnical properties of soil. In recent years, the human and material losses in the study area have increased considerably as a result of landslides. The assessment of the final landslides hazard map was divided into three classes: 'low', 'moderate', and 'high' hazard. This assessment gives an opportunity for planners to take appropriate steps necessary to reduce or mitigate these losses. This method can also be applied to other watersheds throughout Taiwan.

Nguyen et al. (2007) used GIS (logistic regression) to build a map of the landslide risk assessment based on weighted scores. Through the results extracted from GIS, it was found that a higher weighted score leads to a higher potential for landslide data. The data inserted into the system (GIS) was collected through field work for the catchment area (along with the Kalibawang channel, west of the KulonProgo region Yogyakarta, Indonesia). According to the results of the multivariate statistical analysis, the data collected for the study area led to the following conclusions: 1) the controlling factors in landslide occurrence include slope, lithology, and groundwater, 2) to generate correct results; the amount of rainfall should be recorded daily in order to establish a consistent relationship between rainfall durations and landslide occurrence. Rainfall is a major cause of the failure of soil and the occurrence of landslides.

Dahal et al. (2007) applied weights-of-evidence quantitative integration method to create a map of landslide susceptibility. This study chose two small catchments (Moriyuki and Monnyu) in Northeastern Japan, because this region is most prone to landslides, due to heavy rainfalls. Five classes were considered in the created landslide susceptibility maps. These classes vary from "very low" to "very high". The final results of landslides susceptibility maps were verified for both catchments. It was determined that the Moriyuki catchment had an accuracy of 80.7 percent, while the accuracy of the

Monnyu catchment was 77.6 percent. The authors concluded that the model of weights-of-evidence , when used in GIS, provides the best results if applied in small catchments.

By using the GIS technique (Stability Index Mapping (SINMAP), Kuthari (2007) proved that the main trigger mechanism causing landslides in the Garhwal Himalayas in India are heavy rainfall and slopes. According to the records, in the study area, the highest amount of rainfall was received between July and September. The resolution of the digital elevation map (DEM) for the study area is 15-meters which derives slope values and presents results for prediction of landslide hazards obtained from the GIS model were validated. The success rate of prediction for this model is 74 percent.

Godt et al. (2008) used GIS to calculate the factors of safety and pore pressures at each pixel just north of Seattle, Washington. The parameters used in the model included topographic data (using Light Detection and Ranging (LiDAR) data with a high-resolution of 1.8-meters), the distribution of initial pore-pressure in the study area, the rainfall, hydraulic properties, and the strength of material data. The data was gathered from the field, in laboratory tests, and also from experiential data of rainfall intensity-duration. The results were verified by comparing the predicted and historic landslide occurrences near Seattle. The results determined that the rainfall intensity across multiple periods was the main reason for trigger landslides in the study area.

Pradhan et al. (2008) used GIS (logistic regression method) and remote sensing technology to calculate the probability of landslide hazard and risk in Malaysia. The key factors aiding in landslide occurrence include rainfall (recorded rainfall each month, approximately ranging from 58.6 to 240 millimeters), topographical and geological information, and satellite images. The final results of the study area were divided into five regions. Each region was verified based on data of previous landslide location; it is noted that the accuracy of the verification process reached 83, 72, 82, 79 and 81 percent respectively. This study has helped planners and engineers make well-informed decisions in the management and mitigation of landslide risk, and will thus reduce human and property losses.

Tassetti et al. (2008) used GIS analysis models (used Certainty Factors (CF) as a function of probability) and remote sensing technology to create a map with which one can observe and evaluate landslide susceptibility in the Western Italian Alps. One of the main factors responsible for landslide incidence in the region observed was heavy rainfall. The average annual rainfall documented ranged anywhere from 250 to 800 millimeters, with the highest value in the northern region and the lowest value recorded in the southern part of the study area. Other factors used for evaluation include slope, aspect, morphological, geological, human activity, and lithology. The final results were classified as risk maps to five classes: 1) high stability and very low certainty, 2) medium stability and low certainty, 3) low

stability and low certainty, 4) medium stability and medium certainty, and 5) high instability and high certainty.

Mukhlisin et al. (2010) used GIS (the overlay index method) to produce a landslide hazard map in Malaysia. The main factors considered to affect the occurrence of landslides were a slope, aspect, geology, land use, and the distribution of precipitation. After analysis, the final landslide hazard map was reclassified into five classes: 'very low', 'low', 'medium', 'high', and 'very high' hazard. This study assisted planners and engineers, especially in the Ulu Klang region, to take the appropriate action to continue planning safe development of this region, in spite of the existence of such landslide hazards. The verification of the final results was based on the data collected for the locations of previous landslides within the study area.

Sulaiman et al. (2010) used a GIS-based slope stability deterministic model to predict the occurrence of landslides by producing a landslide susceptibility map at a catchment in Pahang, Malaysia. The main causes of landslides in this study area were rainfall and hill slopes. The important factors used in developing the model include bulk density, friction angle, cohesion, and hydraulic conductivity. This data was collected from the site, laboratory testing, and previous geotechnical reports. Landslide sites within the study area were identified and inventoried by GPS, aerial photographs, and satellite images. The final results of the landslide susceptibility map illustrated that the unstable region (FS < 1) was concentrated in an area with rainfall of 110 millimeters. The ratio of impact on these areas was 69.51 and 69.88 percent at soil depths of two and four meters respectively.

Akbar and Ha (2011) developed a GIS and Remotely Sensed data model (information model value Ii) to predict landslide susceptibility zonation in the western portion of the Himalayan Kaghan Valley of Pakistan. The most important factors to in this model were land use, rainfall intensity, and distance from the road to the river which has more effect on a landslide compared with alternative factors. The final results confirmed the accuracy of landslide hazard zonation map to be 100 percent. Akbar and Ha observed the occurrence of landslide concentration, and categorized these hazard zones as 'moderate', 'high', or 'very high'; whereas the hazard zones where no landslides occurred were categorized to be 'low' or 'very low'. The map of landslide hazard zones illustrates that the zones categorized as 'high' or 'very high' hazard lie along the main road close to the valley. From the study's results, the authors were able to suggest two new, safer alternative road routes through the application of the GIS model.

Pradhan et al. (2011) used GIS (landslide hazard index (LHI) formula) and remote sensing techniques to compute the probability of landslide hazards and risk in Penang Island, Malaysia. The factors used for analysis included rainfall data (in the form of maps containing information supplied by

the Malaysian Meteorological Department), 10-meter interval contour maps, and a digital elevation model (DEM). From the DEM, the slope angle, slope aspect, and slope curvature were calculated, and from the topographic data, the distance from drainage or to the road could be determined. The accuracy of the final results to evaluate landslide hazards was determined to be 89 percent, confirming this technique's accuracy and usefulness when mitigating the hazard of landslides and assisting engineers in land use planning.

Akgun et al. (2012) used GIS (logistic regression modeling approach) and remote sensing techniques to evaluate the landslide risk in West Turkey (Izmir city). Input data representing the common trigger factors affecting the occurrence of landslides were divided into two groups: first precipitation data and secondly lithology (i.e., slope gradient, slope aspect, distance from roads, faults, and drainage lines). The final risk maps illustrated future landslides would concentrated in the north and southern most parts of the study area. The study area had a large urban development, so planners and engineers took advantage of the results presented in the risk maps during the planning and design of local and use.

Fowze et al. (2012) adopted the GIS approach (weighted overlay method) to create landslide susceptibility map in Thailand. Factors analyzed for impacting landslides occurrences in the study area included rainfall,, elevation, rock type, landform, land use and land cover, topography, inventory, watershed, drainage, and soil depth. The Research Division at the University of Kasetsart included the engineering properties of materials such as plasticity and grain size distribution as well. This data was used to determine the cumulative rainfall for three days in order to create accurate landslide susceptibility maps. The final results determined that rainfall increased soil moisture, and thus affected the establishment of the buildings on the slopes of the study area.

Li et al. (2012) implemented a GIS-based approach to assess landslide susceptibility by using the back-propagation Artificial Neural Network model (ANN) in Qingchuan County in China. The information from previous landslides was collected from an investigation in the field and through the analysis of an aerial photo. The number of landslides that occurred in the study area before the Wenchuan earthquake was 473 landslides. The majority of these incidents were caused by rainfall. In order to distinguish the difference between landslides that have occurred as a result of rainfall and earthquakes, a comparison between the spatial allocation of landslides and conditioning factors was done. To understand the different impacts of rainfall and earthquakes on landslide occurrence, Variation in landslide spatial distributions and the factors affecting landslide conditions were compared. The results showed that areas with high slopes and rainfall were more prone to landslides.

There was immense damage to roads and villages due to landslides in Dena city in Iran, so Moradi et al. (2012) used a GIS model and the analytical hierarchy process (AHP) to produce landslide susceptibility maps for the region. The scale used in this study for all topographic maps was 1:50,000. Several factors were taken into consideration, including rainfall, slope, weathering of lithology, land cover, and distance to a stream or road. This study has given engineers the ability to make appropriate engineering decisions to reduce human loss and prevent damage.

Shahabi et al. (2012) developed a GIS technique by using the landslide susceptibility index (LSI) equation and remote sensing data to create a landslide susceptibility map in the province of West-Azerbaijan in Iran. The landslide occurrence factors used in this analysis are precipitation, slope, aspect, distance to road, drainage network, faults, land use, elevation, and geological factors. The final results of the landslide hazard maps were classified and split into four classes: 51.37 percent of the region was a low hazard, 29.35 percent of the region was a moderate hazard, 11.10 percent of the region was high hazard, and 8.18 percent of the region was a very high hazard. The results of landslide hazards were verified based on the locations of previous landslides obtained from field studies of the study area.

Park et al. (2013) researched and developed a hydrogeological model and an infinite slope model using GIS to evaluate the shallow landslide susceptibility in Korea. The input parameters used in this model consist of soil properties, such as cohesion and friction angle, and spatial parameters like the depth of initial pore water pressure. The resulting landslide inventory map was used to validate the results obtained from the prior analysis. The probability proved that the prediction is perfect compared to previous landslide data. Furthermore, the results revealed the accuracy of predicting shallow landslide susceptibility and its dependence on suitable consideration and understanding.

Chen et al. (2013) developed a GIS-based Logistic Regression model to assess landslide hazards at the Alishan Forestry Railway, Taiwan. The factors related to landslide incidents in the study area included the geology, topographic aspect, terrain roughness, profile curvature, distance to the river, and rainfall for various durations. The final results of the landslide hazards map were divided into four classes: ‘low hazard’, ‘medium hazard’, ‘high hazard’, and ‘very high hazard’. As a result, areas most prone to landslides were classified as ‘high hazard’. These results aided planners and engineers in taking the appropriate measures for the reconstruction of the railway of the Alishan Forestry, after the Typhoon Morakot damage.

Within the last decade, Pardeshi et al. (2013) developed a GIS and remote sensing technique to evaluate landslide hazards. The data used in Pardeshi’s techniques are derived from aerial photographs and high-resolution satellites. The final results of this study showed that the main factor responsible for

the frequent occurrence and size of landslides was heavy rainfall. This study also showed that similar techniques can not only detect or monitor landslides but can predict landslides in the future.

Raia et al. (2014) adapted the TRIGRS approach to predict landslides in Mukilteo, Washington, USA. In their TRIGRS model, researchers used a probability approach to calculate the FS for each pixel. Additionally, the TRIGRS model was able to utilize GIS to identify the entire behavior of a slope. Therefore, TRIGRS is determined to be a high-quality model for predicting landslides.

In a part of the Upper Tiber River Basin area in Central Italy, Alvioli et al. (2014) applied the TRIGRS model to predict landslide susceptibility and the corresponding characteristics of slope stability/instability that results from rainfall. The outcomes of the study conducted by Alvioli concluded that TRIGRS is capable of reproducing the frequency of the terrain patch size. The model matched the statistics for frequency size and predicted that the terrain was unstable in the area. The results presented by Alvioli et al. (2014) demonstrated the mechanisms that lead to increase the properties of landslide scaling.

Kritikos et al. (2014) developed a GIS approach (Fuzzy logic method) to create shallow landslide susceptibility maps of New Zealand. A key factor that can affect a slope's failure is heavy rainfall. Besides rainfall, there are several parameters evaluated in this technique, such as slope angle, slope aspect, lithology, stiffness of the soil, and proximity to faults and drainage networks. The final results produced three maps which assessed landslide hazard levels. These maps assisted planners and engineers in land use planning, and in the mitigation and prevention of hazardous landslides.

Musinguzi et al. (2014) developed a GIS-based analysis model to evaluate landslide risk in Uganda. The main technique used in the analysis was DEM. The data used in this technique was precipitation, soils, cover for vegetation, and population. This data was collected from several different sources, including literature reviews and expert proposals. The final results produced a map illustrating the landslide hazards in Uganda. It is noted that the map shows that landslides are concentrated in regions consisting of clay soil, high slopes, and heavy rainfall. After synchronizing the risks of landslide regions with the occurrence of recent landslides, Musinguzi found that there is a strong need to utilize GIS techniques in the management of natural disasters in Uganda.

Ahmed et al. (2014) adopted the GIS technique by using weighted overlay and fuzzy logic techniques to produce landslide hazard maps in Indus. Datasets used in this technique were divided into two groups: 1) environmental risk with respect to slope angle, slope aspect, elevation, lithology maps and, 2) the main factors causing landslides such as rainfall and seismic activity. The final results verified

the location of landslides previously recorded in the study area. The main results obtained from this study in the mountainous regions of Indus, analyzed landslides by using unique means and techniques in order to reduce costs.

Gaprindashvili et al. (2014) applied the GIS technique (using the hazard index formula) to evaluate landslide hazards in Georgia. The main factors that caused landslides in the study area included rainfall, seismic activity, erosion and weathering, ground water table effects, and human activities. Using local data, topographic and geological and historical landslide maps were created in GIS. The main factors causing landslides include slope, aspect, geomorphology, lithology, land-use, and depth of soil. This data was used in GIS with certain weight applied according to their impact on the occurrence of landslides. The final results of the analysis determined that 34.13 percent of the residential buildings were within high risk, and the land use of government and private zones were within the same risk zone by 39.9 percent and 40.9 percent respectively. Planners can take advantage of these results to reduce human and property losses.

Arunkumar et al. (2014) used the GIS system (spatial analysis tools) to find a relationship between the quantity of rainfall and areas prone to landslides along the Udhagamandalam–Mettupalayam Highway, Tamilnadu. This study is based on the Institution of Water Studies rainfall data for the period of 2003 to 2012. This data was interpreted and analyzed on an annual and seasonal basis, using GIS, then - correlated with landslide locations. The final results illustrated that the landslide that occurred in the Coonoor and Wellington region, was due to high rainfall, and the landslides evident in the Kotagiri and Ooty region were a result of moderate rainfall.

Rajamohan et al. (2014) developed a method using GIS (ranks and weights method) and remote sensing technology to find out the main reasons for landslide occurrence in India, especially in the western part of the Kodaikanal Rjon region. The collected landslide data revealed that over the past 10 years, 35 out of 66 landslide events, in the Kodaikanal region, were influenced by heavy rainfall. The hills located in the Kodaikanal area, tend to be more susceptible to weathering processes that increase the probability of sliding when exposed to large amounts of rainfall. For this reason, landslide occurrence in this region is high. There were other factors used in the analysis of landslide occurrence, in addition to rainfall including slope, geology, geomorphology, faults, drainage system, land use, and land cover. The final landslide hazard maps enabled planners to take the necessary measures to reduce the occurrence of these landslides, and thus prevent human and material losses in the Kodaikanal hills area.

Saleh et al. (2015) used GIS technologies (weight and combine dataset) to determine landslide risk zones in Southeastern Sinai, Egypt. The key factors triggering landslides in their study area were

heavy rain-falls, seismic events, elevation, steep slopes, and the structure of the rock. Soil and rock movement occurred as a result of landslides, in various forms in this study area, including rock fall, toppling, rock debris flow, and sliding. The final map depicted landslide risk zones segregated into three classes: 'very high risk', 'high-risk', 'moderate risk'. The final results made it easier for hazard management planners and engineers to assess, reduce, and mitigate the landslide hazards.

Eshaghi et al. (2015) used GIS (a multivariate regression model) to generate a landslide susceptibility map in Iran. There are several factors used in GIS models that have led to the occurrence of landslides in the study area including an amount of rainfall (annual rainfall ranges from 329 to 1278 millimeters), lithology, distance from the river, roads, and fault, elevation, land-use, and slope angle. According to the final results of the analysis, the landslide susceptibility maps were classified into the following, 'very low susceptibility', 'low susceptibility', 'medium susceptibility', 'high susceptibility', and 'very high susceptibility'. The final landslide susceptibility map was verified and found to have a high correlation between previous landslides and the landslide susceptibility map generated using GIS.

Jana et al. (2015) used the weighted overlay analysis technique in GIS and remote sensing data to produce landslide hazard maps in Papua New Guinea. The main factors considered during this study include rainfall, slope, soil type, geological, geomorphologic terrain, land use, and land cover. The final results of the analysis are classified into five classes: 'low hazard', 'medium hazard', 'medium to high hazard', 'high hazard', and 'very high hazard'.

In Penang Island, Khodadad et al. (2015) used the GIS technique by (analytical hierarchy process (AHP)) to identify and classify the probability of ground failure by creating hazard landslide maps. These maps were created based on seven important factors: rainfall, slope, distance to roads, rivers, and faults, lithology, land use, and land cover. The annual rainfall data collected from the three major climate stations in the study area were interpolated using the Inverse Distance Weighting (IDW) method in ArcGIS software. The final results of the analysis classified landslide susceptibility into five classes: 'very high', 'high', 'moderate', 'low', and 'very low'. The results also demonstrated that 75 percent of the landslides located in the areas, which have 'very high' and 'high' susceptibility.

Sarma et al. (2015) used GIS and the TRIGRS model to evaluate landslide susceptibility and hazard in the Guwahati region. All indicators and studies emphasize that previous landslides that had occurred in the study area are concentrated in the hills due to a high slope, and also due to heavy rainfall. The input dataset used in these models included hydrogeological data, soil characteristics, rainfall, and topography. The final results computed the safety factor values associated with landslides: a safety factor

less than one (FS < 1) is unstable, and a safety factor greater than one (FS > 1) is stable. These results helped establish appropriate solutions to the problems of landslides in the Guwahati region.

From the literature review presented above, it can be concluded that numerous studies on GIS-based assessment of landslides induced by rainfall were conducted in the past years and decades. However, none of these studies dealt with the GIS-based analysis of landslide susceptibility induced by rainfall in the sensitive marine clays, in the Ottawa region. This research gap and need will be addressed in this thesis.

2.6 Literature Review on Previous Studies of GIS Based Assessment of Landslide Susceptibility, Hazards, or Risks Induced by Snowmelt.

There is a paucity of GIS based modeling studies of landslides induced by snowmelt. Relevant past studies are discussed below.

Gorsevski et al. (2000) used GIS (multivariate normal probability plot) to predict landslide hazard in the Clearwater National Forest. Environmental information included slope, aspect, elevation, profile, plan, and tangential curvature, area of upslope, and flow path, and. The triggers analyzed for mass failure (landslides) in the study area were snowmelt, heavy rainfall, and flow from the High River during the winter of 1995-1996. Data on landslides of the study area has been derived from the interpretation of aerial photographs and field inventory together. The final results map classifies the landslide hazards into three classes: ‘landslide’, ‘low hazard’, and ‘high hazard’.

Hofmeister et al. (2002) used GIS to create a map of the landslide hazards in Western Oregon. The study area is prone to landslides largely as a result of the rapid melting of snow as well as the earthquakes and volcanoes. The final results were checked and compared to the field data and the information recorded related to previous landslides within the study area. The final maps illustrated the areas that are more prone to landslide occurrence due to their proximity to the mouth of a channel or steep slopes. In other words, the landslide hazard is largely concentrated across Western Oregon due to its mountainous regions (steep slopes), in addition to the few drainage channels.

Ayalew et al. (2004) developed a GIS model to create a landslide susceptibility map in the Tsugawa area of the Agano River based on the analysis of the spatial database collected for 791 landslides. Landslides occurred in the study area as a result of exposure to large amounts of snow and rainfall, in spite of the existence of dense vegetation. Six factors were used in this GIS analysis including lithology, slope, aspect, elevation, and plan and profile curvatures.The study results determined that

landslides in mid-slopes within the study area were composed of weak rocks (e.g. sandstone, mudstone, tuff).

Meusburger (2010) used GIS, a logistic regression model, and remote sensing technique to evaluate the risk of soil erosion as a result of landslides and sheet erosion in the Urseren Valley (Central Swiss Alps). Processes related to soil erosion in this research focused on soil erosion by water (sheet erosion) and gravity (landslides). The main factors triggering landslides and sheet erosion included heavy rainfall, snowmelt, steep slope, earthquakes, man-made activities, changes in landuse, and water seepage. In the study area, it was observed that the snowmelt causes slope failures because it was transported and separated from the soil materials, leading to the movement of soil slopes downhill. The data collected and mapped, was based on the interpretation of air photography and satellite images. The authors showed that the GIS and remote sensing techniques can be applied in areas often inaccessible in Alpine regions, yet prone to slope failure. The final results can be used by planners to avoid the risk of soil erosion and landslides in Alpine regions.

Wang et al. (2012) used the GIS-based limit equilibrium stability analysis model to calculate the probability of landslide hazards in Minamata–Hougawachi. There are many natural events that can be triggered and induce landslide occurrence. The events considered during this study included heavy rainfall and snowmelt for long duration, or an earthquake. The analysis process was not limited to finding a relationship between landslides and the factors that cause them, but also to better predict future landslides and evaluate their risks. The final results included predicted landslide risk maps. Their results suggested appropriate measures to reduce and mitigate future landslide damage in the study area.

Othman and Gloaguen (2013) predicted the locations and size of landslides were anticipated due to rapid snowmelt near Kurdistan. (Northeastern Iraq). In addition to snowmelt, several other natural factors have caused landslides. Those considered in this study include precipitation, rugged topography, homogeneous geology, and geomorphology. The Dukan Lake dam construction operations also contributed toward increasing the probability of landslide in the study region. Data was processed using ArcGIS10 and R (programming language) for statistical analysis. The final results could accurately evaluate the risk of landslides with an accuracy of 92.7 percent.

Khezri et al. (2013) used multivariate analysis models (logistic regression modeling) in GIS to create a landslide susceptibility map in the province of West-Azerbaijan in Iran. The key factors considered in their analysis which led to the landslides included precipitation, slope, aspect, elevation, distance to road, drainage network, and fault, land use, and geological properties. Khezri et al. also considered the particularly sudden snow melting as a controlling factor, which could trigger mass water

movements, thus increasing underground hydrostatic levels, and thus, the pore water pressure. Note that the melting of snow increases the groundwater table in the soil, which increases the probability of a slope failure. The calculated risk of landslides were ranked into five classes: 'very low', 'low', 'moderate', 'high', and 'very high' risk. Each class covers an area of95.46 square kilometers, 100.46 square kilometers, 46.1 square kilometers, 158.38 square kilometers, and 120.96 square kilometers, respectively.

Federico et al. (2014) implemented GIS and the integrated hydrological–geotechnical (IHG) model to analyze and predict landslide hazards over a large area in Liguria, Italy. The researchers found that the rainfall and snowmelt were the major factors of landslide occurrence in the study area. Their GIS technique utilized various data, such as soil, slope, geotechnical parameters (like cohesion and friction angle), and hydraulic parameters (like the water table level). The final outcomes were validated. The study results offered adequate information related to landslides and their correlation to the seasonal period of rainfall and snowmelt. The authors concluded that GIS is a tool that can be employed by planners in monitoring and managing land use to mitigate the risks associated with landslides.

Arifianti et al. (2014) used GIS tools and the weight of evidence method to create a map of landslide susceptibility in the Cianjur Regency, in West Java, Indonesia. This study was required for remote sensing data, to create a database for landslide inventory, field surveys, geotechnical parameters, groundwater table, and failure depth. The key factors triggering landslides used with the GIS tool includes precipitation (rainfall/snowmelt), slope angle, slope aspect, elevation, and distance from drainage or lineament, lithology, and land use/land cover. The final result classified the ratio of susceptibility of landslide in the study area into four classes: high (greater than 70 percent), moderate (ranging from 15 to 70 percent), low (between 5 to15 percent), very low (between 0 to 5 percent). The verification of the final outcome was evaluated based on historic landslides in the study area, which confirmed the GIS tool as a good way to estimate landslide susceptibility. The tool developed can be adopted by planners to prevent or mitigate the damage caused by the landslides.

From the literature review presented above, it can be concluded that only few studies on GIS-based assessment of landslides induced by snowmelt were conducted in the past years and decades. Furthermore, none of these studies dealt with GIS-based analysis of landslide susceptibility induced by snowmelt in the sensitive marine clays, in the Ottawa region.

2.7 Conclusion

Sensitive clays are some of the most problematic soils due to their variable characteristics. For example, clays are subject to sudden loss of shear strength due to a disturbance or an increase in moisture content. These sensitive clays are common in various parts of the world, especially northern countries like Canada (e.g., Ottawa), Sweden, Norway, and America's Alaska, that were previously covered by glaciers (Brand & Brenner 1981). These sensitive clays are prone to landslides.

In the past decades, the geographic information system (GIS) model has become an important tool for landslide susceptibility assessment and mapping, mainly due to its ability to offer various functions that include the handling, processing, analyzing, and reporting of geospatial data. Landslide susceptibility assessment based on expert evaluation and statistical approaches can be successfully done in a GIS environment. With regards to the TRIGRS method, it has been found that the use of probability distribution functions is more accurate at predicting shallow, rainfall-induced landslides than the original TRIGRS method. This was determined by measuring various metrics used to determine instability conditions, and comparing the results to landslide maps depicting recent rainfall or snowmelt induced landslides.

The literature review of previous studies on GIS-based assessment of landslide susceptibility has shown that no study was carried out to assess the landslide susceptibility (induced by rainfall or snowmelt) in the Ottawa sensitive marine clay by using GIS and TRGRIS. This gap of knowledge will be addressed in the following chapters of this thesis. This research gap and need will be addressed in this thesis.

2.8 Reference

A Risk management standard © Published by AIRMIC, ALARM, IRM (ARMS), 2002. https://www.theirm.org/media/886059/ARMS_2002_IRM.pdf.

Ahmed, M.F., Rogers, J.D. and Ismail, E.H., 2014. A regional level preliminary landslide susceptibility study of the upper Indus river basin. Eur. J. Remote Sens, 47, pp.343-373.

Akbar, T.A. and Ha, S.R., 2011.Landslide hazard zoning along Himalayan Kaghan valley of Pakistan—by integration of GPS, GIS, and remote sensing technology. Landslides, 8(4), pp.527-540.

Akgun, A., Kıncal, C. and Pradhan, B., 2012. Application of remote sensing data and GIS for landslide risk assessment as an environmental threat to Izmir city (west Turkey). Environmental Monitoring and Assessment, 184(9), pp.5453-5470.

Alvioli, M., Guzzetti, F. and Rossi, M., 2014. Scaling properties of rainfall induced landslides predicted by a physically based model. Geomorphology,213, pp.38-47.

Andrews, J. T., 1986. The pattern and interpretation of restrained, post-glacial and residual rebound in the area of Hudson Bay. Geological Survey of Canada Paper 49-62.

Arifianti, Y., Triana, Y.D., Ika, W., Irawan, W. and Suantika, G., 2014.The aplication of landslide inventory data base of Indonesia (LIDIA) for supporting landslide susceptibility mapping in Cianjur Regency, west Java, Indonesia. GSTF Journal of Geological Sciences (JGS), 1(2).

Arunkumar, M., Gurugnanam, G., Isai, R., Suresh, M., 2014. Geospatial technology based rainfall precipitation assessment with landslides in Udhagamandalam – Mettupalayam highway, Tamilnadu. International Journal of Recent Scientific Research Vol. 5, Issue, 8, pp.1506-1508.

Ayalew, L., Yamagishi, H. and Ugawa, N., 2004. Landslide susceptibility mapping using GIS-based weighted linear combination, the case in Tsugawa area of Agano River, Niigata Prefecture, Japan. Landslides, 1(1), pp.73-81.

Aylsworth, J.M., and Hunter, J.A., 2004. A geophysical investigation of the geological controls on landsliding and soft deformation in sensitive marine clay near Ottawa.57TH Canadian Geotechnical Conference.5th Joint Cgs/Iah-Cnc Conference. Geological Survey of Canada, Ottawa, Ontario, Canada

Baker, G.H., 2005. A vulnerability assessment methodology for critical infrastructure sites.

Barredo, J. I. ,Hervás, J. Lomoschitz, A., Benavides, A., Westen, C. v. 2000. Landslide hazard assessment using GIS and multicriteria evaluation techniques in the Tirajana basin, Gran Canaria Island. European Commission - Joint Research Centre, University of Las Palmas de Gran Canaria.

Baum, L., Savage, W.Z. and Godt, J.W., 2008. TRIGRS-a Fortran program for transient rainfall infiltration and grid-based regional slope-stability analysis, version 2.0, US Geological Survey Open-File Report 2008–1159, available at: http://pubs. usgs. gov/of/2008/1159.

Baum, R.L., Savage, W.Z. and Godt, J.W., 2002. TRIGRS—a Fortran program for transient rainfall infiltration and grid-based regional slope-stability analysis. US geological survey open-file report, 424, p.38.

Benjumea, B., Hunter, J.A., Aylsworth, J.M. and Pullan, S.E., 2003. Application of high-resolution seismic techniques in the evaluation of earthquake site response, Ottawa Valley, Canada. Tectonophysics, 368(1), pp.193-209.

Bhutia, S. L., Pradhan, R. Ghose, M.K., 2015. A survey on landslide susceptibility mapping using soft computing techniques. IOSR journal of applied geology and geophysics. e-ISSN: 2321–0990, p-ISSN: 2321–0982.Volume 3, Issue 1 Ver. I, PP 16-20. www.iosrjournals.org.

Bilaşco, Ş., Horvath, C., Roşian, G., Sorin, F. and Keller, I.E., 2011. Statistical model using GIS for the assessment of landslide susceptibility. Case-study: The Someş Plateau. Rom J Geogr, 2, pp.91-111.

Bordoni, M., Meisina, C., Valentino, R., Bittelli, M. and Chersich, S., 2014.From slope-to regional-scale shallow landslides susceptibility assessment using TRIGRS. Natural Hazards and Earth System Sciences Discussions, 2, pp.7409-7464.

Bui, D.T., Pradhan, B., Lofman, O., Revhaug, I. and Dick, Ø.B., 2013. Regional prediction of landslide hazard using probability analysis of intense rainfall in the HoaBinh province, Vietnam. Natural hazards, 66(2), pp.707-730.

Capacity Building in Asia using Information Technology Applications (CASITA) 2000, Model 2, http://www.adpc.net/casita/course-materials/Mod-2-Hazards.pdf.

Carrivick, J.L. and Tweed, F.S., 2013. Proglacial lakes: character, behaviour and geological importance. Quaternary Science Reviews, 78, pp.34-52.

Chau, K.T., Sze, Y.L., Fung, M.K., Wong, W.Y., Fong, E.L. and Chan, L.C.P., 2004. Landslide hazard analysis for Hong Kong using landslide inventory and GIS. Computers & Geosciences, 30(4), pp.429-443.

Chen, H.X., Zhang L.M., GaoL., Zhu H., Zhang S. 2015. Presenting regional shallow landslide movement on three-dimensional digital terrain. Engineering Geology 195:122-134.

Chen, S.C., Chang, C.C., Chan, H.C., Huang, L.M. and Lin, L.L., 2013.Modeling typhoon event-induced landslides using GIS-based logistic regression: a case study of Alishan Forestry Railway, Taiwan. Mathematical Problems in Engineering, 2013.Crovelli, R.A., 2000. Probability models for estimation of number and costs of landslides. Reston, VA: US Geological Survey.

Dahal, R.K., Hasegawa, S., Nonomura, A., Yamanaka, M., Masuda, T. and Nishino, K., 2008. GIS-based weights-of-evidence modelling of rainfall-induced landslides in small catchments for landslide susceptibility mapping. Environmental Geology, 54(2), pp.311-324.

Dai, F.C., Lee, C.F. and Ngai, Y.Y., 2002. Landslide risk assessment and management: an overview. Engineering geology, 64(1), pp.65-87.

Dohare E., D., Vaghela E.,G.,R. 2014. Management, Modelling & Maintenance of water and wastewater using GIS- a review. International Journal of Engineering Sciences & Research Technology. ISSN: 2277-9655, 3(12).

Eden W. J. and Crawford. B., 1957. Geotechnical Properties of Leda Clay in the Ottawa Area. Soil Mechanics Section, Division of Building Research, Ottawa, Canada.

Eshaghi, A., Ahmadi, H., Motamedvaziri, B. and Samani, A.N., 2015, July. A GIS-based statistical model for landslide susceptibility mapping: A case study in the Taleghan watershed, Iran. In Biological Forum (Vol. 7, No. 2, p. 862).Research Trend.

Federici, B., Bovolenta, R. and Passalacqua, R., 2015. From rainfall to slope instability: an automatic GIS procedure for susceptibility analyses over wide areas. Geomatics, Natural Hazards and Risk, 6(5-7), pp.454-472.

Flentje, P. and Chowdhury, R.N., 2005.Managing landslide hazards on the Illawarra escarpment.

Fowze, J.S.M., Bergado, D.T., Soralump, S., Voottipreux, P. and Dechasakulsom, M., 2012. Rain-triggered landslide hazards and mitigation measures in Thailand: From research to practice. Geotextiles and geomembranes, 30, pp.50-64.

Fransham, P.B. and Gadd, N.R., 1977. Geological and geomorphological controls of landslides in Ottawa Valley, Ontario. Canadian Geotechnical Journal, 14(4), pp.531-539.

Freeman-Lynde, R.P., Hutchinson, D.R., Folger, D.W., Wiley, B.H. and Hewett, M.J., 1980.The origin and distribution of subbottom sediments in southern Lake Champlain. Quaternary Research, 14(2), pp.224-239.

Gadd, N.R., 1986. Llthofacles of Leda clay in the Ottawa basin of the Champlain sea. Geological Survey of Canada Paper 85-21.

Gaprindashvili, G., Guo, J., Daorueang, P., Xin, T. and Rahimy, P., 2014.A new statistic approach towards landslide hazard risk assessment. International Journal of Geosciences, 5(1), p.38.

García-Rodríguez, M.J., Malpica, J.A., Benito, B. and Díaz, M., 2008.Susceptibility assessment of earthquake-triggered landslides in El Salvador using logistic regression. Geomorphology, 95(3), pp.172-191.

Godt, J.W., Baum, R.L., Savage, W.Z., Salciarini, D., Schulz, W.H., Harp, E.L., 2008. Transient deterministic shallow landslide modeling: requirements for susceptibility and hazard assessments in a GIS framework. Eng. Geol. 102 (3), p. 214–226.

Gorsevski, P.V., Gessler, P. and Foltz, R.B., 2000. Spatial prediction of landslide hazard using discriminant analysis and GIS.

Guzzetti, F., Reichenbach, P., Cardinali, M., Galli, M. and Ardizzone, F., 2005.Probabilistic landslide hazard assessment at the basin scale. Geomorphology, 72(1), pp.272-299.

Hartford, D.N.D. and Hydro, B.C., 2007. Justification of risk-taking through reasoning, reasonableness and practicability. Risk Acceptance and Risk Communication (March 26-27, 2007), Joint Committee on Structural Safety, Engineering Mechanics Division, ASCE, Stanford University, Stanford, CA.

Hofmeister, R.J., Miller, D., Mills, K., Hinkle, J. and Beier, A., 2002.Hazard map of potential rapidly moving landslides in Western Oregon. Interpretive Map Series IMS-22, Oregon Department of Geology and Mineral Industries.

Hong, Y., Adler, R.F. and Huffman, G., 2007. An experimental global prediction system for rainfall-triggered landslides using satellite remote sensing and geospatial datasets. Geoscience and Remote Sensing, IEEE Transactions on, 45(6), pp.1671-1680.

Iverson, R.M., 2000. Landslide triggering by rain infiltration. Water Resource Res 36:1897–1910.

Jana, S.K., Sekac, T., Pal, D.K., 2015.Landslide hazard investigation in Papua New Guinea-a remote sensing &GIS approach. International Journal of Scientific Engineering and Research (IJSER), ISSN (Online): 2347-3878, Volume 3 Issue 3.

Jha, M.K., Chowdhury, A., Chowdary, V.M. and Peiffer, S., 2007. Groundwater management and development by integrated remote sensing and geographic information systems: prospects and constraints. Water Resources Management, 21(2), pp.427-467.

Johnston, W.A., 1917. Pleistocene and recent deposits in the vicinity of Ottawa, with a description of the soils (Vol. 101). Government Printing Bureau.

Khodadad, S. and Jang, D.H., 2015.A comparative study of Analytical Hierarchy Process and Ordinary Least Square methods for landslide susceptibility mapping using GIS technology. The Online Journal of Science and Technology, 5(2).

Kim, D., Im, S., Lee, S.H., Hong, Y. and Cha, K.S., 2010. Predicting the rainfall-triggered landslides in a forested mountain region using TRIGRS model. Journal of Mountain Science, 7(1), pp.83-91.

Kimura, T., Hatada, K., Maruyama, K. and Noro, T., 2014. A probabilistic approach to predicting landslide runout based on an inventory of snowmelt-induced landslide disasters in Japan. International Journal of Erosion Control Engineering, 7(1), pp.9-18.

Kritikos, T. and Davies, T., 2015. Assessment of rainfall-generated shallow landslide/debris-flow susceptibility and runout using a GIS-based approach: application to western Southern Alps of New Zealand. Landslides, 12(6), pp.1051-1075.

Kumpulainen, S., 2006.Vulnerability concepts in hazard and risk assessment. Special Paper-Geological Survey of Finland, 42, p.65.

Kuthari, S. 2007. Establishing precipitation thresholds for landslide initiation along with slope characterization using GIS- based modelling. International Institute For Geo-Information Science And Earth Observation Enschede, The Netherlands and Indian Institute Of Remote Sensing (Nrsa) Dehradun, India.

Lee, S., 2005.Application of logistic regression model and its validation for landslide susceptibility mapping using GIS and remote sensing data. International Journal of Remote Sensing, 26(7), pp.1477-1491.

Li, Y., Chen, G., Tang, C., Zhou, G. and Zheng, L., 2012. Rainfall and earthquake-induced landslide susceptibility assessment using GIS and Artificial Neural Network. Natural Hazards and Earth System Science, 12(8), pp.2719-2729.

Liao, Z., Hong, Y., Kirschbaum, D., Adler, R.F., Gourley, J.J. and Wooten, R., 2011. Evaluation of TRIGRS (transient rainfall infiltration and grid-based regional slope-stability analysis)'s predictive skill for hurricane-triggered landslides: a case study in Macon County, North Carolina. Natural hazards,58(1), pp.325-339.

Lin, P.S., Lin, J.Y., Lin, S.Y. and Lai, J., 2006.Hazard assessment of debris flows by statistical analysis and GIS in Central Taiwan. Int J ApplSci Eng,4(2), pp.165-187.

Malczewski, J. 2004.GIS-based land-use suitability analysis: a critical overview. Progress in Planning 62, 3–65.Department of Geography, University of Western Ontario, London, Ont., Canada.

Meaden, G.J. and Aguilar-Manjarrez, J., 2013. Advances in geographic information systems and remote sensing for fisheries and aquaculture.

Meusburger, K., 2010. Soil erosion in the Alps: causes and risk assessment (Doctoral dissertation, University_of_Basel).

Mitchell, R.J., 1970. On the yielding and mechanical strength of Leda clays. Canadian Geotechnical Journal, 7(3), pp.297-312.

Moradi, M., Bazyar, M.H., Mohammadi, Z., 2012.GIS-based landslide susceptibility mapping by AHP method, a case study, Dena city, Iran.Journal of Basic and Applied Scientific Research 2(7)6715-672.www.textroad.com.

Mukhlisin, M., Idris, I., Salazar, A.S., Nizam, K. and Taha, M.R., 2010. GIS based landslide hazard mapping prediction in Ulu Klang, Malaysia. Journal of Mathematical and Fundamental Sciences, 42(2), pp.163-178.

Musinguzi, M. and Asiimwe, I., 2014. Application of geospatial tools for landslide hazard assessment for Uganda. South African Journal of Geomatics, 3(3), pp.302-314.

Nader, A., 2014. Engineering characteristics of sensitive marine clays-examples of clays in eastern Canada (Doctoral dissertation, Universitéd'Ottawa/University of Ottawa).

Nader, A., Fall, M., Hache, R., 2015. Characterization of sensitive marine clays by using cone and ball penetometers – example of clays in eastern Canada.Journal of Geotechnical and Geological Engineering, DOI 10.1007/s10706-015-9864-x.

Nguyen, T.D., Aoki, K., Mito, Y., Suryolelono, K.B., Karnawati, D. and Pramumijoyo, S., 2007. Landslide riskmicrozonation by using multivariate statistical analysis and GIS. International Journal of the JCRM, 3(1), pp.7-15.

Numetu R., 2005: A GIS-based slope stability analysis of the applachian and ridge province under seismic loading, PhD thesis. University of Houghton, Michmigan. Othman, A.A. and Gloaguen, R., 2013. Automatic extraction and size distribution of landslides in Kurdistan Region, NE Iraq. Remote Sensing, 5(5), pp.2389-2410.

Pardeshi, S.D., Autade, S.E. and Pardeshi, S.S., 2013.Landslide hazard assessment: recent trends and techniques. SpringerPlus, 2(1), p.523.

Park H. J., Lee J. H., Woo Ik. 2013. Assessment of rainfall-induced shallow landslide susceptibility using a GIS-based probabilistic approach. Engineering Geology 161:1-15

Park, H.J., Lee, J.H. and Woo, I., 2013. Assessment of rainfall-induced shallow landslide susceptibility using a GIS-based probabilistic approach. Engineering Geology, 161, pp.1-15.

Pascale, S., Sdao, F. and Sole, A., 2010.A model for assessing the systemic vulnerability in landslide prone areas. Natural Hazards and Earth System Science, 10(7), pp.1575-1590.

Persson, M., 2014.Predicting spatial and stratigraphic quick-clay distribution in SW Sweden.https://scholar.google.ca/scholar?q=Predicting+Spatial+and+Stratigraphic+Quick-clay+Distribution+in+SW+Sweden&btnG=&hl=en&as_sdt=0%2C5&as_vis=1

Pradhan, B. and Lee, S., 2009. Landslide risk analysis using artificial neural network model focusing on different training sites. Int J Phys Sci, 3(11), pp.1-15.

Pradhan, B., Mansor, S., Pirasteh, S. and Buchroithner, M.F., 2011.Landslide hazard and risk analyses at a landslide prone catchment area using statistical based geospatial model. International Journal of Remote Sensing, 32(14), pp.4075-4087.

Quinn, P. E., 2009. Large landslides in sensitive clay in eastern Canada and the associated hazard and risk to linear infrastructure. PhD thesis, Queen's University Kingston, Ontario, Canada.

Raia, S. M., Alvioli, M., Rossi, R.L., Baum, J.W., Godt, F., Guzzetti, 2014. Improving predictive power of physically based rainfall-induced shallow landslide models: a probabilistic approach. 1CNR IRPI, via Madonna Alta 126, 06128 Perugia, Italy.US Geological Survey.

Raia, S., Alvioli, M., Rossi, M., Baum, R.L., Godt, J.W. and Guzzetti, F., 2013. Improving predictive power of physically based rainfall-induced shallow landslide models: a probabilistic approach. arXiv preprint arXiv:1305.4803.

Rajamohan, M.R., Anand, B., Balakrishnan, P., Durai, P. and Joy Johnson, A., 2014. Landslide hazard zonation using geospatial technology in parts of Kodaikanal hill region, Tamilnadu. International Journal for Innovative Research in Science and Technology, 1(1), pp.11-17.

Rankka, K., Andersson-Sköld, Y., Hultén, C., Larsson, R., Leroux, V. and Dahlin, T., 2004. Quick clay in Sweden. Swedish Geotechnical Institute Report, 65, p.145.

Regmi, N.R., Giardino, J.R. and Vitek, J.D., 2010.Modeling susceptibility to landslides using the weight of evidence approach: Western Colorado, USA. Geomorphology, 115(1), pp.172-187.

Saha, A.K., Gupta, R.P. and Arora, M.K., 2002. GIS-based landslide hazard zonation in the Bhagirathi (Ganga) Valley, Himalayas. International Journal of Remote Sensing, 23(2), pp.357-369.

Salciarini D., Godt J.W., Savage W.Z., Pietro C., Baum R.L., Michael J.A., 2006. Modeling regional initiation of rainfall-induced shallow landslides in the eastern Umbria Region of central Italy. Landslides 3:181–194 DOI 10.1007/s10346-006-0037-0

Salciarini, D., Godt, J.W., Savage, W.Z., Conversini, P., Baum, R.L. and Michael, J.A., 2006. Modeling regional initiation of rainfall-induced shallow landslides in the eastern Umbria region of central Italy. Landslides, 3(3), pp.181-194.

Saleh, A.S. and Saleh, S.S., 2015. Geo-informatics application in determining, analyzing, evaluating and mitigating landslides hazards in the slopes of the canyon of watier valley, southeastern Sinai, Egypt. Journal of Geosciences and Geomatics, 3(1), pp.7-16.

Sarkar, S., Kanungo, D.P., Patra, A.K. and Kumar, P., 2012. GIS based landslide susceptibility mapping–a case study in Indian Himalaya.

Sarma, C.P., Krishna, A.M. and Dey, A., 2015. Landslide hazard assessment of Guwahati region using physically based models.

Shahabi, H., Ahmad, B.B. and Khezri, S., 2012. Application of satellite remote sensing for detailed landslide inventories using frequency ratio model and GIS. International Journal of Computer Science, Issues, 9(4), pp.108-117.

Sulaiman, W.N.A. and Rosli, M.H., 2010. Susceptibility of shallow landslide in Fraser hill catchment, Pahang Malaysia. Environment Asia, 3(Special Issue), pp.66-72.

Taha, A.M., 2010. Interface shear behavior of sensitive marine clays-leda clay (Doctoral dissertation, University of Ottawa (Canada)).

Taha, A.M., Fall, M., 2014. Shear behavior of sensitive marine clays - concrete interface. Journal of Geotechnical and Geo-Environmental Engineering 139(4): p. 644–650.

Tassetti, N., Bernardini, A. and Malinverni, E.S., 2008. Use of remote sensing data and GIS technology for assessment of landslide hazards in Susa valley, Italy. EARSeLeProceedings, 7(1), pp.59-67.

Thapa, P.B. and Esaki, T., 2007.GIS-based quantitative landslide hazard prediction modelling in natural hillslope, Agra Khola watershed, central Nepal. Bulletin of the Department of Geology, 10, pp.63-70.

Tilahun, T.K., 2013. The identification of quick clay layers from various sounding methods.

Tsihrintzis, V.A., Hamid, R. and Fuentes, H.R., 1996. Use of geographic information systems (GIS) in water resources: a review. Water resources management, 10(4), pp.251-277.

Vahidnia, M.H., Alesheikh, A.A., Ali mohammadi, A. and Hosseinali, F., 2009. Landslide hazard

Van Westen, C.J., Van Asch, T.W. and Soeters, R., 2006. Landslide hazard and risk zonation—why is it still so difficult? Bulletin of Engineering geology and the Environment, 65(2), pp.167-184.

Varnes, D.J., 1984. Landslide hazard zonation: a review of principles and practice (No. 3). International Association of Engineering Geology Commission on Landslides and Other Mass Movement on slopes. Published by the United Nations Educations Educational Scientific and cultural Organization.

Wang, C., Marui, H., Furuya, G., Watanabe, N., 2012. A Two-step procedure for web landslide susceptibility information system (WebLSIS).

Westen, C.V. and Terlien, M.J.T., 1996. An approach towards deterministic landslide hazard analysis in GIS.A case study from Manizales (Colombia).Earth Surface Processes and Landforms, 21(9), pp.853-868.

Wint Sandra M. E. 2004, An overview of risk, RSA (The Royal Society for the encouragement of Arts, Manufactures & Commerce), is registered in England & Wales as a charity, number 12424. http://documents.mx/documents/an-overview-of-risk.html.

Wolleb, G., Daraio, A., 2009. Regional challenges in the perspective of 2020 regional disparities and future challenges. A report to the Directorate-General for Regional Policy Unit Conception, forward studies, impact assessment.

Won, J.Y., 2013. Anisotropic strength ration and plasticity index of natural clays. In Proceedings of the 18th international conference on soil mechanics and geotechnical engineering, Paris (pp. 445-448).

CHAPTER 3

3 Study Area

3.1 Introduction

This chapter provides information about the geographical, geomorphological, geotechnical, and geological characteristics of the study region. Furthermore, this chapter will describe the climatic conditions in the study area, including rain and melting snow conditions.

3.2 Geographical and Geomorphological Characteristics

3.2.1 Location of the Study Area

The Ottawa region is located between the latitudes of 45.00 N and 45.50 N and 75.50 W to 76.00 W longitudinally. Ottawa is located in the eastern portion of the province of Ontario, Canada and contains several municipalities like Gatineau, and neighboring the city of Ottawa lies the scenic Outaouais area situated 114 meters above sea level Figure (3-1) (Gagnéa et al., 2015; Jack, 2007). Ottawa can be found in the southeast part of the province of Ontario, and the city maintains an approximate area of 2,778 square kilometers. The Ottawa region is bounded to the north by the Ottawa River, and the historic Rideau River and Rideau Canal flows from north to south across the city of Ottawa.

3.2.2 Geographic Setting and Geomorphology

Ottawa represents the southern bank of the Ottawa River, which contains the mouths of both the Rideau River and Rideau Canal. The Lower Town (older part of Ottawa City) is located between the Rideau Canal and Ottawa River. The Downtown of Ottawa City covers the area west of the canal (Jack, 2007). Although the Ottawa region consists of gentle to semi-flat slopes in most areas, the slope of the region can range from 0 to 33 degrees. Areas of high slopes are located in the western regions, and are thus more prone to landslide. Similar areas are also found in Northern Ottawa, close to the Ottawa River.

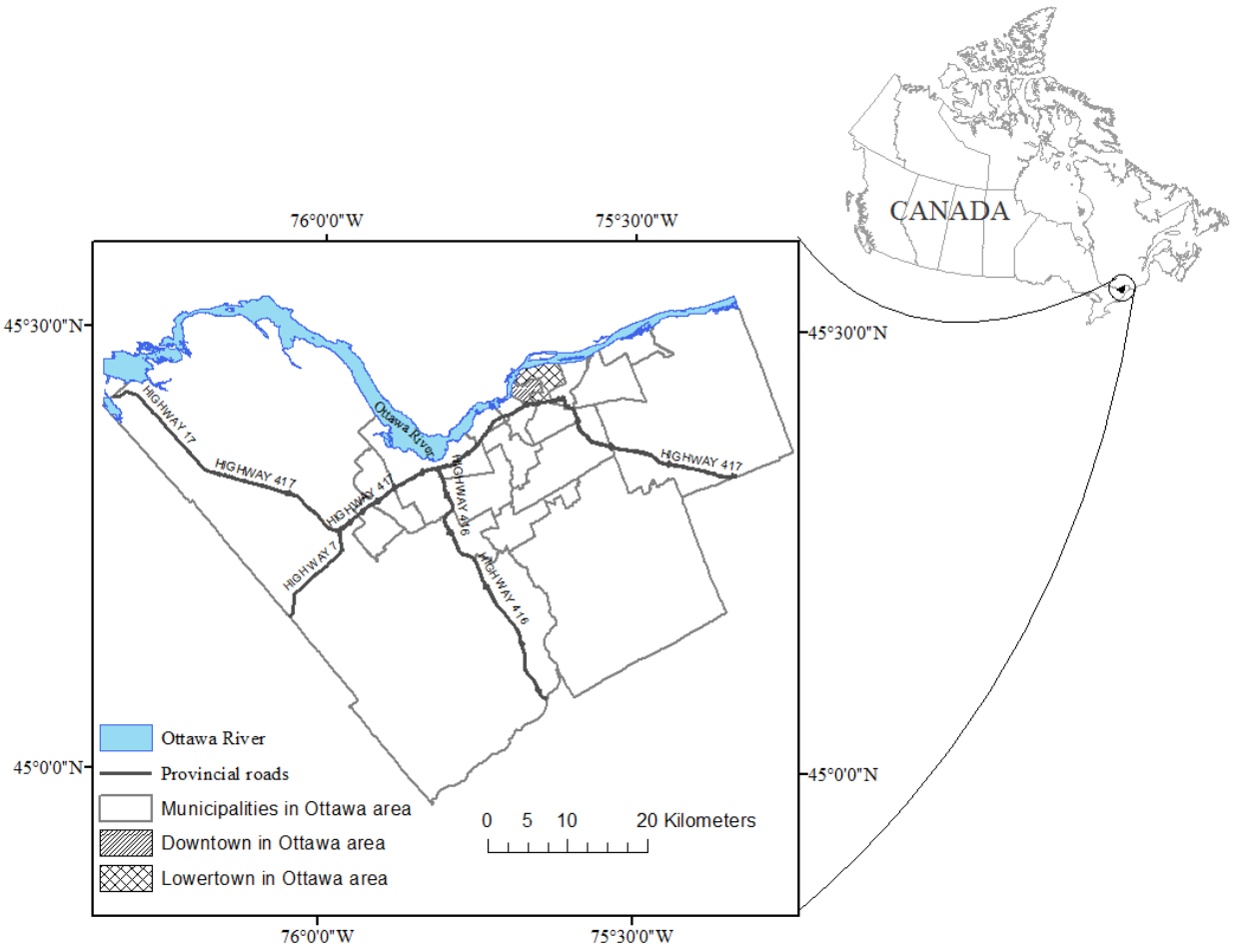

Figure 3-1 Study area (Ottawa Region)

The valley extends northwest and to the east of the city, and ends by flowing to meet the St. Lawrence River in Western Montreal (Nicholas, 2009). There are many highway networks connecting Ottawa city, the largest provincial highway is Highway 417 (also known as Queensway). Other roadway networks connecting the city include, the Ottawa-Carleton Regional Road 174 (previously called Provincial Highway 17), and Highway 416 (Veterans' commemorative highway), which connects Ottawa to the rest of the 400 Series highway network in Ontario. Highway 417 represents the Ottawa portion of the Trans-Canada Highway.

3.2.3 Physiography

Physiography is a way to determine and categorize the terrain in various regions. There are four major physiographic regions that can be noted in the Ottawa-Carleton map: the North Gower drumlin field, the Smiths Falls limestone plain, the Russell Prescott sand plains, and the Ottawa Valley clay

plains. Figure (3-2) illustrates the locations of these areas that make up the geography of Ottawa-Carleton (Nicholas, 2009; Schut and Wilson, 1987).

The western portion of the Rideau Township maintains a flat topography dominated by shallow limestone and dolomite bedrock formations. The Rideau Township is compiled from the Smiths Falls limestone plain, the greater part of Goulbourn Township, and a large fraction of Southwestern Carleton Township. Throughout the wetland regions, a few deposit fans and dispersed deposits of clay and sand still remain. The Rideau and Jock rivers are the chief drainage channels of this area (Schut and Wilson, 1987).

The North Gower drumlin field is located in the eastern half of Rideau Township and the greater part of Osgoode Township. This region consists of drumlins and till plains characterized by gently rising and falling hills creating a reasonably sloping landscape. Lower elevation areas closest to these deposits usually are composed of finer clays and silts of the Champlain Sea. In general, the deposits which are found in the lower region are not sufficiently drained (Schut and Wilson, 1987). The esker deposits surrounding the Western side of the Rideau River occur from the south to north direction. Reformulations of these deposits occur locally along the surface edge near the Champlain Sea. The ensuing topography is bordered by an esker characterized by moderate slopes and plains in various spots. Intermittent limestone plains and stream swamp deposits also arise throughout the drumlin field area (Nicholas, 2009; Schut and Wilson, 1987). The Rideau River is considered to be a major drainage canal for the region. Smaller canals nearby include the Mud and Steven Creeks in South Castor and Eastern Ottawa. However, it can be mentioned that these areas also have a high proportion of poor drainage compared to the requirements enforced by the municipal drainage network (Nicholas, 2009; Schut and Wilson, 1987). Clay plains are highly concentrated in the Ottawa Valley, occurring throughout the majority of the western regions of the valley. Likewise, Western Ottawa maintains a mixture of clay plains and bedrock uplands evident due to faulting. Similarly, Eastern, Central, and Southern Ottawa maintain a nearly homogenous border composed of clay (Nicholas, 2009; Schut and Wilson, 1987). Alternatively, the southern part of the Olden River canal and the Cumberland and Northern Osgoode Townships maintains sandy plains throughout the physiographic area. The sand deposits evident in this region were initially considered part of the early Ottawa River delta.

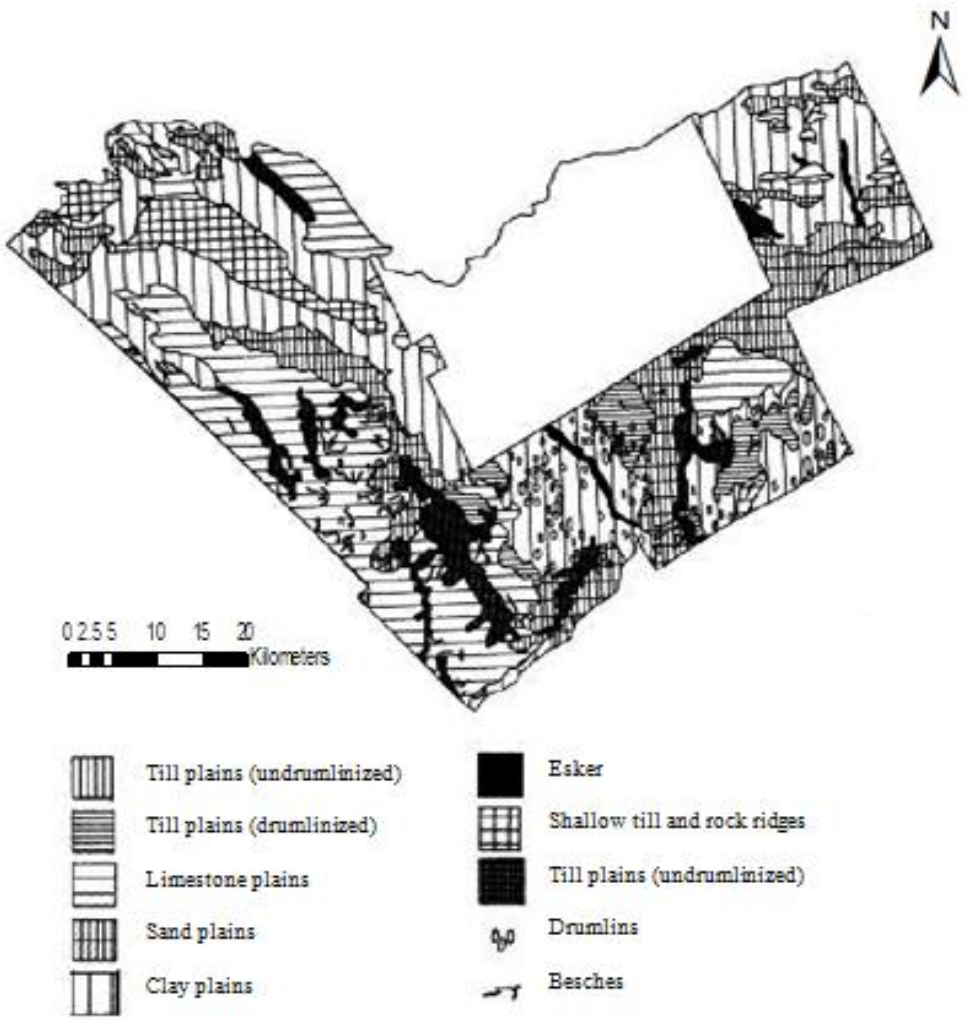

Figure 3-2 Physiography of the Ottawa-Carleton Region (modified from Schut and Wilson 1987)

3.3 Geological Characteristics of the Study Area

3.3.1 Introduction

The rocks and soils of Ottawa region have been extensively studied by geologists. The sedimentary rocks of this area mainly belong to the Paleozoic era. They cover the ancient Precambrian rocks and continue to remain exposed in the Gatineau Hills north of Ottawa. Even though they developed millions of years ago, the rock registry in the Ottawa is a small part of the geological history (Gall, 2010).

3.3.2 Geologic Overview

Typically, Ottawa region rocks are categorized based on four different eras: Cenozoic, Mesozoic, Paleozoic, and Precambrian. The earliest sediment layer in the Ottawa region consists of unconsolidated sediments that were deposited beginning in the Pleistocene at the end of the Ice Age. The sediment layer deposited throughout the Pleistocene era covers the primary Paleozoic sedimentary rocks (earliest geologic layer). The time between the age of early Paleozoic rocks and the Pleistocene layer is about 438 million years (Gall, 2010).The study area is positioned inside a physiographic area identified as the Ottawa Valley Clay Plain. This region contains a high proportion of sensitive marine silty clay deposits, characterized as relatively thick, deposited within the Champlain Sea basin subsequent to previous glaciations. Such deposits, typically occurring in Champlain Sea clay or Leda clay, begin to overlie glacial till which in turn ascends the bedrock. There are several large sedimentary rocks underlying the region including sandstones, dolostones, limestone, and shale. Additionally, silty sand covers areas of the Champlain Sea clay, and organic soils occur most often in badly drained regions (Gall, 2010; Adams, 2003). The compressibility of the sensitive marine Champlain Sea clay is one of the most important characteristics to be dealt with by projects underlined by this soil. There is a large amount of these deposits evident throughout the study area so that it will be a problem for many future projects (Gall, 2010).

3.3.2.1 Surficial Geology

Ottawa is a developed region that maintains fill deposits approximately three meters high along the region's border. These deposits often occur as either peat, sand, and clay, or glacial till, in the following sequence: 1) bedrock, 2) covered by glacial deposits, 3) soil deposits from the regression of the Champlain Sea, 4) surface soil from the Champlain Sea recession (Stantec Consulting Ltd., 2010). Based on the generalized surficial geology and prior knowledge of shear wave velocity ranges in the Ottawa region, three geotechnical units where identified: 1) late and post-glacial sediments (Leda Clay, 65 percent), 2) bedrock outcrop (20 percent), and 3) glacial sediment (15 percent) (Hunter et al. 2009) as shown in Figure (3-3).

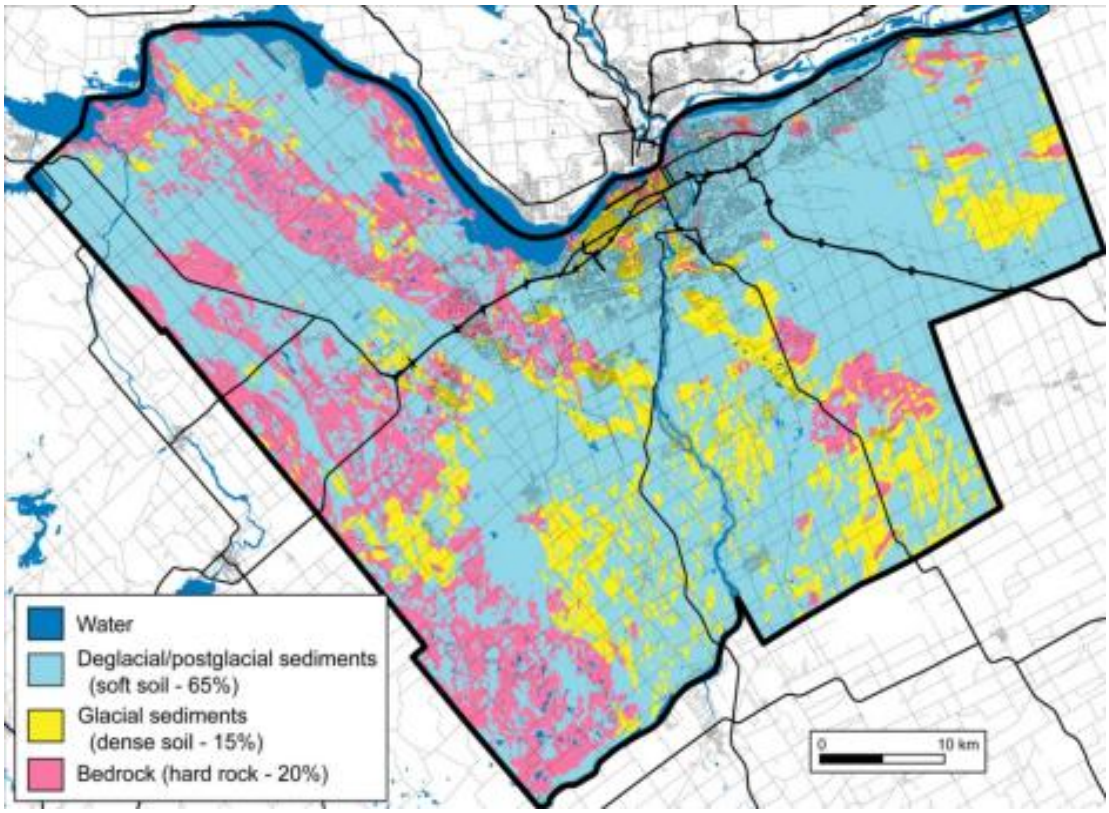

Figure 3-3 Surficial geology of the Ottawa region (CSRN 2010)

3.3.2.2 Organic Deposits/Peat

Southern Ottawa, at shallow depths, is often composed of deposits of organic material such as peat. Organic materials are often loose, excessively soft, dark brown or black, and potentially formless in shape. This organic material forms marshes in areas with poor drainage. Peat deposits usually arise beneath a stratum of fill. The fill material is often formed of variable quality and has a high percentage of organic content with moisture content in excess of 200 percent, even though it is of limited thickness (2 meters or less). Beneath the layer of the fill material, and the layer of organic material, clay soils are often present (Stantec Consulting Ltd., 2010).

3.3.2.3 Offshore Marine Clay

The offshore marine environment consists of post-glacial Champlain Sea clay close to the surface of the ground, and deposits of sand and peat lying at shallow levels below the ground. Stratigraphically, the clay is often found near the glacial till. Clay sediments are extremely fine and well arranged, and the moisture content of soil and depth define the characteristics of the clay. For example, the upper layer (1

to 3 meters deep) is often dried and weathered, forming a firm, solid crust. With depth, moisture content increases and shear strength drops, so strength is lost and the soil becomes highly compressible (Stantec Consulting Ltd., 2010; Gall, 2010).

3.3.2.4 Glacial Till

The stratum of glacial till is often located directly above bedrock and below the silty clay layer; glacial till is usually not found at shallow depths. Typically, the till mixture of sediment is homogeneous and ranges in size from clay to boulders. The composition of till can vary considerably, from silty sand to gravel to clay, cobbles, or boulders. Granular till is typically dense to very dense and considered to be a non-cohesive soil. Water content of the till can range anywhere from 10 to 30 percent. In the Ottawa region, the top of the glacial till layer contains sandy silt, silty sand, and sand (Stantec Consulting Ltd., 2010; Gall, 2010).

3.3.2.5 Bedrock Geology

According to the maps created by the Ontario Geological Survey in 1984, the Carlsbad Bedrock Formation lies beneath the entire region. This Ottawa bedrock is composed of fossiliferous calcareous siltstone, dark grey shale, and silty limestone. Depth to bedrock can be anywhere from 6 meters, in the southeast, and 14 meters, in the northeast and southern regions (Stantec Consulting Ltd., 2010; Gall, 2010).

3.4 The Geotechnical Properties in the Study Area

Geotechnical data used in the GIS model for the present study was obtained from previous geotechnical studies performed by researchers and accredited companies in the city of Ottawa (e.g., Inspec-Sol Inc, 2014; Houle Chevrier Engineering, 2013; Kollaard Associates Engineers, 2013; Trow Associates Inc., 2010; Stantec Consulting Ltd., 2010**;** Golder Associates Ltd., 2008). Soil samples were taken from different sites, which are well and densely distributed throughout the study area. All of the soil samples were visually examined in the field, logged, specified, and reported. Laboratory tests carried out on the soils provided several geotechnical parameters of the marine clay, such as hydraulic conductivity, clay fraction, specific gravity, plasticity, moisture content, unit weight, shear strength parameters, and porosity. These studies also provided alternative technical data from standard penetration tests (SPTs).

According to these studies, the lithology of the study area consisted of two layers of sensitive marine clay: 1) shallow layer of silty clay - clay, located at a depth of between 1.8 and 5.25 meters and 2) deep layer of clay - clayey silt, located at a depth of between 6.5 and 12 meters. Standard penetration tests values (SPT) of 5 to 10 blows and 5 to 20 blows were recorded for the shallow layer and the deep layer respectively. The liquid limit (LL) of the shallow layer varied from 22 to 80 percent, and the plasticity index (PI) fell between 8 and 48 percent, while at the deep layer, the liquid limit and plasticity index values ranged from 50 to 70 percent, and 28 to 52 percent, respectively. The specific gravity was found in general to be between 2.70 to 2.80 for all of the sites, as expected for clay (Houle chevrier Engineering 2013; Sorensen et al. 2013; Stantec Consulting Ltd. 2010; Trow Associates Inc. 2010; Joel 2008; Golder Associates Ltd. 2008; Catana 2006;Tan 2003). The clay fractions were determined from available hydrometer testing data from local reports. The clay fractions range between 56 and 87 percent. The reported unit weight ranges between 14 and 22 kN/m^3.The generated results agree with those reported in the literature (Taha and Fall, 2014; Quinn, 2009). Furthermore information about the geotechnical characteristics of the study area are given in the technical papers of this thesis manuscript.

Furthermore information about the geotechnical characteristics of the study area are given in the technical papers of this thesis manuscript.

3.5 Climate Condition

Ottawa has a humid continental climate, which is accompanied by large temperature changes. High temperatures are found during July, where the average daily maximum temperature is 23.5°C.

Alternatively, low temperatures occur in January with a mean daily minimum value of -16.4°C Throughout the winter season, snow and ice prevail in this region. Recently, average annual rainfall of 714 millimeters has been observed, while the average annual snowfall is 208 millimeters (Canadian Council of Professional Engineers 2008). These precipitation rates are incremental, as it has been observed that the annual rainfall in Ottawa continues to increase over the past several decades. An increase in the annual maximum 24-hour rainfall has been recorded by the Ottawa CAD station for the period of 1960 to 2004 to of 0.57 millimeters per year, as shown in Figure (3-4) (Auld et al., 2009).

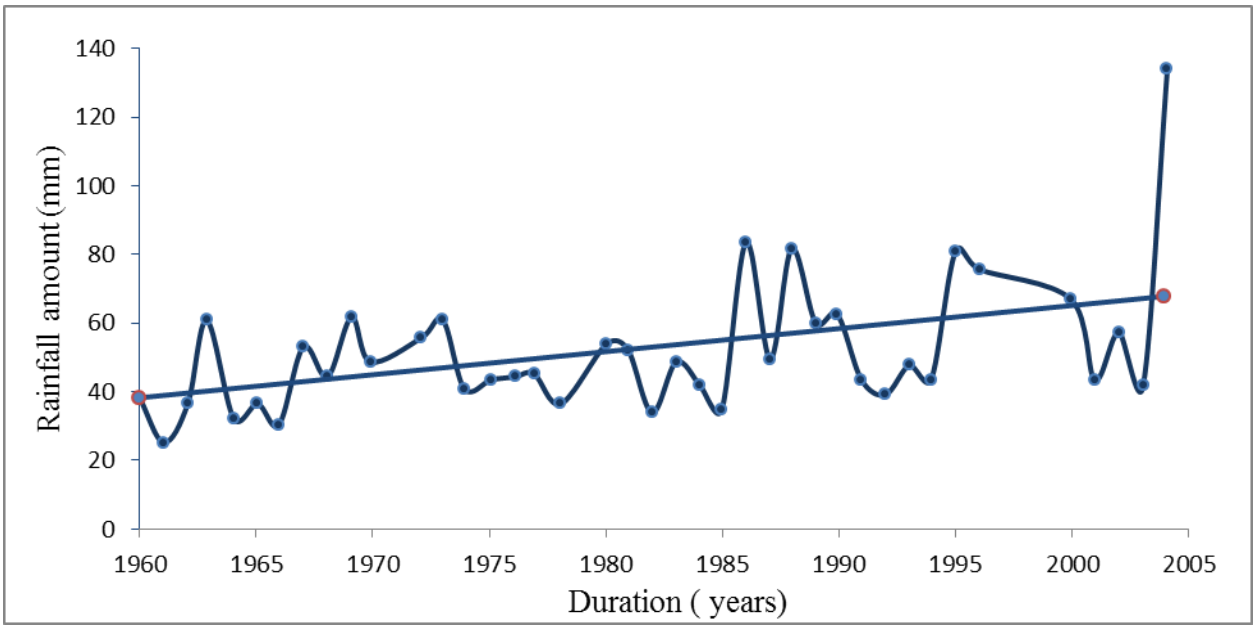

Figure 3-4 Annual maximum 24-hour rainfalls (mm), Ottawa CAD (1960 – 2004) (Modified from Auld et al. 2009).

Snow and ice prevail in this region, as snowfall can occur in Ottawa in every month of the year except July and August (see Figure (3-5)). The duration of winter and snowfall is not constant in a typical Ottawa winter. Typically, a long-lasting snow cover starts from mid-December until early April. Freeze-thaw cycles take place during the winter, causing a few days throughout the cycle to reach the freezing point, followed by nights that are well below 0°C (32°F) (EEPL, 2014). Freezing rain and high wind chills are also very common. Summers are relatively warm and humid in Ottawa, even though they are typically short in length. The cold air from the north plays an important role in reducing humidity (EEPL, 2014). Generally, the most snowfall in the Ottawa region occurs from November to March with snowfall range of 208 millimeters per annum (Auld et al., 2009). Recently, rates of rainfall and snowfall were subjected to increment. The highest extreme daily snowfall of 383 millimeters was recorded in the years 1960 and 1971.

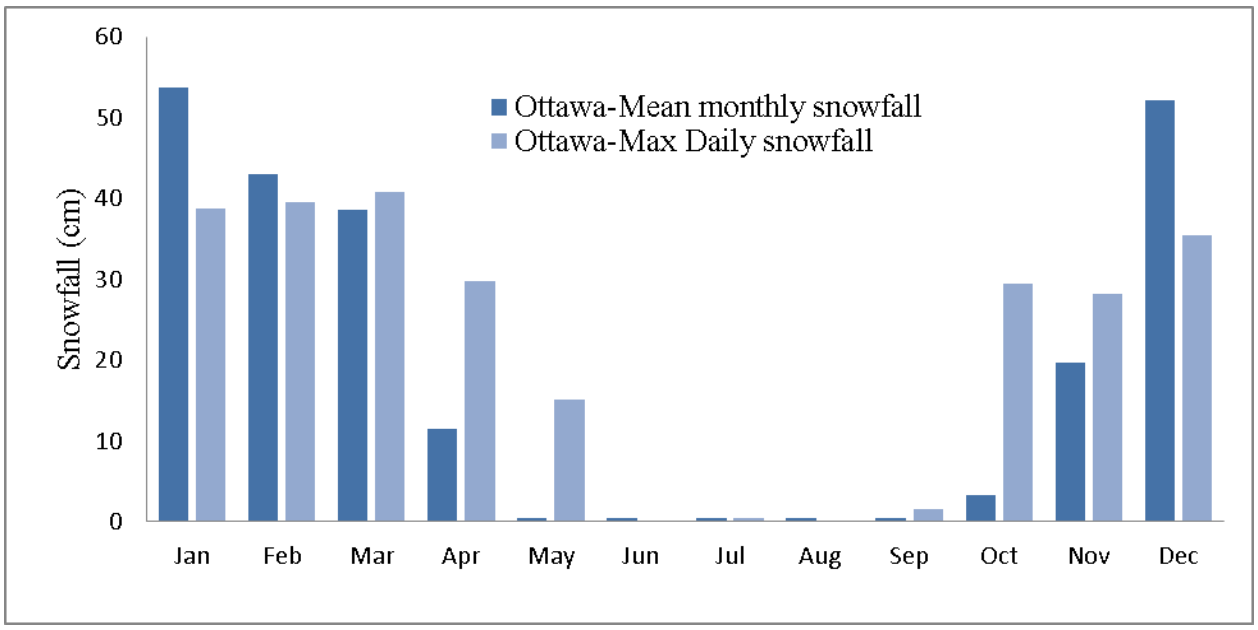

Figure 3-5 Mean monthly and maximum daily snowfalls (1981–2010), Ontario East (Modified from EEPL, 2014)

3.6 Population

According to government statistics and the city's economic profile, Ottawa growth expectations in the long term in population, housing and employment are the main factors in city planning shown in Figure (3-6).

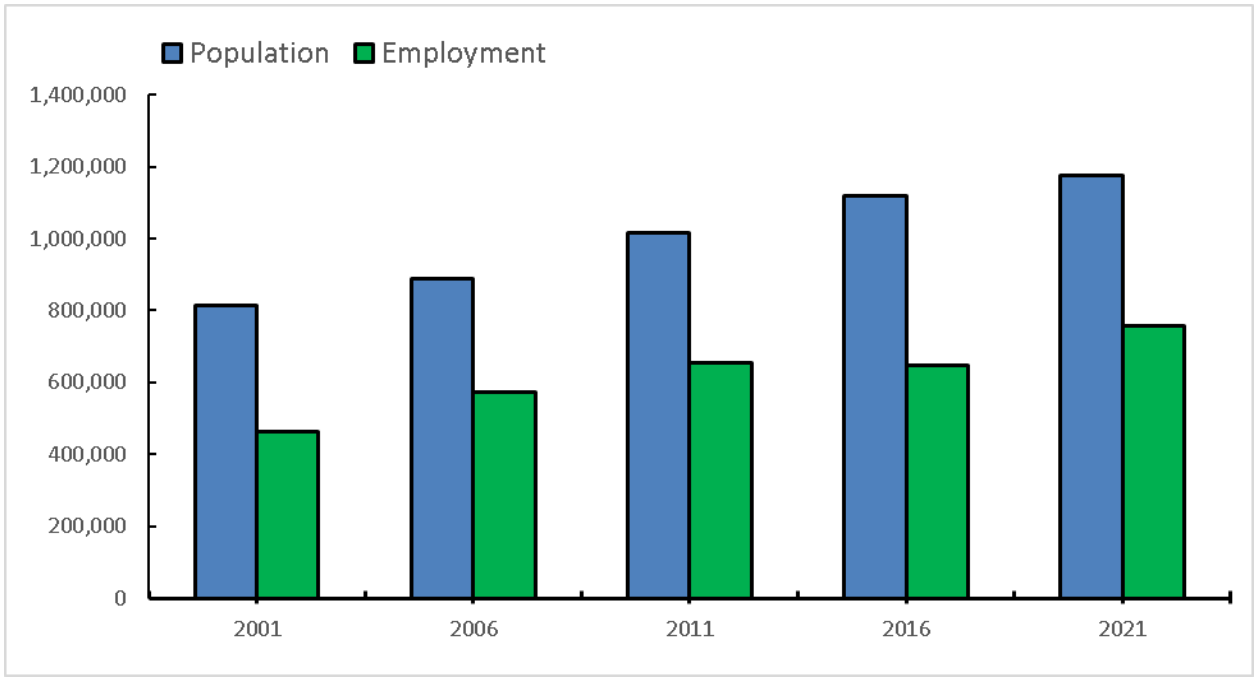

Figure 3-6 Projected population and employment growth, Ottawa, 2001-2021. (From city of Ottawa)

The city of Ottawa maintains a population of approximately 870,250, which represents an increase of 7.9 percent since 2001. Ottawa's rate of growth has been quicker than the rate of Ontario (6.2 percent) and the rate of Canada overall (4.8 percent). The population of Ottawa accounts for about two-thirds of residents concentrated in the largest Ottawa-Gatineau region, which has a collective population of 1,282,500, and is expected to continue growing. In 2003, the city was predicted to have 37 percent population growth over the next 15 years. Although initial population growth rates were slower than expected, current growth rates remain higher than the anticipated average. Immigration is considered one of the main causes of this accelerated growth which is continuously increasing and surpassing the population growth rates of Ontario or Canada (City of Ottawa 2006). From 2006 to 2011, the Ottawa population grew by 8.8 percent, or roughly twice the growth period between 2001 to 2006. If this trend continues, the population of Ottawa will exceed a million marks in 2016 (City of Ottawa, 2006)

3.7 Conclusion

Geotechnical, geological, and geographical characteristics of the study area were assessed in order to consider them in the landslide susceptibility modelling. Morphologically the Ottawa area is flat land in most regions (characterized by low slopes), yet exposed to heavy rainfall and snowfall - often leading to slope failure. The Ottawa Valley has several areas containing sensitive clays that are prone to landslides. Historical landslide data and maps are used during preliminary site investigations by the local engineer and regional planner to show areas where landslides have occurred in the past and where potential problems might occur during future land use and development. Gaining more insight into the regional stratigraphic profile, soil physics, and geological history offers a better understanding of the types of sediments and their geotechnical characteristics.

3.8 Reference

Adams, J. and Halchuk, S., 2003. Fourth generation seismic hazard maps of Canada: values for over 650 Canadian localities intended for the 2005 National Building Code of Canada (p. 155). Geological Survey of Canada.

Auld, H., Don, M., Joan, K., Shouquan, C., Neil. C., Sharon, F. 2009. Adaptation by design: climate, municipal infrastructure & buildings in the Ottawa area. Environment Canada.

Bowman, S., 2007. Sustainability assessment and the Ottawa 20/20 growth management strategy.

Canadian Council of Professional Engineers, 2008.Adapting to climate change Canada's first national engineering vulnerability of public infrastructure. Public Works and Government Services Canada and Engineers Canada.

Candian Seismic Reasearch Network (CSRN) 2010.A combined research team from Carleton University and GSC have been surveying the Ottawa to obtain site classifications.

City of Ottawa 2006. Economy and demographics, long-range financial plan III(part 1 and part 2). http://ottawa.ca/en/long-range-financial-plans/long-range-financial-plan-iii-part-1-and-part-2/economy-and-demographics

Dix, G. R, 1997. Lithostratigraphy and sequence stratigraphy of the lower paleozoic succession in the Ottawa valley. Geological Association of Canada.; Mineralogical Association of Canada.; Joint Annual Meeting, Geological Association of Canada, Mineralogical Association of Canada (1997: Ottawa, Ont.).

Fulton, R.J. and Richard, S.H., 1987. Chronology of late quaternary events in the Ottawa region. Quaternary Geology of the Ottawa Region, Ontario and Quebec. Edited by RJ Fulton.Geological Survey of Canada, Paper, pp.86-23.

Gagné, S.A., Eigenbrod, F., Bert, D.G., Cunnington, G.M., Olson, L.T., Smith, A.C. and Fahrig, L., 2015.A simple landscape design framework for biodiversity conservation. Landscape and Urban Planning, 136, pp.13-27.

Gall, Q., 2010.geology Of Ottawa Area, Ottawa - Gatineau Geoheritage project, Field trip.

Golder Associates 2007, Geotechnical investigation guidelines for development applications in the city of Ottawa Planning, Transit and Environment Department Planning Branch.

Hunter, J.A., Crow, H., Brooks, G.R.,Pyne, M., Lamontagne M., Pugin, A.,Pullan, S.E., Cartwright, T., Douma, M., Burns, R.A., Good, R. L. 2009. City of Ottawa seismic site classification map from combined geological/geophysical data. Geological Survey of Canada.

Jack, R. and Montminy, S., 2007. Rideau canal pedestrian bridge-20 years from conception to construction. In 2007 Annual Conference and Exhibition of the Transportation Association of Canada: Transportation-An Economic Enabler (Les Transports: Un Levier Economique).

Nicholas, R.A., 2009. An archaeological assessment (stages 1 & 2). Proposed Metcalfe Subdivision Andrew Simpson Drive & 8 Line Road the East Half Lot 19, Concession 7 Geographic Township of Osgoode City of Ottawa.

Schut, L.W., Wilson, E.A. and Ontario Institute of Pedology, 1987. Soils of the regional municipality of Ottawa-Carleton (excluding the Ottawa urban fringe) [document cartographique]. Le Centre

Sharma, S., Dix, G.R. and Riva, J.F., 2003. Late ordovician platform foundering, its paleoceanography and burial, as preserved in separate (eastern Michigan Basin, Ottawa Embayment) basins, southern Ontario. Canadian Journal of Earth Sciences, 40(2), pp.135-148.

Stantec 2010, Geotechnical inventory and evaluation, Johnston Road Land Use Study.City of Ottawa, Project No. 122410116 (1042983).

Wikimedia Commons, the free media repository (W.M.C.) 2014.https://commons.wikimedia.org/wiki/File:Newottawamap.png#filehistory. This page was last modified on 7 December 2014, at 18:31.

CHAPTER 4

4 Technical Paper I: GIS Based Assessment of Rainfall-Induced Landslide Susceptibility of Sensitive Marine Clays

Mohammad Al-Umar, Mamadou Fall, Bahram Daneshfar,
Department of Civil Engineering – University of Ottawa, Ottawa, Ontario, Canada

Abstract

Sensitive marine clays (also identified as Leda clay or Champlain Sea clay) cause frequent landslides in Ottawa. These landslides are often triggered by rainfall. A Geographic Information System (GIS) model is developed in order to assess and predict rainfall-induced landslides in sensitive marine clays of the Ottawa region. To assess landslide susceptibility, this approach requires topographic, geologic, hydrologic, and geotechnical information of the studied area, in addition to rainfall intensity data for different periods of time. In this study, spatial analyses are conducted by using rainfall intensity records of different durations (5 minutes, and 6, 12, 18, and 24 hours), as well as the historical data on previous landslides in the study area. The Transient Rainfall Infiltration and Grid-based Regional Slope-stability (TRIGRS) model is used in a GIS framework to investigate the influence of rainfall on shallow landslides over the Ottawa region, with respect to time and location. The assessment result maps illustrate that steep slopes of Leda clay are more prone to landslides. Furthermore, susceptibility to landslides in these areas increases with long periods of intense rainfall. The proposed GIS - based model is verified by comparing the predicted areas of landslides induced by rainfall with previous shallow landslides that occurred in the Ottawa region. The comparison results show that there is a good agreement between the predicted areas of landslides and previous landslides reported. Moreover, the results indicate that not all of the previous landslides in Leda clay are triggered by rainfall. The proposed GIS–TRIGRS combined modeling approach can therefore be considered a potential tool for assessing and predicting rainfall induced landslides in sensitive marine clays in Ottawa.

Keywords: Leda Clay, Rainfall, GIS, TRIGRS, Landslide, Sensitive Clay

4.1 Introduction

In Canada, sensitive marine clays are widely found, particularly in the Ottawa area. In the Canadian geotechnical engineering literature, sensitive marine clays are known as Leda or Champlain Sea clay. The micro-structure of the clay particles of Leda clay is arranged in an orientation that resembles a card house structure. When disturbed, the structure collapses. Upon remolding and excessive wetting, Leda clay can suddenly collapse and flow (Nader et al., 2015; Haché et al., 2015; Quinn, 2009). Landslides have therefore taken place in this type of clay in Eastern Canadian formations during the past years and decades (see Figure (4-1)) (Taha and Fall, 2014; Quinn, 2009; Fransham and Gadd, 1977).

Historically, the slopes in many municipalities around Ottawa, such as Orleans, Beacon Hill in Gloucester, and the city of Casselman, have been exposed to several landslides on the terrace slopes of Champlain Sea sediments (Leda clay) (Aylsworth et al., 1997). On the other hand, landslides have been established as a regular phenomenon of river valley growth. Most of these landslides cover a large area, and could rapidly take place without any warning. Rainfall is a primary trigger of landslides in sensitive marine clay formations, particularly in the Ottawa region (Quinn, 2009). The population of Ottawa has steadily increased to about one million. This growth has contributed to the development and construction of new infrastructure facilities, which include the construction of many residential areas, highways, pipelines, and even light rail transportation facilities in the problematic areas of sensitive marine clays. Thus, these sensitive clays which lie underneath the massive areas that cover the Ottawa region pose landslide hazards to the population and infrastructures. In the context of protecting the population and infrastructures against marine clay landslides as well as to effectively manage hazards related to shallow landslides in the Ottawa region, landslide susceptibility mapping is a valuable tool that assists in related decision making (Nader et al., 2015; Quinn, 2009).

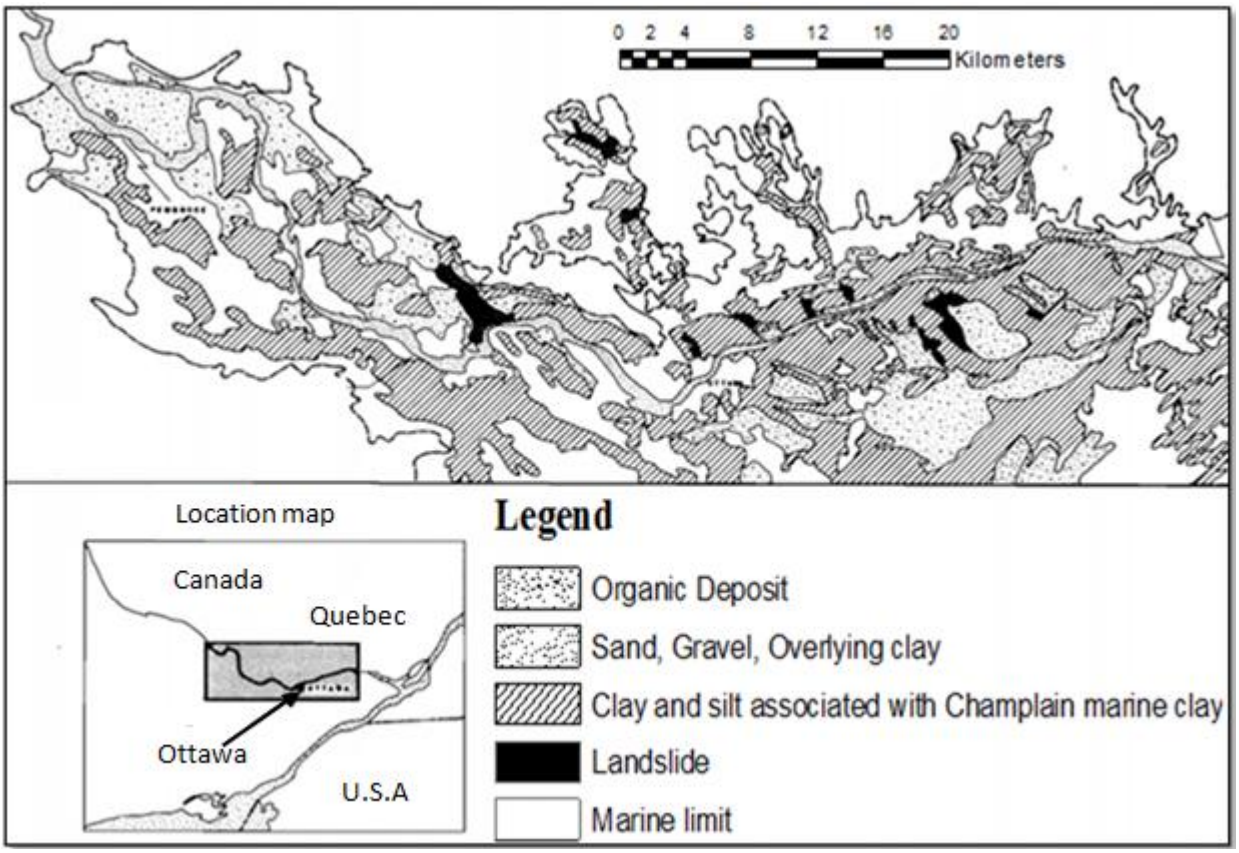

Figure 4-1 Distribution of sensitive clay and associated landslides in Ottawa Valley
Modified from Fransham and Gadd (1977).

Three types of techniques were generated to determine landslides susceptibility and areas of instability: (i) expert evaluation (inventories of past landslides, heuristic approaches); (ii) statistical approaches; and (iii) deterministic approaches (Park et al., 2013a, b; Quinn 2009; Fall et al., 2006; Fall and Azzam, 2001; van Westen et al., 1997). Landslide inventory maps highlight the position and dimensions of recorded landslides. Therefore, they are a simplified form of landslide susceptibility maps. On the other hand, a heuristic approach determines the extent of landslide hazards based on only quasi-static variables (Fall et al., 2006). Many researchers have used these approaches for the evaluation of landslide hazards, such as Fall et al. (1996), Aylsworth et al. (1997), Atkinson and Massari (1998), Guzzetti et al. (1999), and Wu and Li (2014). Nevertheless, these methods are highly subjective. In order to reduce the subjectivity, statistical methods were developed to statistically determine the various combinations of variables that could have caused previous instability events (Lee and Fei, 2015; Fall et al., 2006; Dai and Lee, 2001). Many other researchers also prefer to use statistical approaches in their work, such as Carrara et al. (1991), Carrara and Guzzetti (1995), and Atkinson and Massari (1998).

Each analysis method maintains certain strengths and limits that have been detailed in various publications (e.g., Lee and Fei, 2015; Fall et al., 2006; Dai and Lee, 2001). In the past decades, geographic information system (GIS) has become an important tool for landslide susceptibility assessment and mapping (Chen et al., 2015), mainly due to its ability to offer various functions that include the handling, processing, analyzing, and reporting of geospatial data. Landslide susceptibility assessment based on expert evaluation and statistical approaches can, and has, been successfully done in a GIS environment (Mukhlisin et al., 2010). For instance, Chung and Fabbri (1999) prepared training sets consisting of historic landslides and corresponding multi-layer spatial data from the Rio Chincina region in Colombia. The multi-layer spatial data was used to offer a unified probabilistic framework to carry out predictive modeling. The hazard at each point or pixel in the probability models that they used to predict landslide hazard was assumed to be the joint conditional probability that there will be a future landslide from (or contingent to) the information obtained from the spatial input data at the pixel (Chung and Fabbri, 1999). In their modeling, the authors provided five estimation procedures and an innovative method that is used to visualize, interpret, and confirm the prediction results. Thapa and Esaki (2007) also used GIS modeling as a quantitative technique for multivariate analysis. The analysis was performed to predict the elements of landslides and analyze related observations for various levels of risks in central Nepal. The predicted landslide susceptibility was validated and the relevance of the spatial prediction was established. They found that the occurrence and probability of slope failures are most significant with slopes that are associated with bedrock layering. Thapa and Esaki (2007) also indicated that a quantitative method effectively models landslide hazards based on spatial relevance. Their analysis showed that the reliability of the final hazard map is improved with the use of geomorphological and geological variables. Mukhlisin et al. (2010) used GIS in landslide susceptibility mapping in Malaysia, in which hazardous areas were analyzed and mapped. The hazardous areas were then classified on the landslide susceptibility maps as very low, low, medium, high, and very high hazard. The analysis outcomes were compared with the locations of historic landslides and the validated results confirmed that their model is applicable for determining landslide hazard and creating landslide hazard maps.

Similarly, GIS was utilized by Quinn (2009) to examine landslide susceptibility in the western half of the former Champlain Sea, which occupies parts of eastern Ontario and southern Quebec in Canada. All of the landslide features are located in or near areas designated as having low to moderate, or moderate to high landslide susceptibility. Moreover, the infinite slope stability model has also been incorporated into GIS to determine the spatial distribution of factors of safety (FS) within a given region

(Sorooshian et al., 2015; Quinn, 2009; Fall, 2006; van Westen et al., 1997). GIS and digital topographic data have been very helpful in assessing and evaluating the potential of landslides (Godt et al., 2008).

Furthermore, Transient Rainfall Infiltration and Grid-based Regional Slope-stability (TRIGRS), a program in FORTRAN, has been applied in some studies as a deterministic method to calculate the factor of safety (FS) with time and location (e.g., Raia et al., 2014; Park et al., 2013; Baum et al., 2008; Salciarini et al., 2006). The TRIGRS model is suitable for analyzing the susceptibility of shallow landslides. Application of models such as TRIGRS in a GIS context for landslide susceptibility assessment necessitates digital spatial topographic, geologic, and hydrologic information as well as any records of previous rainfall-induced landslides, which are vital to the model results. Such data also allows for the development of different analytical approaches (Chen et al., 2014). Some studies have combined TRIGRS and GIS to assess landslide susceptibility in different areas. For example, Raia et al. (2014) attempted to predict landslides in Mukilteo, near Seattle, Washington, USA. They adapted the TRIGRS approach to their study by modifying the model using a probabilistic Monte Carlo approach for the distributed modeling of rainfall-induced shallow landslides. The model uses a probability approach to compute the safety factor cell by cell. The TRIGRS model can use a GIS framework to analyze a slope's behavior. The TRIGRS model is physically based so site specific conditions can easily be studied and landslides predicted. Salciarini et al. (2006) used TRIGRS to model the development of rainfall-induced shallow landslides in Central Italy. In their work, the TRIGRS model was coupled with a one-dimensional analytical solution to determine the transient pore-pressure response to rainfall infiltration with an infinite-slope stability analysis. This set up was used to investigate both the timing and location of shallow landslides in response to rainfall over broad regions in a GIS framework. More details on the TRIGRS approach can be found in Park et al. (2013a, b).

There are several advantages of using a combined model of GIS and TRIGRS. For example, in the TRIGRS program, a simple infinite-slope model is used to compute the FS cell by cell, which makes the calculations more sensitive to changes in input data regardless of their size (Baum et al., 2008). By combining that with the ability of GIS to map changes for any area regardless of its size, the outcome information will be much more detailed and functional (Baum et al., 2002; 2008). Although improvements in accuracy are necessary, this module is nevertheless very useful for preliminary spatio-temporal assessments of large areas. To preserve horizontal heterogeneity, material properties, rainfall and other inputs were allowed to vary.

This program can be used together with GIS software for preparation of input grids and visualization of modeling results (Bordoni et al., 2015; Raia et al., 2014; Baum et al., 2008, 2002). Also, GIS-TRIGRS models can be used with different elapsed time to observe how the desired property (such as the safety factor) can change in parallel with input variations (i.e., rainfall intensity).

Accordingly, this study aims to develop a GIS-TRIGRS model to assess the landslide susceptibility in Ottawa sensitive marine clays triggered by rainfall and create a landslide danger map for these marine clays.

4.2 Study Area

This study deals with the Ottawa region, which is located in Eastern Ontario. The Ottawa municipality covers approximately 2,778 km² and extends from latitude of 45.00 N to 45.50 N and longitude of 75.50 W to 76.00 W Figure (4-2). Ottawa includes several municipalities and rivers as depicted in Figure (4-2). Ottawa River is located in the north of Ottawa, and the Rideau river flows from north of the city to the south (Gagnéa et al., 2015; Jack, 2007).

4.2.1 Geographic Setting and Geomorphology

Ottawa is located on the southern banks of the Ottawa River, which contains the mouths of both the Rideau River and Rideau Canal. The older-part of the city is called Lower Town, which occupies the land area between the Rideau Canal and Ottawa River. The downtown of Ottawa city is located to the west of the canal (Jack, 2007). The Ottawa region consists of gentle to semi-flat slopes in most areas. These slopes range from 0^o to 33^o. Areas of steep slopes which are located in the western region are more prone to landslides. Similar areas are also found in northern Ottawa, close to the Ottawa River.

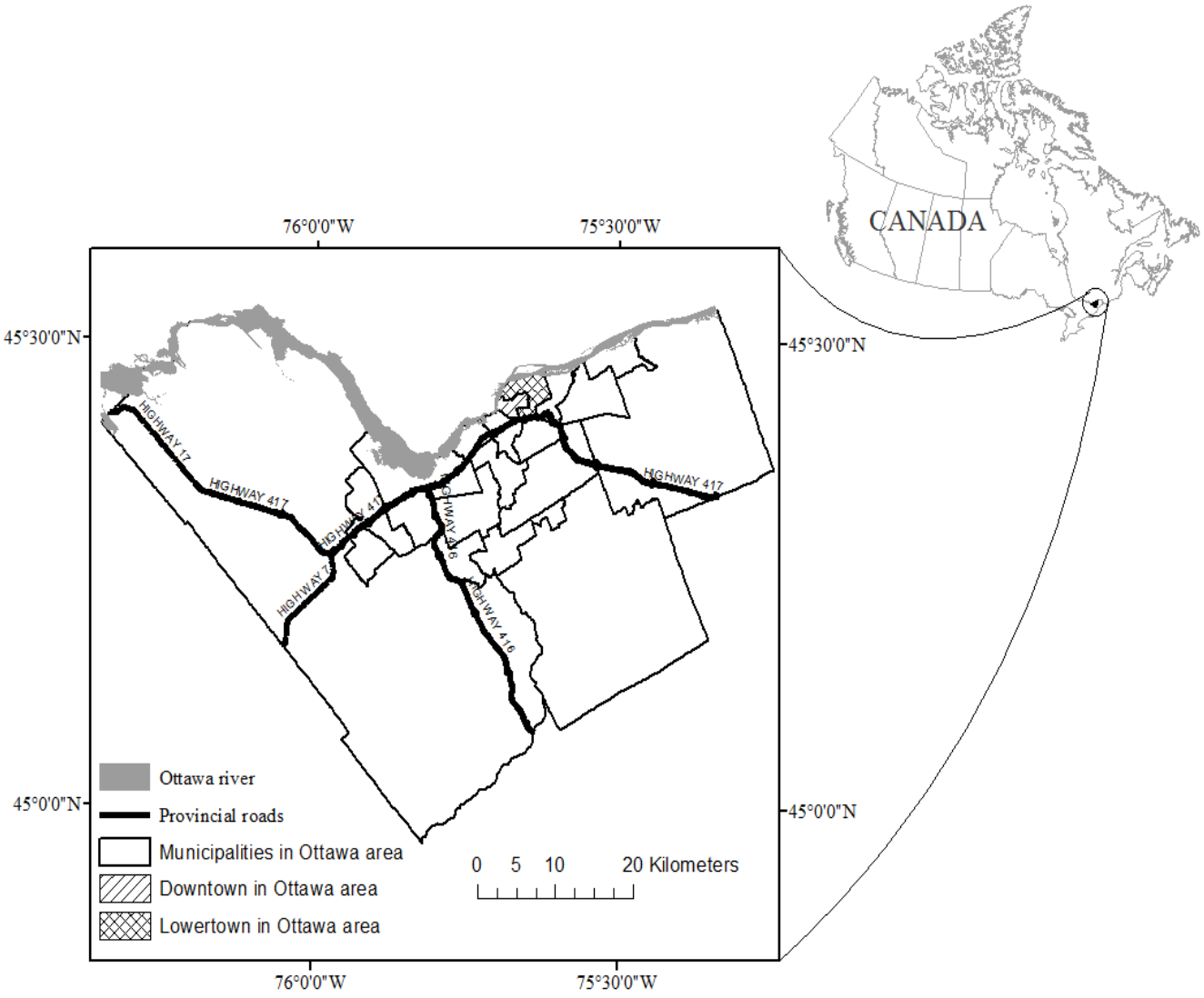

Figure 4-2 Studied area (Ottawa region).

4.3 Geological setting

The study area is positioned in a physiographic area identified as the Ottawa Valley Clay Plain. This region contains a high proportion of sensitive marine silty clay deposits, which are relatively thick and were deposited in the Champlain Sea basin after subsequent glaciations. Such deposits are defined as Champlain Sea or Leda clay. They overlie the glacial till, which in turn, overlies the bedrock (Schut and Wilson, 1987). There are many types of sedimentary rocks that are found in this region, such as sandstones, dolostones, limestones, and shale. In addition, the last deposits of silty sand locally overlie the Champlain Sea clay. Organic soils (like peat) have also been found in certain badly drained regions (Schut and Wilson, 1987). Although some of the organic soils may not have originated from some of the

areas, layers of peat, sand, clay, and glacial till are common types of soil material that are found in the entire area. Within the variety of marine clays, two major units can be found. The upper unit consists of clay, silty clay, and silt overlain by small amounts of sand and silty sand. The lower unit is blue grey clay, and spotted in some parts. Typically, underlying the clay is coarse glaciofluvial sediment, glacial lacustrine sediments, or till up to one meter in thickness. These deposits overlie relatively flat lying limestone (Schut and Wilson, 1987). The surface soils are deposits which exist as a result of the recession of the Champlain Sea (Stantec Consulting Ltd., 2010).

4.4 Climatic Conditions

Ottawa has a humid continental climate, which is accompanied by large temperature changes. High temperatures are found during July, where the average daily maximum temperature is 23.5°C, while low temperatures occur in January with a mean daily minimum value of -16.4°C. Recently, average annual rainfall of 714 millimeters has been observed, and the average annual snowfall is 208 millimeters (Canadian Council of Professional Engineers, 2008). These precipitation rates are incremental; as it has been observed that the annual Ottawa rainfall has incrementally increased over the past decades. An increase in the annual maximum 24-hour rainfall of 0.57 mm/year has been recorded by the Ottawa CAD station from 1960 to 2004, as shown in Figure (4-3) (Auld et al., 2009).Throughout the winter season, snow and ice prevail; although the duration of the winter period and snow duration are not constant in a typical winter in Ottawa, often times a long-lasting snow cover starts from mid-December until early April. Freeze-thaw cycles take place during the winter with a few days that reach the freezing point, followed by nights that are well below 0°C. Freezing rain and high wind chills are also very common. Summers are relatively warm and humid in Ottawa, even though they are typically short in length. The cold air from the north plays an important role in reducing humidity (Canadian Council of Professional Engineers, 2008).

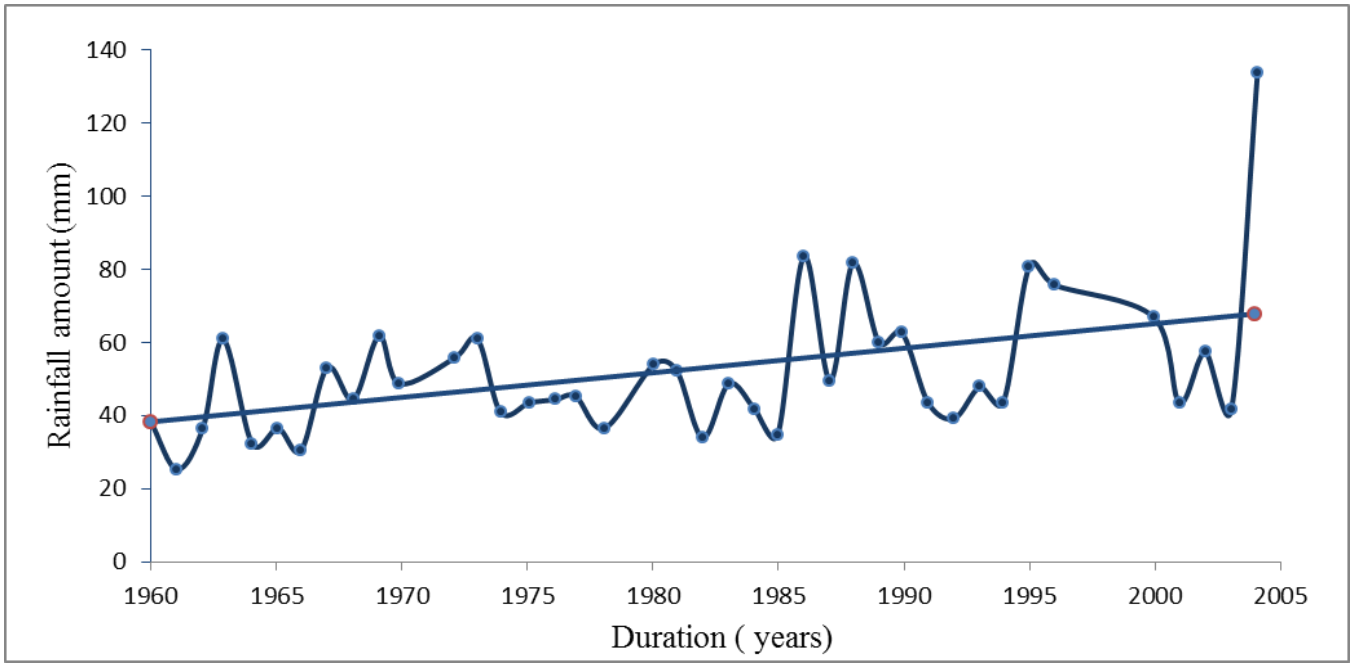

Figure 4-3 Annual maximum 24- hour rainfalls (mm), Ottawa CAD (1960 – 2004). (Modified from Auld et al. 2009).

4.5 Geotechnical Characteristics of the Soils in the Study Area

The geotechnical data used in the GIS model for the present study are obtained from previous geotechnical studies performed by accredited companies throughout Ottawa (e.g., Inspec-Sol Inc., 2014; Engineering Solutions, 2014; Kollaard Associates, 2013; Houle Chevrier Engineering Ltd., 2013; Stantec Consulting Ltd., 2010; Trow Associates Inc. 2010; Golder Associates Ltd., 2008). The soil samples in the studies were taken from different sites, which are thorough and evenly distributed across the study area. All of the soil samples were visually tested in the field, logged, specified and reported. Laboratory tests carried out on the soils have provided the geotechnical parameters of the marine clay, such as hydraulic conductivity, clay fraction, specific gravity, plasticity, moisture content, unit weight, shear strength parameters, and porosity. These studies also provide alternative technical data from standard penetration tests (SPTs). All of the geotechnical data obtained from these studies was used as input data for this GIS assessment.

According to these studies, the underground lithology of the study area consists of two layers of sensitive marine clay, a shallow layer of silty clay (clay located at a depth between 1.8 and 5.25 meters), and a deep layer of clay (clayey silt between 6.5 and 12 meters in depth). The SPT values of 5 to 10 blows and 5 to 20 blows were recorded for the shallow and the deep layers respectively. The liquid limit (LL) of the shallow layer varied from 22 to 80 percent, and the plasticity index (PI) was 8 to 48 percent,

while in the deep layer, the LL and PI values ranged from 50 to 70 percent, and 28 to 52 percent, respectively. The specific gravity was found in general to be 2.70 to 2.80 for all of the sites, typical for clay (Houle Chevrier Engineering Ltd., 2013, Sorensen and Okkels, 2013; Stantec Consulting Ltd., 2010; Trow Associates Inc., 2010; Golder Associates Ltd., 2008). The clay fractions were determined via hydrometer testing from the available data. The clay fractions ranged between 56and 87 percent. The reported unit weight ranged between 14 and 22 kN/m^3. These values agree with those reported in the peer reviewed literature (e.g., Taha and Fall, 2014; Quinn, 2009).

4.6 Historical Landslides

Landslides are a fairly common phenomenon along the slopes of river valleys and terraces in Ottawa areas that have Leda clay. The slides are resultant of slips that normally propagate backwards over large distances on slopes and in some cases, may develop into large flow slides.

Fransham and Gadd (1977) stated that early in the history of the Ottawa region, the significantly larger Ottawa River cut numerous broad channels through the sediment, which resulted in many large landslides during that period. They provided in their work, seventeen maps at a scale of 1:50,000 that show the distribution of sensitive clay deposits and the accompanying landslides in the Ottawa Valley (Fransham and Gadd, 1977).

Radiometric dating and site investigations have indicated that the Ottawa region had experienced several prehistoric landslide events. One of them was at 4550 BP and caused by geologically destructive earthquakes. The magnitude of these earthquakes probably exceeded 6.5 (Brooks et al., 2013; Aylsworth et al., 1997). Moreover, a landslide dated 1140 BP was discovered in the Beacon Hill area in 1960. This landslide was noted along with a scarp that was eroding in postglacial marine clay through the proto-Ottawa River. The maximum retrogression of the slope crest into the original surface was 260 meters, and the volume of the landslide was about two cubic meters (Aylsworth et al., 1997). Moreover, in the last century, several landslide events were recorded. For example, in 1965, a rainfall-induced landslide event took place on the slopes in Orleans, a suburb of Ottawa. In Orleans there were numerous landslides in the Champlain Sea sediments located on the terrace slopes above the community, but widespread housing expansion obscures most of the features that can be previously detected on pre-development aerial photographs (Aylsworth et al., 2004; 1997). No comprehensive geotechnical analysis is available for these landslides; however, a detailed geotechnical study was carried out by Eden and Jarrett (1971) on a small landslide near a side hill of a road cut south of a shopping plaza in October 1965. After five

years, the landslide occurred due to the excavation of a hill and a period of heavy rain. The landslide was shallow with a sliding surface that was circular in shape, and the extent of the landslide was small.

Another landslide event took place in 1971 along the South Nation River from Casselman, located about 50 kilometers east of Ottawa along Highway 417. This event occurred during a night with a heavy thunderstorm in which the ground became fully saturated after the slow melt of exceptionally heavy snow (Aylsworth et al., 1997). This landslide involved an area of 28 hectares, a maximum retrogression distance of 490 meters, and an estimated volume of ($7x10^6$) cubic meters. Singhroy et al. (2000) showed patterns in the Ottawa Valley by combining airborne SAR and Landsat TM images and used SAR interferometric techniques to classify the morphological features of the landslides. The airborne SAR images in the Ottawa Valley revealed flow slides on the sensitive marine clays. The activating mechanism was the extreme rainfall. Hugenholtz and Lacelle (2004) selected Green's Creek Valley as the area for a case study and examined its landslide activity through aerial photographs from 1928 to 1999. They concluded rainfall to be a key trigger for many landslides that took place in this area. Figure (4-4) illustrates areas that were historically subjected to landslide events in the study area (Zones A and B), which include the areas subjected to landslides in the eastern and western parts of the study area respectively. It should be indicated that, in our study area, it was assumed that the inventory of past or historical landslides is not complete since some might not have been identified or destroyed by human activities (e.g., land use, construction, excavation, or transportation facilities).

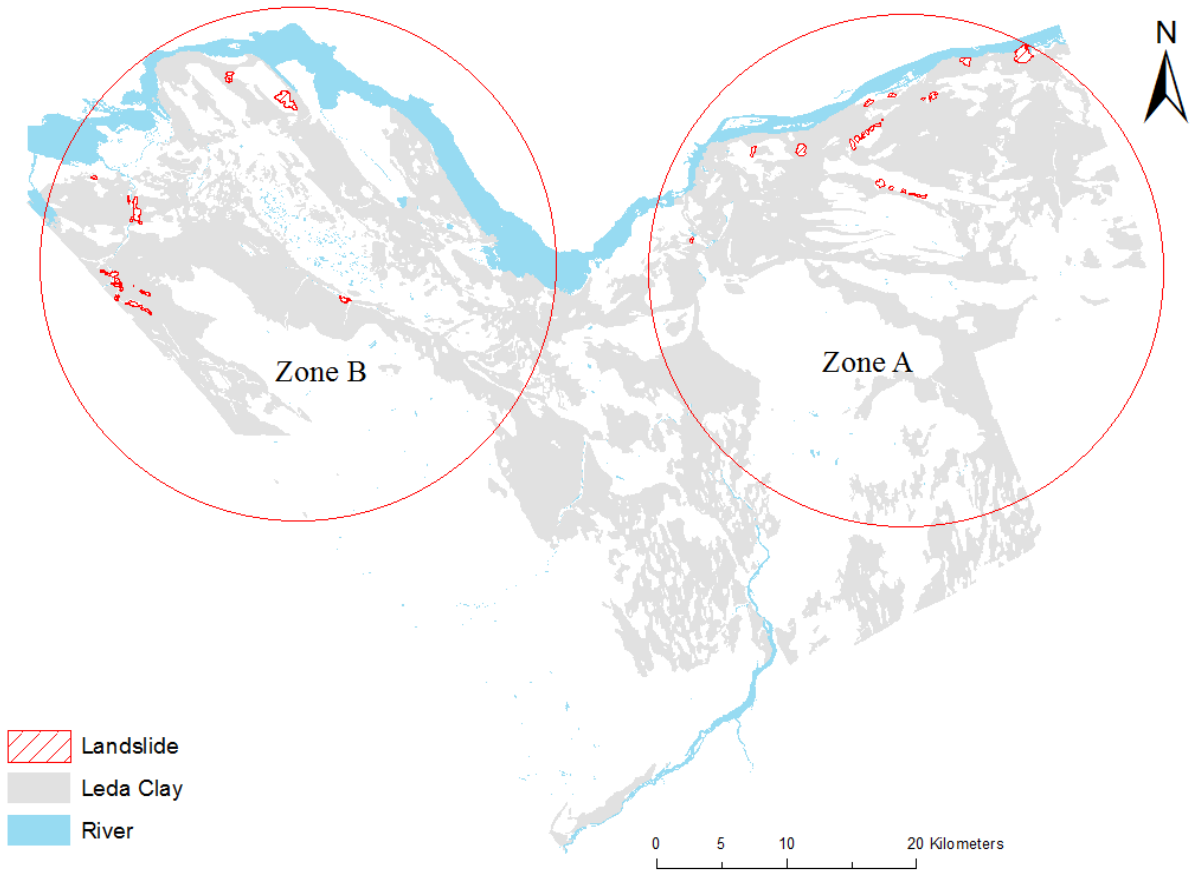

Figure 4-4 Map shows areas subjected to landslides in the past (historical landslides) as recorded in the literature.

4.7 Methodology

An approach that involves multiple steps was applied to assess slope stability for areas consisting of sensitive marine clays susceptible to landslides as a result of rainfalls. These steps are represented as a flowchart in Figure (4-5).

The first step consisted of collecting geotechnical, climate, hydrogeological, and spatial data (Table 4-1). This data was collected from several sources, such as governmental agencies, and consulting and technical firms that have a good work history in the Ottawa region. The information on the geotechnical subsurface properties in the study area, such as shear strength parameters, consistency limits (liquid limit, plastic limit, etc.), moisture content, depth, thickness, and type of subsurface layer were collected from previous geotechnical investigations (e.g. Trow Associates Inc., 2010, Taha, 2010).

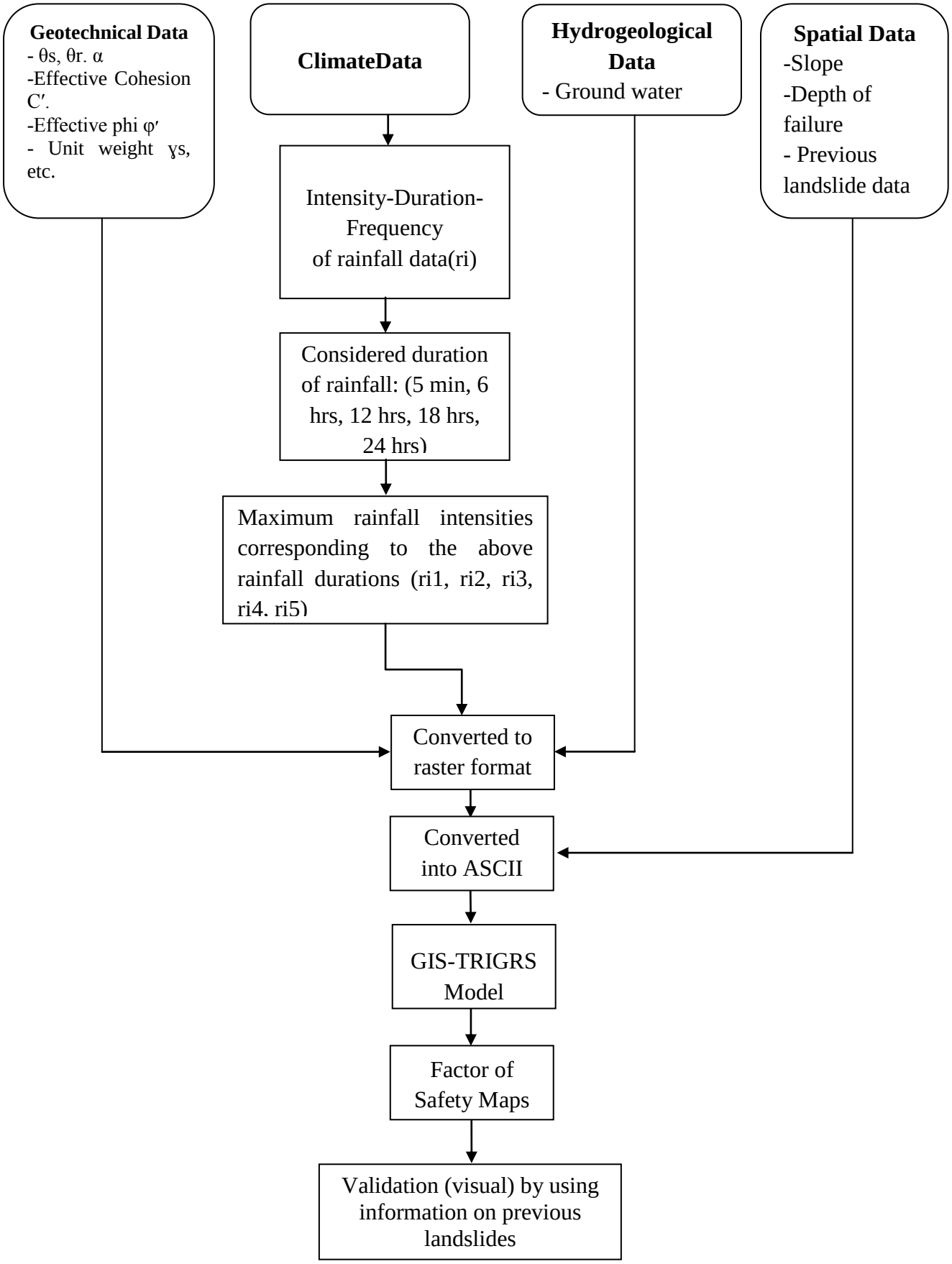

Figure 4-5 Map Methods in landslide susceptibility assessment.

In the second step, climate data, comprised of rainfall intensity-duration frequency data curves, from Environment Canada was used. The data from five stations located in the Ottawa region and the surrounding areas were extracted for this study (see Figure (4-6)): Ottawa CAD (45^{o} 23′N, 75^{o} 43′W), Ottawa Macdonald –Cartier (45^{o} 19′N, 75^{o} 40′W), Kemptville (45^{o} 0′N, 75^{o} 38′W), Cornwall ONT Hydro (45^{o} 2′N, 75^{o} 48′W), and Brockville PCC (44^{o} 36′N, 75^{o} 40′W).

The rainfall intensity-duration frequency curves represent the relationship between rainfall intensity and the return periods of 2, 5, 10, 25, 50 and 100 years. An example of a rainfall intensity-duration frequency curve is provided in Figure (4-6). The rainfall data used in this paper is from the Canadian Weather Energy and Engineering Datasets (CWEEDS) of Environment Canada. The datasets (rainfall intensity and duration) span the period of 1905 to 2003. The rainfall intensity was obtained based on data recorded from rain gauged over long periods of time, such as 25 years or more. This helps to determine the frequency of occurrence of a given intensity, and consequently the intensity-frequency-duration relationships. The entire rainfall record in a year was analyzed to find the maximum intensities for various durations of 5 minutes, and 6, 12, 18, and 24 hours. Thus, each storm provides the value of maximum intensity for a given duration. The largest of all such values was taken as the maximum intensity in that year for a corresponding duration. Likewise, the annual maximum intensity was obtained for different durations. By analyzing each duration for specific return periods and the intensity, the intensity-duration curves can be plotted. The connection of rainfall intensity of various durations with concurrent return periods is shown in Figure (4-6) (DHV Consultants BV & DELFT HYDRAULICS, 2002).

Likewise, the initial groundwater levels were gathered from hydrogeological data, which were taken from data provided by the Provincial Groundwater Monitoring Network (PGMN) Program. There are presently 474 wells in the PGMN program that are not used to provide water, but rather to observe and monitor the groundwater conditions. The groundwater levels are measured on an hourly basis. These wells are designed to obtain the pore water of aquifers located in overburden, bedrock, and the interface between the two. The location and elevation information of these wells have been determined by using latitude and longitude data, and applying them to the Provincial Digital Elevation Model (DEM) (Rogojin, 2014).

In the third step, the Digital Elevation Model (DEM) data files, obtained from the U.S. Geological Survey, were used. These have adequate resolution and scale required for the deterministic modeling of shallow landslide susceptibility. In this study, 1:50,000 DEM raster (publicly available from Natural Resources Canada) was imported into the GIS. Since the study area is likely to be in highly

dissected terrain with high relief, high-resolution data of 10 by 10 meters is typically required; the resolution of the original raster image for the DEM was 10 by 10 meters. The slope of the topography was calculated from the DEM by using the Spatial Analyst of ArcGIS Figure (4-7A). Furthermore, by recognizing that this study is dealing with predicted landslide events, the raster image of the lower boundary (predicted slope failure plane) Figure (4-7B) was calculated in the GIS by using an exponential function of slope (Godt et al., 2008).

$$d_{lb} = 7.72e^{-0.04\,\delta} \qquad (4\text{-}1)$$

Where d_{lb} is the depth of failure, and δ is the slope angle, which were proposed by Godt et al. (2008). Raster images of the geological distribution of Leda clay in the studied area were also created Figure (4-7C). The resolutions of all of the created raster images were then converted into a grid of 25 by 25 meters. Then, the raster images for the obtained geotechnical data and rainfall intensity for all durations were created for the entire study region.

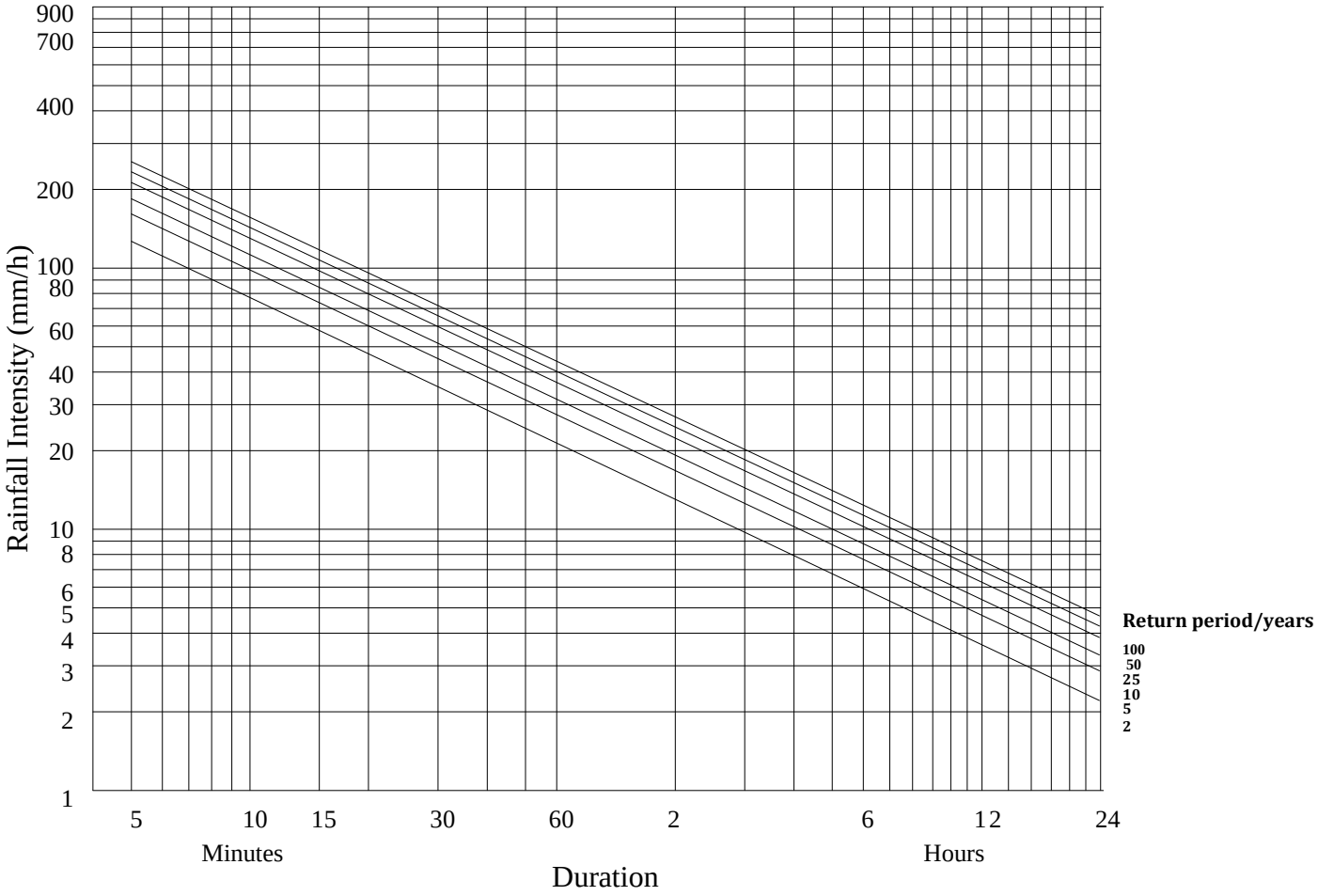

Figure 4-6 Short duration of rainfall intensity - duration-frequency data
(Modified from Environment Canada, 2010).

In the fourth step, all of the data obtained from the previous steps were converted into ASCII format files in order to run the TRIGRS model, including raster images of the following geotechnical parameters (e.g., ϕ', c', θs, θr, α), rainfall intensity, slope, depth of failure, and hydraulic conductivity (Ks) and soil water diffusivity (D_Ψ) (see Table 4-1). This format is convenient for TRIGRS modeling. Data conversions were done by using the ESRI ArcGIS program. Subsequently, the data was introduced into the TRIGRS model by following the method in Baum et al. (2008), and then the TRIGRS model was run to calculate the safety factor (by using infinite slope modeling) for the entire studied area for rainfall durations of 5 minutes, and 6, 12, 18, and 24 hours.

Table 4-1Summary of input data used in the GIS-TRIGRS model

Data type	Collected data							
	Range of values of the sub-sections in the studied area[1]							
Geotechnical Data [2]	C′ kPa	ϕ′ Degree	Unit Weight kN/m^3	θs	θr	Ks $\times 10^{-7}$ m/s	D_ψ $\times 10^{-6}$ m/s^2	α
	12 - 20	21 - 30	14 - 22	0.2 – 0.9	0.02 – 0.34	0.01 – 1	0.0005 - 4	(-0.5) – (- 3.2)
Climate Data [3]	Rainfall Intensity (mm/s)		Rainfall Duration (sec)		Rainfall (mm)		Return Period	
	see Figure (4-6)							
Hydrogeological Data[4]	Initial Ground Water Table (for 474 water wells/boreholes)							
	(0.65 – 5.6) m							
Spatial Data[5]	Slope δ (Degree)				Failure Depth (m)			
	0- 33				2.1 – 7.7			

C′: effective cohesion, ϕ′: effective internal friction, θs: volumetric water content at saturation,θr: residual water content , Ks: saturated hydraulic conductivity, D_ψ: soil water diffusivity α: inverted capillary fringe.

[1] The studied area was divided in small sub-areas or sub-sections; each sub-section has its own geotechnical data which are used as the input data in the GIS model.

[2] Geotechnical reports issued by Trow Associates Inc. 2010; Golder Associates Ltd. 2008; Houle Chevrier Engineering Ltd. 2013, Stantec Consulting Ltd. 2010; Inspec-Sol Inc., Engineering Solutions 2014, Kollaard Associates Engineers 2013.

[3] Environment Canada.

[4] The Provincial Groundwater Monitoring Network (PGMN) Program

[5] Natural Resources Canada.

In the fifth step, the obtained result files obtained from TRIGRS (in an ASCII file format) were converted back into raster format so the data could be used in the GIS model. The outputs were analyzed to understand the behavior of landslides in the studied area for five different durations of rainfall. These results are discussed in the next section. Finally, the sensitivity of the predicted landslide areas to the

changes in the input data was assessed, followed by a comparison of the predicted landslide areas with the location of the historical landslides recorded in the study area. For visual comparison, the historical landslide areas were overlaid in GIS on the maps of the predicted landslide susceptibility. This allows observation of the similarities between the general spatial trends of the historical landslides and potential landslide zones identified as the result of this study.

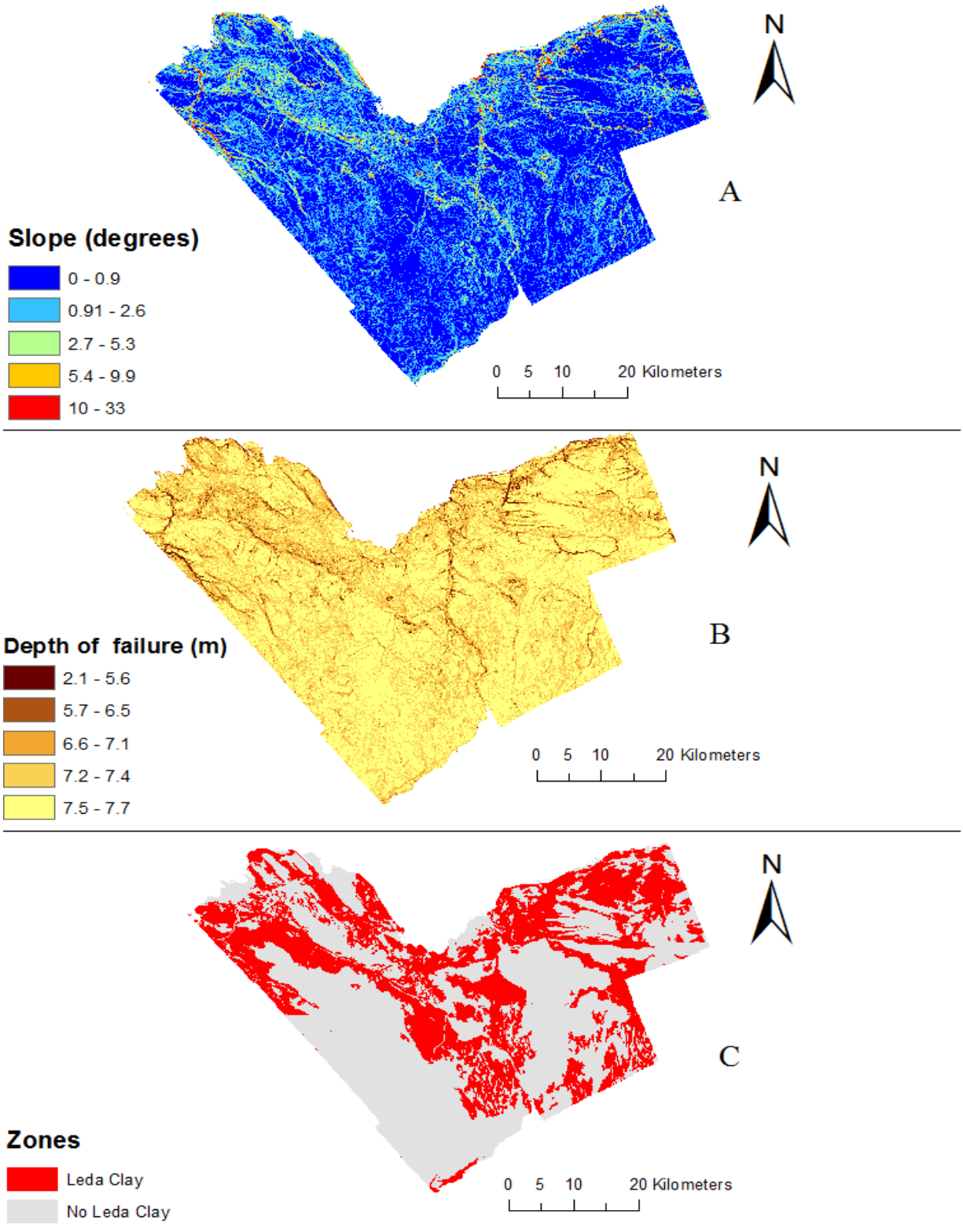

Figure 4-7 Geological maps of the studied area: (A) topographic slope, (B) depth to the lower boundary, and (C) simplified geology (Leda clay).

4.8 Slope Stability Model

Infinite slope stability analysis is a common tool for assessing and evaluating landslides because of its simplicity and feasibility (Iverson, 2000). This method is applicable to the case of landslides with shallow depth relative to their length and width. The above deterministic approach to slope stability analysis based on one-dimensional infinite-slope stability analysis has been studied and tested using digital topography. Infinite-slope stability analysis assumes that landslides are exceptionally long with planar failure surface. This applies to landslides with shallow depth compared to their length and width. They are triggered by extensive regions of elevated pore-water pressure or a decrease in soil suction (Godt et al., 2008). Slope stability analysis in unsaturated soil is widely used to assess slope failure. The main triggers that reduce the shear strength or increase the driving force are heavy rainfall and infiltration. This is due to elevated pore-water pressure and the dissipation of matric suction (Zhao and Zhang, 2014; Yeh et al., 2008). Therefore, infinite slope modeling is used in this work to calculate the safety factor (FS); and thus slope stability (see Figure (4-8)). The FS is reduced by an increase in the pore-water pressure head or a reduction in the soil suction (Bhandary et al., 2013). The factor that leads to slope failures is the matric suction (negative pore water pressure) which begins to decrease when water starts to penetrate unsaturated soil. The loss of matric suction reduces the shear strength of the soil mobilized along the slip surface. To best establish increases in matric suction, the relationship between the matric suction of the soil and the water content, must be defined. This relationship is called the soil water characteristic curve (SWCC). The SWCC is plotted using Equations (4-2) and (4-3) as proposed by Fredlund and Xing (1994) (given that the distribution of grain size and moisture content of the soil is known). These soil parameters are obtained from the collected geotechnical data (the borehole data), and Equations (4-2) and (4-3) are used to fit the SWCC.

$$\theta = C(\Psi)\frac{\theta s}{\left\{\ln\left[e+\left(\frac{\Psi}{a}\right)^{n}\right]\right\}^{m}} \qquad (4\text{-}2)$$

Where θ the volumetric water is content, θs represents the saturated volumetric water content, Ψ is the total suction. The three fitting parameters a, n, and m can be calculated from the soil-water characteristic curve. The influence of this parameter is variable. It can be observed that the parameter a is closely related to the air-entry value when n and m are fixed. Usually, the value of a would be higher than the air-entry value. $C(\Psi)$ is a correction function determined from:

$$C(\Psi) = 1 - \frac{ln\left(1+\frac{\Psi}{\Psi r}\right)}{ln\left(1+\frac{1000000}{\Psi r}\right)} \qquad (4\text{-}3)$$

Where Ψr , is the suction corresponding to the residual water content θr.

The FS is computed with Equation (4-4) for transient pressure heads at multiple depths Z. Failure is predicted when the FS < 1, and stability holds when the FS > 1. Thus, the depth Z where the FS first reaches 1 will be the depth where the landslide is initiated. This initiation depth will differ with variations in time as well as the depth of the pressure head which, in turn, is based on the rainfall history. Equation (4-4) (Salciarini et al., 2008; Terzaghi, 1943) was used to determine the FS with respect to the coordinate system and ground water conditions in the slope above and impermeable lower boundary below the ground surface, as

$$\mathrm{FS} = \frac{\tan\phi'}{\tan\delta} + \frac{\mathrm{c}' - \Psi(\mathrm{Z},\mathrm{t})\,\gamma_{\mathrm{w}}\,\tan\phi'}{\gamma_{\mathrm{s}}\mathrm{d}_{\mathrm{Ib}}\,\sin\delta\,\cos\delta} \qquad (4-4)$$

As c' is the soil cohesion, ϕ ' is the soil friction angle, Ψ is the ground-water pressure head as a function of depth Z and time t , δ is the slope angle, and γ_w and γ_s the unit weights of water and soil, respectively.

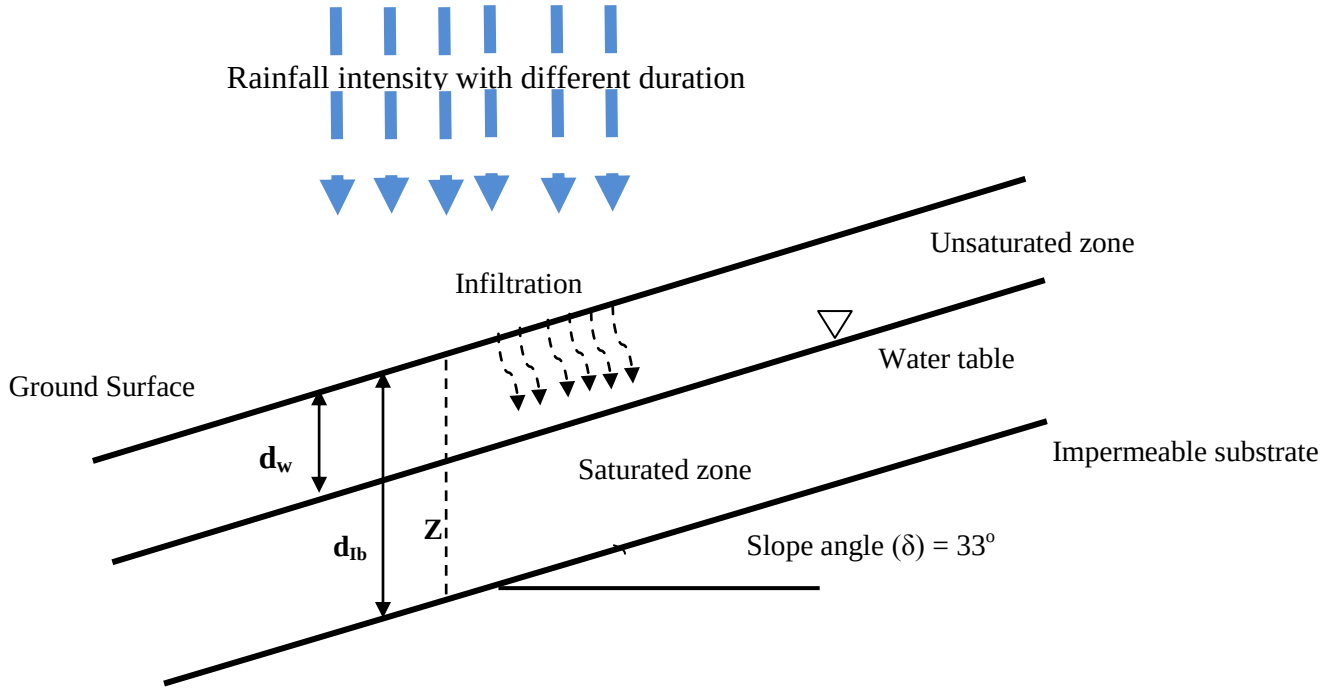

Figure 4-8 Proposed infinite slope stability analysis of studied area

4.9 Hydrological Model

This section describes the TRIGRS hydrological model and formulas therein used to represent the flow behavior in the studied area, in both saturated and unsaturated conditions.

4.9.1 Infiltration Models for Saturated Initial Conditions

Under saturated initial conditions, the groundwater flow field is modeled in two states: steady and transient. The steady-state seepage groundwater flow field depends on the water table level and infiltration rate. The steady state flow direction in both directions (x and z planes) is determined on the basis of the infiltration rate, saturated hydraulic conductivity, and slope angle (Baum et al. 2008; Iverson 2000). The FS values obtained by the TRIGRS model are very sensitive to the initial steady seepage conditions. Thus, accurate initial conditions are important for modeling. To obtain accurate initial conditions, a considerable number of field observations are required, and most likely supplemented with steady flow modeling to generalize the result between the different observations. When there is a lack of accurate initial conditions, TRIGRS is only suitable for modeling hypothetical scenarios (Godt et al., 2008; Baum et al., 2002). Transient groundwater flow in one dimensional (vertical), and maintains a set intensity and length at the earth´s surface for a specific flux. At the starting time the zero flux condition is present at the basal boundary located at an infinite depth (Baum et al., 2002). Combining TRIGRS and

Heavy side step functions rainfall at a constant intensity and varied surface fluxes were characterized (Iverson, 2000; Baum et al., 2002). The solution used in TRIGRS is given in Equation (4-5) (Iverson, 2000):

$$\Psi(Z,t) = (Z-d)\beta + 2\sum_{n=1}^{N}\frac{I_{nz}}{K_s}\left\{H(t-t_n)[D_1(t-t_n)]^{\frac{1}{2}}\text{ierfc}\left[\frac{Z}{2[D_1(t-t_n)]^{\frac{1}{2}}}\right]\right\} - 2\sum_{n=1}^{N}\frac{I_{nz}}{K_s}\left\{H(t-t_{n+1})[D1(t-t_{n+1})]^{\frac{1}{2}}\text{ierfc}\left[\frac{Z}{2[D_1(t-t_{n+1})]^{\frac{1}{2}}}\right]\right\} \quad (4-5)$$

Where t is time, $Z = z/cos\,\delta$, Z is the vertical coordinate direction, z is the slope-normal coordinate direction, $\beta = cos^2\delta - (I_{ZLT}/K_s)$, where K_s is the hydraulic conductivity in the Z direction, I_{ZLT} is the steady surface flux, and I_{nz} is the surface flux of a given intensity of the nth time interval. $D_1 = D_0/cos^2\,\delta$, where D_0 is the saturated hydraulic diffusivity, N is the total number of intervals, and $H(t-t_n)$ is the heaviside step function, t_n is the time at nth time interval in the rainfall infiltration sequence (Godt et al. 2008). The function $ierfc\,(\eta)$ is in the following form (Godt et al. 2008).

$$\text{Ierfc}(\eta) = \frac{I}{\sqrt{\pi}\exp(-\eta^2)} - \eta\text{erfc}(\eta) \quad (4\text{-}6)$$

Where $\text{Ierfc}(\eta)$ is the complementary error function. In Formula (4-5) the steady component of a solution is signifies by the first term, and the second term signifies the transient component of flow. The first few expressions of the infinite series provide an acceptable degree of accuracy so that the computation of Equation (4-5) is very effective and can be helpful above broad areas on a cell-by-cell basis in a GIS framework that yields time-varying pore-pressure and FS for each grid cell as a function of depth in response to rainfall (Baum et al., 2002). When modeling with TRIGRS, limitations maybe imposed, so that at any depth Z, the maximum pressure head under a downward gravitational flow can not exceed the water table pressure at the ground surface if the original flow direction and hydraulic gradient are maintained (Godt et al., 2008, Baum et al., 2002). This is given by Equation (4-7):

$$\Psi(Z,t) \leq Z\beta \quad (4\text{-}7)$$

4.9.2 Infiltration Models for Unsaturated Initial Conditions

In order for the TRIGRS model to apply to a wider range of initial conditions and have validity in doing so, an analytic solution has been added for unsaturated flow as an alternative for estimating the infiltration at the ground surface. The alternative condition analyzes the soil as having two layers: a saturated zone and an unsaturated zone. The unsaturated zone absorbs ground surface water and begins to fill up towards the initial water table (Baum et al., 2002). The unsaturated zone has lower permeability that prevents or reduces surface infiltration to deeper strata or ground. This model utilizes four factors (θs, θr, α, Ks) to produce the SWCC for the wetting of the unsaturated soil, as well as an one-dimensional infiltration process (Srivastava and Yeh, 1991). The infiltrating water moves to the bottom of the unsaturated region; as a result, the water table will rise. The increase in water over the primary water table spreads like a diffusive pressure wave or waves consequently increases the pore pressure at deeper ground. The pressure waves moved quickly in thin, saturated zones (like on hillsides). An independent and distinct analytical solution models the transmission of these pressure waves over the saturated zone. In order to describe the infiltration at the ground surface and upright flow through the unsaturated zone, Richard's equation was applied in a one-dimensional form (Baum et al., 2008). The coordinate transformation described by Iverson (2000) is applied to explain for the effects of a sloping ground surface, see Equation (4-8).

$$\frac{\partial \theta}{\partial t} = \frac{\partial}{\partial z}\left[K(\Psi)\left(\frac{1}{\cos^2\delta}\frac{\partial \Psi}{\partial z} - 1\right)\right] \qquad (4\text{-}8)$$

In this model, the dependence of hydraulic conductivity, $K(\Psi)$, and the fluid content, θ, on the pressure head in Richard's equation is specified with the following formulas, see Equations (4-9) and (4-10) (Baum et al., 2008).

$$K(\Psi) = Ks \exp(\alpha \Psi^*) \qquad (4\text{-}9)$$

$$\theta = \theta r + (\theta s - \theta r)\exp(\alpha \Psi^*) \qquad (4\text{-}10)$$

In Equations (4-9) and (4-10), Ψ is the pressure head, Ψ* = Ψ - Ψo, where Ψo is a constant. K_s denotes the saturated hydraulic conductivity, K(Ψ) is the hydraulic conductivity function, θ is the volumetric water content, θ_r is the residual water content, and θ_s represents water content at saturation. α is sourced by bringing together Formula (4-9) and soil curves. By Substitutions Formulas (4-6) and (4-7) into Richard's equation (see Equation 4-5), a solution is givin in Formulas (4-11) and (4-12) (Srivastava and

Yeh, 1991). To apply this process to a sloping ground surface, the following relationship is used: α1 = α cos2δ.

$$q(d_u, t) = \begin{Bmatrix} I_z - 4\,(I_z - I_{ZLT})\exp\left(\frac{\alpha_1 \; d_u}{2}\right)\exp\left(-D_\Psi \frac{t}{4}\right) \\ \sum_{m=1}^{\infty} \frac{\Lambda_m \sin(\Lambda_m \alpha_1 d_u)}{1+\frac{\alpha_1 d_u}{2}+2\Lambda_m^2 \alpha_1 d_u}\exp[-\Lambda_m^2 D_\Psi t] \end{Bmatrix} \quad (4\text{-}11)$$

$$D_\Psi = \frac{\alpha_1 K_s}{(\theta_s - \theta_r)} \quad (4\text{-}12)$$

D_Ψ is the soil-water diffusivity, $D_\Psi t$ is equivalent to non-dimensional time and $\alpha_1 d_u$ corresponds to the non-dimensional depth used by Srivastava and Yeh (1991). d_u is the vertical depth to the top of the capillary fringe, and the values of Λm are the roots of the characteristic equation given in Baum et al. (2008). All other parameters have been used and identified in previous formulas (Srivastava and Yeh, 1991).

4.10 GIS-TRIGRS Model Sensitivity Analysis and Validation

Validation work was carried out to test the ability of the developed GIS-based model to predict rainfall-induced landslides in the studied sensitive marine clays before its application to the study area. Since it is well known that the uncertainties related to the input parameters (e.g., data quality, spatial variability of the data) can significantly affect the accuracy or reliability of a landslide susceptibility map, it is necessary to take into consideration these parameter uncertainties in the model validation, and subsequently in the model application to the studied area. Therefore, the model was first used to simulate the landslide susceptibility for three scenarios with respect to the values of the geotechnical input data for each model:

(i) A "normal "scenario: the average value of the geotechnical parameters (e.g., cohesion, internal friction angle) in each domain of the study areas was used as the input data. Figures (4-9a) and (4-10a) show the landslide susceptibility map obtained with a normal scenario for a steady rainfall duration of 24 hours;

(ii) A worst case scenario: the most negative ("pessimist") values (with respect to impacts on the FS) were used as the geotechnical parameters in this scenario as the input data. For example, for the shear strength parameters, the lowest values of cohesion and the internal friction angles obtained from previous geotechnical studies in each domain of the study area was used as the input data. This

is a conservative approach, but the landslide susceptibility map obtained by using these values will better reduce the susceptibility of slope failure. Figures (4-9b) and (4-10b) show the landslide susceptibility maps obtained for the worst scenario with a constant rainfall duration of 24 hours; and

(iii) An "optimistic" or "ideal" scenario: the most optimistic values (with respect to impacts on the FS) were used as the geotechnical parameters in the scenario. For example, for the shear strength parameters, the highest values of cohesion and the internal friction angles obtained from previous geotechnical studies in each domain of the studied area were used as the input data. Figures (4-9c) and (4-10c) show the landslide susceptibility maps obtained for an optimistic scenario with constant rainfall duration of 24 hours.

As expected, a comparison of Figures (4-9a, b and c) with Figures (4-10a, b and c) respectively shows that there are more vulnerable areas prone to landslides in the worst case scenarios Figures (4-9b) and (4-10b) than in the normal scenario Figures (4-9a) and (4-10a). There are also more vulnerable areas prone to landslides in the normal scenario than in the optimistic scenario. These findings, therefore, confirm that the landslide susceptibility model is sensitive to any changes in the input geotechnical parameters.

Secondly, the predicted landslide areas (model results) for the various scenarios were compared with previous landslide areas mapped or identified in the Ottawa region. Typical validation results are shown in Figures (4-11) and (4-12). The results of the GIS-TRIGRS model were evaluated by comparing the predicted unstable sites (areas with FS < 1) with the location of previous landslides in the studied area. An analysis of Figures (4-11) and (4-12), shows that much of the predicted areas with a low FS, which represent potential locations of future landslides induced by rainfall, fall within the same general trends (often elongated trends) as the areas that were affected by historical landslides in the Ottawa region (i.e. the predicted landslides are close to or on the same path or trend of the previous landslides). In other words, there is good agreement between the model's predicted results and the spatial distribution of historical landslides in the area. This suggests that the developed GIS-based model is able to predict rainfall-induced landslide susceptibility in the marine clays of Ottawa. However, it can be observed that there are previous landslides in Ottawa that were not triggered by rainfall. This results is also consistent with the results of previous geotechnical investigations on landslides in Ottawa, which show that besides rainfall; snowmelt and earthquake are other key triggers of landslides in the sensitive marine clays (e.g., Quinn, 2009; Aylsworth et al., 1997; Eden and Mitchell, 1969).

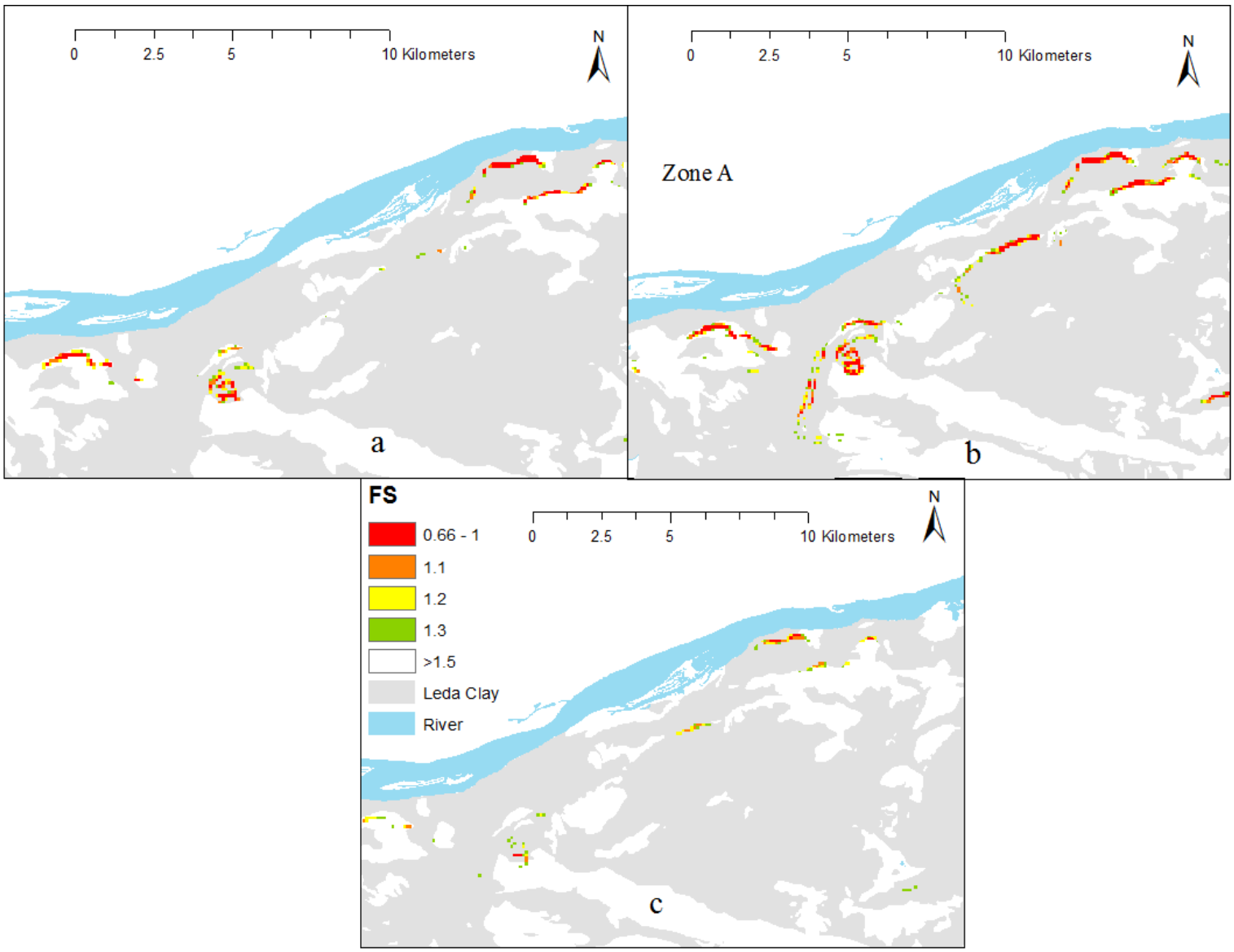

Figure 4-9 Factor of safety distribution in Zone A of studied area with respect to changes in input data, a: normal scenario, b: worst case scenario, c: ideal scenario

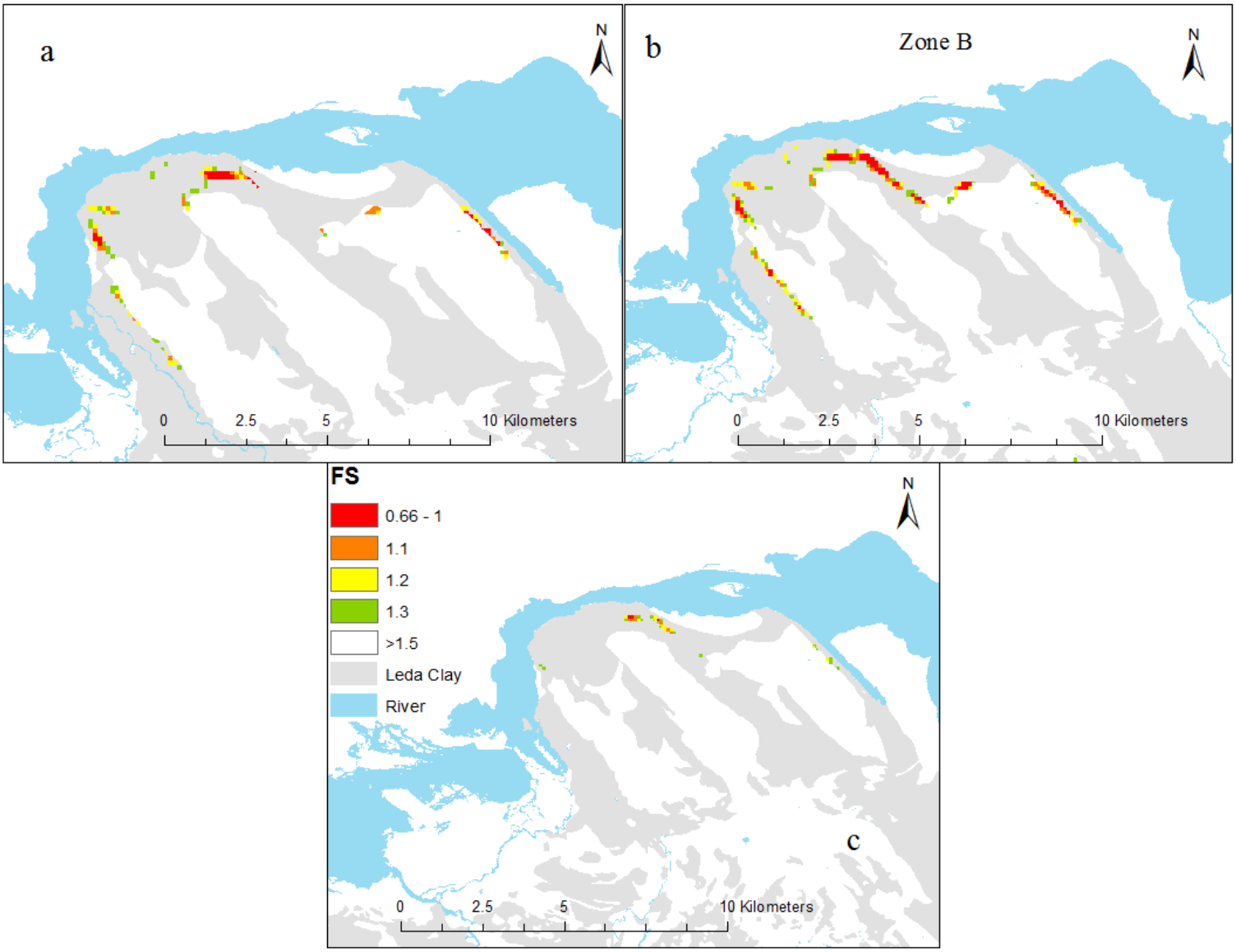

Figure 4-10 Factor of safety distribution in Zone B of studied area with respect to changes in input data, a: normal scenario, b: worst case scenario, c: ideal scenario

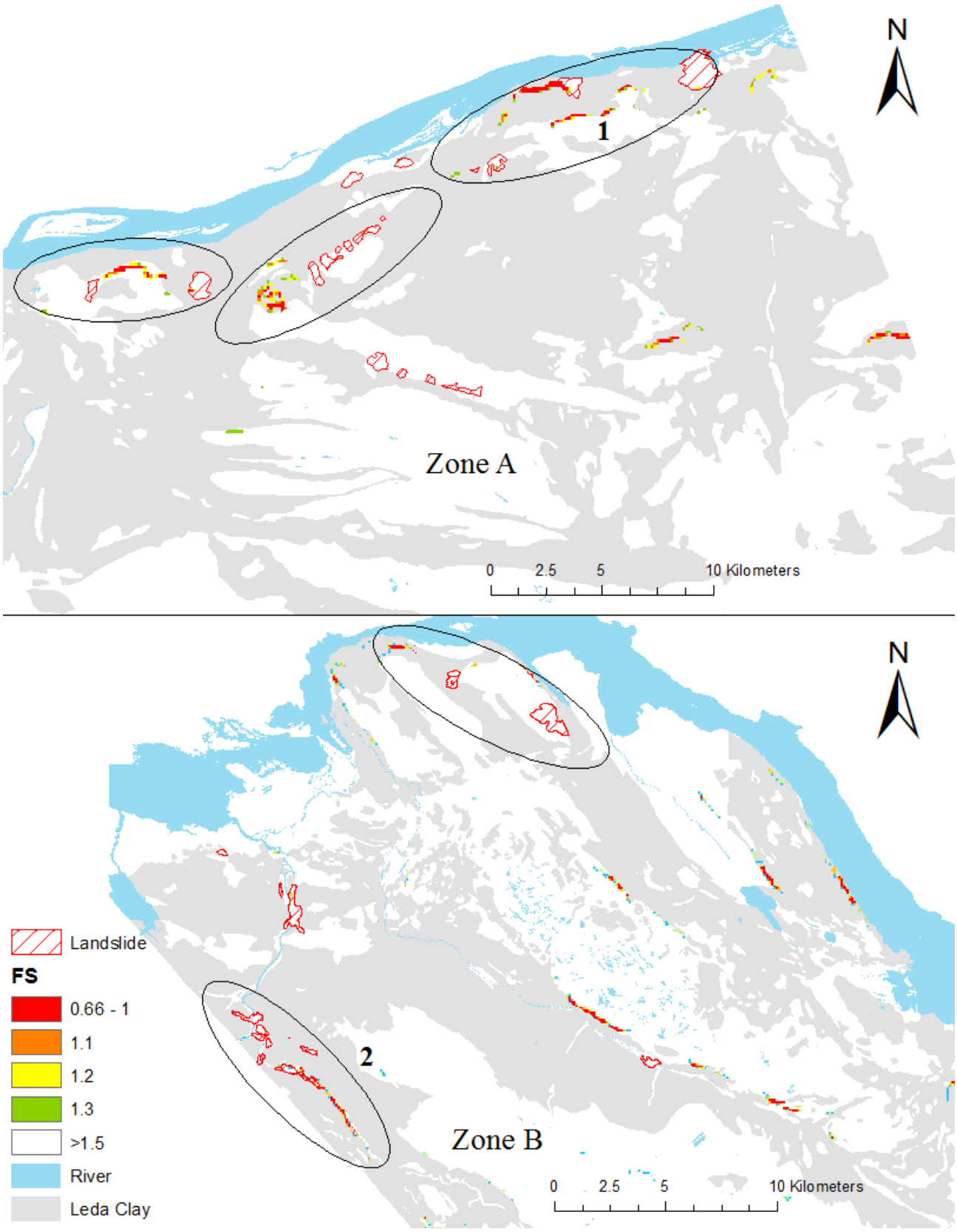

Figure 4-11A Location of historical landslides and map of predicted FS (normal case scenario): Details of Zones A and B

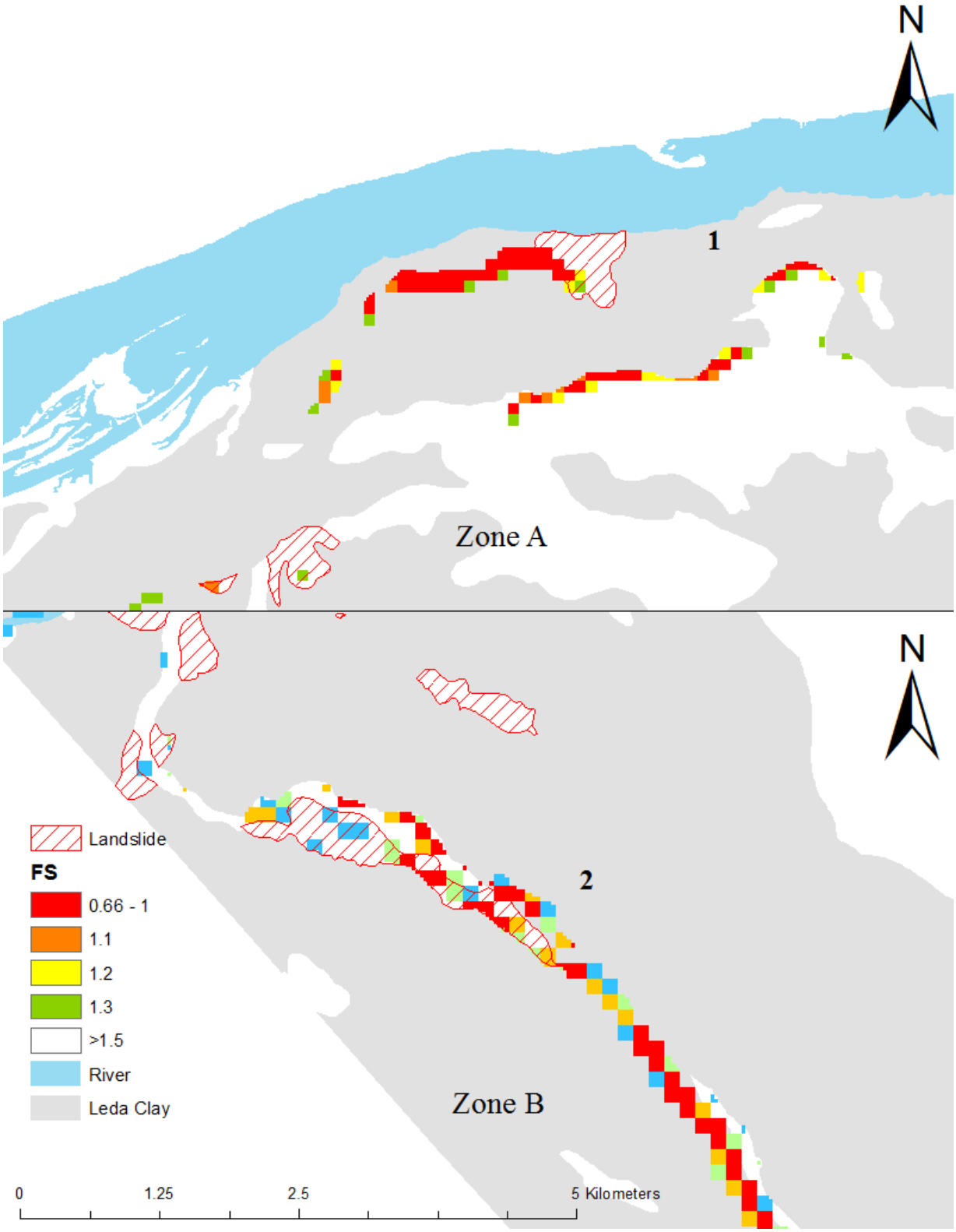

Figure 4-11B Details of Zones A and B, location of historical landslides and map of predicted FS (normal case scenario).

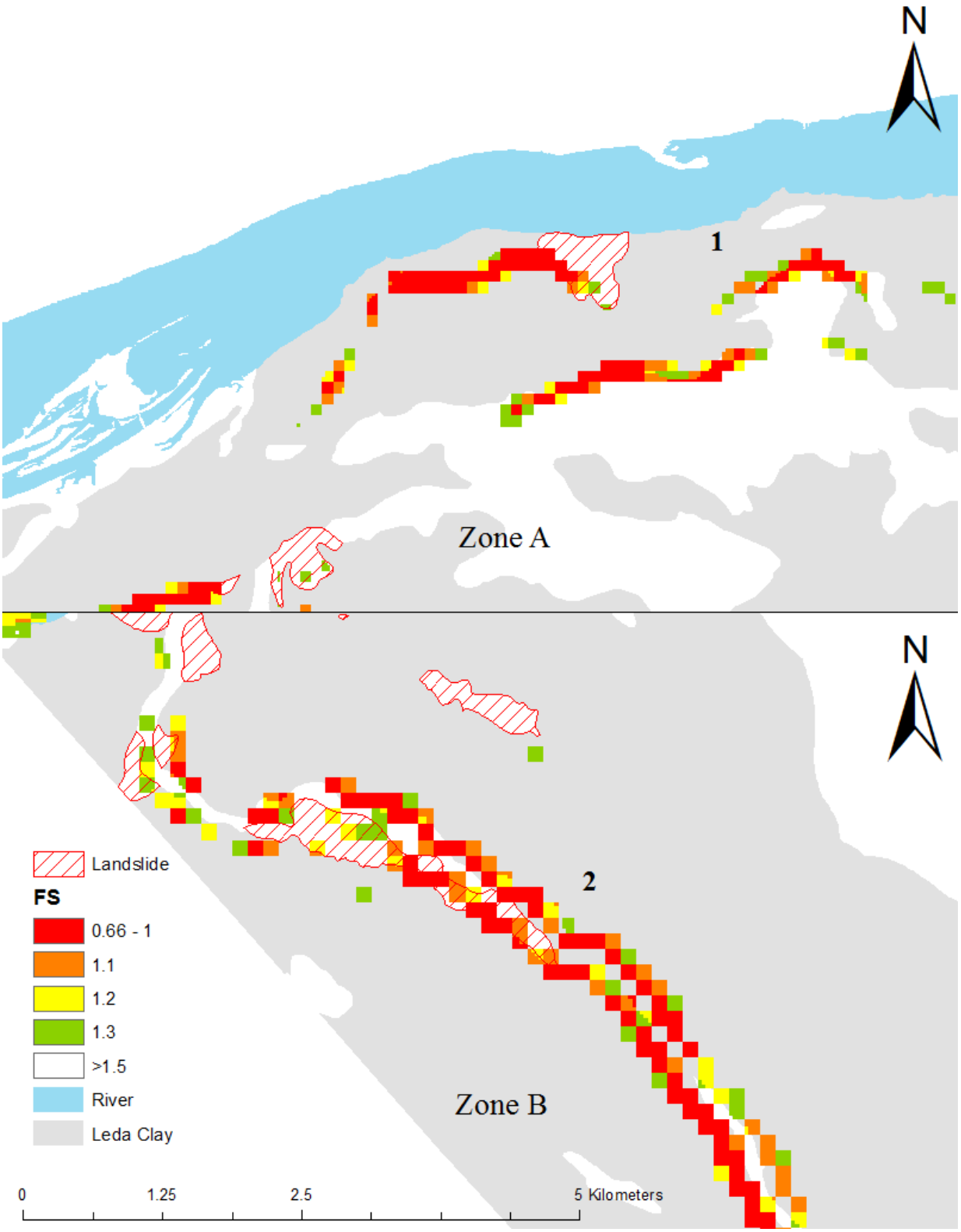

Figure 4–12 Details of Zones A and B, location of historical landslides and map of predicted FS (worst case scenario)

4.11 Application of the Model to the Study Area to Identify Landslide Susceptible Areas

The developed and validated model was then applied to the study area to identify the area's most prone to landslides induced by rainfall; in other words, a landslide danger map of rainfall-induced landslides was developed. The input data for rainfall (rainfall duration and intensity) used in the GIS-TRIGRS model of the landslide susceptibility is shown in Figure (4-6). As previously mentioned, this figure represents the intensity-duration frequency curves in the studied area, and thus, provides the relationship between rainfall intensity and duration and the concurrent return period. The considered return periods are 2, 5, 10, 25, 50 and 100 years. From Figure (4-6), it can be observed that the greatest rainfall intensity occurs after 5 minutes and then constantly decreases until 24 hours. The rainfall durations and their corresponding rainfall intensity values in Figure (4-6) were selected to simulate or predict the landslide susceptible areas. The results are presented in Figures (4-13) to (4-17).

Figures (4-13) to (4-17) illustrate the areas that are susceptible to rainfall-induced landslides in the study area for rainfall durations of 5 minutes, and 6, 12, 18, and 24 hours, respectively, for normal and worst case scenarios, and its associated rainfall duration and intensity. A slope with a safety factor less than one was determined to be susceptible to rainfall-induced landslides. The figures show that the areas which are most susceptible to rainfall-induced landslide are located in Eastern and Western Ottawa. Areas with steep, Leda clay slopes are also highly susceptible to landslide. Lastly, areas that see low rainfall intensities across a longer duration have a greater probability of being prone to landslide.

This means that landslides in this study area are triggered more so by rainfall events of long duration and low intensity, than those that are short in duration and high in intensity. Indeed, from the results of the prediction conducted with rainfall duration of 5 minutes and rainfall intensity of 250 millimeters per hour as presented in Figure (4-13). Notice that almost all of the slopes in the Ottawa region have safety factors greater than or equal to one ($FS \geq 1$), i.e. they are not susceptible to landslides. In contrast, in Figure (4-17), it can be observed that in the predicted landslide susceptible areas for rainfall duration of 24 hrs and rainfall intensity of around 4.5 mm/h, many slopes (compared to Figure (4-13)) show an $FS < 1$, i.e. they are potentially unstable. This finding is also consistent with the results of previous studies on rainfall-induced landslides, which showed that long duration of rainfall and low rainfall intensity are key triggers of landslides (e.g., Salciarini et al., 2008, Hasegawa et al., 2009, Li et al., 2013).

This higher sensitivity of the FS to rainfall duration is due to the fact that long rainfall durations and low intensity favor the infiltration of water into the soil. This infiltration will result in the reduction of the shear resistance of Leda clay, and thus reductions in the safety factor and slope stability. This argument is consistent with previous geotechnical investigations that have shown that the upper parts of Leda clay formations are unsaturated (e.g., Nader et al., 2015; Haché et al., 2015; Taha and Fall, 2014; Quinn, 2009; Fall et al., 2006; Dai and Lee, 2001). Accordingly, this unsaturated state was also considered in the model predictions of this study. Thus, infiltrating water will reduce the matric suction, which is obviously associated with a decline in the shear strength of Leda clay and thus reductions in the safety factor (FS). The higher sensitivity of the FS to rainfall duration is due to long rainfall durations of low intensity, that of which commonly result in the infiltration of water into the soil.

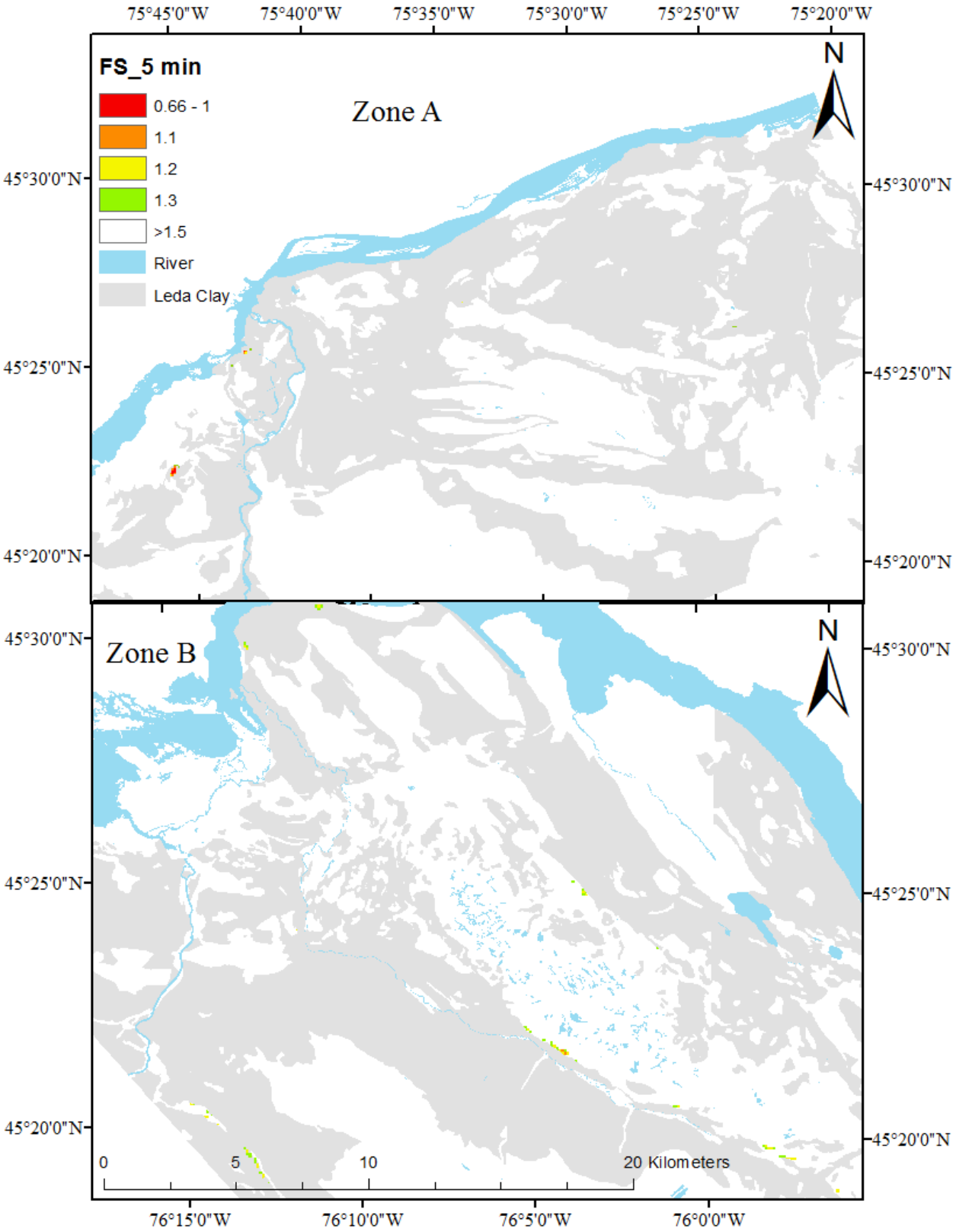

Figure 4–13A FS map and areas prone to landslides for rainfall duration of 5 min (normal case scenario).

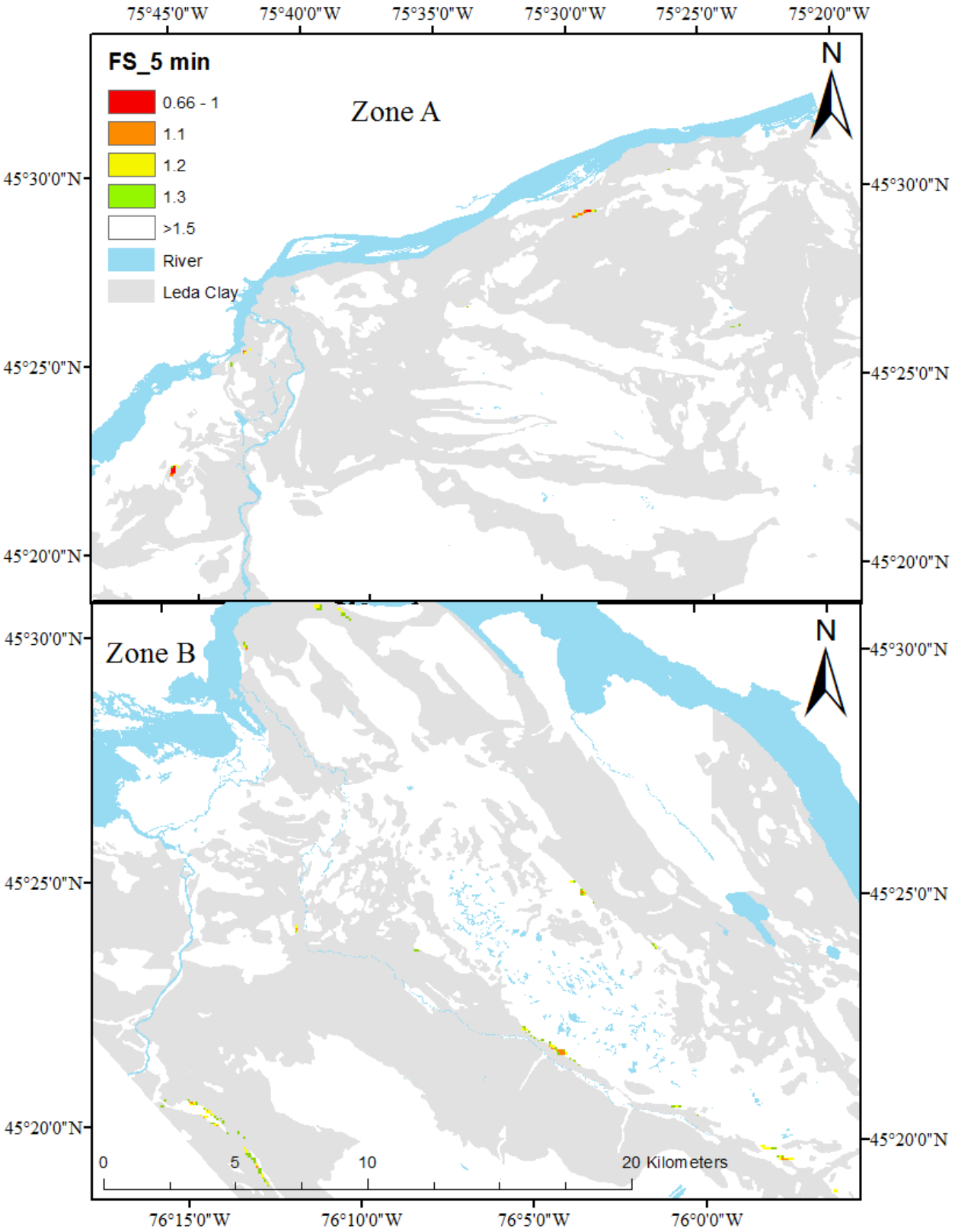

Figure 4–13B FS map and areas prone to landslides for rainfall duration of 5 min (worst case scenario).

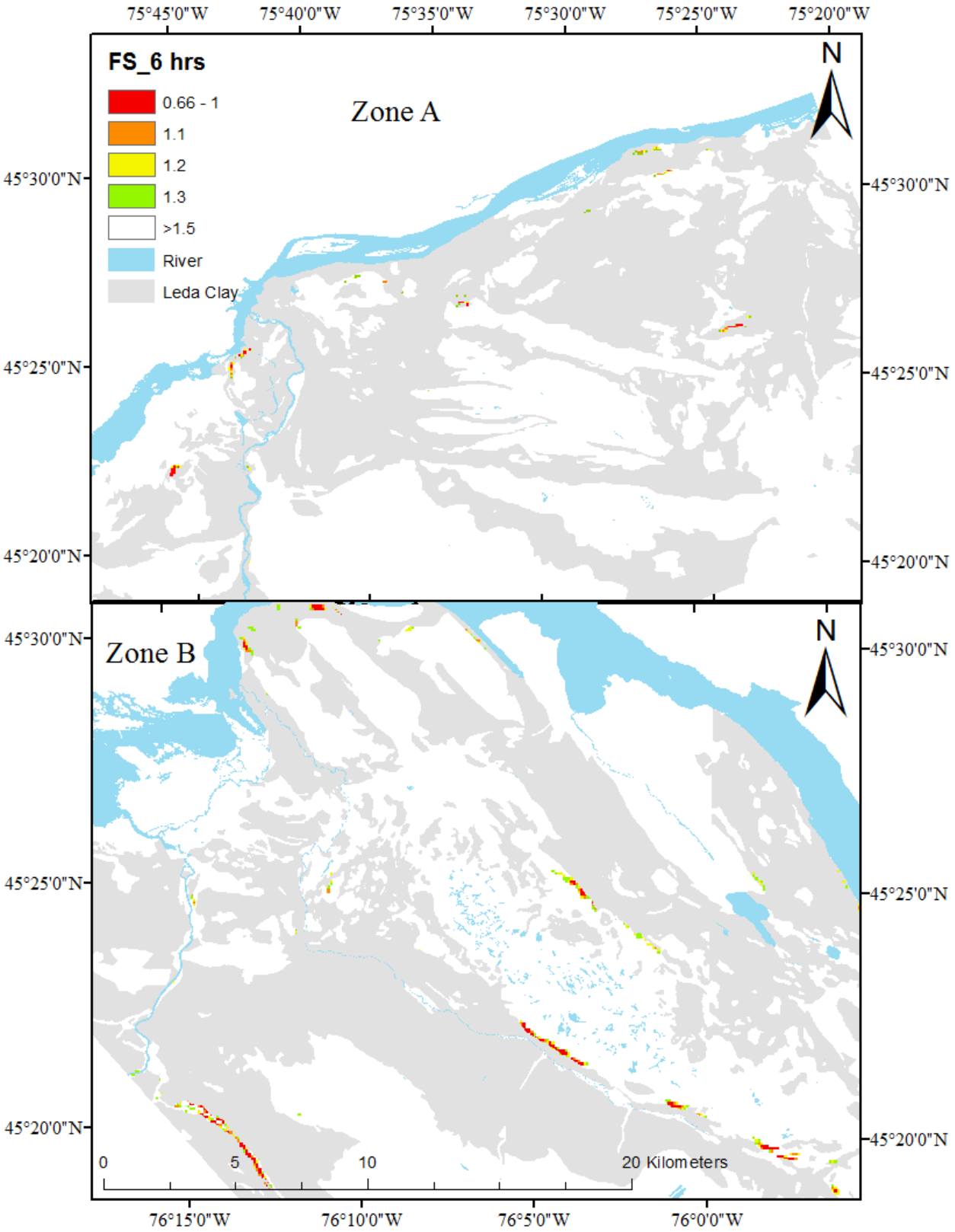

Figure 4–14A FS map and areas prone to landslides for rainfall duration of 6 hrs (normal case scenario).

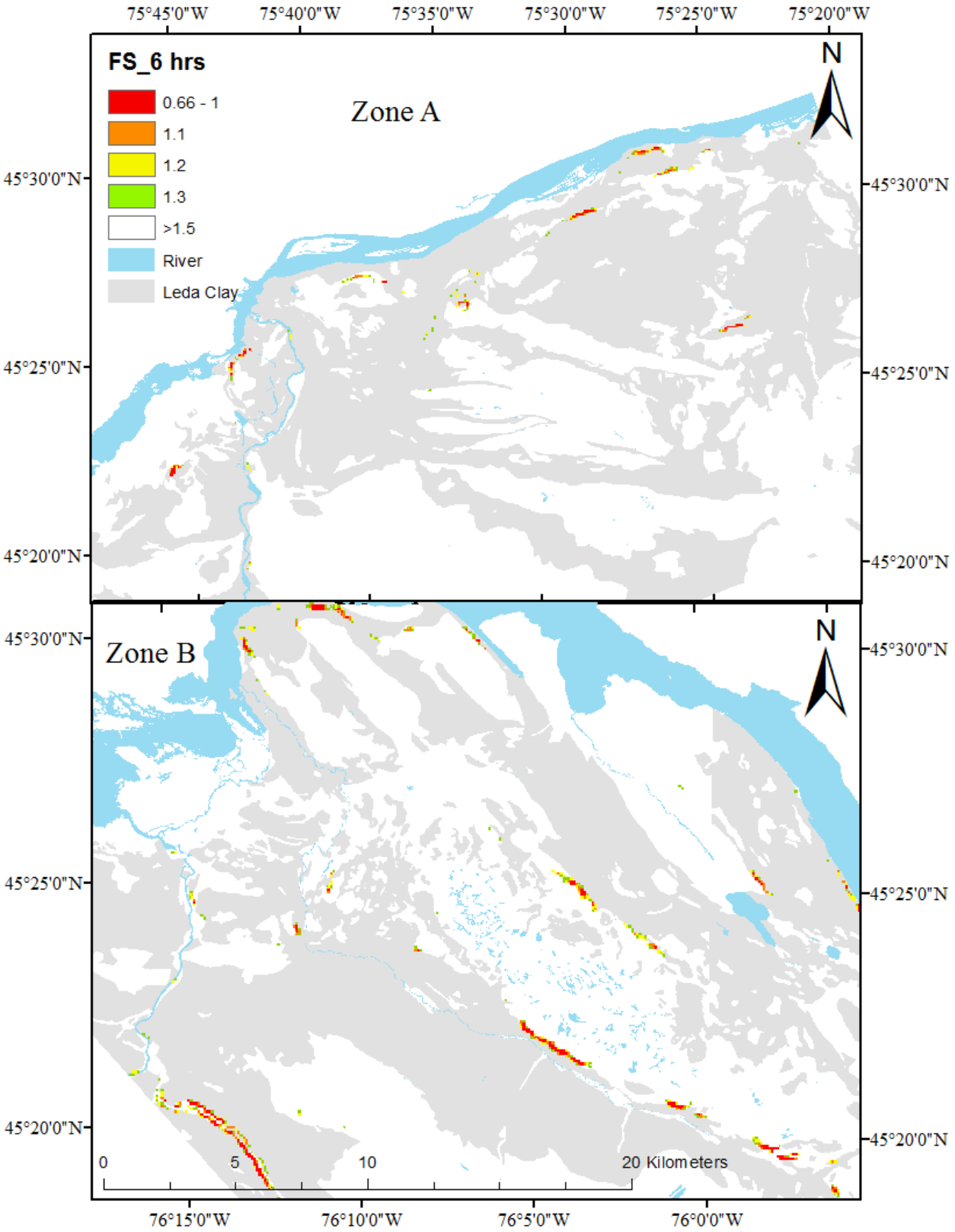

Figure 4–14B FS map and areas prone to landslides for rainfall duration of 5 min (worst case scenario).

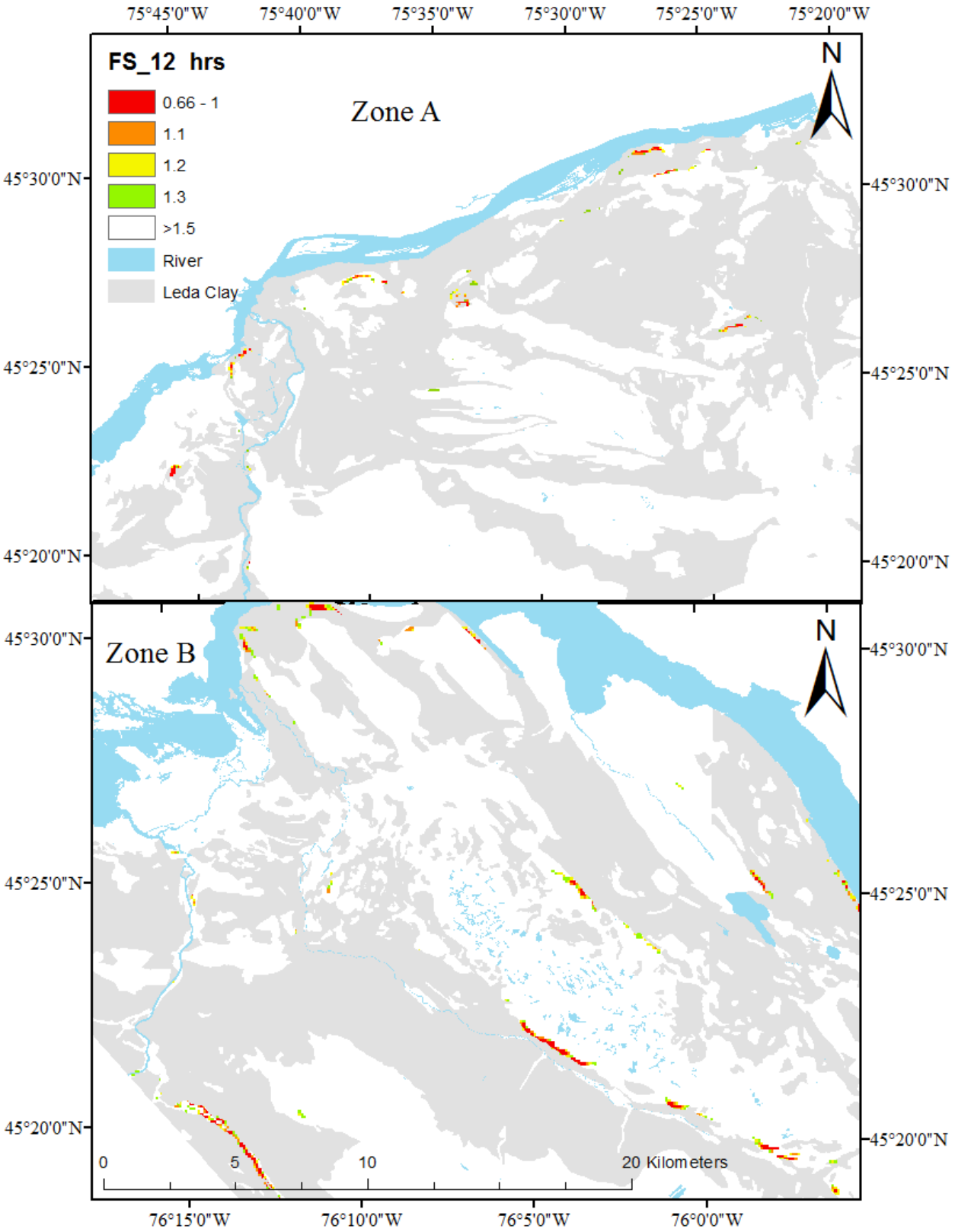

Figure 4–15A FS map and areas prone to landslides for rainfall duration of 12 hrs (normal case scenario).

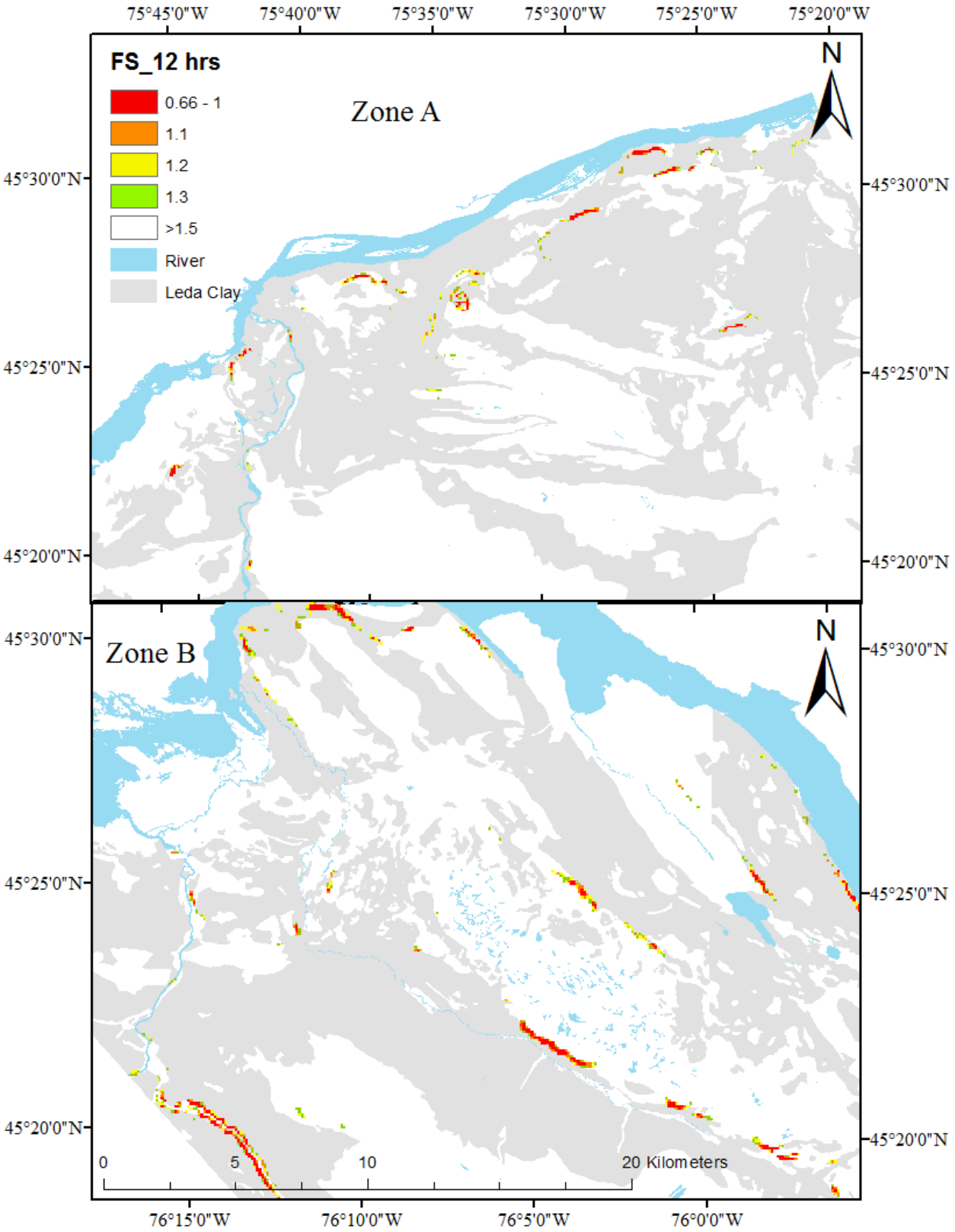

Figure 4–15B FS map and areas prone to landslides for rainfall duration of 12 hrs (worst case scenario).

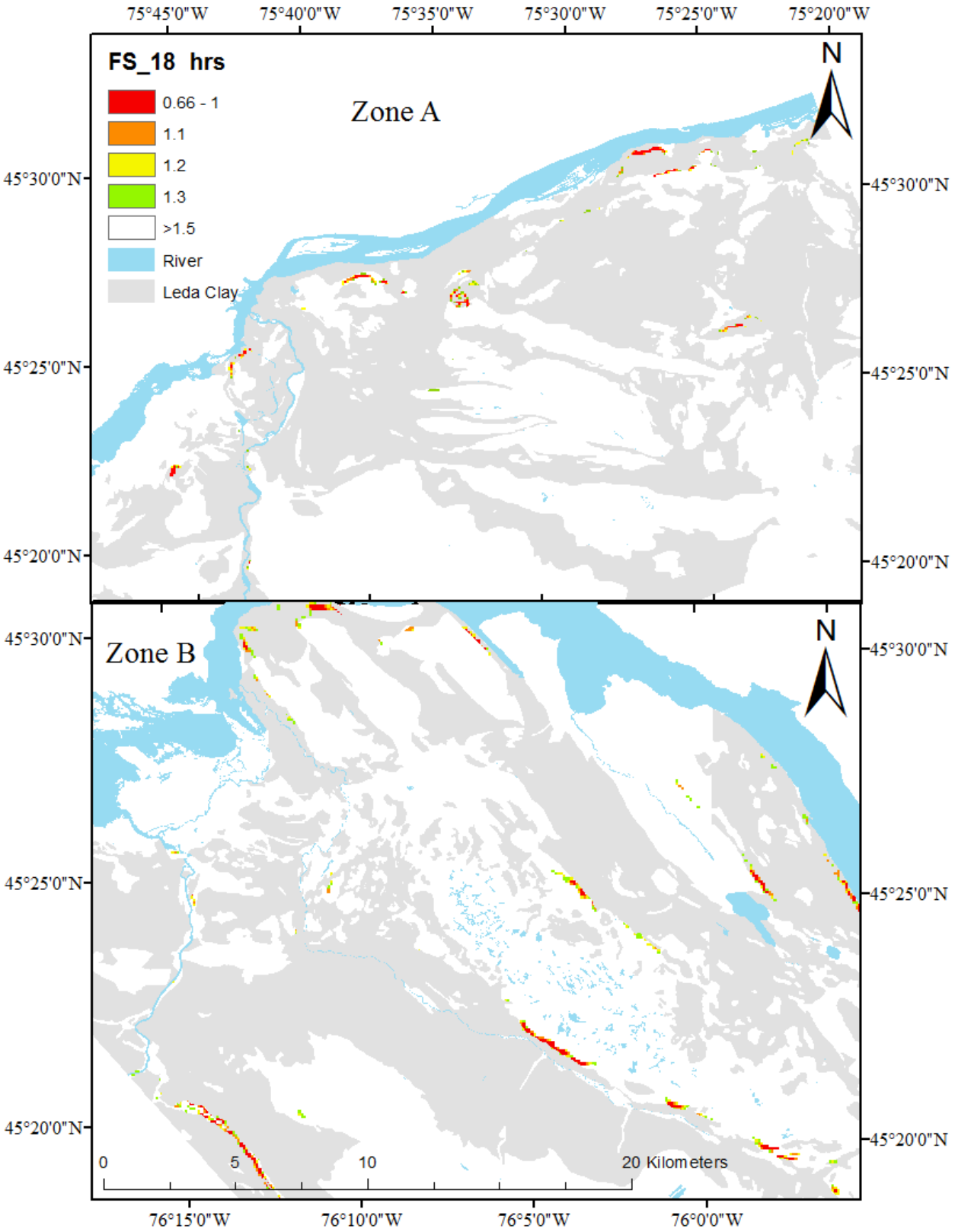

Figure 4–16A FS map and areas prone to landslides for rainfall duration of 18 hrs (normal case scenario).

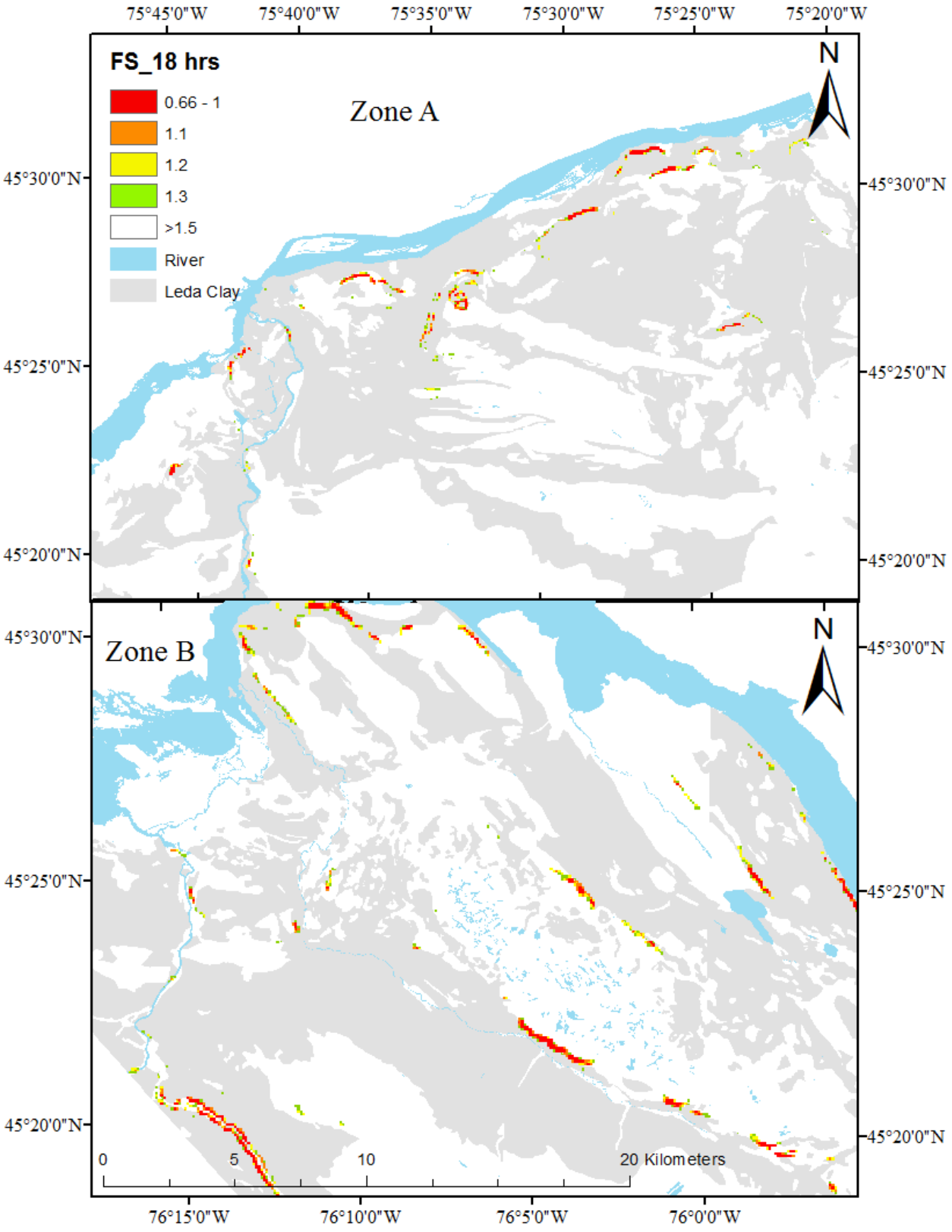

Figure 4–16B FS map and areas prone to landslides for rainfall duration of 18 hrs (worst case scenario).

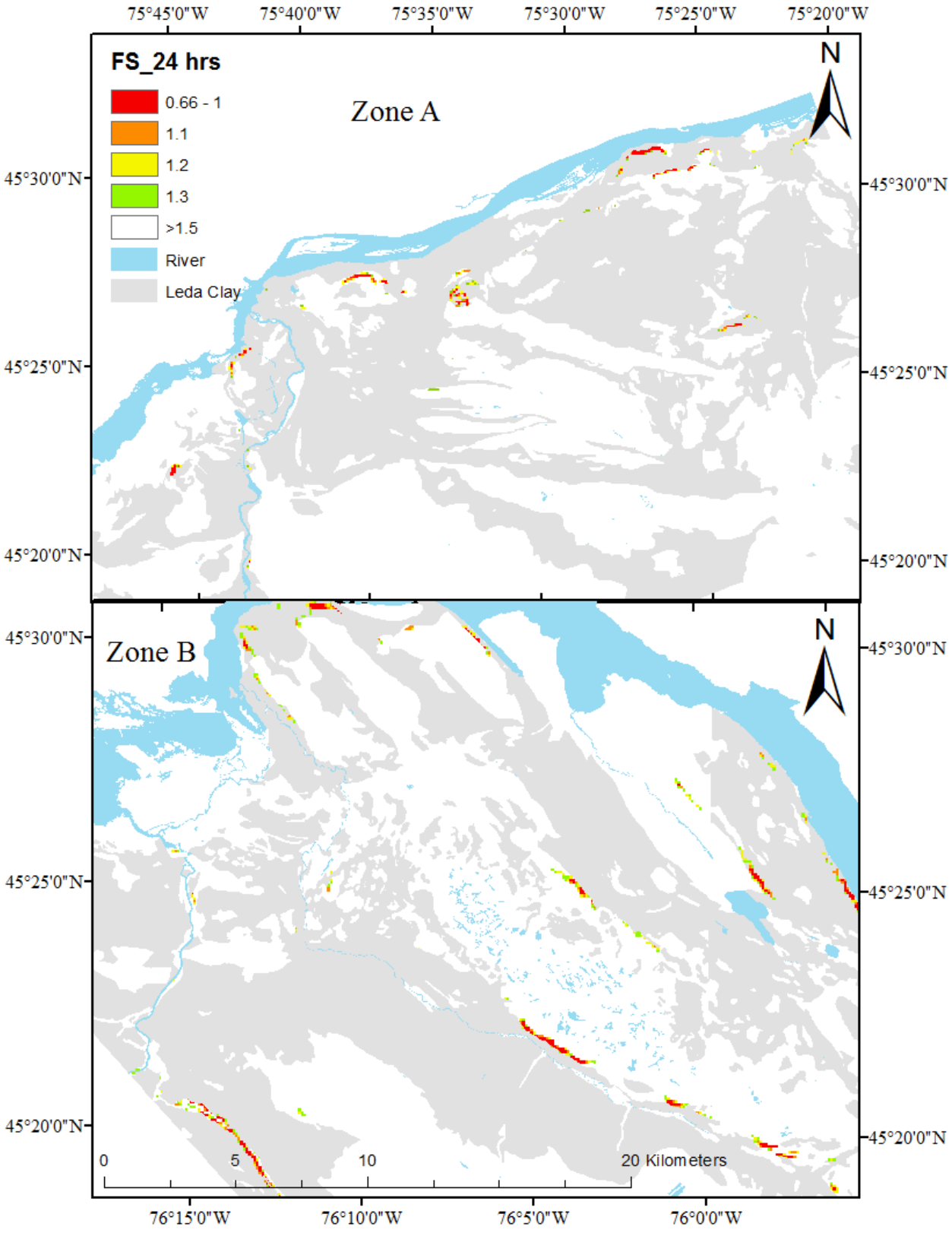

Figure 4–17A FS map and areas prone to landslides for rainfall duration of 24 hrs (normal case scenario).

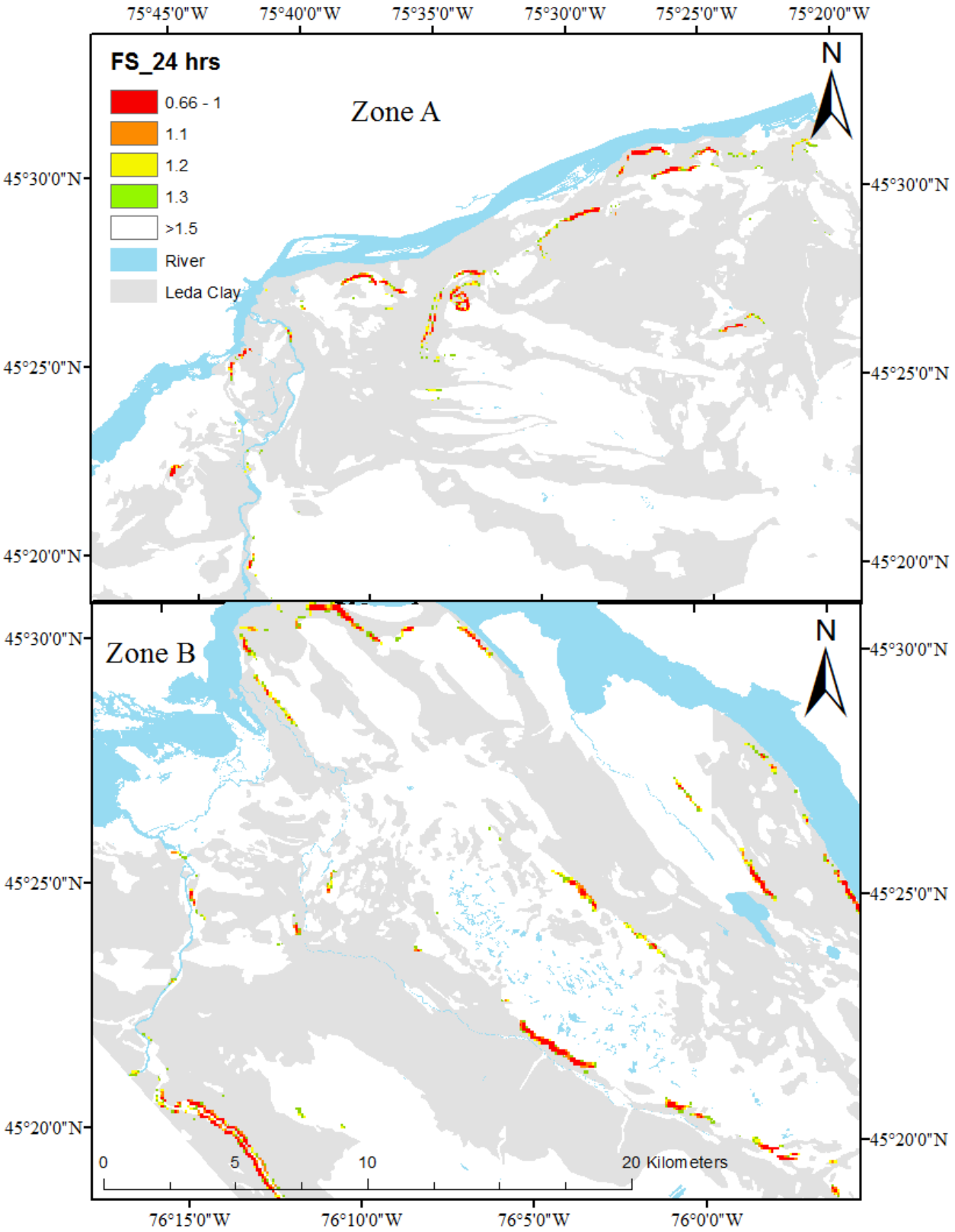

Figure 4–17B FS map and areas prone to landslides for rainfall duration of 24 hrs (worst case scenario).

4.12 Conclusions

The GIS-TRIGRS model was developed and applied to the Ottawa region, an area consisting of primarily sensitive marine clays. This model can be used to assess the susceptibility of landslide due to rainfall. The validation of model results indicated that predicted areas that are susceptible to rainfall-induced landslide were found to be in good agreement with historical landslide occurrences. The results have also revealed that not all previous landslides recorded in these sensitive marine clays are due to rainfall events. Other factors, such as snowmelt and/or earthquakes may have triggered the landslides. The application of the GIS-TRIGRS model to the studied area has allowed for the identification of the Leda clay slopes most prone to rainfall-induced and has explained the triggering mechanism of landslides in these Leda clay formations. This model determined that areas in eastern and western Ottawa were susceptible to landslides induced by rainfall. This was found to be true due to the Leda clay and steep slopes in the area. The study also reveals that Ottawa landslides are typically triggered by rainfall events of low intensity (4.5 mm/h) and long duration (24 hrs). This is because these rainfall events more commonly result in the infiltration of water into the Leda clay formations, of which the upper parts remain unsaturated. This infiltration will result in the reduction of the shear resistance of Leda clay (due to a reduction in the matric suction), and thus, a reduction in the safety factor and slope stability. The method and GIS-based tool for the assessment of rainfall-induced landslides in Ottawa sensitive marine clays developed in this study can serve to optimize the planning designs in land development in the city of Ottawa.

4.13 References

Atkinson, P.M., Massari, R., 1998. Generalized linear modelling of landslide susceptibility in the central Apennines, Italy. Computers & Geosciences 24, 373– 385.

Auld, H., Don, M., Joan, K., Shouquan, C., Neil. C., Sharon, F. 2009. Adaptation by design: climate, municipal infrastructure & buildings in the Ottawa area. Environment Canada.

Aylsworth, D.E., Lawrence and Evans, S.G., 1997. Landslide and settlement problems in sensitive marine clay, Ottawa Valley. Geological Survey Canada.

Aylsworth, J.M., and Hunter, J.A., 2004. A geophysical investigation of the geological controls on landsliding and soft deformation in sensitive marine clay nearOttawa.57TH Canadian

Geotechnical Conference.5th Joint Cgs/Iah-Cnc Conference. Geological Survey of Canada, Ottawa, Ontario, Canada

Baum, R. L., Savage, W. Z., Godt, J. W., 2002. TRIGRS - a Fortran program for transient rainfall infiltration and grid-based regional slope-stability analysis. U.S. Geological Survey.

Baum, R.L., Savage, W.Z., Godt, J.W., 2008. TRIGRS - a Fortran program for transient rainfall infiltration and grid-based regional slope stability analysis, Version 2.0. U.S. Geological Survey. Accessed: http://pubs.usgs.gov/of/2008/1159/

Bhandary, N.P., Yatabe, R., Kumar Dahal, K., Hasegawa, S., Inagaki, H., 2013.Areal distribution of large-scale landslides along highway corridors in central Nepal. Georisk 7 (1), p.1–20.

Bordoni, M., Meisina, C., Valentino, R., Bittelli, M. and Chersich, S., 2015. Site-specific to local-scale shallow landslides triggering zones assessment using TRIGRS. Natural Hazards & Earth System Sciences, 15(5).

Brooks G.R., MedioliB.E.,Aylsworth J.M., Lawrence D.E., 2013. A compilation of radiocarbon dates relating to the age of sensitive clay landslides in the Ottawa valley, Ontario Québec. Geological Survey Of Canada Open File 7432.

Burgess, M.M., Lawrence, D.E., MacDonald, J., Desrochers, D.T., 1995. Hot spots on wood chip insulated slopes, Norman wells pipeline, Northwest Territories. Geological Survey of Canada, open file 3093.

Canadian Council of Professional Engineers, 2008. Adapting to climate change Canada's first national engineering vulnerability of public infrastructure. Public Works and Government Services Canada and Engineers Canada.

Carrara, A., Cardinali, M., Detti, R., Guzzetti, F., Pasqui, V., Reichenbach, P., 1991.GIS techniques and statistical models in evaluating landslide hazard. Earth Surface Processes and Landforms 6, 427–445

Carrara, A., Guzzetti, F. (Eds.), 1995.Geographical information systems in assessing natural hazards. Kluwer Academic Publisher, Dordrecht, The Netherlands. 353 pp.

Chen, H.X., Zhang L.M., GaoL., Zhu H., Zhang S. 2015. Presenting regional shallow landslide movement on three-dimensional digital terrain. Engineering Geology 195:122-134.

Chen, H.X., Zhang, L.M., 2014. A physically-based distributed cell model for predicting regional rainfall-induced shallow slope failures. Department of Civil and Environmental Engineering, The Hong Kong University of Science and Technology, Clear Water Bay, Hong Kong Engineering Geology (176): p.79–92. Chris, R., Associates Inc. Ottawa – Fall 2012.

Chung, C. F., Fabbri, A. G., 1999. Probabilistic prediction models for landslide hazard mapping. American Society for Photogrammetry and Remote Sensing. Vol. 65, No. 12, pp. 1389-1399.

Dai, F.C., Lee, C.F., 2001. Terrain-based mapping of landslide susceptibility using a geographical information system: a case study. Canadian Geotechnical Journal 38, p. 911 – 923.

Jack, R. and Montminy, S., 2007. Rideau canal pedestrian bridge-20 years from conception to construction. In 2007 Annual Conference and Exhibition of the Transportation Association of Canada: Transportation-An Economic Enabler (Les Transports: Un Levier Economique).

DHV Consultants BV & DELFT Hydraulics, with HALCROW, TAHAL, CES, ORG & JPS, 2002. How to analyse rainfall data. Hydrology Project Training Module, New Delhi. http://www.cwc.gov.in/main/HP/download/12%20How%20to%20analyse%20rainfall%20data.pdf

Eden, W. J., Jakrett, P. M., 1971.Landslide at Orleans, Ontario. Tech. Paper 321, Division of Building Research, National Research Council

Eden, W.J., Mitchell, R.J., 1969.The mechanics of landslides in Leda Clay. Canadian Geotechnical Journal Vol 7 (3): p. 285-296.

Fall, M., 2009. A GIS-based mapping of historical coastal cliff recession. Bulletin of Engineering Geology and Environment 68(4): 473-482.

Fall, M., Azzam, R. 2001. Ingenieurgeologische und numerische Standsicherheitsanalysen der Basaltkliffe in Dakar, In International Journal Felsbau 19 (1): 51-57.

Fall, M., Azzam, R., Noubactep., C., 2006. A multidisciplinary study of the stability of natural slopes and landslide hazard mapping. Engineering Geology 82 (4): p. 241-263.

Fall, M., Dia, A., Fall, Meï.,Gbaguidi, I., Diop, I. 1996. Uncasd'instabilité de pentenaturelle: le versant des madeleines: analyse, cartographie des risques et prévention. In Bulletin of Engineering Geology and Environment 53: 65-74.

Fransham, P. B., Gadd, N. R. 1977. Geological and geomorphological controls of landslides in Ottawa Valley, Ontario, Geological Survey of Canada. Presented at the 29th Canadian Geotechnical Conference, Vancouver, B.C. Accessed: http://mysite.science.uottawa.ca/idclark/courses/GEO2334_files/Lectures/Week%202/Fransham%20and%20Gadd%20Landslides%20in%20Ottawa%20valley.pdf

Fredlund, D. G., Xing, A. 1994. "Equations for die lOiJ-water characteristic curve."Can. Geotech.J., 31, p.533-.546.

Gagnéa, S. A., Eigenbrod, F., Bert D. G., Cunnington G. M., Olson, L.T., Smith, A. C., Fahrig, L., 2015. A simple landscape design framework for biodiversity conservation. Landscape and Urban Planning 136 p.13–27.

Godt, J.W., Baum, R.L., Savage, W.Z., Salciarini, D., Schulz, W.H., Harp, E.L., 2008. Transient deterministic shallow landslide modeling: requirements for susceptibility and hazard assessments in a GIS framework. Eng. Geol. 102 (3), p. 214–226.

Golder Associates Ltd. 2008. Geotechnical investigation proposed commercial building 1455 Youville drive, Ottawa, Ontario.
http://webcast.ottawa.ca/plan/All_Image%20Referencing_Site%20Plan%20Application_Image%20Reference_D07-12-12-0132%20Geotechnical%20Investigation.PDF.

Guzzetti, F., Carrara, A., Cardinali, M., Reichenbach, P., 1999. Landslide hazard evaluation: a review of current techniques and their application in a multi-scale study, central Italy. Geomorphology 31 (1–4), 181– 216.

Haché, R., Nader A., Gudina S., Fall, M., 2015. Evaluation of the undrained shear strength of Champlain Sea clays (Leda) in Ottawa.GeoQuebec 2015 – the 68th Canadian Geotechnical Conference (CGC) and 7th Canadian Permafrost Conference, Sep. 20-23 2015, Quebec, Canada CD rom.

Hasegawa S., Dahal, R.K., Yamanaka, M. Bhandari, N.P. Yatabe, R, Inagaki, H. 2009. Causes of large landslides in the Lesser Himalaya of central Nepal. Environ Geol 57:1423-1434.

Houle Chevrier Engineering Ltd. 2013.Geotechnical Investigation Proposed Garden Centre 2710 March Road, Ottawa, Ontario.
http://webcast.ottawa.ca/plan/All_Image%20Referencing_Site%20Plan%20Application_Image%20Reference_D07-12-13-0162%20Geotechnical%20Report.PDF

Consulting Engineers Ltd. 2014 The Pond Clinic,

Geospatial Foundation 2015 Provincial Groundwater Monitoring Network (PGMN) Program: Groundwater Level Data, Groundwater Chemistry Data, https://www.javacoeapp.lrc.gov.on.ca/geonetwork/srv/en/metadata.show?id=13677

Hugenholtz, C.H., Lacelle, D., 2005. Geomorphic Controls on Landslide Activity in Champlain Sea Clays along Green's Creek, Eastern Ontario, Canada. Physical Geography and Quaternary, vol. 58, No. 1, p. 9-23

Inspec-Sol Inc., Engineering Solutions, 2014. Technical memorandum – geotechnical update commercial development 2717 Stevenage Drive Ottawa, Ontario, Reference No.: T020952-A1.

Iverson, R.M., 2000. Landslide triggering by rain infiltration. Water Resource Res 36:1897–1910.

Kollaard Associates, 2013. Additional geotechnical investigation proposed light industrial building 1358 Coker Street Osgoode Ward, Greely, City Of Ottawa, Ontario. http://webcast.ottawa.ca/plan/All_Image%20Referencing_Site%20Plan%20Application_Image%20Reference_D07-12-13-0086%20Geotechnical%20Study%20FINAL.PDF

L'Heureux, J.S., Eilertsen, R.S., Glimstad, S., Issler, D., Solberg, I.-L., &Harbitz, C.B. 2012. The 1978 quick clay landslide at Rissa, mid-Norway: subaqueous morphology and tsunami simulations. In: Y. Yamada et al. (eds.), Submarine Mass Movements and Their Consequences, Advances in Natural and Technological Hazards Research 31, Springer Science+Business Media B.V. DOI 10.1007/978-94-007-2162-3_45.

Lee, C.T., and Fei, L.Y., 2015. Nationwide landslide hazard analysis and mapping in Taiwan. In: Engineering Geology for Society and Territory, Springer International Publishing, Vol. 2, pp. 971-974.

L'Heureux, J S, 2013. Natural Hazards project, Work Package 6 - Quick clay, Characterization of historical quick clay landslides and input parameters for Q-Bing. Publisher: Norwegian Water Resources and Energy Directorate in collaboration with Norwegian Public Roads Administration and Norwegian National Railways Administration. Prepared by Norwegian Geotechnical Institute (NGI).

Li, WC Lee, L.M., Cai, H., Li, H.J., Dai, F.C., Wang, M.L. 2013. Combined roles of saturated permeability and rainfall characteristics on surficial failure of homogeneous soil slope. Eng. Geol, 153:105-113.

Mukhlisin, M., Iyias, I., Al Sharif, S., Khairul, N., &Mohd, R. T., 2010. GIS based landslide hazard mapping prediction in UluKlang, Malaysia, ITB J. Sci. Vol. 42 A, No. 2, p. 163-178

Nader, A., Fall, M., Hache, R., 2015. Characterization of sensitive marine clays by using cone and ball penetometers – example of clays in Eastern Canada. Journal of Geotechnical and Geological Engineering, DOI 10.1007/s10706-015-9864-x.

Park, D. W., Nikhil, N. V., Lee, S. R., 2013a. Landslide and debris flow susceptibility zonation using TRIGRS for the 2011 Seoul landslide event. Korea Advanced Institute of Science and Technology, Daejeon, Republic of Korea.

Park H. J." Lee J. H., Woo Ik. 2013b. Assessment of rainfall-induced shallow landslide susceptibility using a GIS-based probabilistic approach. Engineering Geology 161:1-15

Quinn, P. E., 2009. Large landslides in sensitive clay in Eastern Canada and the associated hazard and risk to linear infrastructure. PhD thesis, Queen's University Kingston, Ontario, Canada.

Raia, S. M., Alvioli, M., Rossi, R.L., Baum, J.W., Godt, F., Guzzetti, 2014. Improving predictive power of physically based rainfall-induced shallow landslide models: a probabilistic approach. 1CNR IRPI, via Madonna Alta 126, 06128 Perugia, Italy.US Geological Survey.

Rogojin, V., 2014. Provincial Groundwater Monitoring Network (PGMN) Program: Groundwater Level Data, Groundwater Chemistry Data, and precipitation Data. Metadata Management Tool (LIO). Ministry of Environment (Ontario). Accessed:

Salciarini D., Godt J.W., Savage W.Z., Pietro C., Baum R.L., Michael J.A., 2006. Modeling regional initiation of rainfall-induced shallow landslides in the eastern Umbria Region of central Italy. Landslides 3:181–194 DOI 10.1007/s10346-006-0037-0

Salciarini, D. D., Godt, J.W., Savage, W.Z., Baum, R. L., Conversini, P., 2008. Modeling landslide recurrence in Seattle, Washington, USA. Engineering Geology 102, p. 227–237.

Schut, L.W., Wilson, E.A, 1987. The soils of the regional municipality of Ottawa - Carleton, Report No. 58 Of the Ontario Institute of Pedology Volume 1. Accessed http://sis.agr.gc.ca/cansis/publications/surveys/on/on58/on58-v1_report.pdf

Singhroy, V.K.E., Mattar, A.L., Gray, 2000. Landslide characterization in Canada using interferometric SAR and combined SAR and TM images. Canada Centre for Remote Sensing, 588 Booth St., Ottawa, Canada, K1A 0Y7.

Sorensen, K.K., Okkels, N., 2013. Correlation between drained shear strength and plasticity index of undisturbed over consolidated clays. Proceedings of the 18th International Conference on Soil Mechanics and Geotechnical Engineering, Paris.

Sorooshian, S., Li, W., Yusof Ismail, M.D., 2015. Landslide susceptibility mapping: a technical note. Vol. 20 [2015], Bund. 22.

Srivastava, R. T.C., Yeh, J., 1991. Analytical solutions for one-dimensional, transient infiltration toward the water table in homogeneous and layered soils. Water Resour. Res. 27: 753-762

Stantec Consulting Ltd., 2010.Geotechnical Inventory and Evaluation, Johnston Road Land Use Study. City of Project No. 122410116 (1042983).

Taha, A. M. 2010. Interface shear behavior of sensitive marine clays-Leda clay. Master thesis, University of Ottawa, 152 p.

Taha, A.M., Fall, M., 2014. Shear behavior of sensitive marine clays - concrete interface. Journal of Geotechnical and Geo-Environmental Engineering, 139(4): p. 644–650.

Terzaghi, K., 1943. Theoretical soil mechanics. John Wiley and Sons, New York. 510 pp.

Thapa, P. B. and Esaki, T., 2007. GIS-based quantitative landslide hazard prediction modeling in natural hillslope, Agra Khola watershed, central Nepal, Bulletin of the Department of Geology, Tribhuvan University, Kathmandu, Nepal, Vol. 10, p. 63–70.

Trow Associates Inc., 2010. Updated geotechnical investigation proposed residential development 280-282 Crichton Street, Ottawa, Ontario, Trow Associates Inc., Accessed http://webcast.ottawa.ca/plan/All_Image%20Referencing_Site%20Plan%20Application_Image%20Reference_Geotechnical%20Study%20D07-12-10-0219.PDF

Van Westen, C.J., Rengers, N., Terlien, M.T.J., 1997. Prediction of the occurrence of slope instability phenomena through GIS-based hazard zonation.GeologischeRundschau 86, 4004– 4414.

www.chrisrobinsontravelshow.ca.

Wu, Y. and Li, W., 2014. 'A GIS based landslide susceptibility mapping using multi-criteria decision analysis model at a regional scale' The Electronic Journal of Geotechnical Engineering, 20(12), 4445-4460.

Yeh, H. F., Lee, C. C., Lee, C.H., 2008. A rainfall-infiltration model for unsaturated soil slope stability. Department of Resources Engineering, National Cheng Kung University Tainan 701, Taiwan. J. Environ. Eng. Manage, 18(4), p. 261-268.

Zhao, H.F., Zhang, L.M., 2014. Instability of saturated and unsaturated coarse granular soils. J. Geotech. Geoenviron. Eng. ASCE 140 (1), p. 25–35.

CHAPTER 5

5 Technical Paper II: GIS-Based Modeling of Snowmelt-Induced Landslide Susceptibility of Sensitive Marine Clays

Mohammad Al-Umar, Mamadou Fall, Bahram Daneshfar,
Department of Civil Engineering – University of Ottawa, Ottawa, Ontario, Canada

Abstract

Landslides triggered by snowmelt or a snowmelt-rainfall combination during spring are common in slopes made of sensitive marine clays, particularly in the Ottawa region (Canada). In this study, a Geographic Information System (GIS)-based tool is developed to assess and predict the snowmelt-induced landslides in areas of sensitive marine clays in the Ottawa region. Topographic, geologic, hydrologic, and geotechnical information of the study area, in addition to snowmelt intensity data for different periods, was required to conduct this modeling study. Snowmelt intensity records for periods of 6–48 hours, 3–15 days, 25 days, and 30days, as well as the information on historical landslides in the study area, were used to examine both the timing and location of shallow landslides due to snowmelt across the Ottawa region in a GIS-based framework. The developed model is validated by comparing the predicted landslide-susceptible areas with the historical landslide maps in the study area. A good agreement between the predicted and recorded historical landslides was obtained, which suggests that the developed GIS-based model can predict relatively well the snowmelt-induced landslide susceptibility in the sensitive marine clays. The modeling results show that high slope areas of sensitive marine clay are more prone to snowmelt-induced landslides. As a result, this developed GIS-TRIGRS modeling approach can be considered a potential tool for assessing and/or predicting snowmelt-induced landslides in different areas of the Ottawa region.

Keywords: Leda Clay, Snowmelt, GIS, TRIGRS, Landslide, Sensitive Clay

5.1 Introduction

There are many types of soils that cause geotechnical problems. Sensitive marine clay is one of these soils; they will significantly lose their shear strength if their structure is disturbed. During the last glacial era, glaciers covered many areas of the world, especially in the northern regions of the earth. These areas are found to contain these problematic soils(Theenathayarl 2015).These include the state of Alaska in the United States, as well as many other countries, such as Canada, Sweden, and Norway. The provinces of Quebec and Ontario (particularly in the Ottawa region) in Canada have sensitive marine clays (locally called Leda clay or Champlain sea clay), which cover relatively large areas. These Canadian marine clays, younger than 12,000 years, are considered to be young glacial deposits (Haché et al., 2015; Taha, 2010).

Several landslides have previously occurred in these soils. For instance, there were over 500 victims due to 1,345 landslide events occurring in the Norwegian Gaula Valley. In 1893, 116 people died because of a sensitive marine clay (quick clay) landslide that occurred in Verdal (L'Heureux, 2013). In Sumatra, significant shearing of highly sensitive marine clay was suggested for a landslide event that occurred along the length of the Siak River bank in 1993. Moreover, numerous landslides have also occurred in the Canadian sensitive marine clay formations (see Figure (5-1)). Aylsworth et al. (1997) indicated that three landslide episodes took place in different areas or localities of the Ottawa region (Ontario province), such as Orleans, Beacon Hill in Gloucester, and the city of Casselman. A key trigger of these landslides has been identified as snow melting in the spring (Quinn, 2009). Ontario has a continental climate that sees great amounts of snowfall in the winter. Winter precipitation is typically stored as snow or ice on the ground. During the snowmelt in the spring, huge quantities of snowmelt water is released, which has a negative effect on the stability of the slopes.

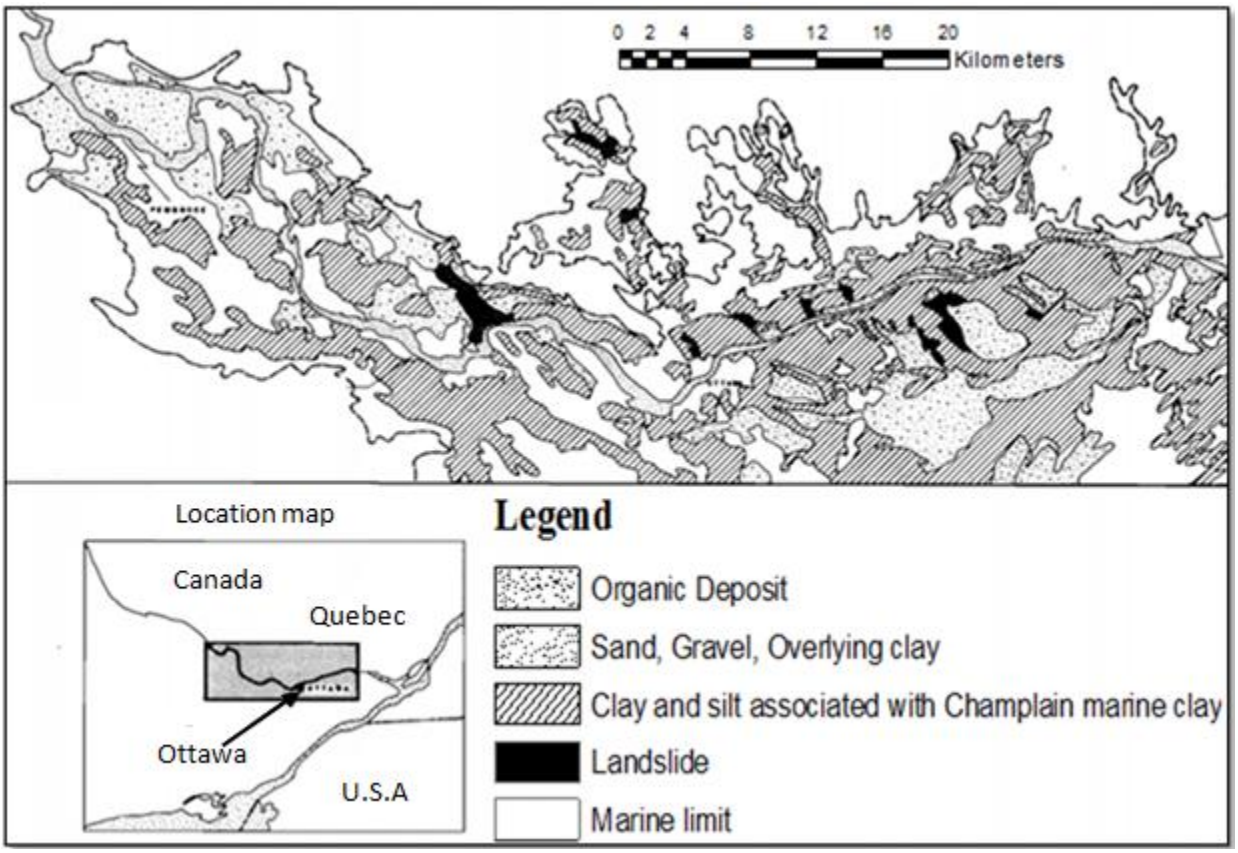

Figure 5-1 Distribution of sensitive clay and associated landslides in Ottawa Valley Modified from Gadd (1977).

As the population of the Ottawa region is steadily rising (currently at approximately 900,000) (City of Ottawa, 2015) there is a continuous growth in infrastructure facilities, including residential and other buildings, transportation infrastructure, and utilities located on the problematic marine clay. However, the presence of sensitive clay slopes in the Ottawa region and presence of snowmelt in the spring, poses a landslide hazard for both the population and infrastructure (Nader et al., 2015; Taha, 2010; Quinn, 2009). A good engineering practice to reduce this landslide hazard and potential impact on people and infrastructure is to identify or assess the sensitive marine slopes that are susceptible to snowmelt-induced landslides, as well as develop a tool that can assess and predict these snowmelt-induced landslides in Ottawa sensitive marine clay. Indeed, landslide susceptibility mapping is an important tool for decision-making processes with respect to protecting the population and infrastructure against marine clay landslides (Nader et al., 2015).However, until now, no tool has been developed to assess and map the sensitive clays slopes in Ottawa that are susceptible to landslides induced by snowmelt. This knowledge gap is addressed in the present study.

It should be emphasized that studies on snowmelt-induced landslides are rare compared to rainfall-induced landslides. For instance, in the Clearwater River Basin in Central Idaho, Gorsevski et al. (2000) used a Digital Elevation Model (DEM) to derive analyses of snowmelt and rainfall triggered landslides on a small watershed named Rocky Point. Kimura et al. (2014) used a probabilistic approach to estimate landslide hazard. According to the topography for the study area, GIS analysis was used to classify these landslides into three groups. Khezri et al. (2013) used a GIS system to predict landslide susceptibility in the central Zab basin of the West-Azerbaijan province in Iran. This study, claims that the key factor of mass movement is the sudden melting of snow as a result of the presence of water in the soil, increasing the porewater pressure and hydrostatic level. The final results classified a landslide map into five classes of risk assessment: very low, low, moderate, high and very high. The area for each class covered 95.46 km^2, 100.46 km^2, 46.1 km^2, 158.38 km^2 and 120.96 km^2, respectively. Kawagoe et al. (2009) analyzed snowmelt's effect on landslide occurrence by using a probabilistic model based on multiple logistic regression analysis. The analysis included several parameters pertinent to landslide occurrence including hydraulic, geographical, and geological parameters. The analysis was executed by using a logistic regression model to produce landslide susceptibility maps across Japan. The results revealed that across Western Japan (throughout the mountain ranges near the Japan Sea), there exists a 95 percent landslide probability. Ayalew et al. (2004) created a landslide susceptibility map near the Agano River in Tusgawa using a GIS based analysis of the spatial database collected for 791 landslides. Most often, landslides were triggered by heavy amounts of snow and rainfall. Ayalew's analysis found that landslides were concentrated in the mid-slopes of the Tusgawa region in areas consisting of weak rocks (e.g., sandstone, mudstone, and tuff). However, no studies on snowmelt induced landslides in the sensitive marine clays in the Ottawa have been conducted.

Several approaches have been established to evaluate landslide susceptibility and identify the potential of unstable slopes/regions. Such approaches can be divided into three key groups: (i) expert evaluation (i.e. inventory, heuristic approaches), (ii) statistical approaches, and (iii) deterministic approaches (Quinn, 2009; Fall et al., 2006; Van Westen et al., 1997). The advantages and disadvantages of each technique have been outlined in numerous publications (e.g. Fall et al., 2006; Dai and Lee, 2001). Moreover, landslide susceptibility mapping in large areas usually involves the handling, processing, and interpretation of a large amount of geospatial data. Therefore, during the past decades, the Geographical Information System (GIS)

has been successfully used in several studies (Chen et al., 2015; Mukhlisin et al., 2010; Quinn, 2009; Thapa and Esaki, 2007; Chang et al., 1999) to conduct landslide susceptibility assessment and mapping. Additionally, the infinite slope stability model has also been merged with GIS to assess shallow landslide potential and the distribution of the factor of safety in a specified region (e.g., Sorooshian et al., 2015; Quinn, 2009; Fall, 2006; Van Westen et al., 1997). Furthermore, Transient Rainfall Infiltration and Grid-based Regional Slope-stability (TRIGRS) (Baum et al., 2008), a deterministic, spatially distributed model that combines a hydrologic 1-D transient infiltration model (Iverson, 2000) and an infinite slope stability model to calculate the factor of safety with respect to time and location, have been applied in several studies for modeling the timing and spatial distributions of shallow landslides and to compute their factor of safety with respect to time and location (e.g. Raia et al., 2014; Park et al., 2013; Salciarini et al., 2008). The TRIGRS model, when used for either saturated or unsaturated soils, is appropriate for shallow landslide susceptibility analysis. When using the infinite-slope approximation, the failure surface in each cell is considered to be of unlimited extent, planar, at a fixed depth, and parallel to the topographic surface (Raia et al., 2014). The application of models like TRIGRS in a GIS environment for landslide susceptibility evaluations requires digital spatial topographic, geologic, and hydrologic data in addition to any previous snowmelt and rainfall-induced landslide accounts, which are fundamental to test the model results (Baum et al., 2008; Baum et al., 2002). Based on the facts mentioned above, in this work, the TRIGRS model combined with GIS will be applied to the study area to assess snowmelt induced landslides, and to develop snowmelt induced landslide maps. This study aims to develop a GIS-TRIGRS model and map to assess the shallow and snowmelt-induced landslide susceptibility in sensitive marine clays in Ottawa.

5.2 Study Area

The Ottawa region Figure(5-2), is located between the latitudes of 45.00–45.50 N and the longitudes 75.50–76.00 W. Ottawa is located within the southeast part of the province of Ontario, with an approximate area of 2,778 km². The Ottawa region is bounded to the north by the Ottawa River. The historic Rideau River and Rideau Canal flow north to south across Ottawa city, which is positioned in the eastern part of the province of Ontario in Canada, and the region contains several municipalities (Gagnéa et al., 2015; Jack, 2007).

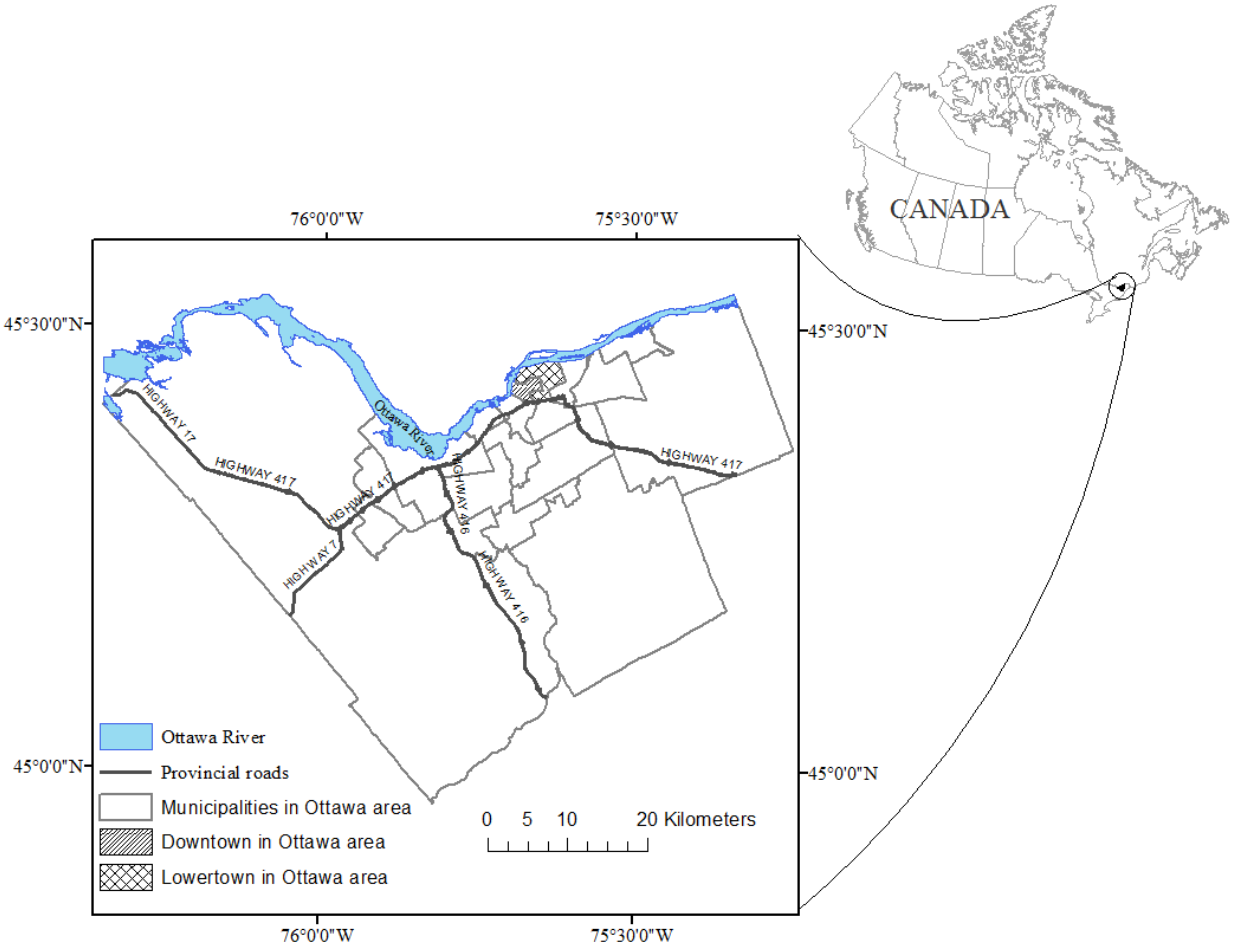

Figure 5-2 Study area (Ottawa region).

5.2.1 Geographic Setting and Geomorphology

Ottawa is a region consisting of gentle slopes ranging from 0 to 33 degrees; although, Western and Northern Ottawa maintain higher slopes prone to landslides. Along the southern bank of the Ottawa River, the city of Ottawa can be found. The oldest portion of the city lies between the Rideau Canal and the Ottawa River. Alternatively, the center of Ottawa covers the region just west of the canal (Jack, 2007).

5.2.2 Geological Setting

In the study area the stratigraphy is characterized by deltaic and estuarine soil consisting of fine to medium grained silty sands of 1.8 to 6 meter thickness underlain by the deposits of Ottawa sensitive marine clays, which were deposited within the Champlain Sea basin following previous glaciations. These deposits consist of glacial till overlain by relatively thick layers of sensitive marine silty clay deposits called Champlain Sea clay (also known as Leda Clay), which were deposited as a result of the recession of the Champlain Sea. This physiographic region is underlain by different types of sedimentary rocks (such as sandstones, dolostones, limestones and shales). In addition, the final deposits of silty sand overlie Champlain Sea clay. Organic soils (like peat) are also found in certain badly drained regions (Schut and Wilson, 1987). Although some may not exist in some areas, layers of peat, sand, clay, and glacial till are common types of soil material that are found in the entire area. Within the marine clays, two major units can be distinguished: the upper and lower unit. The upper unit mainly consists of sand thinly interbedded with silty sand, and locally overlay layers of clay, silty clay and silt, generally the higher parts are mottled or laminated reddish-brown and bluish-gray. The blue-gray clays dominate, and the laminations are less frequent (Schut and Wilson, 1987). The lower unit is blue-gray clay, sometimes mottled. Below the upper layer of clay are coarse galciofluvial and glacial lacustrine sediments that vary in thickness (up to one meter). These deposits lie atop relatively flat limestone (Schut and Wilson, 1987). The surface soils are deposits that occur as a result of the recession of the Champlain Sea. Although some areas may not contain some of these layers, the common types of soil material found across the entire area are peat, sand, clay, and glacial till (Stantec Consulting Ltd., 2010).

5.2.3 Geotechnical Characteristics of the Soils in the Study Area

In this study, geotechnical data was used in the GIS program. This data was obtained from geotechnical studies or reports and further completed by accredited companies in different sites within the city of Ottawa (Trow Associates Inc., 2010). All the samples of soil were visually tested in the field, specified, and logged by Inspec-Sol Inc. (2014), Kollaard Associates Engineers (2013), Houle Chevrier Engineering (2013), Stantec Consulting Ltd. (2010), and Golder Associates Ltd. (2008).

Based on these studies, the subsurface lithology of the study area entailed two layers of sensitive marine clay, a shallow layer of silty clay (1.8 to 5.25 meters in depth) and a deep layer of clay and clayey silt, between 6.5 and 12 meters in depth. Normal penetration tests values (SPT) of 5 to 10 blows and 5 to 20 blows were logged for the shallow layer and the deep layer, respectively. Furthermore, the liquid limit (LL) of the shallow layer varies from 22 to 80 percent, and the plasticity index (PI) is 8 to 48 percent, while in the deep layer, the liquid limit and plasticity index values were 50 to 70 percent and 28 to 52 percent, respectively. The specific gravity was discovered overall to be 2.70 to 2.80 for all of the sites in the reports as anticipated for clay (Houle Chevrier Engineering, 2013; Sorensen et al., 2013; Stantec Consulting Ltd., 2010; Trow Associates Inc., 2010; Golder Associates Ltd., 2008). The clay fractions were as well established from hydrometer testing as from the existing data in the reports. The clay fractions extend between 56 and 87 percent. The stated unit weights were between 14 and 22 kN/m^3. These values are in accord with those described in the literature (e.g., Taha and Fall, 2014; Quinn, 2009).

5.2.4 Climatic Conditions

Ottawa has a continental humid climate with an average annual relative humidity of 62.8 percent. The average monthly relative humidity ranges from 53 percent in May, to 75 percent in January. High temperatures are present in July, where the average daily maximum temperature is 23.5°C; comparatively, in winter, the mean daily minimum temperature is -16.4°C (Auld et al., 2009). The annual rainfall is 714 to 869.5 millimeters (Canadian Council of Professional Engineers, 2008). In Ottawa, snow and ice are typically present throughout the year except in July and August (see Figure (5-3)).

Generally, the most snowfall in the Ottawa region occurs from November to March with a snowfall range of 208 millimeters annually (Auld et al., 2009). The highest daily snowfall of 383 millimeters was recorded in Ottawa region in the years 1960 and 1971. The duration of the winter and snow are not steady in a typical winter in Ottawa; long-lasting snow cover starts from mid-December until early April. Freeze-thaw cycles take place during the winter with a few days lying well above the freezing point, followed by nights well below it (EEPL, 2014). Freezing rain and high wind chills are also very common. Summers are relatively warm and humid in Ottawa, even though they are typically short. Cold air from the north plays an important role in reducing humidity (EEPL, 2014).

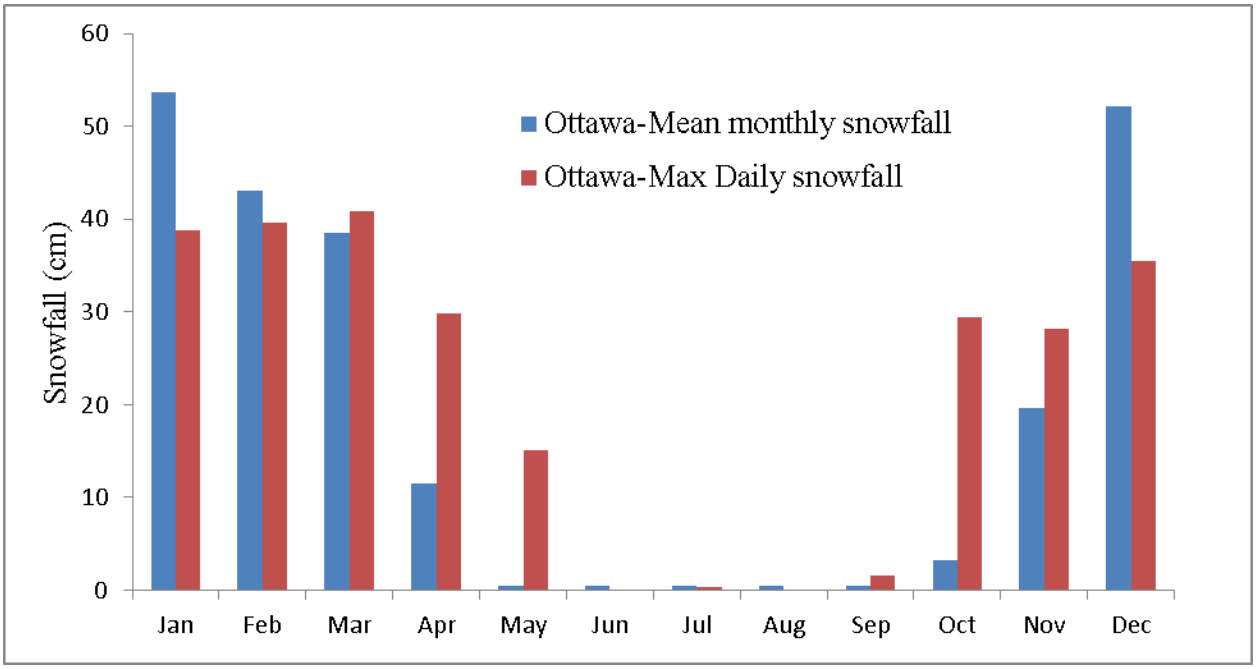

Figure 5-3 Mean monthly and maximum daily snowfalls (1981–2010), Ontario East (Modified from EEPL, 2014)

5.2.5 Historical Landslides

Numerous landslides have occurred in the Ottawa region in the past. Fransham and Gadd (1977) noted that several huge landslides promptly occurred once the Ottawa River sliced numerous broad channels over with sediment. This study was organized using 17 maps at a scale of 1:50,000 exhibiting how the spread of sensitive clay deposits and accompanying landslides in Ottawa Valley were gathered. Theses maps display the spreading of sensitive clay and related landslides in the Ottawa Valley. The site investigation results and radiometric age dating shows that the Ottawa region has suffered several prehistoric landslide events, one of which was in the year 4550 B.P., produced by geologically destructive earthquakes, causing widespread landslides in the region's sensitive marine clays. The magnitude of these earthquakes may have surpassed 6.5. In addition, in 1960, a landslide occurring in the year 1140 B.P. was discovered in the Beacon Hill area, located along a sharp, eroding edge in postglacial marine clay along the Proto-Ottawa River. The maximum retrogression was found to be around 260 meters, from the slope crest to the original surface. The volume of the landslide is of the order of magnitude 2.0 $\times 10^6$cubic meters. In the past century, other numerous landslides have been recorded. For instance, in 1971, a snowmelt landslide event occurred on the slopes in Casselman (Aylsworth et al., 2004; Aylsworth et al., 1997).

The sediments of Champlain Sea on the terrace over Orleans slopes were exposed to several landslides. However, noticeable developments in the home construction on the slopes of Orleans have hidden the construction traces that were shown in the aerial photos of the area before development. No comprehensive geotechnical analysis was available on the Orleans landslides. However, Eden and Jarrett (1971) provided a detailed geotechnical study on a small landslide that occurred in October 1965 close to the hillside cut near the Orleans Shopping Center. After five years, the landslide took place due to the hill's cut excavation. Landslides have also occurred on the South Nation River in the small city of Casselman, Ontario, sited about 50 kilometers east of Ottawa on Highway 417 on the South Nation River; heavy rainfall and snowmelt made the ground soil saturated, and thus, increased the landslide occurrence probability (Aylsworth et al., 1997). This landslide comprised an area of 280,000 square meters. The maximum distance of retrogression was 490 meters, and had a volume of 7×10^6 cubic meters.

There is a 20-kilometer range of the South Nation River downstream from Casselman that was the focal point of several landslides. Singhroy et al. (2000) presented outlines in the Ottawa Valley of the skill of linking airborne SAR and Landsat TM pictures, and interferometric means for organizing the morphological features of landslides. Airborne SAR pictures showed flow slides on sensitive marine clays in the Ottawa Valley. Hugenholtz et al. (2005) selected the Green Creek valley as a case study and extended it thorough aerial photograph profiles (1928 to 1999); since then, several landslides have followed. Rainfall is generally observed as a key hydrologic trigger for various kinds of landslides in the study area. Figure (5-4) shows the distributions of previously identified historical landslide zones in the study areas (Zones A and B). Zones A and B shield the areas exposed to landslides in both the eastern and western parts of the study area. It should be highlighted that, in the study area, it was assumed that the inventory of historical landslides is not complete since some might not have been identified or destroyed by human activities (e.g., land use, construction, excavation, or transportation facilities).

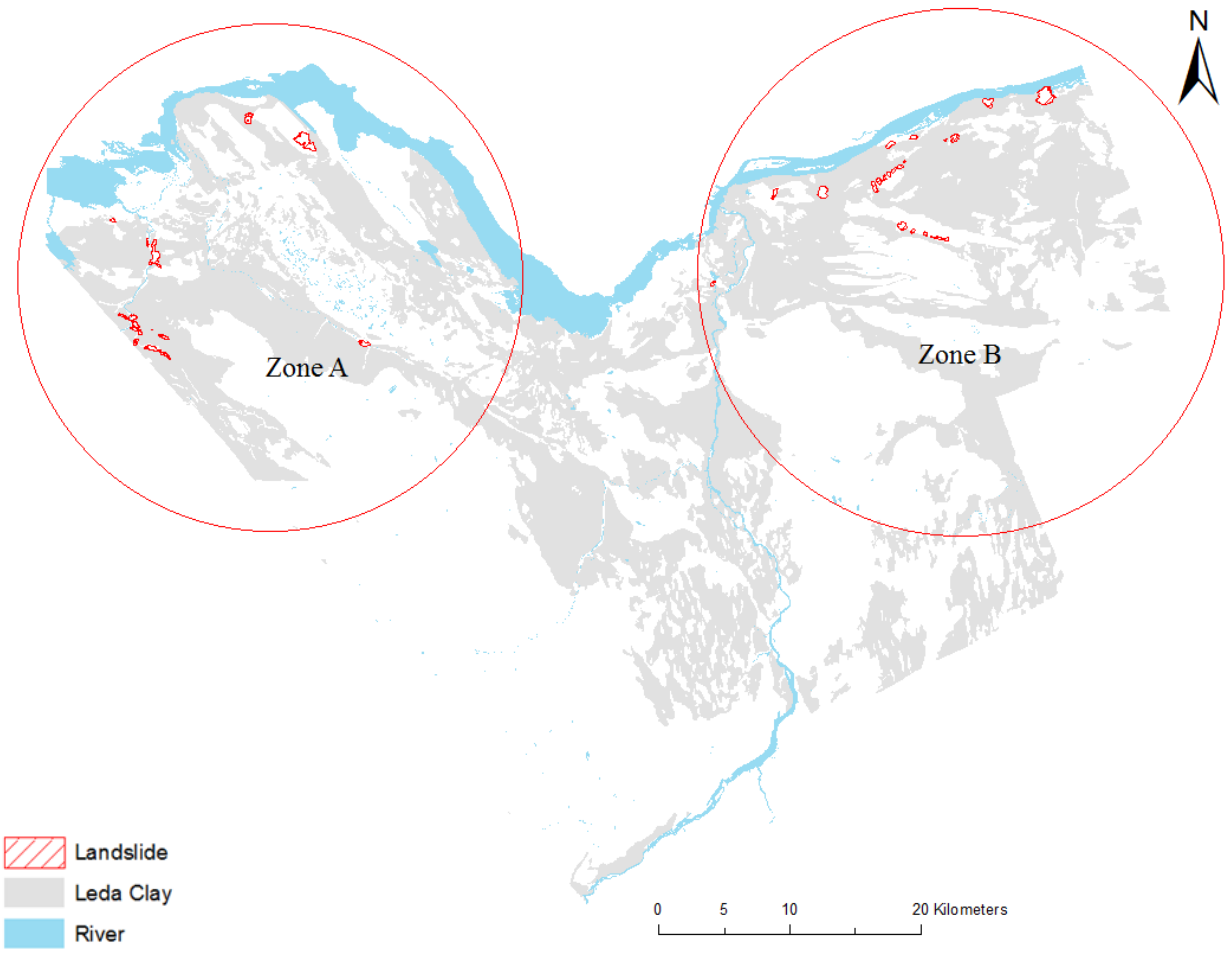

Figure 5-4 Distribution of areas subjected to landslides in the past (historical landslides) in both zones (A & B) as recorded in the literature.

5.3 Methodology

This study takes a multi-stage approach to evaluate landslide susceptibility induced by snowmelt. This methodology is summarized by the six main stages presented in the flowchart, Figure (5-5).

The first stage consists of collecting the input data needed for this study. This data includes information about the geotechnical characteristics as well as the climate, hydrogeological, and spatial data of the study area (Table 5-1). The government, consulting, and engineering agencies with extensive work experience throughout Ottawa sourced several key soil properties in the area. The property data retrieved from previous geotechnical investigations include standard penetration test (SPT) results, consistency limits (liquid limit, plastic limit, etc.),

shear strength parameters, moisture content, depth, thickness, and the relevant types of subsurface layers are all present in Table 1 (e.g. Trow Associates Inc. 2010; Taha 2010).Data for Ottawa snowmelt was gathered from Environment Canada. Snowmelt data was recorded at the Ottawa CAD station located in Ottawa from 1890 to 2007. The bar chart is shown in Figure (5-6) represents the relationship between the time of a recorded landslide and the corresponding snowmelt intensity. Greatest snowmelt intensity was recorded in 1960 and 1971. Snowmelt intensities were selected for periods of 6–48 hours, 3–15, 25, and 30 days.

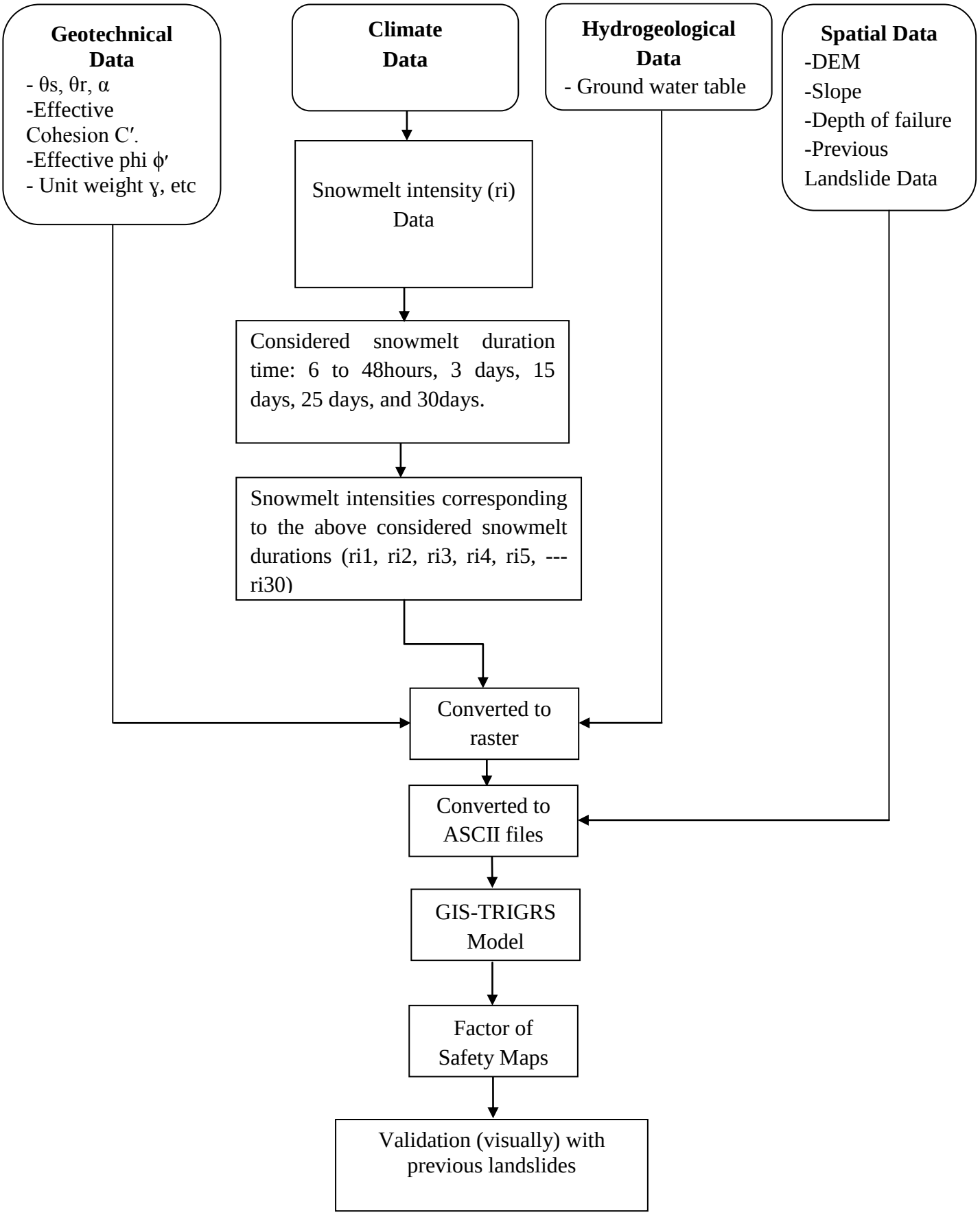

Figure 5-5 Methodology Flowchart.

By monitoring several hundred wells, hydrogeological data was collected by the Provincial Groundwater Monitoring Network (PGMN) Program. The PGMN program collected initial groundwater levels of the 474 wells by observing and monitoring water table on an hourly basis. The wells monitored were located at the interface between the soil and bedrock, allowing for easy retrieval of the pore water of each aquifer. Using each well's latitude and longitude, the location and elevation of each well were identified using the Provincial Digital Elevation Model (DEM) (Rogojin 2014). For this GIS-TRIGRS model, groundwater level recordings were used for March since snowmelt begins in spring in Ottawa.

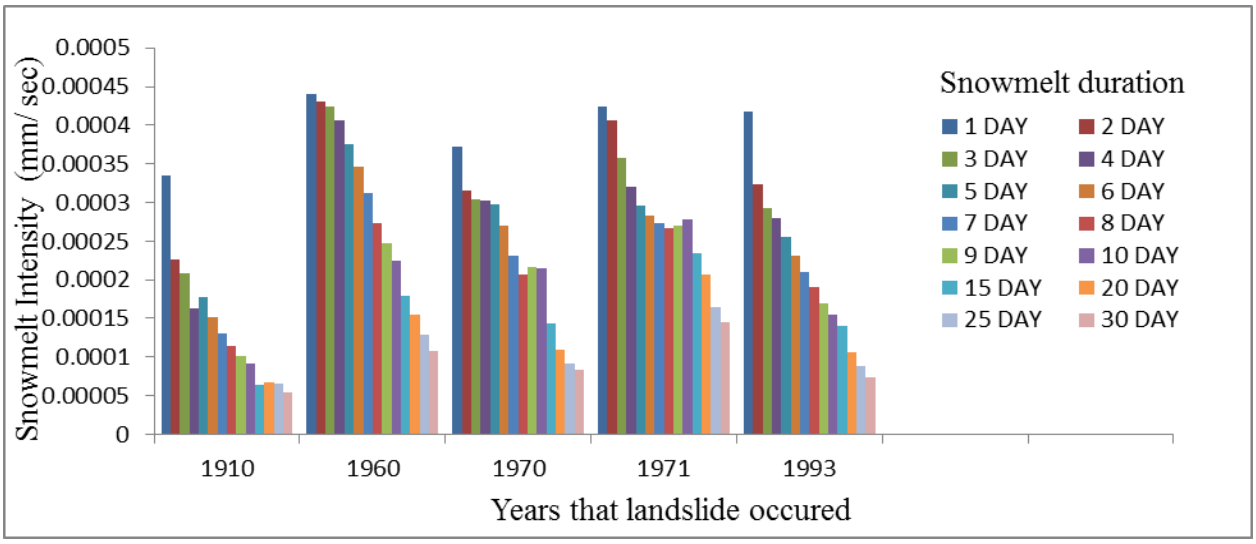

Figure 5-6 Relationship between snowmelt intensity and landslides that occurred in Ottawa region

Moreover, a suitable resolution and raster scale of 1:50,000 was used in the Digital Elevation Model (DEMs) published by the Natural Resources Canada. The DEM was applied to the GIS model to evaluate shallow landslide susceptibility modeling. The original DEM raster resolution of ten by ten meters was used, as applied to the high relief terrain evident in the study area. The terrain's slope was calculated using the Spatial Analyst in ArcGIS (see Figure (5-7A). The lower boundary raster was calculated by using the following exponential equation (1) by Godt et al. (2008):

$$d_{lb} = 7.72e^{-0.04\,\delta} \qquad (5-1)$$

Where d_{lb} represents the depth of failure (see Figure (5-7B)), δ is the slope angle. Additionally, raster images of the geological distribution of the sensitive clays in the study area were also generated (see Figure (5-7C)). The resolution of all created raster images was then

transformed to 25 by 25 meters to fit the TRIGRS requirement. Later, raster images for the acquired geotechnical information, and for snowmelt intensity for all periods, was generated for the entire study area. Furthermore, the digital data of the spatial distributions of the historical landslides identified in the study area was also acquired (see Figure (5-4)). This data is needed to test the landslide prediction ability of the developed model.

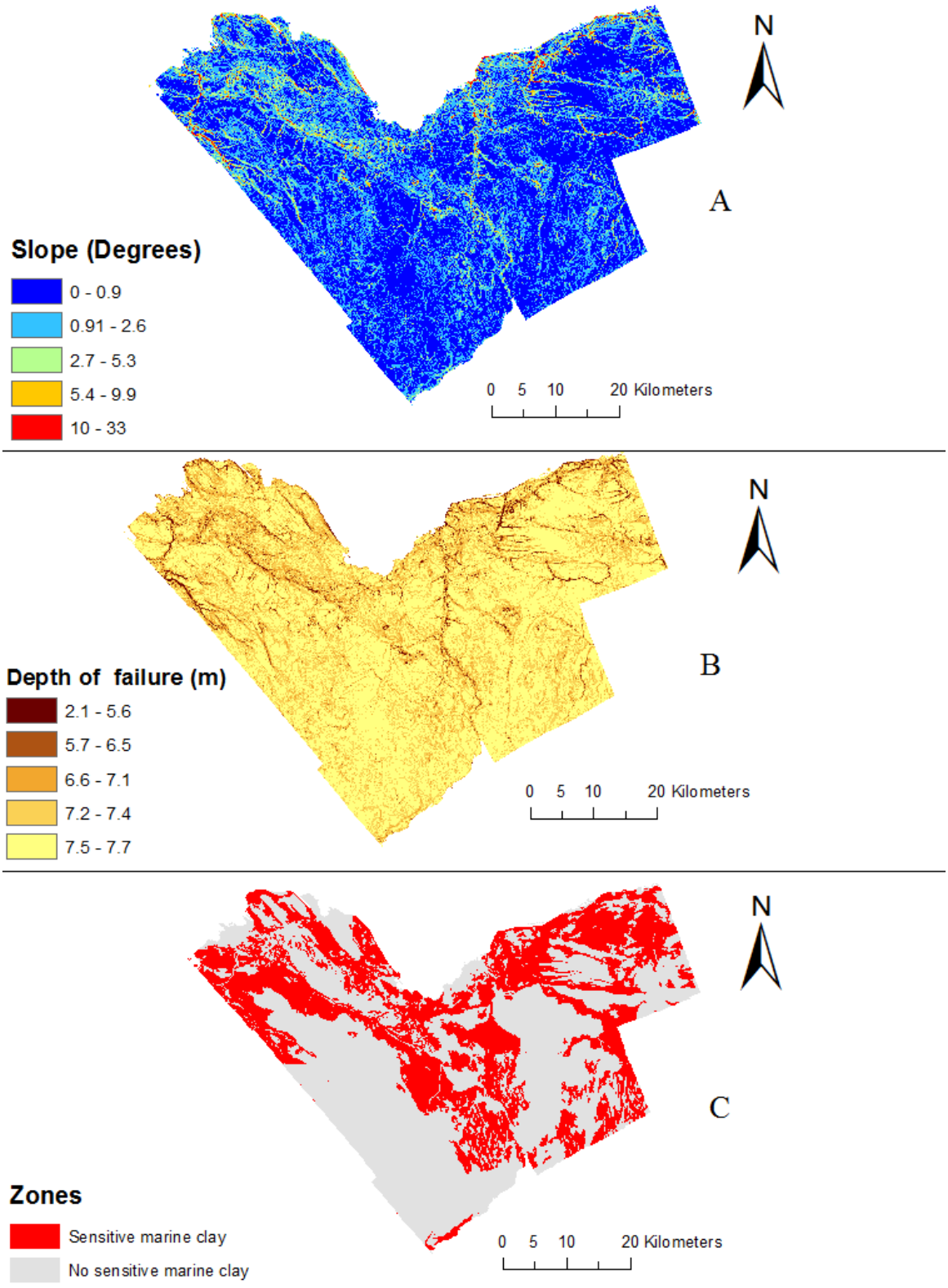

Figure 5-7 Geological maps of the study area, showing (A) topographic slope, (B) depth of failure, and (C) simplified geology (sensitive marine clay distribution).

In the second stage, all data obtained from the previous stage was converted to the ASCII file format in order to run the TRIGRS model including the raster images of geotechnical parameters (e.g., ϕ′, c′, θs, θr, α), rainfall intensity, slope, depth of failure, hydraulic conductivity (Ks), and soil water diffusivity (D_Ψ) (see Table 5-1). This format is convenient for the TRIGRS model. Data conversions were performed using the ESRI ArcGIS program. The above data was entered into the TRIGRS model using the Baum et al. (2008) method. In the third stage, the TRIGRS model was run to assess the stability of the slope in the study area, for various snowmelt durations and intensities (by using the infinite slope model to compute the safety factor, as described below).

Table 5-1 Summary of input data used in the GIS-TRIGRS model

Data typep	Collected data							
	Range of values							
Geotechnical Data [1]	C′ kPa	ϕ′ Degree	Unit Weight kN/m^3	θs	θr	Ks $\times 10^{-7}$ m/s	D_Ψ $\times 10^{-6}$ m/s^2	α
	12 – 20	21 – 30	14 – 22	0.2 – 0.9	0.02 – 0.34	0.01 – 1	0.0005 – 4	(-0.5) – (-3.2)
Climate Data [2]	Snowmelt Intensity (mm/s)				Snowmelt Duration (s)			
	see Figure (5-6)							
Hydrogeological Data[3]	Initial Groundwater Table (for 474 water wells/boreholes)							
	(0.2 – 3.5) m							
Spatial Data[4]	Slope δ (Degree)				Failure Depth (m)			
	0–33				2.1 – 7.7			

C′: effective cohesion, ϕ′: effective internal friction, θs: volumetric water content at saturation, θr: residual water content, Ks: saturated hydraulic conductivity, D_Ψ: soil water diffusivity α: inverted capillary fringe.

[2] Geotechnical reports issued by Inspec-Sol Inc., Engineering Solutions 2014; Kollaard Associates Engineers 2013; Houle Chevrier Engineering Ltd. 2013; Trow Associates Inc. 2010;Stantec Consulting Ltd. 2010; Golder Associates Ltd. 2008.

[2] Environment Canada.

[3] Provincial Groundwater Monitoring Network (PGMN) Program.

[4] Natural Resources Canada.

In the fourth stage, the obtained result files from the TRIGRS model (in ASCII file format) were converted back to raster format to work in GIS. Each raster was reclassified; including the number of pixels recorded using the ArcMap program. This allows for the mapping of the distribution of unstable slopes in the region. This distribution data is based on the safety factors calculated for the snowmelt durations and intensities studied in the area (unstable slopes maintain a FS < 1). In the last stage, the modeled landslide susceptibility map was validated by comparing the predicted landslide areas, with the locations of historical landslides. An analysis of the sensitivity of the TRIGRS-GIS model to the variations in the input data was also performed.

5.4 Infinite Slope Stability Model

The infinite slope stability model is used alongside TRIGRS to analyze the stability of the slopes. It is assumed that the landslides have a shallow depth relative to their length and width. Figure (5-8) depicts a schematic representation of the conceptual infinite slope model of the study area to compute the factor of safety (and thus slope stability) by using a TRIGRS model. Upon landslide occurrence, the upper part of the slope is typically left unsaturated, as observed in the previous geotechnical studies mentioned in Section 5.2.3. The initial ground water table in the study area was reconstructed based on the observations of groundwater levels in wells within PGMN described previously and is interpolated in ArcView GIS analysis. The equation to compute the safety factor by snowmelt water infiltration at a depth, Z, for the infinite slope model (see Figure (5-8)) is given by (Salciarini et al., 2008; Terzaghi, 1943):

$$FS = \frac{\tan\phi'}{\tan\delta} + \frac{c' - \Psi(Z,t)\,\gamma_w \tan\phi'}{\gamma_s d_{lb} \sin\delta \cos\delta} \qquad (5-2)$$

Where c' is soil cohesion, ϕ' is soil friction angle, Ψ is groundwater pressure head as a function of depth Z and time t, δ is slope angle, and γ_w, and γ_s are the unit weights of water and soil, respectively. The infinite slope is stable when FS > 1, in an equilibrium state when FS =1, and FS < 1 indicates unstable conditions. Thus, the depth of landslide initiation is the depth, Z, where FS reaches 1.

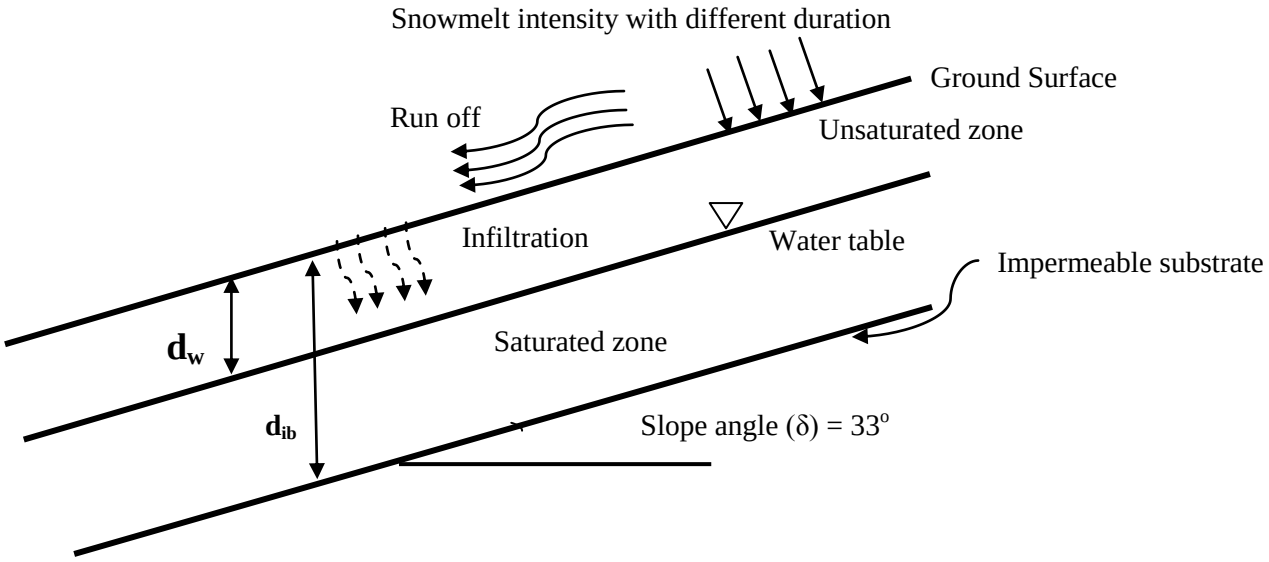

Figure 5-8 Proposed Infinite Slope Stability Analysis for the Study Area.

5.5 Hydraulic Factors

The infiltration of snowmelt water was used as the main parameter to represent the hydraulic boundary condition in this study, because the infiltration of snowmelt water results in a change in the hydraulic gradient. The hydraulic gradient (defined by head loss, h, over horizontal length, L) is derived by analyzing the soil during unsaturated infiltration and by using Richard's equation (Cobin, 2013; Kawagoe et al., 2010). The unsaturated infiltration analysis uses soil data, slope angle, and snowmelt (represents the snow water quantity) as the main input data.

5.5.1 The Degree-Day Method

Several methodologies can be used to quantify snowmelt. To quantify snowmelt, Environment Canada used a heat balance equation (based upon a process of heat transfer). The heat balance equation utilizes radiation and both sensible and latent heat fluxes. The degree-day method was used to estimate snowmelt via the degree-day equation below (Kawagoe et al., 2010; Kazama et al., 2008; Hultstrand et al., 2006).

$$\mathrm{SM} = \mathrm{K} \times \mathrm{T} \qquad (5-3)$$

Where K is the degree-day parameter (mm/°C/day) and T is the mean daily temperature (°C).

If T is less than zero degrees Celsius, snowmelt is not evaluated (because water remains solid) and the negative snowmelt value is discarded. The equation contains only one degree-day parameter, making it easy to determine the optimized degree-day parameter when correlating the estimated snow area with satellite images. With respect to input data, this method requires the following parameters to estimate snowmelt: precipitation, temperature, and elevation data. Precipitation and temperature directly affect snowmelt, because snow is generated from precipitation and temperature, and elevation directly affects the temperature of the snow (Clow et al., 2012; Kawagoe et al., 2010; Kazama et al., 2008).

5.5.2 Infiltration Analysis

Using the TRIGRS model is one of the simplest means to route the surface runoff of saturated cells. Infiltrability is known as the amount of water that can infiltrate soil as excess precipitation (known as runoff) continues to flow downhill (Godt et al., 2008; Baum et al., 2008; Raia et al., 2013). Routing surface runoff is necessary because the cells filled with excess surface water remain adjacent to downslope cells where the water can either infiltrate or flow farther downslope (known as infiltrability) (Godt et al., 2009, Baum et al., 2008). Routing surface runoff effectively can minimize the loss of excess water that cannot infiltrate the soil, and to improve performance in existing urbanized or impervious areas. When storm drains are used to divert stormwater, runoff routing is unnecessary. Runoff is assumed to occur when the precipitation and runoff supplied to a cell exceed its infiltrability (Raia et al., 2013; Godt et al.2008; Baum et al., 2008).

The saturated hydraulic conductivity is represented by Ks . The infiltration, I , at each cell is computed as the sum of the precipitation, P , in addition to any runoff from upslope cells, Ru . The runoff is limited by infiltration and it cannot exceed the saturated hydraulic conductivity, Ks .

$$\mathrm{I} = \mathrm{P} + \mathrm{Ru} \quad \text{if} \quad \mathrm{I} = \mathrm{P} + \mathrm{Ru} \leq \mathrm{Ks} \qquad (5-4)$$

$$\mathrm{I} = \mathrm{Ks} \quad \text{if} \quad \mathrm{P} + \mathrm{Ru} > Ks \qquad (5-5)$$

Provided the infiltration is less than the saturated hydraulic conductivity, Baum et al. (2008) argue that TRIGRS use a simplified method for modeling surface runoff from cells which contain excess surface water, to neighboring cells by infiltrating or flow downslope (Baum et al., 2002). At each cell where $P + Ru$ is greater than the saturated hydraulic conductivity, Ks, the excess flow is considered runoff, Ru, and is diverted to adjacent cells.

$$Rd = P + Ru - Ks, \quad \text{if} \quad P + Ru - Ks \geq 0 \qquad (5-6)$$

$$Rd = 0, \quad \text{if} \quad P + Ru - Ks < 0 \qquad (5-7)$$

During analysis, overland flow is assumed to be instant; therefore, this study does not model the rate of overland flow. Storm duration during analysis should be long enough for excess surface runoff to flow downslope. The routing method used ensures mass balance throughout the storm. Ensuring mass balance confirms that the total precipitation in the cells is equal to the water infiltrating the soil cells and the excess water flowing outside the region's border. TRIGRS models do not consider runoff between time steps nor do they track water exiting the system (via storm drains). TRIGRS models for runoff analysis assumes that water infiltrates a different cell or reaches the model's edge (Park et al., 2013; Baum et al., 2008). In addition to excess runoff from cells, water is also assumed to runoff from cells where the water table is initially at the ground surface, and the infiltration rate is initially steady and negative. In this case, water is leaving such cells and runs to adjacent downslope cells.

Alternatively, the TRIGRS model tracks water leaving cells in the mass balance calculations (Raia et al., 2013; Park et al., 2013; Baum et al., 2008).Instead of iterating to reach a solution satisfying mass balance, this model analyzes the infiltration and runoff of cells starting from the ground's surface down to further depths, removing iteration from the analysis. In order to achieve mass balance successfully, the topographic data must be indexed correctly. Digital Elevation Models (DEM) does correctly index topographic data if GIS has already been adjusted so that, the flow can be directed concurrent with the surrounding topography. Mass-balance calculations for any storm verify that water applied as an input, is accounted for as an output via infiltration or runoff (Raia et al., 2013; Park et al. 2013; Godt et al.,2008, Baum et al., 2008).

5.6 Hydrological Model

This section describes the TRIGRS hydrological model and formulas used to analyze and represent the flow behavior of the studied area, for both saturated and unsaturated conditions.

5.6.1 Infiltration Models for Saturated Initial Conditions

Groundwater flow can be modeled in two states when initially in the saturated condition: transient or steady flow. Steady groundwater flow is dependent on the water table level, infiltration rate, saturated hydraulic conductivity, and slope angle. Steady water flow occurs in both the horizontal and vertical planes (Baum et al., 2008; Iverson, 2000).The results obtained from the TRIGRS model are very sensitive to initial steady seepage conditions, so maintaining accurate initial conditions is essential to this analysis. In order to generate accurate recordings of the initial seepage conditions, field observations and steady flow models are imperative. If accurate initial conditions are lacking, TRIGRS is best applied to the modeling of hypothetical contexts (Godt et al., 2008; Baum et al., 2002).

Transient groundwater flow is typically modeled in one dimension (vertical), with a fixed duration time-varying flux and zero flux conditions beyond time equal to zero (Baum et al., 2002). Heaviside step functions were used to determine constant rainfall intensities along varying sequences of variable surface flux intensities and duration (Baum et al., 2002). This solution is achieved using TRIGRS given the Equation (5-8) (Iverson, 2000):

$$\Psi(Z,t) = (Z-d)\beta + 2\sum_{n=1}^{N}\frac{I_{nz}}{K_s}\left\{H(\mathrm{t}-\mathrm{t_n})[\mathrm{D_1}(\mathrm{t}-\mathrm{t_n})]^{\frac{1}{2}}\mathrm{ierfc}\left[\frac{\mathrm{Z}}{2[\mathrm{D_1}(\mathrm{t}-\mathrm{t_n})]^{\frac{1}{2}}}\right]\right\} - 2\sum_{\mathrm{n}=1}^{\mathrm{N}}\frac{\mathrm{I_{nz}}}{\mathrm{K_s}}\left\{\mathrm{H(t}-\mathrm{t_{n+1}})[\mathrm{D1}(\mathrm{t}-\mathrm{t_{n+1}})]^{\frac{1}{2}}\mathrm{ierfc}\left[\frac{\mathrm{Z}}{2[\mathrm{D_1}(\mathrm{t}-\mathrm{t_{n+1}})]^{\frac{1}{2}}}\right]\right\} \qquad (5-8)$$

Where t is time, $Z = z/\cos\delta$ Z is the vertical coordinate direction, z is the slope-normal coordinate direction, $\beta = \cos^2\delta - (I_{ZLT}/K_s)$, where K_s is the hydraulic conductivity in the Z direction, I_{ZLT} is the steady surface flux, and I_{nz} is the surface flux of a given intensity of the nth time interval. The subscript L_T denotes long term, $D_1 = D_0/\cos^2\delta$, where D_0 is the saturated hydraulic diffusivity, N is the total number of intervals, and $H(t-t_n)$ is the Heavy side step

function t_n is the time at nth time interval in the rainfall infiltration sequence (Godt et al., 2008). The function $ierfc\ (\eta)$ is of form (Godt et al., 2008).

$$\mathrm{Ierfc}(\eta) = \frac{\mathrm{I}}{\sqrt{\pi}\exp(-\eta^2)}\eta\mathrm{erfc}(\eta) \qquad (5-9)$$

Here $\mathrm{Ierfc}(\eta)$ is the complementary error function.

The first term in Equation (5-8) represents steady flow, whereas all other terms represent the transient flow. When using the TRIGRS model, limits can be applied to make the maximum pressure head under gravity's pressure not exceed the pressure head at the ground surface if the original flow direction and hydraulic gradient are maintained (Godt et al., 2008, Baum et al., 2002). This model is presented in Equation (5-10):

$$\Psi(\mathrm{Z},\mathrm{t}) \leq \mathrm{Z}\beta \qquad (5-10)$$

5.6.2 Infiltration Models for Unsaturated Initial Conditions

Unsaturated flows required an analytical solution to use the TRIGRS model to scenarios following initial conditions. This method analyzes soil as a two-layered system containing a saturated and unsaturated zone, with a capillary fringe (Baum et al., 2002).The unsaturated zone is assumed to soak up the water penetrating the surface until the water table rises beyond its initial state, while also reducing surface infiltration to the deeper ground due to low permeability. This model is dependent on several input parameters to produce the soil water characteristic curve (SWCC) for the wetting of unsaturated soil: residual water content, volumetric water content, saturated hydraulic conductivity, and the alpha parameter (Srivastava and Yeh, 1991). As water infiltrates the unsaturated soil, it will distribute downwards towards the bottom of the region, causing the water table to rise and pore pressure to increase. These pressure changes and waves spread quickly in very thin saturated zones. Models outside of the TRIGRS model can be used to model the transmission of the pressure waves across the saturated zones. For example, a one-dimensional form of Richard's equation can be used to depict the infiltration of the ground water through the unsaturated zone (Baum et al., 2008). To explain the effect of a sloping ground surface on infiltration, Equation (5-11) by Iverson (2000) can be used

$$\frac{\partial \theta}{\partial t} = \frac{\partial}{\partial z}\left[K(\Psi)\left(\frac{1}{\cos^2\delta}\frac{\partial \Psi}{\partial z} - 1\right)\right] \qquad (5\text{-}11)$$

In this model, the dependence of hydraulic conductivity, K (Ψ), and the fluid content, θ, on the pressure head in Richard's equation is specified with the following formulas, see Equations (5-12) and (5-13) (Baum et al., 2008).

$$K(\Psi) = Ks \exp(\alpha \Psi^*) \qquad (5\text{-}12)$$

$$\theta = \theta r + (\theta s - \theta r)\exp(\alpha \Psi^*) \qquad (5\text{-}13)$$

In Equations (5-12) and (5-13),

Ψ = is represents the pressure head, $\Psi^* = \Psi - \Psi o$, where Ψo is a constant,

Ks = is represents the saturated hydraulic conductivity,

$K(\Psi)$ = is the hydraulic conductivity function,

θ =is the volumetric water content,

θr = is the residual water content, θs is the water content at saturation

5.6.3 Model Validation and Sensitivity Analysis

The GIS-TRIGRS model developed was tested and validated to predict snowmelt induced landslides in sensitive marine clays in the study region before the model was applied in the study area. Uncertainty in any given input parameter (e.g., data quality or spatial variability of the data), can significantly affect the accuracy of a landslide susceptibility map; therefore, it is necessary to consider the uncertainty for each parameter and its application to the study region's model. The model initially was used to simulate landslide susceptibility in three scenarios:

(i) A "normal" scenario: The average values of the study area's geotechnical parameters were used as input data (e.g., cohesion, internal friction angle). Results from scenario one, are shown in Figures (5-9a) and (5-10a), including a depiction of the landslide susceptibility maps obtained in a normal scenario for a constant snowmelt duration of 10 days.

(ii) The "worst case" scenario: The most negative, or pessimistic, values for each geotechnical parameter within the study area was used as input data (chosen with

respect to their impact on the factor of safety (FS). For example, regarding the shear strength parameters, the lowest values for both cohesion and the internal friction angles were obtained from previous geotechnical studies and used as input data for the given parameters. This is a conservative approach, but using the landslide susceptibility map obtained from this scenario will greatly reduce the risk of slope failure. Figures (5-9b) and (5-10b) depict the landslide susceptibility maps obtained in a worst case scenario with constant snowmelt duration of 10 days.

(iii) An "optimistic" or "ideal" scenario: Here, the most positive, or optimistic, values for each geotechnical parameter in the study area were used as input data (with respect to their impact on the FS). For example, for the shear strength parameter the highest values of cohesion and internal friction angles were obtained from previous geotechnical studies in the study area, and used as input data. Figures (5-9c) and (5-10c) depict the results for this scenario via landslide susceptibility maps obtained with constant snowmelt duration of 10 days.

As expected, a comparison of Figures (5-9a), (5-9b), and (5-9c) with Figures (5-10a), (5-10b), and (5-10c) respectively, shows that there are more vulnerable areas prone to landslides in the worst case scenarios Figures (5-9b) and (5-10b), than in a normal Figures (5-9a) and (5-10a), or an optimistic Figures (5-9c) and (5-10c) scenario. Likewise, there are many more vulnerable areas prone to landslides in a normal analysis scenario than in an optimistic scenario. These findings therefore confirm that the landslide susceptibility model is sensitive to any changes in the input geotechnical parameter data.

In order to confirm the results of the GIS-TRIGRS model, a comparison analysis was completed by comparing the locations of the predicted unstable sites (areas with FS < 1) with the locations of historical landslides in the study area (see Figure (5-11)). Note that areas with a low factor of safety (less than one), represent locations with a high possibility of future landslides induced by snowmelt. An analysis of Figure (5-11) shows that many areas predicted to have a high susceptibility of snowmelt-induced landslides, follow similar trends as historical landslides in the Ottawa region. For example, the predicted landslides are approximately on the same path as compared to the historical landslides. The results show that a high correlation exits between the predicted and historical landslide spatial distributions in the region. This validation confirms that the developed GIS-based model can predict snowmelt-induced landslide susceptibility in the

marine clays of Ottawa with relatively good accuracy. However, some historical landslides in Ottawa were not triggered by snowmelt. The model's results remain consistent with this statement and confirm that (alongside previous geotechnical investigations on Ottawa landslides) besides snowmelt, rainfall, and earthquakes are other key triggers of landslides in sensitive marine clays (e.g., Quinn, 2009; Aylsworth et al., 1997; Eden and Mitchell, 1969).

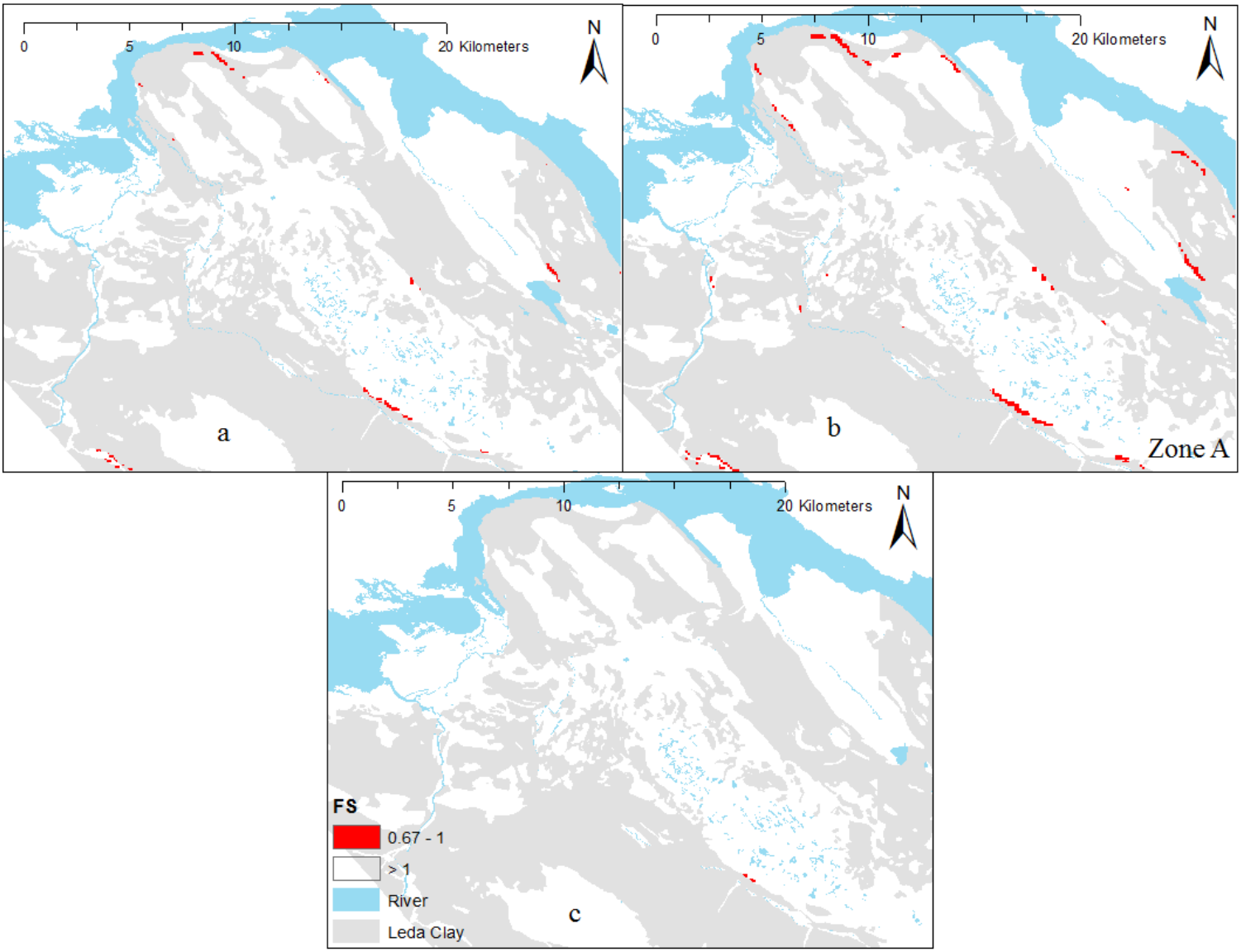

Figure 5-9 Factor of safety distribution in zone A of study area with respect to changes in input data, a: normal case scenario, b: worse case scenario, c: ideal case with respect (worse case) geotechnical

.

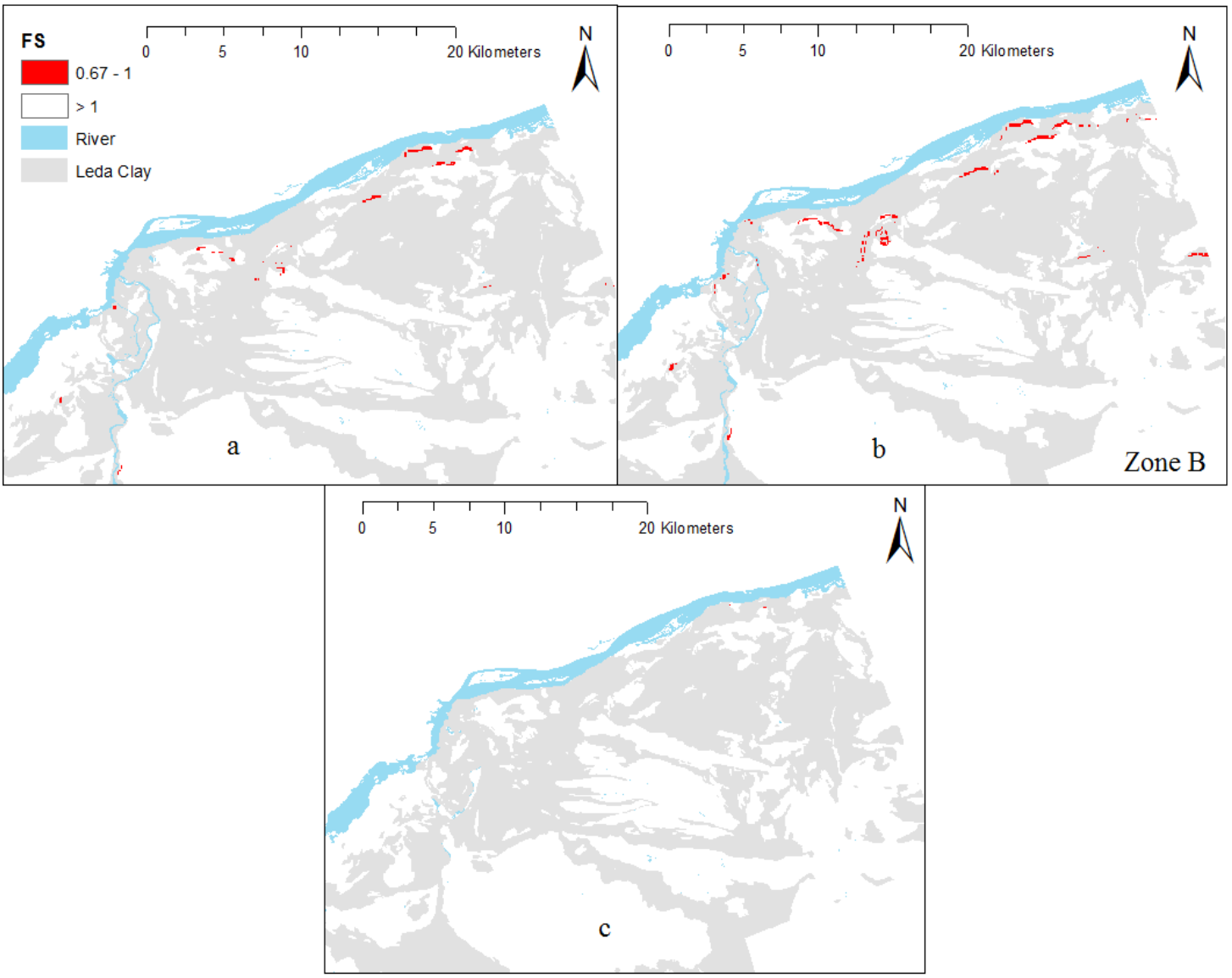

Figure 5-10 Factor of safety distribution in zone B of study area with respect to changes input data, a: normal case scenario, b: worse case scenario, c: ideal case

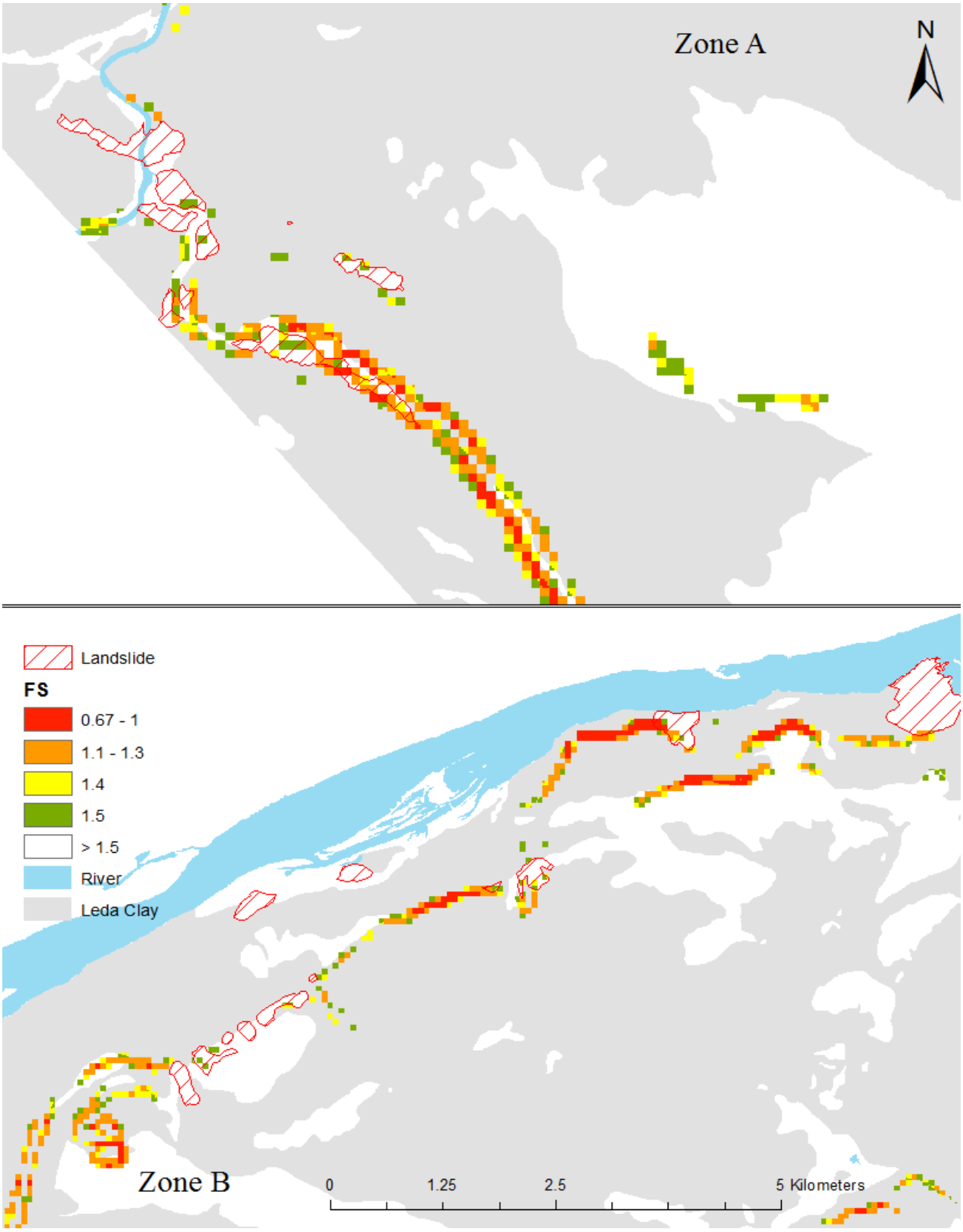

Figure 5-11A Details of Zones A and B, location of historical landslides and map of predicted FS (normal case scenario) with respect geotechnical data.

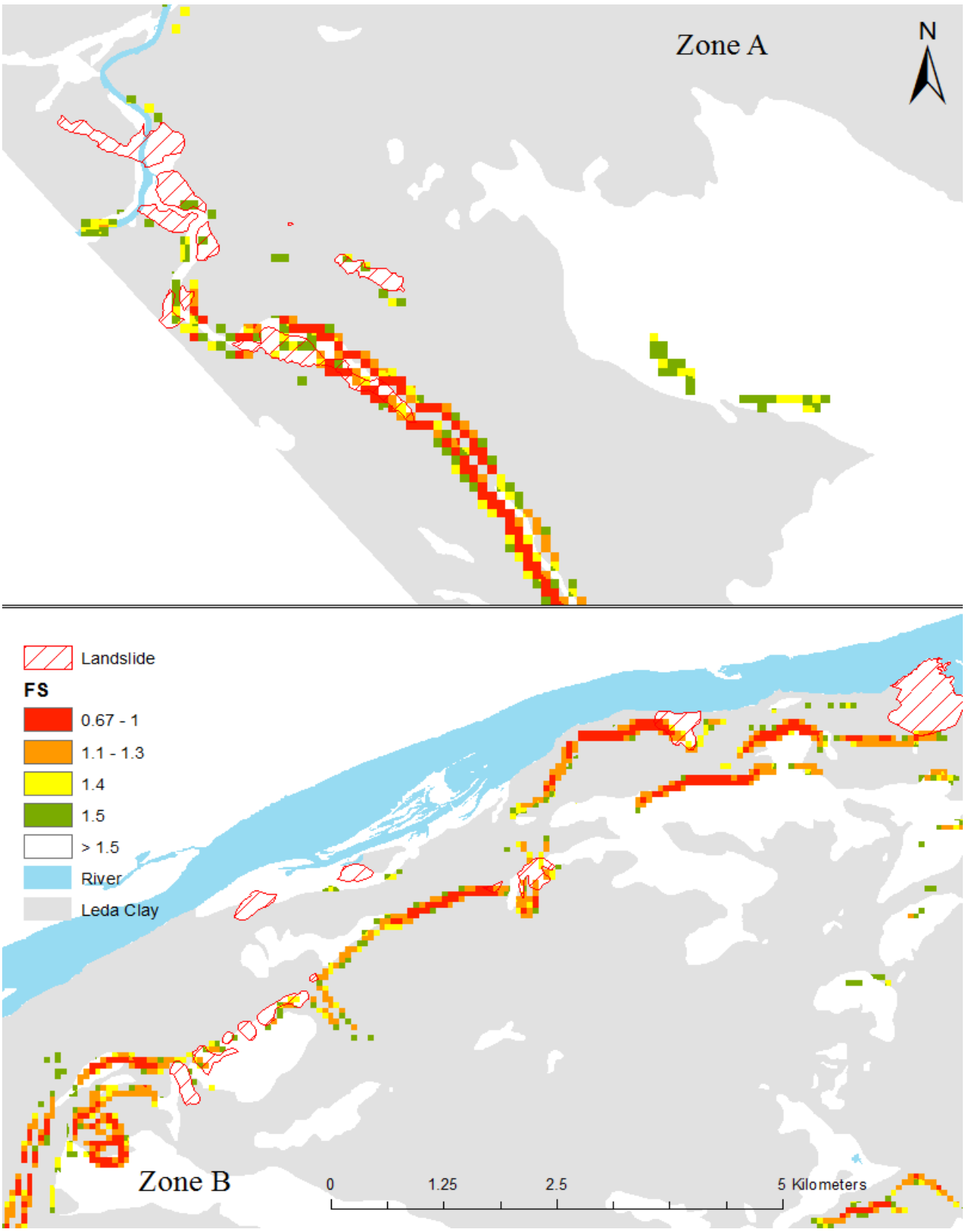

Figure 5–11B Details of Zones A and B, location of historical landslides and map of predicted FS (worse case scenario) with respect geotechnical data.

5.6.4. Application of the GIS-TRIGRS Model to the Study Area to Identify Landslide Susceptible Areas

The model developed was also applied to the study area to create a landslide danger map identifying the regions prone to snowmelt-induced landslides. The input data used for snowmelt (snowmelt duration and intensity) used in the GIS-TRIGRS based model is shown in Figure (5-6) and Table (5-2).The effect of snowmelt intensity on slope stability was analyzed using a GIS-TRIGRS model for the snowmelt durations of 6 to 48hours, 3 to 15 days, 25 days, and 30 days. For both the normal and worst case scenarios, landslide predictions were conducted with snowmelt intensities of 1.53 mm/hrs for 6 hours (see Figure (5-12)). Figures (5-13) to (5-15) depict the results for snowmelt intensities of 1.48 mm/hrs, 1 mm/hrs, and 0.54 mm/hrs for durations of 2 days, 10 days, and 30 days, respectively. As illustrated in both Figures (5-12) and (5-15), the results confirm that the majority of the slopes in the study area are not susceptible to landslides (typically maintaining a FS $\geq$ 1). On the other hand, Figures (5-12) and (5-15) demonstrate that many slopes in the predicted landslide susceptible areas are potentially unstable (FS <1).These landslide susceptibility maps depict the areas which are most susceptible to landslides. In the Ottawa region, eastern and western parts of the city are more prone to landslide due to their sensitive clay and steep slopes of Leda clay. Furthermore, areas prone to landslides (typical FS < 1) are few, in the case of high snowmelt intensity and short snowmelt duration, compared to low snowmelt intensity and long snowmelt duration. These results indicate that, within the Ottawa area, landslides are often triggered by low intensity, long duration snowmelt events compared to high intensity, short duration snowmelt events. This result aligns with the results from previous studies on snowmelt induced landslides, which have confirmed that long duration and low intensity snowmelt are major landslide triggers, such as the landslide that occurred in Shiidomari in September 1999 and the landslide in Katanooin January 2003 (Kawagoe et al. 2009). The characteristic of low intensity, long duration snowmelt that can lead to a landslide event, is due to a factor of safety that changes over time as a result of the water's infiltration of the soil. The factor of safety keeps changing as the infiltration process continues to increase for up to 10 to 11 days of continuous snowmelt (see Figures (5-12) and (5-13)). Thereafter, infiltration becomes constant (see Figures (5-14) and (5-15)). The higher sensitivity of the safety factor is due to the fact that long snowmelt durations at a low intensity encourage the infiltration of water into the soil. This infiltration results in the reduction of shear resistance

in the Leda clay and reduction in the matric suction, and thus reduces the safety factor and soil stability. This argument is consistent with previous geotechnical investigations that have shown that the upper parts of Leda clay formations remain unsaturated (Haché et al., 2015; Nader et al., 2015; Taha and Fall, 2014; Quinn, 2009; Fall et al., 2006; Dai and Lee, 2001). Accordingly, this unsaturated state was also considered in the model developed.

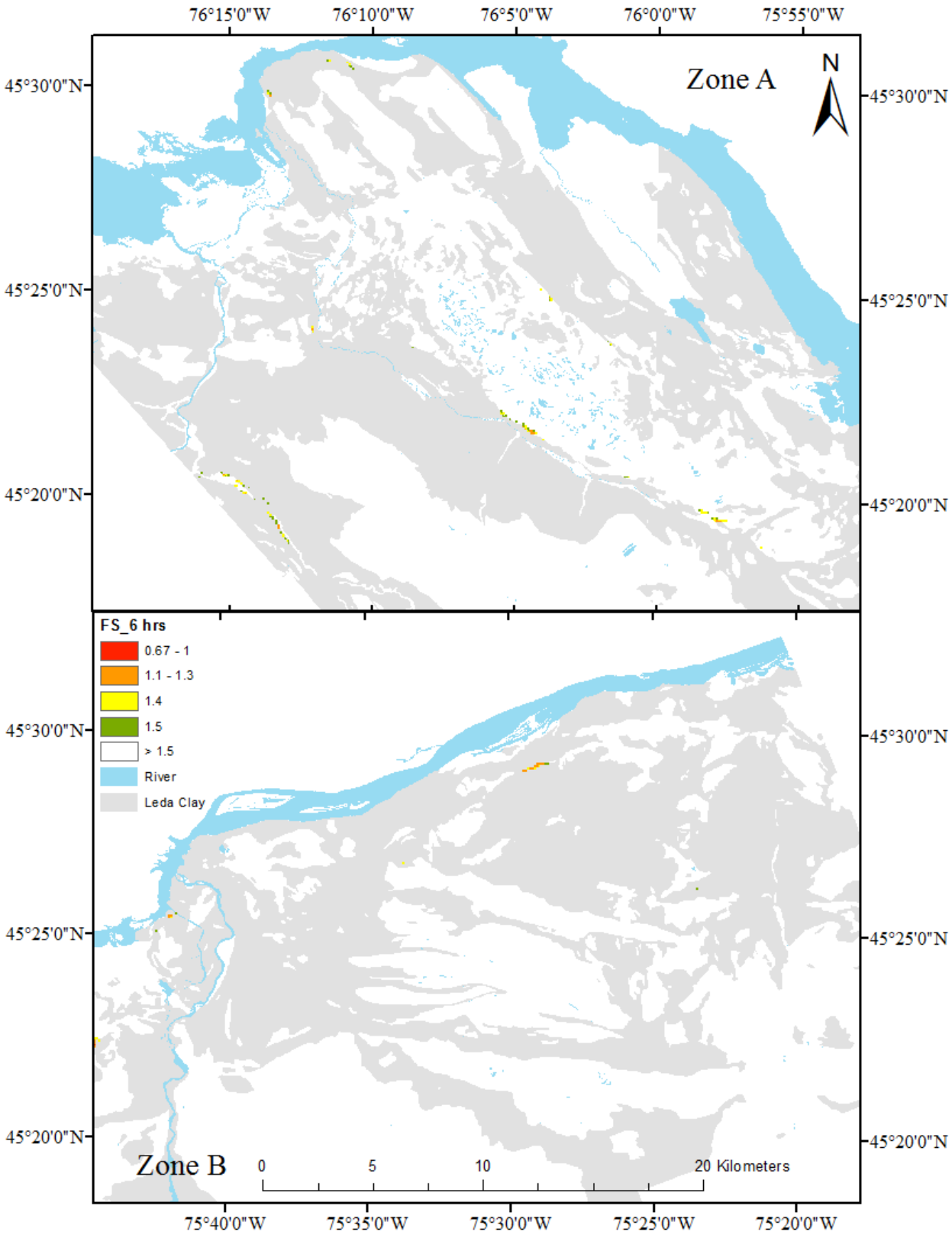

Figure 5–12A FS map and areas prone to landslides for snowmelt duration of 6 hrs and snowmelt intensity of 1.53 mm/hrs based on (normal case scenario) of the geotechnical parameters.

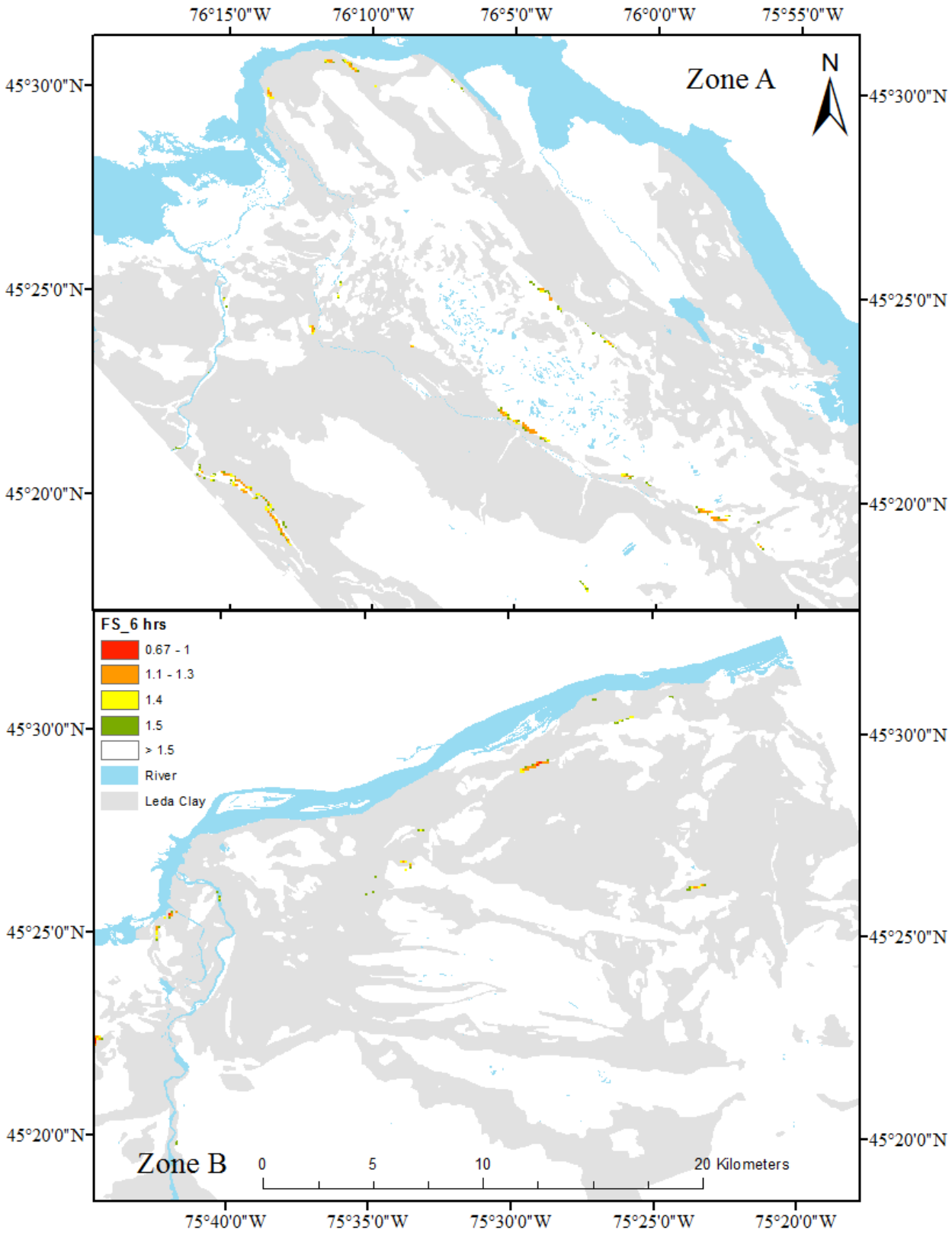

Figure 5–12B F.S map and areas prone to landslides for snowmelt duration of 6 hrs and snowmelt intensity of 1.53 mm/hrs based on (worse case scenario) of the geotechnical parameters.

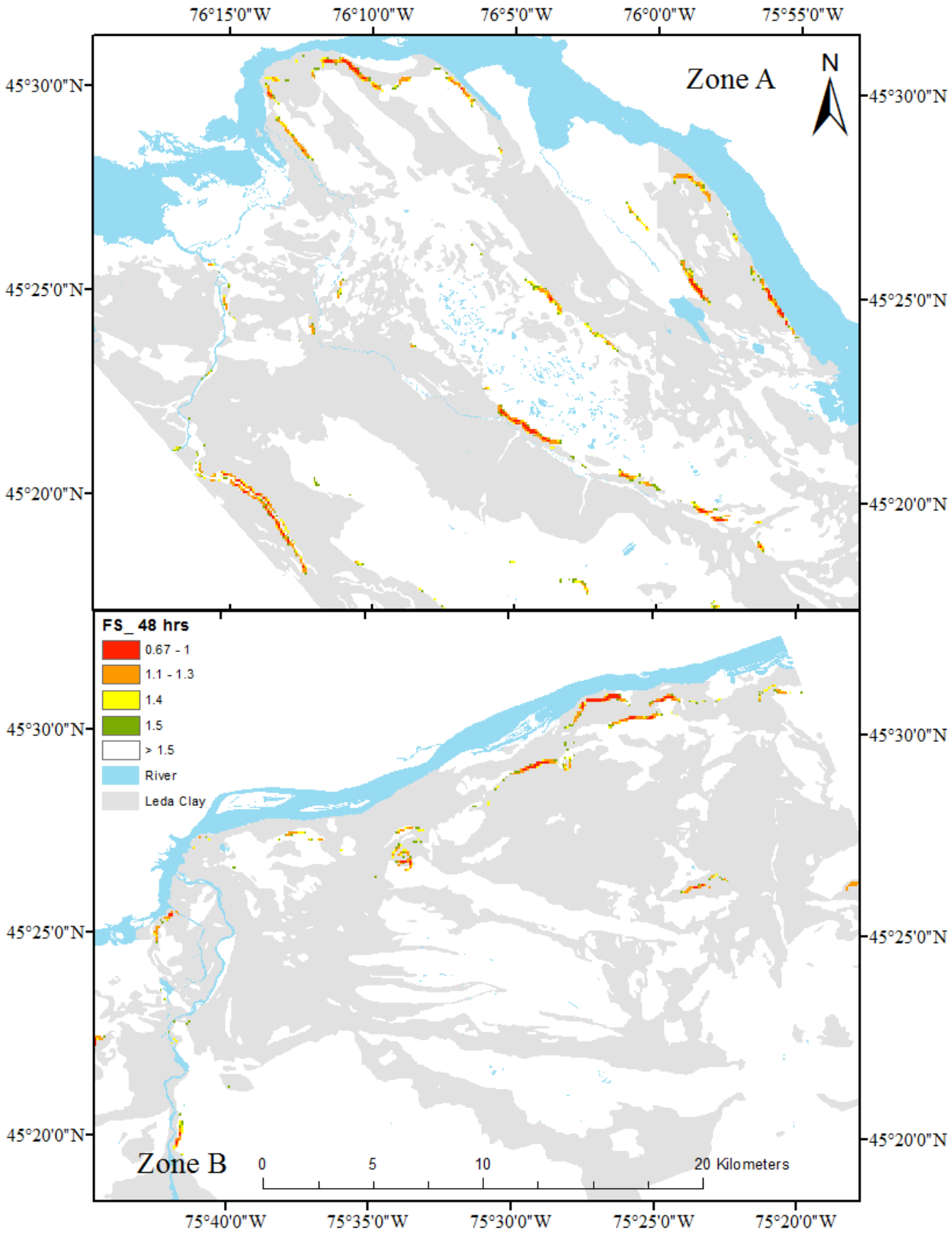

Figure 5–13A FS map and areas prone to landslides for snowmelt duration of 48 hrs and snowmelt intensity of 1.48 mm/hrs based on (normal case scenario) of the geotechnical parameters.

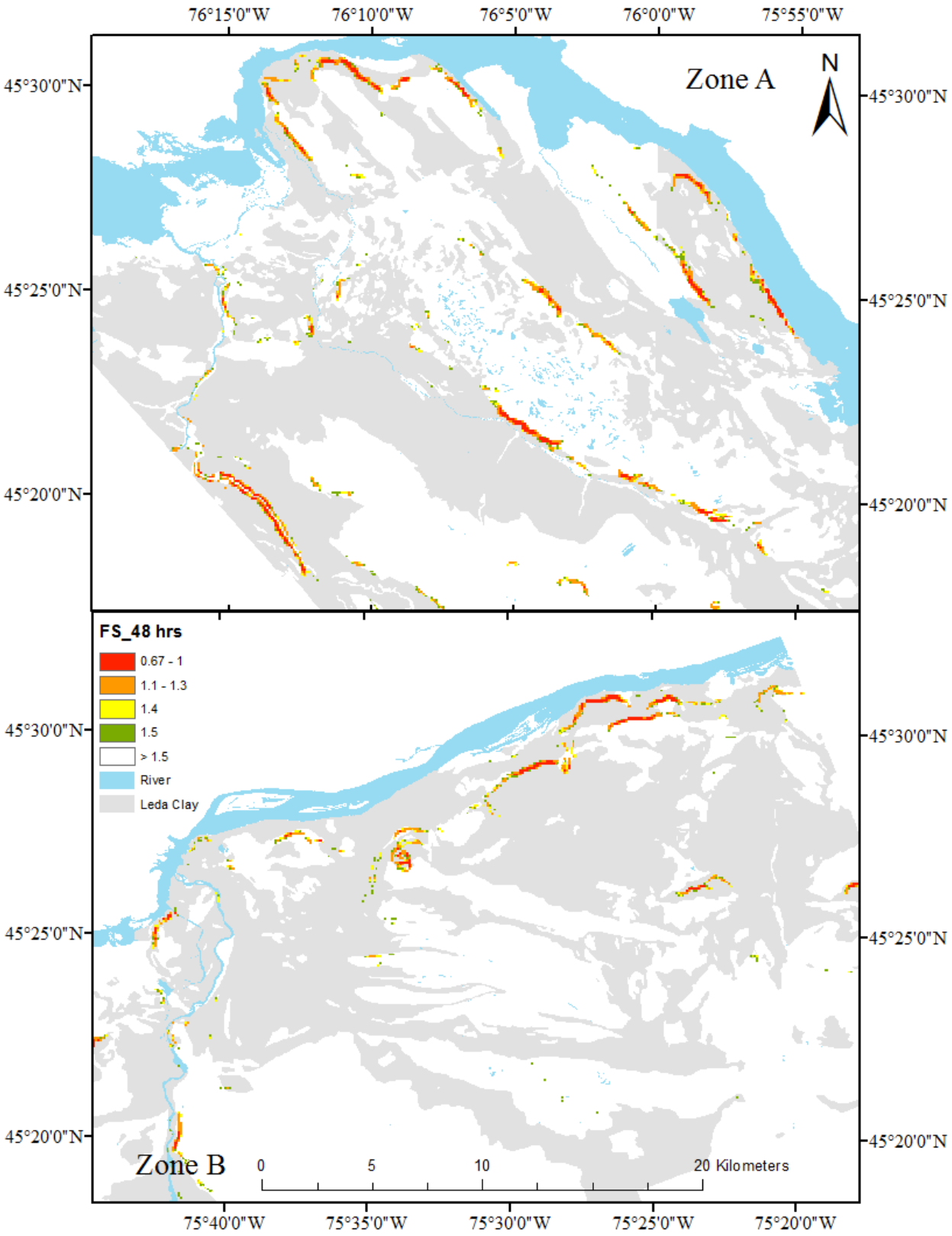

Figure 5–13B FS map and areas prone to landslides for snowmelt duration of 48 hrs and snowmelt intensity of 1.48 mm/hrs based on (worse case scenario) scenario of the geotechnical parameters.

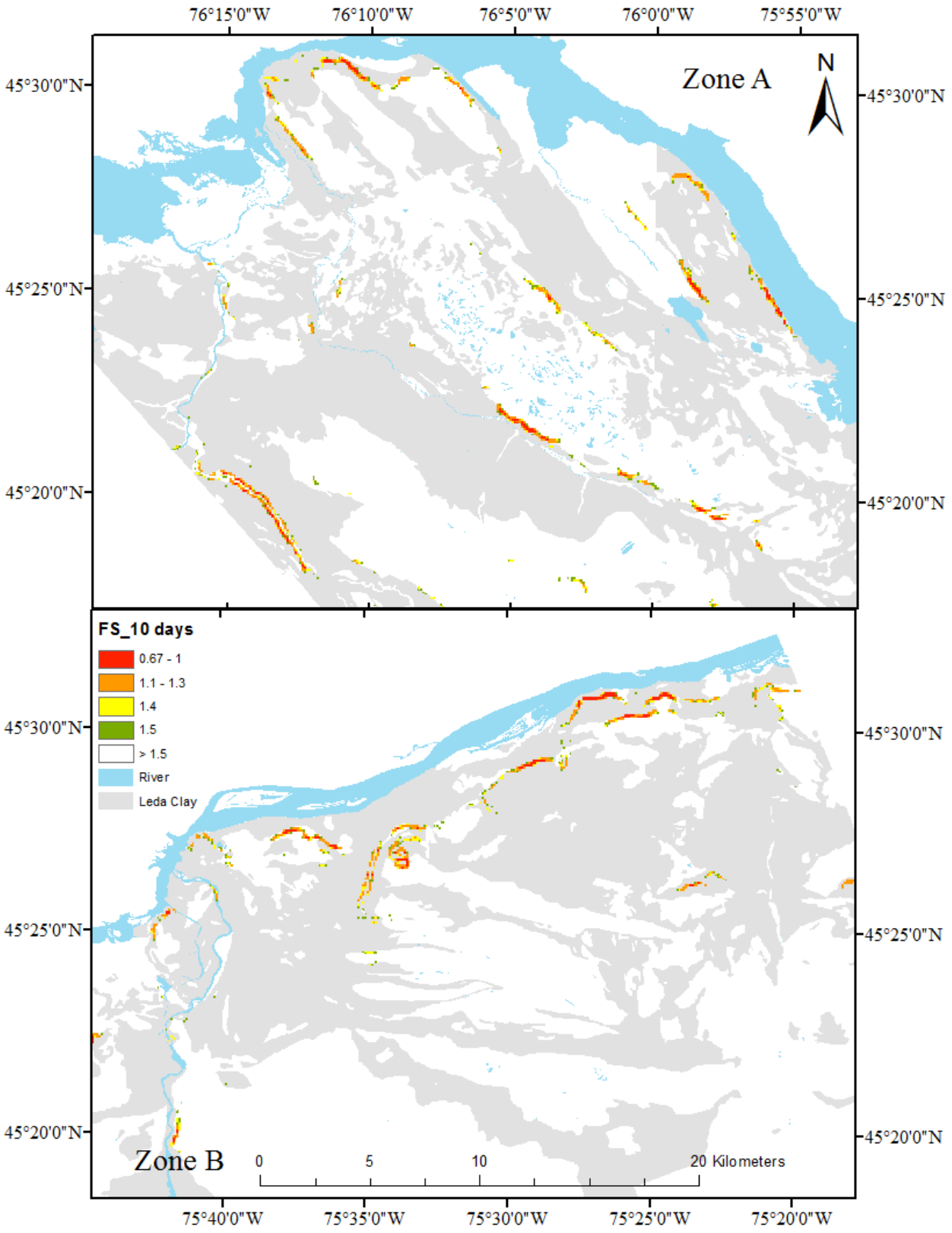

Figure 5–14A FS map and areas prone to landslides for snowmelt duration of 10 days and snowmelt intensity of 1 mm/hrs based on (normal case scenario) of the geotechnical parameters.

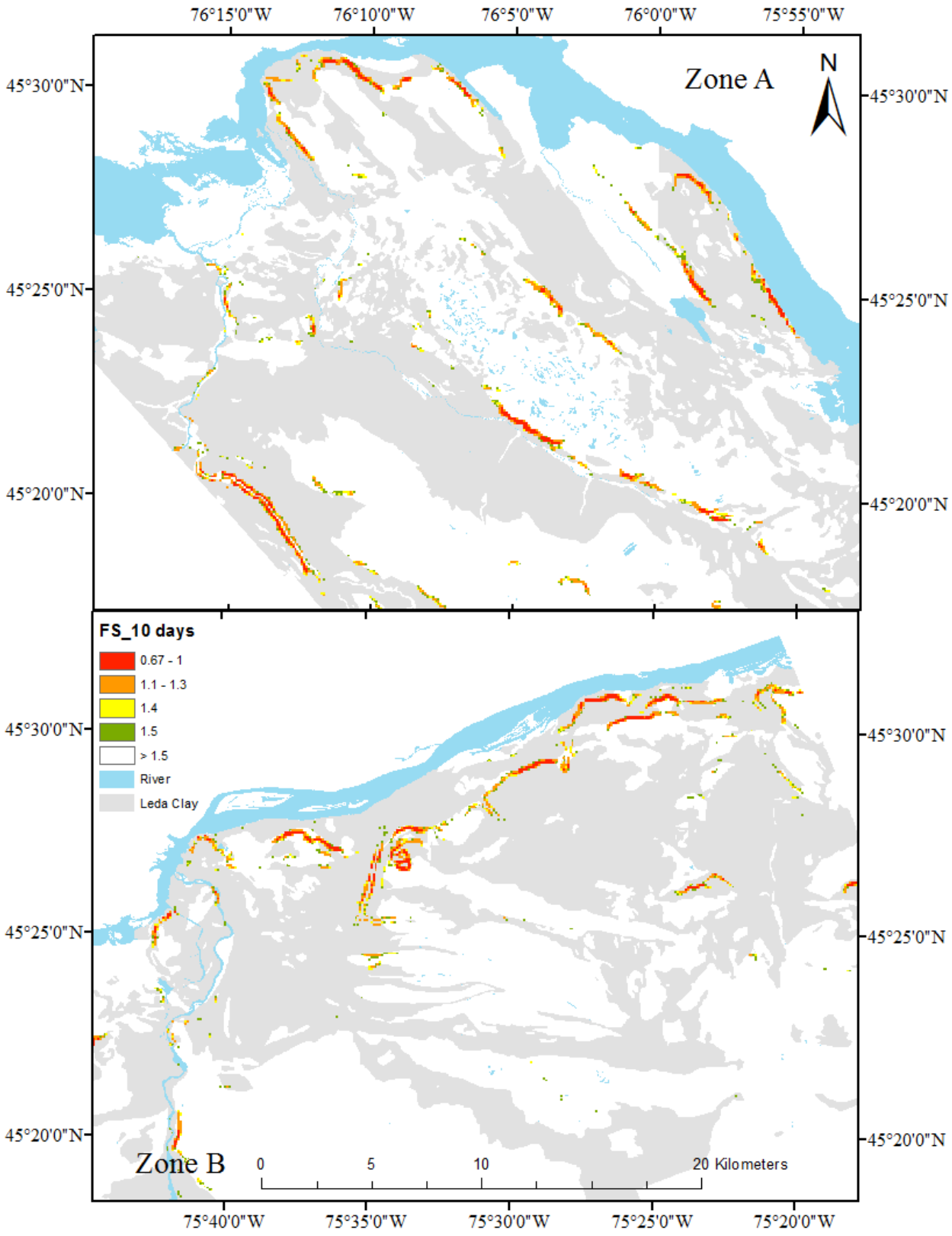

Figure 5–14B FS map and areas prone to landslides for snowmelt duration of 10 days and snowmelt intensity of 1 mm/hrs based on (worse case scenario) of the geotechnical parameters.

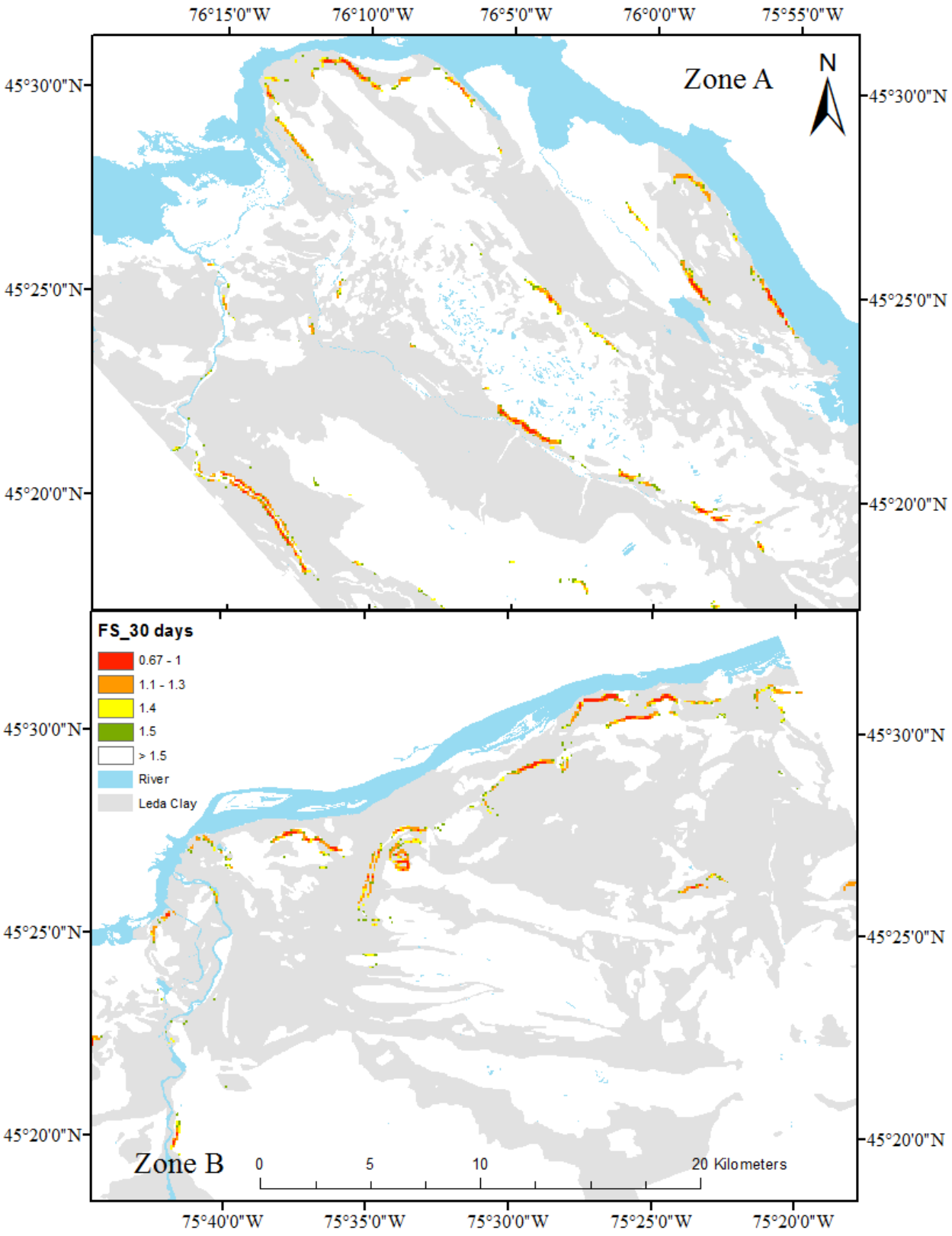

Figure 5–15A FS map and areas prone to landslides for snowmelt duration of 30 days and snowmelt intensity of 0.54 mm/hrs based on (normal case scenario) of the geotechnical parameters.

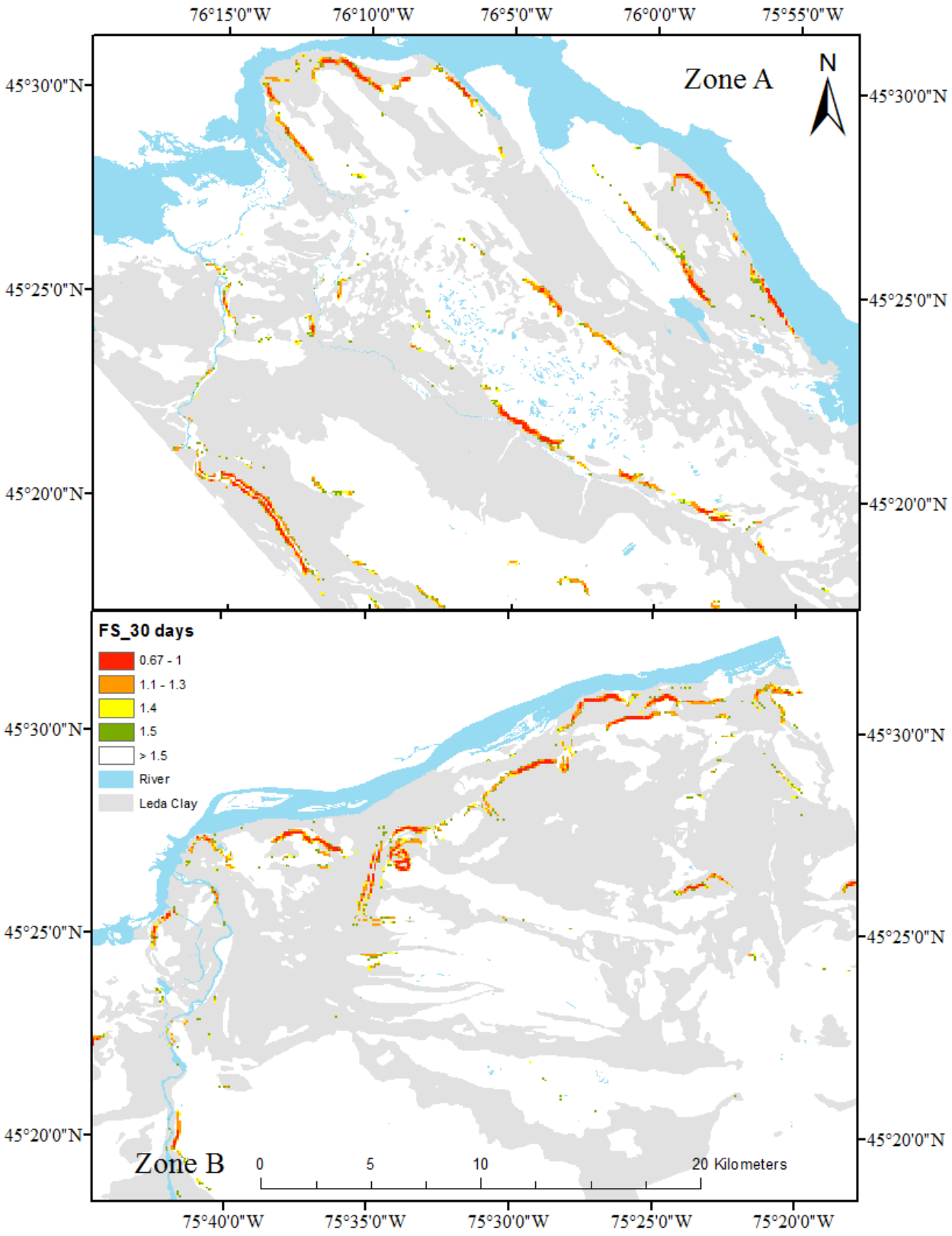

Figure 5–15B FS map and areas prone to landslides for snowmelt duration of 30 days and snowmelt intensity of 0.54 mm/hrs based on (worse case scenario) of the geotechnical parameters. .

5.7 Conclusion

A GIS-TRIGRS model was developed in this study to assess and predict snowmelt-induced landslides in the Ottawa sensitive marine clays. Then, the model was successfully validated by comparing the predicted snowmelt induced landslide areas with the historical landslides maps of the study area. After validation, the model was applied to determine areas prone to snowmelt-induced landslides in the Ottawa region using geotechnical and hydrological information, and a DEM of the study area. Some new areas subjected to landslides were detected by comparing the model results to historically recorded landslides. Coupling GIS-TRIGRS together is a useful predictor for snowmelt-induced landslides. It enables users to create maps showing the distribution of the factor of safety. Thus, the developed approach could be considered a good method for assessing snowmelt induced landslide susceptibility in the Ottawa region. This approach can be improved, by considering more factors that may influence slope stability in different conditions, such as the effect of earthquake activity in seismically active regions. Further studies are recommended to be conducted to continue development of this model.

5.8 References

Atkinson, P.M. and Massari, R., 1998.Generalised linear modelling of susceptibility to landsliding in the Central Apennines, Italy. Computers & Geosciences, 24(4), pp.373-385.

Auld Heather, Don MacIver. Joan Klassen, Shouquan Cheng, Neil. Comer, Sharon Fernandez., 2009. Adaptation by design: climate, municipal infrastructure & buildings in the Ottawa Area. Environment Canada.

Aylsworth, D. E., Lawrence and Evans, S. G., 1977.Landslide and settlement problems in sensitive marine clay, Ottawa Valley. Geological Survey Canada, Ottawa.

Aylsworth, J.M., and Hunter, J.A., 2004. A geophysical investigation of the geological controls on landsliding and soft deformation in sensitive marine clay near Ottawa.57TH Canadian Geotechnical Conference.5th Joint Cgs/Iah-Cnc Conference. Geological Survey of Canada, Ottawa, Ontario, Canada

Baum, L., Savage, W.Z. and Godt, J.W., 2008. TRIGRS-a Fortran program for transient rainfall infiltration and grid-based regional slope-stability analysis, version 2.0, US Geological Survey Open-File Report 2008–1159, available at: http://pubs. usgs. gov/of/2008/1159.

Baum, R.L., Savage, W.Z. and Godt, J.W., 2002. TRIGRS—a Fortran program for transient rainfall infiltration and grid-based regional slope-stability analysis. US geological survey open-file report, 424, p.38.

Bhandary, N.P., Yatabe, R., Dahal, R.K., Hasegawa, S. and Inagaki, H., 2013.Areal distribution of large-scale landslides along highway corridors in central Nepal. Georisk: Assessment and Management of Risk for Engineered Systems and Geohazards, 7(1), pp.1-20.

Canadian Council of Professional Engineers, 2008.Adapting to climate change Canada's first national engineering vulnerability of public infrastructure. Public Works and Government Services Canada and Engineers Canada. Available at: http://www.pievc.ca/e/Adapting_to_climate_Change_Report_Final.pdf

Carrara, A. and Guzzetti, F. eds., 1995. Geographical information systems in assessing natural hazards (Vol. 5).Springer Science & Business Media.

Carrara, A., Cardinali, M., Detti, R., Guzzetti, F., Pasqui, V. and Reichenbach, P., 1991.GIS techniques and statistical models in evaluating landslide hazard. Earth surface processes and landforms, 16(5), pp.427-445.

Chen, H.X. and Zhang, L.M., 2014. A physically-based distributed cell model for predicting regional rainfall-induced shallow slope failures. Engineering geology, 176, pp.79-92.

Chen, H.X., Zhang, L.M., Gao, L., Zhu, H. and Zhang, S., 2015. Presenting regional shallow landslide movement on three-dimensional digital terrain. Engineering Geology, 195, pp.122-134.

City of Ottawa, 2015 http://ottawa.ca/en/long-range-financial-plans/economy-and-demographics/population.

Clow, D.W., Nanus, L., Verdin, K.L. and Schmidt, J., 2012. Evaluation of SNODAS snow depth and snow water equivalent estimates for the Colorado Rocky Mountains, USA. Hydrological Processes, 26(17), pp.2583-2591.

Cobin, P.F., 2013. Probabilistic modeling of rainfall induced landslide hazard assessment in San Juan La Laguna, Sololá, Guatemala.

Dai, F.C. and Lee, C.F., 2001. Terrain-based mapping of landslide susceptibility using a geographical information system: a case study. Canadian Geotechnical Journal, 38(5), pp.911-923.

Eden, W. J., Jakrett, P. M., 1971. Landslide at Orleans, Ontario. Tech. Paper 321, Division of Building Research, National Research Council

Eden, W.J. and Mitchell, R.J., 1970. The mechanics of landslides in Leda clay. Canadian Geotechnical Journal, 7(3), pp.285-296.

Energy East Pipeline Project (EEPL) 2014, Prepared for energy east pipeline Ltd. Calgary, Alberta.

Fall, M., Azzam, R. and Noubactep, C., 2006. A multi-method approach to study the stability of natural slopes and landslide susceptibility mapping. Engineering Geology, 82(4), pp.241-263.

Fransham, P.B. and Gadd, N.R., 1977. Geological and geomorphological controls of landslides in Ottawa Valley, Ontario. Canadian Geotechnical Journal, 14(4), pp.531-539.

Fredlund, D.G. and Xing, A., 1994. Equations for the soil-water characteristic curve. Canadian geotechnical journal, 31(4), pp.521-532.

Gagné, S.A., Eigenbrod, F., Bert, D.G., Cunnington, G.M., Olson, L.T., Smith, A.C. and Fahrig, L., 2015.A simple landscape design framework for biodiversity conservation. Landscape and Urban Planning, 136, pp.13-27.

Godt, J.W., Baum, R.L., Savage, W.Z., Salciarini, D., Schulz, W.H. and Harp, E.L., 2008. Transient deterministic shallow landslide modeling: requirements for susceptibility and hazard assessments in a GIS framework. Engineering Geology, 102(3), pp.214-226.

Golder Associates Ltd. 2008. Geotechnical investigation proposed commercial building 1455 Youville drive, Ottawa,Ontario.http://webcast.ottawa.ca/plan/All_Image%20Referencing_Site%20Plan%20Application_Image%20Reference_D07-12-12-0132%20Geotechnical%20Investigation.PDF.

Gorsevski, P.V., Gessler, P. and Foltz, R.B., 2000. Spatial prediction of landslide hazard using discriminant analysis and GIS.

Guzzetti, F., Carrara, A., Cardinali, M. and Reichenbach, P., 1999. Landslide hazard evaluation: a review of current techniques and their application in a multi-scale study, Central Italy. Geomorphology, 31(1), pp.181-216.

Haché, R., Nader A., Gudina S., Fall, M., 2015. Evaluation of the undrained shear strength of Champlain Sea clays (Leda) in Ottawa. GeoQuebec 2015 – the 68th Canadian Geotechnical Conference (CGC) and 7th Canadian Permafrost Conference, Quebec, Canada CD-Rom.

Houlechevrier engineering Geotechnical Ltd. 2013. Investigation proposed garden center 2410 March Road, Ottawa, Ontario.

Hugenholtz, C.H. and Lacelle, D., 2004. Geomorphic controls on landslide activity in Champlain Sea clays along Green's Creek, eastern Ontario, Canada. Géographie physique et Quaternaire, 58(1), pp.9-23.

Hultstrand, D.M., Fassnacht, S.R. and Stednick, J.D., 2006. Geostatistical methods for estimating snowmelt contribution to an alpine water balance. In Proceedings of the Annual Western Snow Conference (pp. 149-154).

Inspec-Sol Inc. Engineering Solution, 2014.Technical memorandum – geotechnical update commercial development 2717 Stevenage Drive Ottawa, Ontario, Reference No.: T020952-A1

Iverson, R.M., 2000. Landslide triggering by rain infiltration. Water resources research, 36(7), pp.1897-1910.

Jack, R. and Montminy, S., 2007. Rideau canal pedestrian bridge-20 years from conception to construction. In 2007 Annual Conference and Exhibition of the Transportation Association of Canada: Transportation-An Economic Enabler (Les Transports: Un Levier Economique).

Kawagoe, S., Kazama, S. and Sarukkalige, P.R., 2009. Assessment of snowmelt triggered landslide hazard and risk in Japan. Cold Regions Science and Technology, 58(3), pp.120-129.

Kawagoe, S., Kazama, S. and Sarukkalige, P.R., 2010. Probabilistic modelling of rainfall induced landslide hazard assessment. Hydrology and Earth System Sciences, 14(6), pp.1047-1061.

Kazama, S., Izumi, H., Sarukkalige, P.R., Nasu, T. and Sawamoto, M., 2008.Estimating snow distribution over a large area and its application for water resources. Hydrological Processes, 22(13), pp.2315-2324.

Khezri, S., Shahabi, H. and Ahmad, B.B., 2013.Landslide susceptibility mapping in central Zab basin in GIS-based models, northwest of Iran. Environment, 3, p.4.

Kimura, T., Hatada, K., Maruyama, K. and Noro, T., 2014. A probabilistic approach to predicting landslide runout based on an inventory of snowmelt-induced landslide disasters in Japan. International Journal of Erosion Control Engineering, 7(1), pp.9-18.

Kollaard Associates engineers, 2013. Additional geotechnical investigation proposed light industrial building 1358 Coker Street Osgoode Ward, Greely, City Of Ottawa, Ontario.http://webcast.ottawa.ca/plan/All_Image%20Referencing_Site%20Plan%20Application_Image%20Reference_D07-12-13-0086%20Geotechnical%20Study%20FINAL.PDF.

L'Heureux, J.S., 2013. Characterization of historical quick clay landslides and input parameters for Q-Bing. Publisher: Norwegian Water Resources and Energy Directorate in collaboration with Norwegian Public Roads Administration and Norwegian National Railways Administration. Prepared by Norwegian Geotechnical Institute (NGI).

Mukhlisin, M., Idris, I., Salazar, A.S., Nizam, K. and Taha, M.R., 2010. GIS based landslide hazard mapping prediction in UluKlang, Malaysia. Journal of Mathematical and Fundamental Sciences, 42(2), pp.163-178.

Nader, A., Fall, M. and Hache, R., 2015. Characterization of sensitive marine clays by using cone and ball penetrometers: example of clays in Eastern Canada. Geotechnical and Geological Engineering, 33(4), pp.841-864.

Park, D.W., Nikhil, N.V. and Lee, S.R., 2013. Landslide and debris flow susceptibility zonation using TRIGRS for the 2011 Seoul landslide event. Natural Hazards and Earth System Sciences, 13(11), pp.2833-2849.

Pells, P.J.N., 1999. An equatorial quick clay landslide, Sumatra, Indonesia. In Proceedings 8th Australia New Zealand Conference on Geomechanics: Consolidating Knowledge (p. 143). Australian Geomechanics Society.

Quinn, P., 2009. Large landslides in sensitive clay in eastern Canada and the associated hazard and risk to linear infrastructure. A thesis submitted to the Department of Geological Sciences and Geological Engineering, Queen's University Kingston, Ontario, Canada.

Raia, S., Alvioli, M., Rossi, M., Baum, R.L., Godt, J.W. and Guzzetti, F., 2013. Improving predictive power of physically based rainfall-induced shallow landslide models: a probabilistic approach. arXiv preprint arXiv:1305.4803.

Rogojin, V., 2014. Provincial Groundwater Monitoring Network (PGMN) Program: Groundwater Level Data, Groundwater Chemistry Data, and precipitation Data. Metadata Management Tool (LIO). Ministry of Environment (Ontario).

Salciarini, D., Godt, J.W., Savage, W.Z., Baum, R.L. and Conversini, P., 2008. Modeling landslide recurrence in Seattle, Washington, USA. Engineering Geology, 102(3), pp.227-237.

Schut, L. W., Wilson, E. A, 1987. The Soil of the regional municipality of Ottawa - Carleton, Report No. 58 of the Ontario Institute of Pedology

Singhroy, V., Mattar, K.E. and Gray, A.L., 1998.Landslide characterization in Canada using interferometric SAR and combined SAR and TM images. Advances in Space Research, 21(3), pp.465-476.

Sorensen, K.K. and Okkels, N., 2013. Correlation between drained shear strength and plasticity index of undisturbed overconsolidated clays. In Proceedings of the 18th International Conference on Soil Mechanics and Geotechnical Engineering, Paris (pp. 1-6).

Sorooshian, S., Li, W. and Ismail, M.Y., Landslide susceptibility mapping: A Technical Note.Vol. 20 [2015], Bund. 22.

Srivastava, R. and Yeh, T.C.J., 1991. Analytical solutions for one-dimensional, transient infiltration toward the water table in homogeneous and layered soils. Water Resources Research, 27(5), pp.753-762.

Stantec Consulting Ltd., 2010.Geotechnical inventory and evaluation, Johnston Road Land Use Study.City of Project No. 122410116 (1042983).Available at:http://ottawa.ca/calendar/ottawa/citycouncil/occ/2011/04-13/pec/02%20-%20Geotechnical%20Inventory%20and%20Evaluation%20Report%20-%20April%202010%20%282%29.pdf

Taha, A. and Fall, M., 2014. Shear behavior of sensitive marine clay-concrete interfaces. Journal of Geotechnical and Geoenvironmental Engineering, 139(4), pp.644-650.

Terzaghi, K., 1943. Theoretical soil mechanics. John Wiley and Sons, New York.

Thapa, P.B. and Esaki, T., 2007.GIS-based quantitative landslide hazard prediction modelling in natural hillslope, Agra Khola watershed, central Nepal.Bulletin of the Department of Geology, 10, pp.63-70.

Theenathayarl, T., 2015. Behaviourof sensitive Leda clay under simple shear loading (Doctoral dissertation, Carleton University Ottawa).

Trow Associates Inc., 2010. Updated geotechnical investigation proposed residential development 280-282 Crichton street, Ottawa, Ontario, Trow Associates Inc., Available at:http://webcast.ottawa.ca/plan/All_Image%20Referencing_Site%20Plan%20Application_Image%20Reference_Geotechnical%20Study%20D07-12-10-0219.PDF

Van Westen, C.J., Rengers, N., Terlien, M.T.J. and Soeters, R., 1997. Prediction of the occurrence of slope instability phenomenal through GIS-based hazard zonation. GeologischeRundschau, 86(2), pp.404-414.

CHAPTER 6

6 Technical Paper III: GIS-based Mapping of Combined Effect of Rainfall and Snowmelt on Landslide Susceptibility of Sensitive Marine Clays in Ottawa Area

Mohammad Al-Umar, Mamadou Fall, Bahram Daneshfar,
Department of Civil Engineering – University of Ottawa, Ottawa, Ontario, Canada

Abstract

Extensive deposits of Champlain Sea clays are common in Canada. Oftentimes, the Champlain Sea clays are sensitive. Landslides have persisted and played a significant part in the molding of Eastern Ontario's landscape. The main cause of landslide occurrence is due to the saturation of the slope by water. Saturation can ensue in two forms: intense rainfall or snowmelt. In the Ottawa region, the main triggers of landslides are heavy rainfall occurrences throughout spring and the summer, and snowmelt in the late winter or early spring. This paper uses a Geographic Information System (GIS) based method to evaluate and calculate danger maps for rainfall and snowmelt induced landslides in the sensitive marine clays of the Ottawa region. In addition to rainfall and snowmelt intensity, other requirements for the assessment of landslide susceptibility include the topographic, geologic, hydrologic, and geotechnical information of the study area. In this study, the maximum intensity of rainfall and snowmelt were extracted for periods of 24 and 48 hours from Environment and Climate Change Canada historical climate records. Transient Rainfall Infiltration and Grid-based Slope-stability (TRIGRS) was applied to calculate the factor of safety. This model allows for the evaluation of shallow landslide susceptibility in a GIS context. The effect of climate (rainfall and snowmelt) on landslide susceptibility was assessed for various durations using the GIS-TRIGRS model. The calculated factor of safety maps from the GIS-TRIGRS model demonstrates areas of Leda clay, are often located on high topographic slopes that are more prone to rainfall and snowmelt-induced landslides. The developed GIS–TRIGRS modeling approach can be considered a useful tool for evaluating rainfall and snowmelt-induced landslides in diverse Champlain sea clay slopes.

Keywords: GIS-TRIGRS model, landslide, Leda clay, rainfall, snowmelt

6.1 Introduction

Sensitive clays, often present in countries or regions like Russia, Scandinavia, and Canada, lead to landslides that severely impact the community. One of the largest landslides sensitive marine clays recorded throughout history occurred in Norway in the year 1345. The 1345 Norwegian landslide happened in the Guala Valley and impacted the lives of over 500 people physically and emotionally. Similarly, in Verdal, Norway, a landslide in 1893 killed 116 victims (L'Heureux, 2013). Due to its history of landslides, a larger landslide in Rissa, Norway prompted the mapping of landslide susceptibility in the region (L'Heureux, 2013). Such landslides have been analyzed in some other countries too. For example, in Indonesia, Pells (1999) likewise predicted and analyzed landslide occurrences along the Siak River. Through the analysis, Pells successfully discovered the first proof that landslides often occurred due to the shearing of marine clay.

Marine clay is present in many regions of Canada. Thick layers of this sensitive clay (also known as Leda clay or Champlain sea clays) cover large portions of Quebec and Ontario. The sensitive marine clay was left behind by young glacial deposits less than 12,000 years ago (Taha et al., 2010; Haché et al., 2015). Because sensitive marine clay often leads to landslides upon snowmelt or rainfall, Eastern Canada has endured several landslides in the past decades in regions containing Leda clay. The sudden occurrence of multiple landslides of large size is often present in the river valley growth stage. These types of landslides are often induced by rainfall or snowmelt in the spring, causing their beginnings to be sudden and widespread (Quinn, 2009; Taha, 2010; Taha and Fall, 2010).

However, there is a paucity of previous modeling studies on the effect of rainfall and/or snowmelt on the stability of or landslide susceptibility of Champlain sea clay slopes in the Ottawa area. Al-Umar et al. (2017a, 2017b) developed a GIS-TRIGRS model to predict the landslide susceptibility of areas with sensitive clay as the result of either rainfall or snowmelt. Their studies show that rainfall and snowmelt can significantly affect the stability of these clay slopes in Ottawa. However, Al-Umar et. al. (2017a, 2017b) only investigated the isolated effect of rainfall and snowmelt on these slopes; they did not address their combined effects. Moreover, Quinn et al. (2009) used GIS and infinite slope stability models to identify areas of landslide susceptibility as either "low to moderate" or "moderate to high" (Van Westen et al., 1997; Fall, 2006; Quinn, 2009). Quinn's model was successfully applied to the Western Champlain Sea soils

in the lowlands of Eastern Ontario and southern Quebec. Quinn et al. (2009) studied eight different geospatial themes for potential insertion in the model, including soil type, overburden thickness, land use, elevation above sea level, flow accumulation in the drainage network, bedrock, slope angle, and slope aspect. However, Quinn's model cannot assess or predict the combined effect of rainfall and snowmelt on the stability of Champlain sea clay slopes in Ottawa.

From the review of the previous modelling works on landslide susceptibility in sensitive marine clays, particularly in Ottawa, it can be concluded that there is no modeling study on landslide susceptibility in Ottawa sensitive marine clays induced by the combined effects of rainfall and snowmelt. Therefore, this paper studies the spatial distribution of the estimated landslide susceptibility as the result of both rainfall and snowmelt in the study area and maps areas or slopes that can be affected by both.

6.2 Study Area

Within Southeastern Ontario lies Ottawa, a city of 2,778 square kilometers in size. Ottawa is semi-flat topographically with gentle slopes ranging from zero to 33 degrees, yet bounded by rivers to the north and south. The Ottawa River bounds the city to the north Figure (6-1), and the Rideau Canal and River cut the city from the north to the south (Gagnéa, 2015; Jack, 2007). Further south of Ottawa lies the Saint Lawrence River, and further east lies Montréal - the largest city in Canada's Quebec province. The Saint Lawrence Lowland borders the Ottawa Valley to the south. North of the Ottawa Valley is the Canadian Shield.

Sensitive soils like peat, sand, glacial till and clay are sporadic, yet common in the Ottawa region (Stantec 2010). The Ottawa Valley is a depression left behind by the glacier's weight, and the excess salt water from the melted glacier flowed onwards to the southeast - creating the Champlain Sea (Fransham and Gadd, 1977; Schut, 1987).

Over time, Ottawa rainfall has steadily risen to about 714 millimeters annually (Auld et al., 2009). For this study, the climate data of snowmelt was acquired from Environment and Climate Change Canada (The Engineering Climate Services Unit). From this database, the records from 1890 to 2007 from the Ottawa CAD climate station were extracted and applied. The highest recorded snowmelt in one day was 383 millimeters in 1960 and 1971. The length of cold days in Ottawa has been showing fluctuations over several years where snow fall spectrum

begins from mid-December and lasts up to the late March or nearly the beginning of April (Al-Umar et. al, 2017a, 2017b).

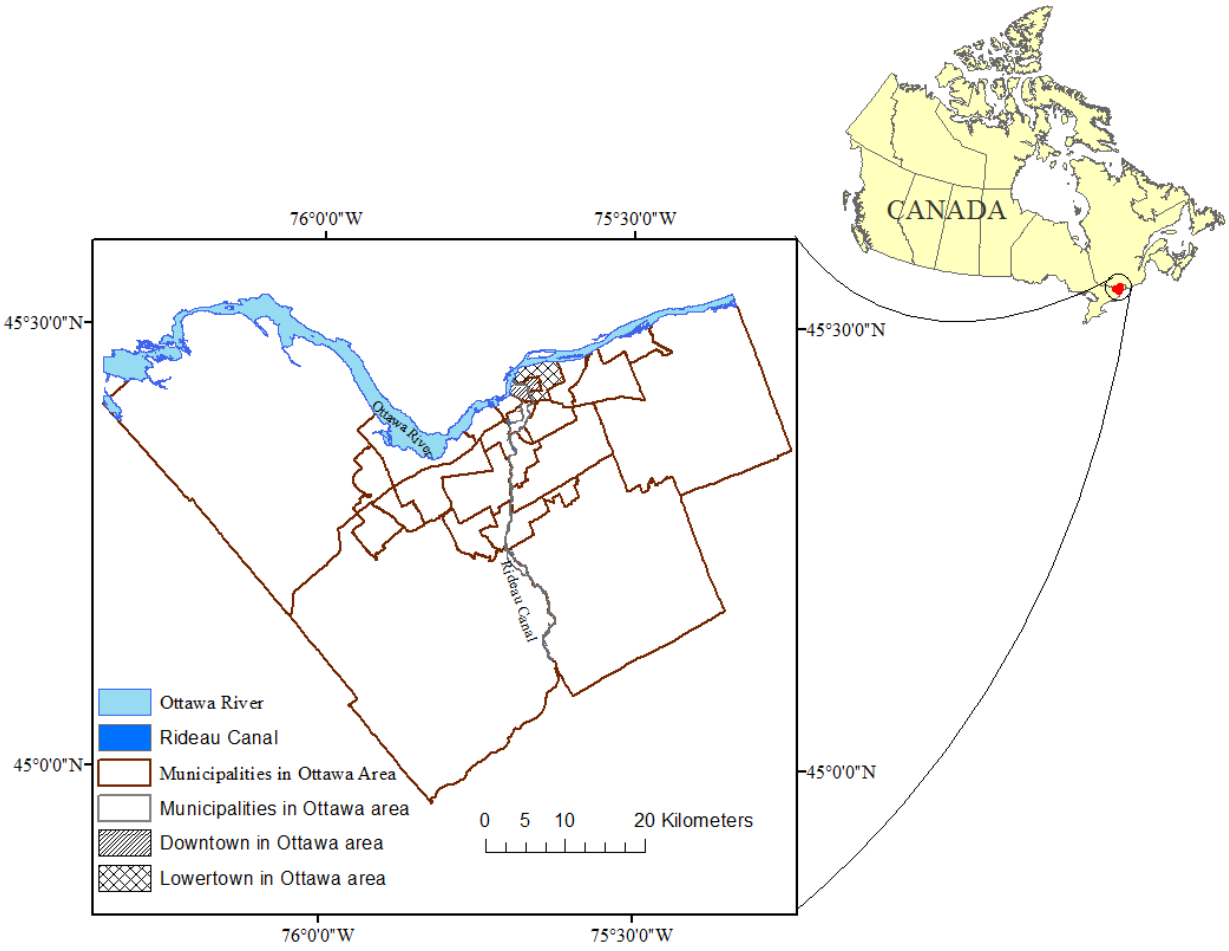

Figure 6-1 Studied area (Ottawa region)

In Ottawa, Canada, large temperature changes are felt throughout the year. The city's humid climate sees an average daily maximum temperature of 23.5°C in the summer (specifically July). Alternatively, winter seasons (specifically in January) may see a mean daily minimum value of -16.4°C. Snow and ice reign throughout Ottawa's winter season, as 208 millimeters of snowfall was seen on average annually (Canadian Council of Professional Engineers, 2008). Typically, snow cover remains in the area from mid-December until early April; although the winter period and snow duration are not constant. During the winter, freeze-thaw cycles occur as temperatures fluctuate above and below 0°C between day and night. Annual

rainfall also prevails in warmer months, averaging about 714 millimeters annually (Canadian Council of Professional Engineers, 2008). This average annual rainfall has incrementally increased over the course of the past decades. Summers are typically humid and warm in Ottawa. Cold air travels from the north to reduce humidity in the area, but rain and high wind chills remain common (Canadian Council of Professional Engineers, 2008).

Ottawa soil properties and data were taken from previous geotechnical reports completed by reputable companies that have completed engineering and construction projects in Ottawa, including Golder Associates Ltd (2008), Stantec (2010), Kollaard Associates Engineers (2013), Houle Chevrier Engineering (2013), and Inspec-Sol Inc (2014). The laboratory tests carried out on the soils from these reports provided the geotechnical parameters of the marine clay, such as hydraulic conductivity, clay fraction, specific gravity, plasticity, moisture content, unit weight, shear strength parameters, porosity, and standard penetration test results (SPTs). The results of the soil analyses indicated that Ottawa is composed of two main soil layers. The upper layer of soil is a shallow layer of silty clay (between 1.8 and 5.25 meters in depth), and the deeper layer of clay is clayey silt (between 6.5 and 12 meters in depth). The SPT performed on the soil determined that the shallow soil layer required 5 to 10 blows, indicating a loose soil packing and low relative density. The SPT performed on the deeper layer of soil required 5 to 20 blows, indicating that second layer of soil has a loose to compact soil packing and a medium relative density. The plasticity index (PI) for each layer resulted in 8 to 48 percent for the shallow layer, and 28 to 52 percent for the deeper layer. These plasticity results indicate that the shallow layer of soil has a great range in plasticity, whereas the deeper soil layer has medium to high plasticity. The specific gravity for the Ottawa region ranged from 2.70 to 2.80 – values typical for clays (Trow Associates Inc. 2010; Golder Associates Ltd. 2008; Stantec 2013; Houle Chevrier Engineering 2013; Sorensen et al. 2013). Using hydrometer testing, the fractions of clay were determined. The hydrometer test results showed that the clay fraction percentage in both soil layers ranged from 56 and 87 percent. The soil's unit weight ranged from 14 to 22 kilonewtons per cubic meter because no soil is entirely uniform (Quinn, 2009; Taha and Fall, 2014; Al-Umar et al., 2017a, 2017b in press).

6.3 Methodology

A multi-step approach Figure (6-2) was applied to assess slope stability and susceptibility to landslide induced by the combined effect of rainfall and snowmelt for areas in Ottawa region, which are composed of sensitive marine clay. This includes the gathering of geotechnical soil data from reputable sources in the Ottawa region (Trow Associates Inc. 2010; Golder Associates Ltd. 2008; Houle Chevrier Engineering Ltd. 2013, Stantec Consulting Ltd. 2010; Inspec-Sol Inc., Engineering Solutions, 2014; Kollaard Associates Engineers, 2013). This step also included the acquisition of Ottawa climate data; specifically, rainfall and snowmelt intensity recordings measured from 1890 to 2007 (in the summer and spring), and distributed by the hydrometeorology group of the Canadian Climate Department. The third set of data included initial groundwater height recordings provided by the Provincial Groundwater Monitoring Network (PGMN) Program (Rogojin, 2014). The input data relevant to shallow landslide susceptibility in GIS included the acquisition of a high-resolution DEM raster image collected from Natural Resources Canada at a scale of 1:50,000 with 10 by 10-meter pixel size.

The GIS analysis was carried out using ESRI ArcGIS to store, access, process and calculate intermediate data to prepare the input data for TRIGRS and finally to visualize and map the TRIGRS model outputs. For instance, the topographic slope was calculated based on the Digital Elevation Models (DEM) of the study area. The spatial extent of the Leda clay in the study area was considered as the masking layer Figure (6-2).

As Figure (6-2) indicates, the developed GIS-TRIGRS model was run separately for rainfall and snowmelt data for the two durations of 24 and 48 hours. The results obtained from (Al-Umar et al., 2017a, 2017b in press) proved that the amount of area susceptible to landslide continues to increase with respect to time. This increase is fast during the preceding periods of (24, & 48 hours). After these periods, the rate at which area susceptible to landslide changes become few; so that the duration of 24 hours,48 hours are considered a critical period. Results are rasters representing factor of safety maps for each case. Since low values of the calculated factor of safety represent higher landslide susceptibility and danger level, the resulting factor of safety rasters of rainfall and snowmelt were integrated with each other by a minimum function. This was carried out separately for the output rasters related to the 24 hrs and 48 hrs simulations. For each of these durations, the results of the combination of a factor of safety rasters represent areas that can be in danger as the result of each by considering the worst of the two. For instance, if in

a certain location (represented in the factor of safety raster by a pixel) the calculated factor of safety value from rainfall is 0.9 and the same for snowmelt is 1.2 then the minimum of these values is considered as the final result which will be 0.9.

$(FS)_{rainfall} = 0.9$, $(FS)_{snowmelt} = 1.2$ then Minimum (0.9, 1.2) = 0.9

or in another pixel if the factor of safety of rainfall is calculated as 1.5 and for snowmelt it is calculated as 0.8 then the overall Minimum (1.5, 0.8) = 0.8 is assigned to the same location

$(FS)_{rainfall} = 1.5$, $(FS)_{snowmelt} = 0.6$ then Minimum (1.5, 0.6) = 0.6

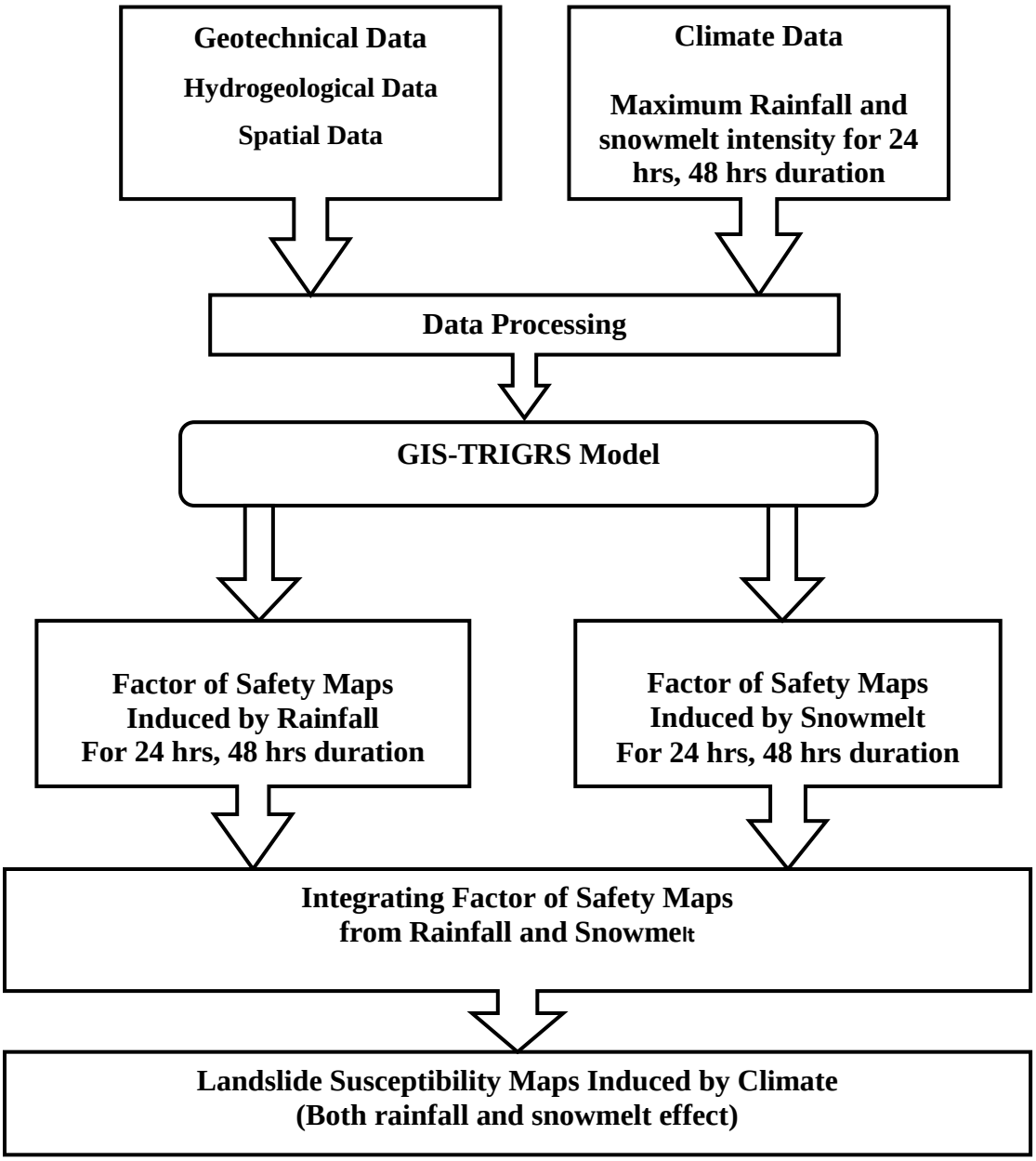

Figure 6-2 Methodology Flowchart

The slope failure plane in this analysis was calculated using the exponential function of slope (see Equation (6-1) (Godt et al., 2008).

$$d_{lb} = 7.72e^{-0.04\beta} \qquad (6-1)$$

Where d_{lb} is the lower boundary and β is the slope angle (Godt et al. 2008).

The next step gathers the data obtained from previous steps and uses ESRI ArcGIS to convert the input raster data into ASCII files. This step is required because this file format is the most convenient to use when working with the TRIGRS model. Using the Baum (2008) method, the converted data was incorporated into the TRIGRS model. The output files from the TRIGRS model have converted once again to raster images. Each pixel of the output rasters from TRIGRS contains the calculated factor of safety value which varies from less than 1 to greater than 1 in different locations. For both 24 and 48 hours durations, maps were created to visualize the distribution of the calculated factor of safety values within the study area. Such maps can be considered as the rainfall and snowmelt induced landslide susceptibility maps. Figure (6-3) illustrates areas that are subject to landslide events in the study area (Zones A and B).

The final step involved integrating the outputs from rainfall and snowmelt factor of safety calculations for each considered duration of rainfall and snowmelt. This step was applied separately to 24 and 48 hours outputs. Minimum of the pixel values of rainfall and snowmelt factor of safety was applied to combine the two pixel values for each location into the single pixel value of the final output. This minimum function was applied in ArcMap using Cell Statistics tool of the Spatial Analyst extension of ArcGIS.

6.4 Slope Stability Model

The infinite slope model is often used to clarify values of slope stability analysis and to find the effect of frequent landslides. Infinite slope stability analysis simply and easily assesses landslides, so it often remains implemented in the field (Iverson, 2000). Slope instability occurs when shear pressure overcomes the shear resistance of the ground. A cause of soil shear strength loss is the effect of groundwater table on pore water pressure. The groundwater level is typically affected by snowmelt, rainfall, and drainage networks (Godt et al., 2008).

TRIGRS model is a deterministic approach that incorporates slope stability calculations with respect to variations in time or location. This method is better applied to rainfall/snowmelt events. This approach relies on a simplified version of Richard's Equation in order to estimate

the pore pressure response, and the infinite-slope method to calculate shallow soil stability throughout a storm (Iverson, 2000; Baum et al., 2002). In this approach, the factor of safety (FS) is computed at a depth, Z, using Equation below (6-2) (Terzaghi, 1943; Salciarini et al., 2008; Al-Umar et al., 2017a, 2017b in press).

$$\mathrm{FS} = \frac{\tan\phi'}{\tan\delta} + \frac{\mathrm{c}' - \Psi(\mathrm{Z},\mathrm{t})\,\gamma_{\mathrm{w}}\,\tan\phi'}{\gamma_{\mathrm{s}}\,\mathrm{d}_{\mathrm{lb}}\,\sin\delta\,\cos\delta} \qquad (6-2)$$

Where c' is soil cohesion, ϕ' is soil friction angle, Ψ is groundwater pressure head as a function of depth Z, and time t , δ is slope angle, and γw, and γs are the unit weights of water and soil, respectively. The infinite slope method identifies stable slopes as those with a safety factors greater than one (FS > 1), slopes in equilibrium have safety factors equal to one (FS = 1), and unstable slopes with safety factors less than one (FS < 1). This model identifies landslide initiation depths to be at the point that the safety factor is equal to one.

TRIGRS infiltration models were developed based upon Iverson's (2000) linear solution and extensions to Richard's Equation by Baum (2008). To determine the pore pressure for an impermeable basal boundary at a finite depth, the following formulas were used:

$$\Psi(Z,t) = (Z-d)\beta + 2\sum_{n=1}^{N}\frac{I_{nz}}{K_s}\left\{H(\mathrm{t}-\mathrm{t_n})[\mathrm{D_1}(\mathrm{t}-\mathrm{t_n})]^{\frac{1}{2}}\mathrm{ierfc}\left[\frac{\mathrm{Z}}{2[\mathrm{D_1}(\mathrm{t}-\mathrm{t_n})]^{\frac{1}{2}}}\right]\right\} - 2\sum_{\mathrm{n}=1}^{\mathrm{N}}\frac{\mathrm{I_{nz}}}{\mathrm{K_s}}\left\{\mathrm{H(t}-\mathrm{t_{n+1}})[\mathrm{D1}(\mathrm{t}-\mathrm{t_{n+1}})]^{\frac{1}{2}}\mathrm{ierfc}\left[\frac{\mathrm{Z}}{2[\mathrm{D_1}(\mathrm{t}-\mathrm{t_{n+1}})]^{\frac{1}{2}}}\right]\right\} \qquad (6-3)$$

$$\mathrm{Z} = \mathrm{z}/\cos\alpha \qquad (6-4)$$

Where t is time, Z is the vertical coordinate direction (positive downward), and z is the slope normal coordinate direction (also positive downward), d is the steady state depth of water table measured in vertical direction, and $\beta = \cos^2\delta - (\mathrm{I_{ZLT}}/\mathrm{K_s})$, where δ is the slope angle, $\mathrm{K_s}$ is the saturated hydraulic conductivity in Z direction, $\mathrm{I_{ZLT}}$ is the steady (initial) surface flux, $\mathrm{I_{nz}}$ is the surface flux of a given intensity for $\mathrm{n^{th}}$ time interval. $\mathrm{D_1} = \mathrm{D_0}/\cos^2\delta$, where $\mathrm{D_0}$ is the saturated hydraulic diffusivity, N is the total number of time intervals, $\mathrm{H(t-t_n)}$ is the

Heaviside step function, and t_n is the time at nth time interval in the rainfall infiltration sequence (Godt et al., 2008). Lastly, ierfc is the complementary error function.

$$\text{ierfc}(\eta) = 1/\sqrt{\pi}\exp(-\eta 2) - \eta\,\text{erfc}(\eta) \qquad (6-5)$$

Baum et al. (2002) states that TRIGRS model offers a simple approach to routing surface runoff of excess groundwater. The model diverts excess runoff to adjacent cells downslope that can infiltrated or flow further downslope (Baum et al., 2002). The infiltration, I, should be less than the saturated hydraulic conductivity K_s.

$$I = K_s \qquad \text{if} \qquad I > K_s \qquad (6-6)$$

Excess water that cannot penetrate the soil's cell must direct itself to adjacent downslope cells. Therefore, for each cell for which I exceed Ks, the excess is considered runoff, Rd, and is diverted to nearby downslope cells. The equation for runoff is:

$$Rd = I - Ks \qquad \text{if} \qquad Rd \geq 0 \qquad (6-7)$$

$$Rd = 0 \qquad \text{if} \qquad Rd > 0 \qquad (6-8)$$

6.5 Result and Discussion

The developed and validated model was then applied to the studied area to identify the areas that are prone to landslides induced by rainfall and/or snowmelt; in other words, a landslide danger map of rainfall/snowmelt-induced landslides was developed. The input data from Environment Canada and Climate Change for rainfall (duration and intensity) was used in the GIS-TRIGRS based model to predict study area landslide susceptibility (Al-Umar et al., 2017a).

The Environment Canada and Climate Change input data for rainfall indicates that the greatest rainfall intensity occurs during the first five minutes of a storm; thereafter, the rainfall intensity constantly decreases for 24 hours. Therefore, through an analysis of the input data, it can be determined that as rainfall intensity decreases, the duration of rainfall will continue to increase. The rainfall duration and intensity data supplied by Environment Canada and Climate Change were used to develop a model to determine the relationship between rainfall intensity and duration over various return periods: 2, 5, 10, 25, 50, and 100 years. The developed model indicated that rainfall-induced landslides were often triggered by long durations of rainfall at a low intensity, a finding consistent with other studies (e.g., Salciarini et al., 2008, Hasegawa et al.,

2009, Li et al., 2013). Areas prone to landslide are typically triggered by low rainfall intensity over longer durations.

Snowmelt intensity can also trigger landslides so the study area was evaluated for the impact of snowmelt duration (6 to 48-hours) and snowmelt intensity on landslides. The GIS-TRIGRS model results indicated that the factor of safety (landslide susceptibility) for unsaturated conditions changes with time. The model determined that areas most prone to a landslide are in the eastern and western parts of the study area and areas containing Leda clay; therefore, these areas had factors of safety less than one, indicating an unstable slope. The study area slope stability is more sensitive to snowmelt duration because long snowmelt durations at a low intensity is a better situation for infiltrating the water into the soil. Marine clay soil infiltration results in reduced soil shear resistance in marine clay due to reduced matric suction, so the slope stability decreases (the slope's safety factor reduces). The model's results are congruent with previous studies that have investigated the behavior unsaturated upper layers of sensitive marine clay (Dai and Lee, 2001; Fall et al., 2006; Quinn, 2009; Taha and Fall, 2010; Nader et al., 2013, 2015; Haché et al., 2015).

The prediction model integrated the landslide susceptibility maps induced by climate (rainfall and snowmelt) as shown in Figures (6-4) to (6-7). The integration was applied to better understand the behavior of sensitive marine clay slopes when exposed to rainfall and snowmelt for 24 and 48 hour durations. To display the details better, the maps of Figures (6-4) to (6-7) divide the study area into two zones (A and B). In each zone, the two areas (1 and 2) are enlarged to show spatial detail with respect to landslide susceptibility change in the area with respect to rainfall and snowmelt. These factor of safety maps represent the gradation of susceptibility to landslide by considering the effect of both the rainfall and snowmelt together for different durations (24 hrs and 48 hrs).

The areas prone to landslides induced by rainfall and snowmelt due to Leda clay concentration are mainly located in high slope areas. The applied integration of this study results in a slight increase in the areas prone to landslide compared to the individual factor of safety maps for only rainfall or snowmelt. In this and previous analyses, slopes with safety factors less than one are considered susceptible to instability (FS < 1); these slopes are therefore more susceptible to rainfall and snowmelt-induced landslides. This study discovered that in both

eastern and western Ottawa there are areas that contain steep slopes of Leda clay. The combination of steep slopes, highly responsive marine clay, and long term water saturation makes these areas most prone to landslide occurrence. The combination of rainfall and snowmelt analysis output maps can be a more realistic representation of the landslide susceptibility for Ottawa area.

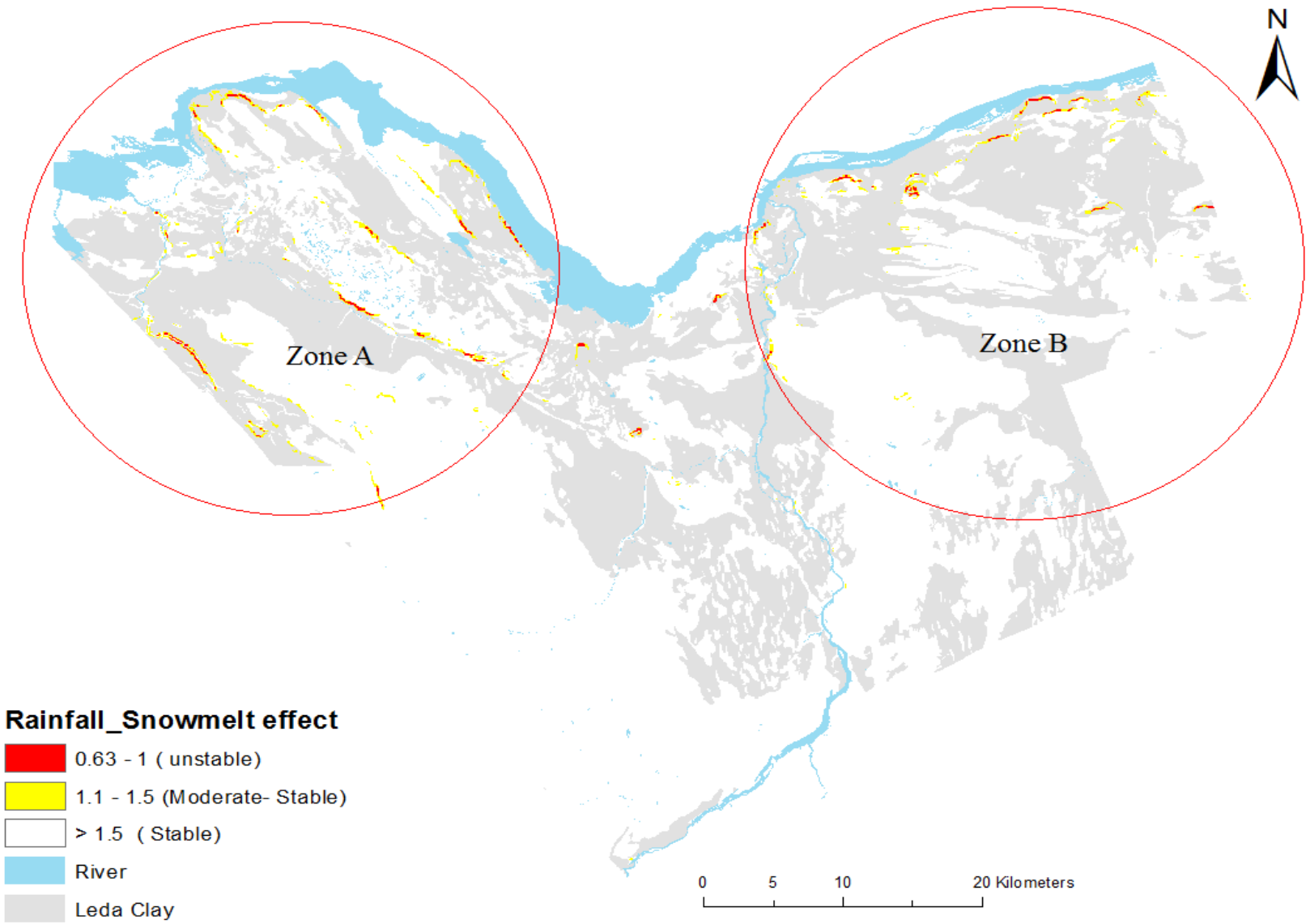

Figure 6-3 Spatial distribution of minimum of the two factors of safety of rainfall and snowmelt..

.

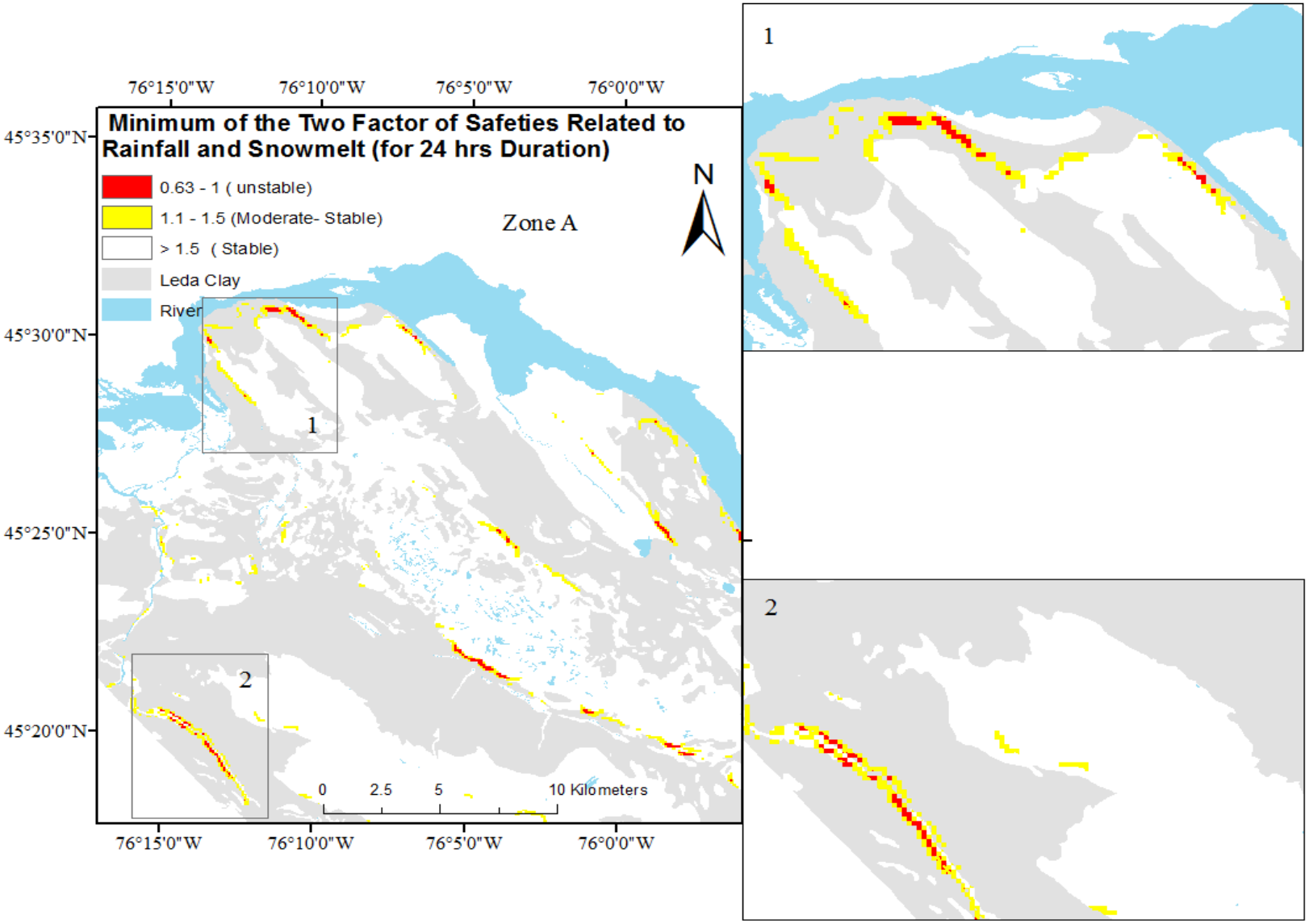

Figure 6-4 Spatial distribution (zone A) of minimum of the two factor of safeties of rainfall and snowmelt (for 24 hours duration).

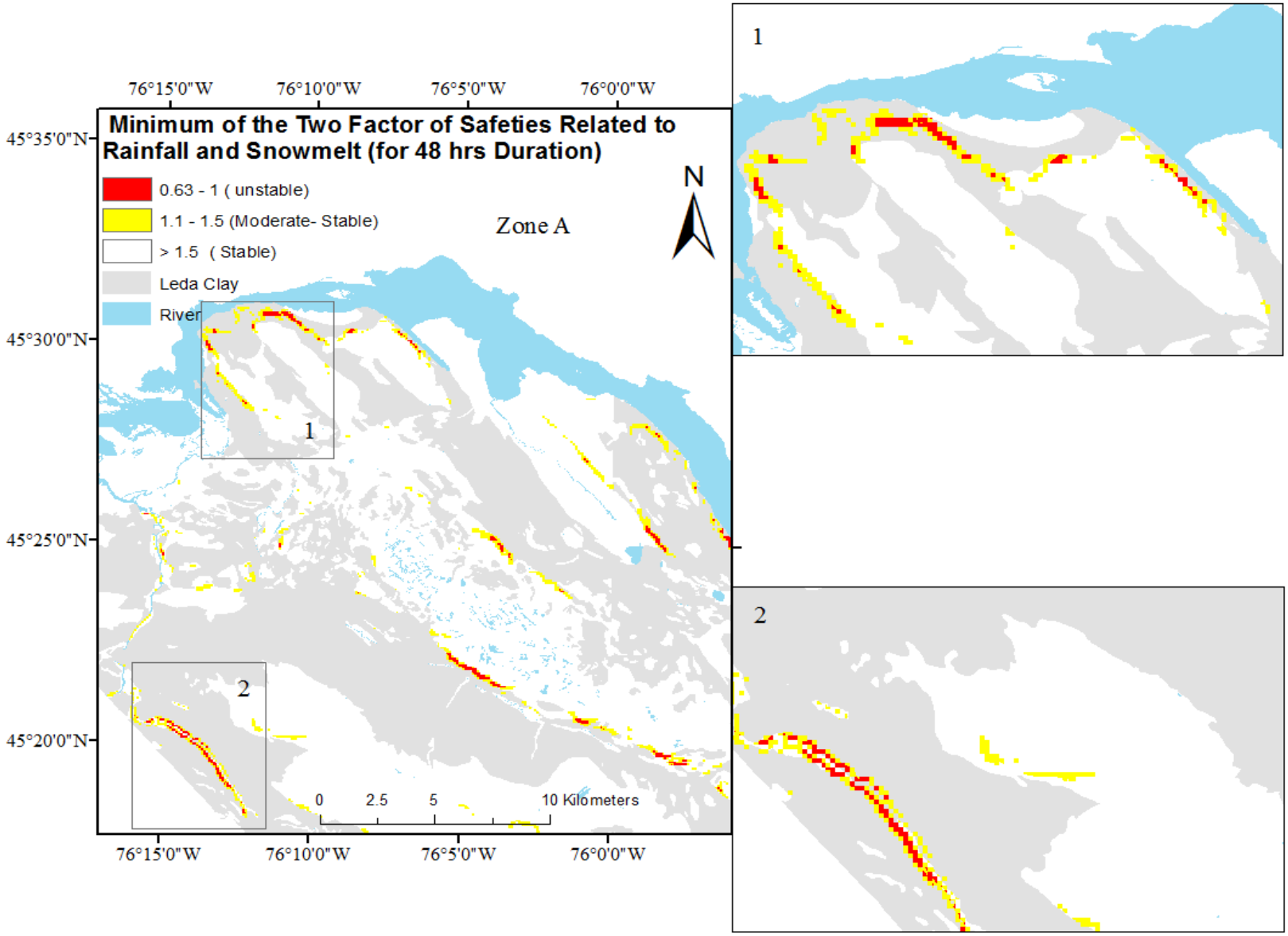

Figure 6-5 Spatial distribution (zone A) of minimum of the two factor of safeties of rainfall and snowmelt (for 48 hours duration).

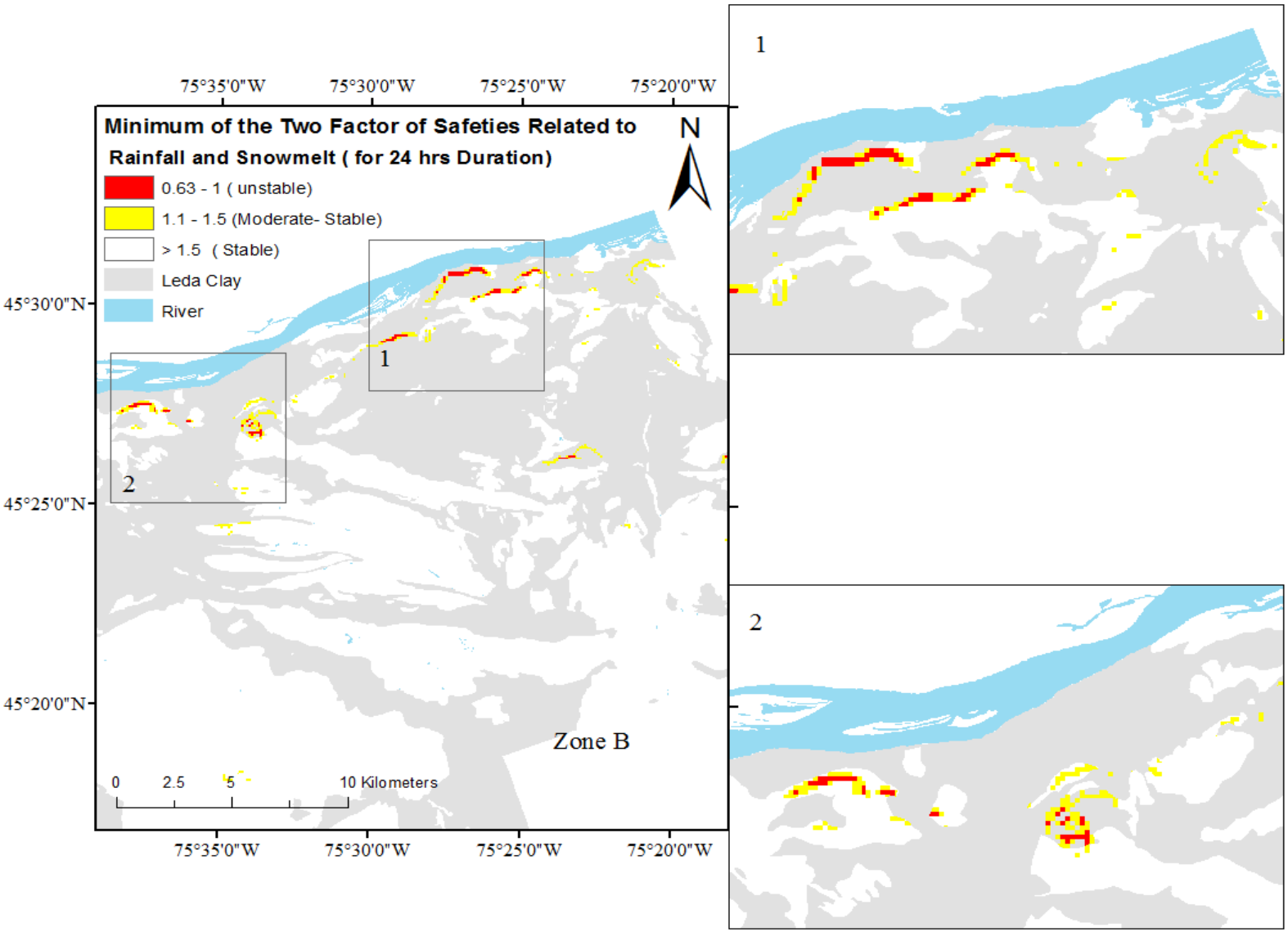

Figure 6-6 Spatial distribution (zone B) of minimum of the two factor of safeties of rainfall and snowmelt (for 24 hours duration).

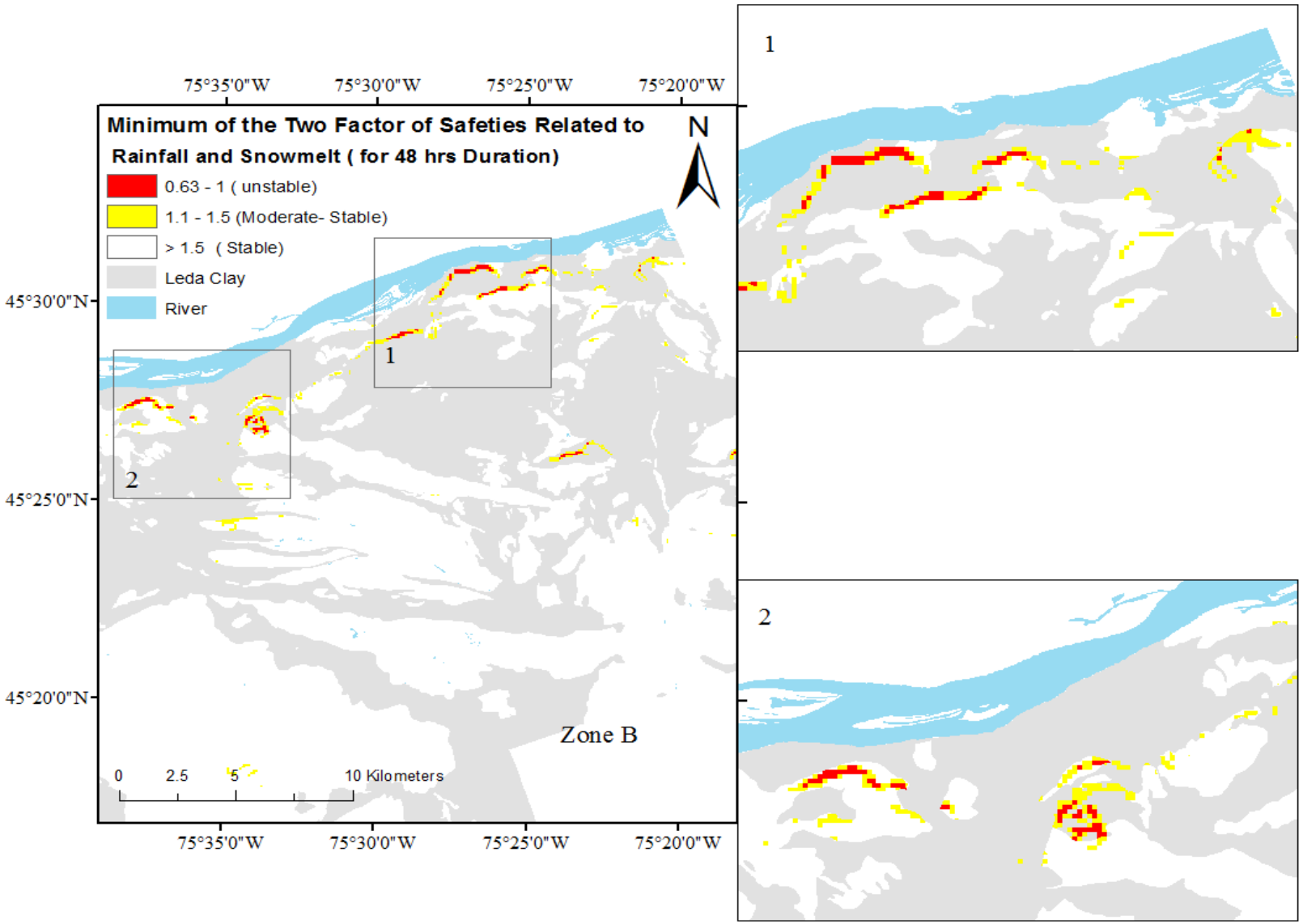

Figure 6-7 Spatial distribution (zone B) of minimum of the two factor of safeties of rainfall and snowmelt (for 48 hours duration).

6.6 Conclusion

This study included the development of a GIS-based model to predict and map expected landslide prone areas in Ottawa, specifically due to both rainfall and snowmelt. The geotechnical and climate input data were gathered from previous research and were applied to assess landslide susceptibility across Ottawa region. This method supports the proper monitoring and mitigation of landslides in the area. The results from this paper identified a slight increase in landslide prone areas as the duration increases from 24 to 48 hours of rainfall and snowmelt. Many areas were located in landslide susceptible regions for both rainfall and snowmelt. These areas had high Leda clay concentrations and steeper slopes. The obtained results and developed model can be used to evaluate landslide probabilities and provide sufficient geotechnical information to help execute efficient slope management and land use planning.

Despite the results obtained, the developed model can be improved by incorporating additional controlling factors that can impact slope stability including sensitive soil, ground water level variation due to climate events, and seismic activity.

6.7 References

Al-Umar, M., Fall, M., Daneshfar, B., (a) GIS based assessment of rainfall-induced landslide susceptibility of sensitive marine clays: A case study. Department of Civil Engineering – University of Ottawa, Ottawa, Ontario, Canada.

Al-Umar, M., Fall, M., Daneshfar, B., (b) GIS based assessment of snowmelt-induced landslide susceptibility of sensitive marine clays: A case study. Department of Civil Engineering – University of Ottawa, Ottawa, Ontario, Canada

Auld Heather, Don MacIver. Joan Klassen, Shouquan Cheng, Neil. Comer, Sharon Fernandez., 2009. Adaptation by Design: Climate, Municipal Infrastructure & Buildings in the Ottawa Area. Environment Canada.

Baum, R.L., Savage, W.Z. and Godt, J.W., 2002. TRIGRS—a Fortran program for transient rainfall infiltration and grid-based regional slope-stability analysis. US geological survey open-file report, 424, p.38.

Baum, R.L., Savage, W.Z., Godt, J.W., 2008. TRIGRS - A FORTRAN program for transient rainfall infiltration and grid-based regional slope stability analysis, Version 2.0. U.S. Geological Survey. Accessed: http://pubs.usgs.gov/of/2008/1159/

Fall, M., Azzam, R. and Noubactep, C., 2006. A multi-method approach to study the stability of natural slopes and landslide susceptibility mapping. Engineering Geology, 82(4), pp.241-263.

Gagné, S.A., Eigenbrod, F., Bert, D.G., Cunnington, G.M., Olson, L.T., Smith, A.C. and Fahrig, L., 2015.A simple landscape design framework for biodiversity conservation. Landscape and Urban Planning, 136, pp.13-27.

Godt, J.W., Baum, R.L., Savage, W.Z., Salciarini, D., Schulz, W.H., Harp, E.L., 2008. Transient deterministic shallow landslide modeling: requirements for susceptibility and hazard assessments in a GIS framework. Eng. Geol. 102 (3), p. 214–226.

Golder Associates Ltd. 2008. Geotechnical investigation proposed commercial building 1455 Youville drive, Ottawa,Ontario.http://webcast.ottawa.ca/plan/All_Image%20Referencing_Site%20Plan%20Application_Image%20Reference_D07-12-12-0132%20Geotechnical%20Investigation.PDF.

Haché, R., Nader A., Gudina S., Fall, M., 2015. Evaluation of the undrained shear strength of Champlain Sea clays (Leda) in Ottawa. GeoQuebec 2015 – the 68th Canadian Geotechnical Conference (CGC) and 7th Canadian Permafrost Conference, Quebec, Canada CD-Rom.

Houle Chevrier Engineering Ltd. 2013.Geotechnical Investigation Proposed Garden Centre 2710 March Road, Ottawa, Ontario.

Houlechevrier engineering Geotechnical Ltd. 2013. Investigation proposed garden centre 2410 March Road, Ottawa, Ontario.

Inspec-Sol Inc. Engineering Solution, 2014.Technical Memorandum – Geotechnical Update Commercial Development 2717 Stevenage Drive Ottawa, Ontario, Reference No.: T020952-A1

Iverson, R.M., 2000. Landslide triggering by rain infiltration. Water Resour Res 36:1897–1910.

Jack, R. and Montminy, S., 2007.Rideau Canal Pedestrian Bridge-20 Years from Conception to Construction. In 2007 Annual Conference and Exhibition of the Transportation Association of Canada: Transportation-An Economic Enabler (Les Transports: Un Levier Economique).

Khezri, S., Shahabi, H. and Ahmad, B.B., 2013.Landslide susceptibility mapping in central Zab basin in GIS-based models, northwest of Iran. Environment, 3, p.4.

Kollaard Associates engineers, 2013. Additional Geotechnical Investigation Proposed Light Industrial Building 1358 Coker Street Osgoode Ward, Greely, City Of Ottawa, Ontario.http://webcast.ottawa.ca/plan/All_Image%20Referencing_Site%20Plan%20Application_Image%20Reference_D07-12-13-0086%20Geotechnical%20Study%20FINAL.PDF.

Kollaard Associates, 2013. Additional Geotechnical Investigation Proposed Light Industrial Building 1358 Coker Street Osgoode Ward, Greely, City Of Ottawa, Ontario.http://webcast.ottawa.ca/plan/All_Image%20Referencing_Site%20Plan%20Application_Image%20Reference_D07-12-13-0086%20Geotechnical%20Study%20FINAL.PDF

L'Heureux, J.S., 2013. Characterization of historical quick clay landslides and input parameters for Q-Bing. Publisher: Norwegian Water Resources and Energy Directorate in collaboration with Norwegian Public Roads Administration and Norwegian National Railways Administration. Prepared by Norwegian Geotechnical Institute (NGI).

Mukhlisin, M., Idris, I., Salazar, A.S., Nizam, K. and Taha, M.R., 2010. GIS based landslide hazard mapping prediction in UluKlang, Malaysia. Journal of Mathematical and Fundamental Sciences, 42(2), pp.163-178.

Nader, A., Fall, M. and Hache, R., 2015. Characterization of Sensitive Marine Clays by Using Cone and Ball Penetrometers: Example of Clays in Eastern Canada. Geotechnical and Geological Engineering, 33(4), pp.841-864.

Pells, P.J.N., 1999. An Equatorial Quick Clay Landslide, Sumatra, Indonesia. In Proceedings 8th Australia New Zealand Conference on Geomechanics: Consolidating Knowledge (p. 143). Australian Geomechanics Society.

Quinn, P., 2009. Large landslides in sensitive clay in eastern Canada and the associated hazard and risk to linear infrastructure. A thesis submitted to the Department of Geological Sciences and Geological Engineering, Queen's University Kingston, Ontario, Canada.

Salciarini, D. D., Godt, J.W., Savage, W.Z., Baum, R. L., Conversini, P., 2008.Modeling landslide recurrence in Seattle, Washington, USA. Engineering Geology 102, p. 227–237.

Stantec Consulting Ltd., 2010.Geotechnical Inventory and Evaluation, Johnston Road Land Use Study.City of Project No. 122410116 (1042983). Available at:http://ottawa.ca/calendar/ottawa/citycouncil/occ/2011/04-13/pec/02%20-%20Geotechnical%20Inventory%20and%20Evaluation%20Report%20-%20April%202010%20%282%29.pdf

Taha, A. and Fall, M., 2010. Shear Behavior of sensitive marine clay-concrete interfaces. Journal of Geotechnical and Geoenvironmental Engineering, 139(4), pp.644-650.

Terzaghi, K., 1943. Theoretical Soil Mechanics. John Wiley and Sons, New York. 510 pp.

Trow Associates Inc., 2010. Updated Geotechnical Investigation Proposed Residential Development 280-282 Crichton Street, Ottawa, Ontario, Trow Associates Inc., Available

at:http://webcast.ottawa.ca/plan/All_Image%20Referencing_Site%20Plan%20Application_Image%20Reference_Geotechnical%20Study%20D07-12-10-0219.PDF

Van Westen, C.J., Rengers, N., Terlien, M.T.J. and Soeters, R., 1997. Prediction of the occurrence of slope instability phenomenal through GIS-based hazard zonation. GeologischeRundschau, 86(2), pp.404-414.

CHAPTER 7

7 Synthesis and Integration of All Results

In the previous chapters, geographic information system (GIS) based modeling tools or models have been developed to assess and predict rainfall, snowmelt, and climate (rainfall and snowmelt)-induced landslides in sensitive marine clays of the Ottawa region. The Transient Rainfall Infiltration and Grid-based Regional Slope stability (TRIGRS) model was used in a GIS framework to assess the landslide susceptibility over the Ottawa region, with respect to time and location. The influences of rainfall and/or snowmelt with different intensities and durations on landslides in Ottawa's sensitive marine clays were investigated by using the developed and validated models. The main results obtained are synthesized and discussed below.

7.1 Model Input Parameters

The model input parameters include geotechnical, climate, hydrogeological, and spatial data that was obtained from several sources, such as governmental agencies, consulting firms and technical firms that have a good work history in the Ottawa region. Since it is well known that the uncertainties related to the input parameters (e.g., data quality, spatial variability of the data) can significantly affect the accuracy or reliability of a landslide susceptibility map, it was necessary to consider these parameter uncertainties in the model development, validation, and subsequently in the model application of the studied area. Therefore, the developed models considered three key scenarios with respect to the potential uncertainties related to the values of the geotechnical input data for each model:

1. The "normal case" scenario: this scenario uses the average geotechnical parameter input values applicable to the study area.

2. The "worst case" scenario: this scenario uses the most negative geotechnical parameter input values applicable to the study area. The most "negative" values used are the most pessimistic based on their impact on the factor of safety. For example, shear strength parameters that most "negatively" impact the factor of safety include the lowest values of cohesion and internal friction angles. Although this approach is conservative, this scenario creates a landslide susceptibility map that will reduce the risk of slope failure.

3. The “ideal case” scenario: this scenario uses the most positive geotechnical parameter input values applicable to the study area. The most “positive” values used are the most optimistic values based upon their impact on the factor of safety. For example, shear strength parameters that most “positively” impact the factor of safety include the highest values of cohesion and the internal friction angles.

The landslide susceptibility maps depicted the areas for each scenario that are susceptible to landslide within the Ottawa region. The “ideal case scenario” contains fewer areas vulnerable to landslide as compared to the normal scenario. The normal scenario contains fewer areas vulnerable to landslide as compared to the worst case scenario, as expected. The amount of predicted landslide prone areas in the worst case scenario was greater than the normal and ideal scenarios. The findings of this study confirm that the landslide susceptibility models are sensitive to changes in input geotechnical parameters. Thus, this sensitivity should be taken into consideration in the assessment and/or mitigation of landslide hazards in Ottawa sensitive marine clays.

7.2 Comparison of the Predicted Landslide Areas with Previous Landslides Areas in Ottawa

The landslide maps developed in this study were compared with historic landslide occurrences in the study area for the purpose of model validation. Indeed, the GIS-TRIGRS model results were evaluated for accuracy by comparing the predicted unstable sites (areas with FS < 1) with historic landslides in the study area. This comparison confirms that a considerable portion of the predicted sites are characterized by low FS values (and thus unstable slopes), indicating potential locations for future landslides induced by rainfall and/or snowmelt. The locations of the landslides fall within the same general trends (often elongated trends) as the areas containing historical landslides in the Ottawa region. Therefore, the models predicted results and the spatial distribution of historically recorded landslides in the Ottawa Region are in good agreement. This suggests that the models are able to predict rainfall and/or snowmelt-induced landslides with a comfortable level of accuracy in the study area. These models can be used to assess or simulate landslide susceptibility in Ottawa sensitive marine clays.

7.3 Effect of Rainfall on Landslide Occurrence or Susceptibility in Ottawa Sensitive Marine Clays

The model was used to investigate the influence of rainfall on shallow landslides over the Ottawa region, with respect to time and location. The study area was analyzed for rainfall durations of 5 minutes, and hourly durations of 6, 12, 18, and 24 hours. The study area was also analyzed for various case scenarios. Several key results were obtained. The landslide susceptibility map depicted that the area's most susceptible to rainfall-induced landslides are located in eastern and western Ottawa due to the region's steep slopes and sensitive Leda clay. The model results also indicated that landslides typically occur after low rainfall over a long duration rather than high intensity rainfall over a short duration. For example, short rainfall durations of 5 minutes at a high intensity of 250mm/h were not susceptible to landslide (FS was greater than or equal to 1). Alternatively, long rainfall durations of 24 hours and low intensity rainfall of 4.5mm/h were susceptible to landslide (FS was less than 1). These findings are consistent with previous study results that indicated that low rainfall across a long duration were key landslide triggers (e.g., Salciarini et al., 2008, Hasegawa et al., 2009, Li et al., 2013). Low intensity, long duration rainfall supports the infiltration of water into soil, resulting in a reduction of the shear resistance of Leda clay (and thus reducing slope stability). Upper parts of Leda clay are considered unsaturated initially. The soils unsaturated conditions change over time due to the infiltration process. Upon the infiltration of water, the clay's matric suction reduces, declining the shear strength of the Leda clay. This argument is congruent with previous studies that indicate that upper parts of Leda clay formations become unstable when saturated (e.g., Dai and Lee, 2001; Fall et al., 2006; Quinn, 2009; Taha and Fall, 2010; Nader et al., 2013, 2015; Haché et al., 2015).

7.4 Effect of Snowmelt on Landslide Occurrence or Susceptibility in Ottawa Sensitive Marine Clays

The developed model was used to assess and predict the snowmelt-induced landslides in areas of sensitive marine clays in the Ottawa region. The obtained results have shown that high slope areas of sensitive marine clay are more prone to snowmelt-induced landslides. Snowmelt intensity was evaluated for its effect on slope stability for durations of 6 to 48 hours, 3 to 15 days, 25 days, and 30 days. An example was executed in the normal and worse case scenarios. In this case, the snowmelt intensity is 16 mm/h and the duration is 6 hours. In this scenario, the slopes are

all stable. Alternatively, for snowmelt intensities of 15.5 mm/h, 10 mm/h, and 6 mm/h for durations of 2, 10 and 30 days the slopes were found to be potentially unstable.

This study result agrees with the results of previous studies completed or snowmelt-induced landslides (Kawagoe et al., 2009). For example, the Shiidomari landslide (in September 1999) and the Katanooin landslide (in January 2003) were examples of low intensity, long duration snowmelt that triggered a landslide. This is due to the change in soil infiltration with time. The soil is more sensitive to snowmelt duration because of the effect it has on increasing the infiltration of water in soil. Infiltrated soil results in reduced soil shear resistance, and thus slope stability. The model takes into account that the soil is initially unsaturated. These results agree with those presented in previous studies (Dai and Lee, 2001; Fall et al., 2006; Quinn, 2009; Taha and Fall, 2010; Nader et al., 2013, 2015; Haché et al., 2015). As previously discussed, upper parts of Leda clay are considered unsaturated initially. This condition changes with time due to snowmelt because of the process of infiltration. Snowmelt infiltration reduces soil suction and the stability of slopes, thus increasing landslide susceptibility in the area. Soil that is infiltrated with water raises the groundwater levels in the area. Saturated soil sees an increase in pore water pressure, a decrease in matric suction, and thus a reduction in the soil's shear strength. The model's results show that at until moment snowmelt intensity reaches the coefficient of permeability of soil at the surface, the soil's stability is not affected. Therefore, the model shows that continued snowmelt infiltration changes the soil from unsaturated to saturated which reduces matric suction to such a small value that its effect is minimized.

7.5 Combined Effect of Snowmelt and Rainfall on Landslide Occurrence or Susceptibility in Ottawa Sensitive Marine Clays

Landslide susceptibility maps were developed and analyzed to understand the behavior of sensitive marine clay after 24 and 48 hours of rainfall and snowmelt duration. These maps considered the effects of rainfall and snowmelt concurrently. These maps depicted how steep slopes and sensitive Leda clay impacted landslide susceptibility in the area when impacted by both rainfall and snowmelt for 24 and 48 hour durations. This integration or coupling of the effects of rainfall and snowmelt resulted in a slight increase in the areas identified as prone to landslide in comparison with the areas affected solely by snowmelt or rainfall. The area's most susceptible to landslide due to rainfall and snowmelt were areas of Leda clay on high slopes. Slopes considered to be prone to instability (and landslide) were areas with safety factors less than one. This study

discovered that the eastern and western portions of the study area contained steep slopes and Leda clay, making them most susceptible to landslide. The landslide susceptibility maps that combine both rainfall and snowmelt create a more realistic representation of landslide susceptibility in the Ottawa area.

7.6 Summary and Conclusions

In summary, the developed GIS-TRIGRS models are able to predict rainfall and/or snowmelt-induced landslide susceptibility in marine clays of the Ottawa Region. The FS values, produced by the models, are sensitive to rainfall and snowmelt duration. The results of the research show a strong influence of rainfall and snowmelt on the occurrence of landslides in the Ottawa Region. Landslides are often triggered by prolonged rainfall and/or snowmelt durations at low intensity, because it favors the infiltration of water into soil. The infiltration will reduce the shear resistance of the Leda clay, and consequently the FS values and slope stability will likewise reduce. The obtained results provide a new insight into the factors influencing landslides in the Ottawa Region and also confirm the reliability of the developed GIS-TRIGRS model.

The results obtained also corroborate the findings of previous geotechnical investigations that have suggested that the upper layers of Leda clay formations remain unsaturated throughout Ottawa (e.g., Dai and Lee, 2001; Fall et al., 2006; Quinn, 2009; Taha and Fall, 2014; Nader et al., 2013, 2015; Haché et al., 2015). The factors of safety values predicted from the GIS-TRIGRS models also reflect the soil in an unsaturated state. This result confirms that infiltrated water will reduce the matric suction, which is accompanied with a decline in the shear strength of Leda clay, reduction of safety factor values, and an increase in slope instability.

CHAPTER 8

8 Conclusions and Recommendations for Future Study

Through the development, testing, and application of a GIS-TRIGRS model, the influence of rainfall and/or snowmelt on landslide susceptibility insensitive Ottawa marine clays was determined. This thesis assesses the influence of rainfall and snowmelt on landslide susceptibility in areas of sensitive marine clays in Ottawa and also evaluates landslide susceptibility induced by climate (both rainfall and snowmelt) for various durations. The developed GIS-TRIGRS model was used to create landslide danger maps to visualize the landslide susceptibility of the Ottawa region. The coupling of GIS and TRIGRS was successfully applied to identify the slopes most prone to rainfall or snowmelt-induced landslides (Eastern and Western Ottawa) within Leda clay areas.

The model results were successfully validated by confirming a high spatial correlation between the historical and predicted landslides throughout the Ottawa region. These applied methodologies and the outputs of this study can be used for evaluating the susceptibility of rainfall or snowmelt induced landslides. They also provide useful geotechnical information for efficient slope management and land use planning. The results also confirm that some recorded landslides in sensitive marine clay may have not been induced by rainfall or snowmelt events.

The GIS-TRIGRS model offers important details related to rainfall and snowmelt-induced landslides. With respect to rainfall, landslides throughout Ottawa are often triggered by high duration and low intensity rainfall events. These rainfall characteristics oftentimes result in the infiltration of water into the Leda clay cells, causing the upper portion of the soil to remain unsaturated, and leaving the area more susceptible to a top soil landslide. The area becomes more susceptible to a landslide because the infiltration results in the reduction of the shear resistance of the Leda clay, and thus, reduces the slope's stability. Similarly, snowmelt-induced landslides occur due to soil infiltration. In this study, there is a slight increase in the areas prone to landslides when the worst of the two calculated factor of safety values from rainfall and snowmelt are considered. Ultimately, the outputs and results of the developed GIS-TRIGRS model for assessment and analysis of rainfall and snowmelt-induced landslides in Ottawa can be applied for the optimization of land use planning and design. It can also be applied to different duration scenarios for the evaluation of the critical duration of rainfall or snowmelt in the area.

To improve the model, the followings are suggested:

- Including other sensitive soils,

- Extended rainfall and snowmelt durations and intensities as a result of climate change associated with increasing climate variability,

- Groundwater level variations due to extreme climatic events, and

- Considering the effect of seismic activities in the area and nearby regions.

This model could also support the investigation of slope material variability over large areas or to assess landslide hazard and risk using rainfall and snowmelt at the regional scale and larger areas in other similar areas. The TRIGRS-unsaturated model developed can characterize slope stability in areas affected by shallow landslides. The model could analyze the impact of plant roots as soil reinforcement in order to optimize agricultural management practices. Lastly, this model could be applied to the analysis of unsaturated slopes that experience a heavy storm after a long-term drought. For proper model verification, the development of strategies for mitigating uncertainty in the model is crucial. This model verification can be done by rechecking the parameters used in the model in order to further correct the result, but further methods must be put into place as well.